NASA CR 72889

FINAL REPORT

DESIGN, FABRICATION, AND TEST OF OMNIDIRECTIONAL FLEXIBLE SEALS FOR THRUST VECTOR CONTROL OF LARGE SOLID ROCKET MOTORS

Prepared by:

E. Y. Wong

Aerojet Solid Propulsion Company
Advanced Technical Operations
Sacramento, California

National Aeronautics and Space Administration
Lewis Research Center
Cleveland, Ohio

J. J. Pelouch, Project Manager

NASA CR 72889

FINAL REPORT

DESIGN, FABRICATION, AND TEST OF OMNIDIRECTIONAL FLEXIBLE SEALS FOR THRUST VECTOR CONTROL OF LARGE SOLID ROCKET MOTORS

Prepared by:

AEROJET SOLID PROPULSION COMPANY
Advanced Technology Operations
Sacramento, California

Author: E. Y. Wong

10 June 1971

Contract NAS3-12049

Prepared for:

NATIONAL AERONAUTICS AND SPACE ADMINISTRATION
Lewis Research Center
Cleveland, Ohio

Technical Management
J. J. Pelouch, Project Manager

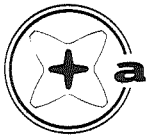

aerojet solid propulsion company

A DIVISION OF AEROJET-GENERAL

TABLE OF CONTENTS

LIST OF TABLES

LIST OF FIGURES

LIST OF FIGURES (Cont.)

LIST OF FIGURES (Cont.)

LIST OF FIGURES (Cont.)

ABSTRACT

Design, fabrication, and test of a large diameter, flight weight, omni-directional flexible seal meeting the requirements of the 260-in.-dia solid rocket motor were accomplished. A simplified flexible element for the seal was designed which consisted of uniform, conical shapes of rubber and steel layers. Individual components of the flexible seal were assembled to form the completed unit by secondary bonding in successive steps using an ambient temperature curing adhesive system. Test data confirmed that the seal met the performance requirements predictably and the performance limits exceeded the design requirements.

I. SUMMARY

This is the final report for the Nozzle Flexible Seal Program performed under NASA Contract NAS3-12049. The objective of the program was to demonstrate the capability to manufacture large diameter, flightweight, laminated, onmi-directional flexible seals meeting the requirements of the 260-in.-dia solid rocket motor.

The scope of work accomplished included design, fabrication, test and evaluation of two flexible seals meeting all the requirements for use in the thrust vector control system of the 260-in.-dia motor. The total work effort was divided into Task I, Design; Task II, Laboratory Support Services; Task III, Fabrication; and Task IV, Test.

Major elements of the finalized seal design were:

- Forward pivot design concept
- Conical reinforcement shims with constant-thickness elastomer pads
- Cylindrical seal body, 108-in. I.D. and 116-in. O.D.
- Five elastomer pads, 0.3-in.-thick natural rubber
- Four reinforcement shims, 0.7-in.-thick steel

All shims were identical in design allowing for interchangeability. The simple geometry of the shims enabled design dimensional tolerances to be readily met with minimum difficulty and hence minimum fabrication cost. The Gen-Shear 44125 pads were net-molded in segments comprising 1/8 of the circumference (45° each), using a two-cavity heated mold and press. Fabrication in segments enabled use of a small mold and minimized the fabrication tooling cost. Each molded segment was thoroughly inspected and only those meeting rigid acceptance standards were authorized for use in seal fabrication. Quality of the elastomer pads was thus assured before their commitment for use in a seal, thus minimizing the risk of rejection in final assembly. The elastomer pads and reinforcement shims were bonded together with Chemlok 304 ambient temperature curing epoxy resin. Integrity of each bondline was verified by nondestructive testing prior to proceeding with bonding of successive components in the assembly. These design features and fabrication methods resulted in high quality seals at minimum cost.

The two seals were fabricated and subjected to performance testing to verify attainment of performance requirement. In these tests, the seals were subjected to 850 psig (5.85×10^6 N/m^2) chamber pressure, 1.15×10^6 lb (5.11×10^6 N) ejection force and $\pm 2°$ (0.0349 rad) deflection. The actuation torque for $\pm 2°$ (0.0349 rad) deflection without the protective boot was 4.98×10^6 in.-lb (5.65×10^6 N-m) which is in good agreement with the design value of 5×10^6 in.-lb (5.65×10^6 N-m) for 1 million lb (4.45×10^6 N) ejection load. Experimental data confirmed compliance with performance requirement and verified the adequacy of analytical techniques used. After performance testing, one seal was subjected to destructive test. This test sequence included over-deflection to 3.3° (0.0575 rad), fatigue test of approximately 1000 cycles, and excessive loading up to 1.5×10^6 lb (6.67×10^6 N) ejection load. Failure was not obtained and testing was discontinued at these conditions which represent limits of test equipment and facility capability.

In summary, the program resulted in a seal design and fabrication method offering significant advantages including low cost and high inherent reliability. Two seals were fabricated and tested to demonstrate adequacy of this design in meeting thrust vector control requirements of the 260-in.-dia motor. These results constitute a major step in development of flexible seal technology.

II. INTRODUCTION

A flexible seal movable nozzle as the means of vectoring the thrust of the large solid rocket motor offers the potential advantages of simplicity, weight, and cost as compared to other candidate methods of thrust vector control. The flexible seal has emerged from only a concept a few years ago to a device currently developed for use on several missile systems. The seal flexible element consists of concentric spherical laminated layers of elastomer and metal shims. Seals have been fabricated by either injection molding or layup of uncured elastomer between shims with the flexible element cured as a unit.

Because of the large nozzle size and low magnitude of steering requirements for a 260-in.-dia solid rocket booster, flexible seals for this application need to be manufactured in a less complicated manner than is currently practical. Accordingly, a program was undertaken to design, fabricate, and test two flexible seals of a size meeting 260-in.-dia motor requirements. The demonstrated capability to fabricate seals of the required size is necessary for the proper consideration of flexible seal movable nozzles for large solid rocket motors.

III. TASK I - DESIGN

A. DESIGN CRITERIA

The flexible seal was designed to meet the requirements of a 260-in. (6.6 m) solid rocket motor. Basic design criteria and performance specifications were established by contract requirements as follows:

1. The seal shall be designed to be used on a motor nozzle with a throat diameter of 90.0 in. (2.28 m) and an entrance-to-throat initial area ratio of 2:1. Allowance shall be made for a nominal 5-in. ablative material thickness at the throat plane exclusive of overwrap.

2. The seal shall be designed for a motor maximum expected operating pressure (MEOP) of 750 psia (5.16×10^6 N/m^2).

3. The flexible seal shall be flightweight and shall consist of chamber and nozzle attachment flanges, the flexible element, and the insulation boot to protect the seal against the thermal environment of the motor.

4. Required vector deflection angle of the seal shall be in accordance with Figure 1.

5. The following minimum factors of safety shall apply to the flexible seal design:

Parameter	Safety Factor	Condition
Metal Stresses	1.25	MEOP and Vectored
Metal Stresses	1.25	MEOP and Null
Elastomer and Bond Line Tension	2.0	Ambient Pressure and Vectored
Metal Shim Compression and Buckling	1.25	MEOP and Vectored or Null, whichever is worse.
Elastomer and Bond Line Shear	2.0	MEOP and Vectored or Null, which ever is worse.

B. PRELIMINARY NOZZLE DESIGN

Preliminary design of a nozzle was prepared to define the envelope and requirements for the detailed design of the flexible seal. Requirements applicable to a full length 260-in. (6.6 m) motor that is suitable for the 260/S-IV vehicle were incorporated into the nozzle design. Test data obtained from previous 260-in. (6.6 m) dia motor tests were utilized in the design analysis.

The nozzle design, Figure 2 was similar to that for the 260-SL-3 nozzle, Reference 1, except the contour was scaled to a 90-in. (2.28 m) throat diameter. The submergence contour from the entrance leading edge to the throat plane was a 3:2 elliptical shape with a major axis corresponding to 75% of the throat radius. Aft of the throat plane, the surface curvature was equal to the throat radius and was tangent to the nozzle divergence contour. A bell-shaped contour with an expansion ratio of 8.5 was selected for the divergence section.

Using a nominal 5-in. (1.27 m) nozzle ablative at the throat plane as the baseline, ablative thicknesses at other nozzle stations were extrapolated on the basis of thermal degradation requirements. Nozzle erosion and char data from 260 in. (6.6 m) dia motor tests were adjusted for differences in throat diameter and motor pressure using Bartz's theory, Reference 2, and applied to the thermal degradation prediction. Predicted erosion, char, and 100°F (311°K) isotherm depths at the various nozzle stations were obtained as tabulated in Table I.

Structural support of the nozzle ablative, as well as the flexible seal, was provided by steel components. A nozzle shell was designed to maintain the stress and strain levels in the ablative liner within the allowable material properties. A bolted joint was incorporated in the shell for assembly to the forward end of the seal. The aft end of the seal was assembled to a steel conical closure, which also had provisions for assembly of the nozzle to the motor case.

From this nozzle design, it can be seen that the envelope for the design of the flexible seal was limited by the nozzle shell and conical closure configurations. Because of the advantages of lower weight and actuation torque, the seal was selected so that the inside diameter was as small as practical within the envelope constraints. This diameter was 108 in. (2.74 m). In addition to the envelope limitation, selection of the interface design between the seal and the nozzle structures included consideration of assembly and disassembly of the seal without interference with the nozzle ablative components.

C. FORWARD AND AFT PIVOT SEAL COMPARISON

Within the envelope defined by the nozzle design outlined above, flexible seals with the pivot point located either forward or aft of the nozzle throat plane can be designed. In the initial seal design effort, both forward and aft pivot design concepts were investigated and comparatively evaluated.

To facilitate this comparative study, the same basic seal configuration was used for both concepts. Differences in rotational angle requirement [1.95° (.034 rad) vs 1.72° (.030 rad)] between the two concepts were neglected. The same flexible element was used, which consisted of five layers of 0.3 in. (.0076 m) rubber pads that were supported alternately by four 0.7 in. (.0178 m) steel conical shims. The seal geometry was a cylindrical body with a 108 in. (2.74 m) I.D. and 116 in. (2.95 m) O.D. Preliminary stress analysis of this seal design, Table II, indicated that shear stress in the rubber pads and compressive and buckling stresses in the steel shims met the design criteria. The seal rotational torque was 13.4% higher for a forward pivot seal with the larger rotational angle requirement.

Some differences were apparent between the nozzle designs for the forward and aft pivot seal concepts, as shown in Figures 3 and 4, respectively. Weights of the two nozzle designs were calculated for comparison. The weight comparison in Table III indicated that the nozzle with a forward pivot seal was 565 lb (256 Kg) less than an aft pivot seal. In terms of cost, the weight difference was equivalent to $9600 calculated on a dollar per lb basis for the various nozzle materials.

For the comparison of actuation system requirements between forward and aft pivot seals, seal rotation torque, internal aerodynamic, axial acceleration and inertia torques were calculated. Although the total torque was 55% higher for a forward pivot seal, the actuation force was actually less because of the longer moment arm as shown in Table IV. Assuming an actuator fluid pressure of 2000 psi (13.8×10^6 N/m^2) and the total stroke for $\pm 2°$ (.0349 rad), hydraulic system flow rates of 60 and 43 GPM (.00379 and .00271 m^3/sec) were required for the forward and aft pivot seals, respectively.

A summary of this comparative study indicated the following advantages of the forward pivot seal concept: (1) lower weight, (2) lower cost, (3) simplicity of nozzle ablative component design in the submerged cavity, (4) longer moment arm to react the actuator torque. Advantages noted for the aft pivot seal concept were: (1) lower total actuation torque, (2) elimination of actuator cross-talk with the plane of actuator attachment coincident with the pivot point, and (3) lower actuation system hydraulic flow rate requirement. From the results of this study, the forward pivot seal concept was selected for detailed design. Concurrence of the NASA/LeRC Program Manager with this selection was obtained.

D. DETAILED FLEXIBLE SEAL DESIGN

1. Design Selection

In addition to the design criteria listed in Section A, the following requirements were determined from the preliminary nozzle design study

for inclusion in the final design and analysis of the flexible seal:

Ejection force	1,000,000 lb (4.45×10^6 N)
Nozzle deflection angle	$\pm$1.95 degree (.034 rad)
Available seal rotation torque	5.0×10^6 in.-lb ($.565 \times 10^6$ N-m)
Available total actuation force	114,000 lb (5.07×10^5 N)
Weight of nozzle movable parts	50,000 lb (2.27×10^4 Kg)

The selected flexible seal design is shown in Figure 5. For simplicity in design and fabrication, a seal with a cylindrical body and conical flexible elements was selected. The inside and outside diameters of the seal were 108 in. (2.74 m) and 116 in. (2.94 m). The angle measured from the nozzle centerline to the centroid of the seal was 50 degree (.873 rad). To meet the rotational angle requirement, the flexible elements of the seal consisted of five layers of 0.30 in. (.0076 m) rubber pads, which were individually supported by four 0.70 in. (.0178 m) steel shims. Steel end rings, which have provisions for assembly of the seal to the nozzle, completed the seal design.

An elastomeric boot for thermal protection of the seal from the motor exhaust gas environment was designed to fit into the envelope defined by the nozzle design with consideration of the required deflection angle. An S-shaped configuration, Figure 5, was selected so that stretching of the boot was minimized during seal deflection.

2. Material Selection

Gen-Shear 44125 rubber, a natural rubber product from General Tire and Rubber Company, was selected as the rubber pad material. The properties of this material were obtained from material characterization studies performed under Task II of this program and Aerojet Independent Research and Development Program. Properties that were used in the seal design analysis included the following:

Young's modulus (E)	81 psi (5.59×10^5 N/m^2)
Shear modulus (G)	27 psi (1.86×10^5 N/m^2)
Bulk modulus (K)	287,000 psi (1.98×10^9 N/m^2)
Ultimate shear strength (F_{su})	403 psi (2.78×10^6 N/m^2)
Ultimate tensile strength (F_{tu})	500 psi (3.45×10^6 N/m^2)
Ultimate shear strain (γ_u)	700%

Young's modulus (E) was assumed to be three times the shear modulus. To maintain conservatism in the design, the upper limit value of the shear modulus was used. This value, 27 psi (1.86×10^5 N/m^2), is about 8% greater than the average shear modulus of 25 psi (1.725×10^5 N/m^2) obtained in tests. Poisson's ratio (ν) was calculated from the elasticity relationship between bulk modulus and shear modulus:

$$\nu = \frac{3K - 2G}{6K + 2G}$$

From this expression Poisson's ratio was found to be 0.49995.

Steel shims and end rings of the seal were made from normalized AISI 4130 steel having the following properties:

Young's Modulus (E)	29×10^6 psi (2.0×10^{11} N/m^2)
Tensile yield strength (F_{ty})	70,000 psi (4.83×10^8 N/m^2)
Compressive yield strength (F_{cy})	70,000 psi (4.83×10^8 N/m^2)
Poisson's ratio (ν)	0.3

The nozzle shell and conical closure were assumed to be made from high nickel maraging steel having a minimum tensile yield strength of 200,000 psi (1.38×10^9 N/m^2).

A butadiene acrylonitrile rubber, V-45, was selected as the elastomeric boot material after comparative evaluation with other candidate materials. This material has the following properties, which were used for design and analysis of the boot:

Shore "A" hardness	85 maximum
Tensile strength	2000 psi (1.38×10^7 N/m^2)
Elongation	200%
Thermal conductivity, max, @150°F	0.15 $\frac{\text{Btu}}{\text{hr ft °F}}$ (389 $\frac{\text{joule}}{\text{m sec °K}}$)
Specific heat, min, @ 150°F	0.32 $\frac{\text{Btu}}{\text{lb °F}}$ (2.2 $\frac{\text{joule}}{\text{Kg °K}}$)

3. Design Analysis

a. Flexible Seal End Rings and Nozzle Support Structure

Nozzle support structure and seal end rings were analyzed as two separate assemblies. One assembly (Part A) consisted of the seal aft ring and the conical closure. The second assembly (Part B) included the seal forward ring and the nozzle shell. Both assemblies were analyzed by means of a finite element computer program which considers the structure to be an assemblage of quadrilateral rings connected at common nodal points. Details of the formulation and method of solution are contained in Reference 3.

In analyzing Part A, the structure was modeled by the grid-work shown in Figure 6. The flange at Point A (see Figure 6) was assumed fixed and a design pressure of 938 psi (6.47×10^6 N/m^2) [1.25 x 750 psi (5.17×10^6 N/m^2)] was applied to the inside surface of the closure. In addition, the ejection force was distributed over the forward surface of the seal aft ring. In actual operation torque is applied to the seal ring as a sinusoidally varying edge load and has the effect of increasing or decreasing the uniformly distributed ejection force on this surface. Since the computer program used is limited to axisymmetric loading conditions, the design value of the distributed axial load was taken as the ejection force plus the maximum value due to torque. A breakdown of this loading is indicated below:

Ejection force:	1,000,000 x 1.25/2π	= 199,000 lb/radian (8.86×10^5 N/rad)
Torque:	5,000,000 x 1.25/56π	= 35,500 lb/radian (1.58×10^5 N/rad)
	Design load	= 234,500 lb/radian (10.44×10^5 N/rad)

Results of the analysis indicated that the maximum stress occurred at Element 31 in Figure 6. The principal stresses in this element were:

Radial stress	-	2,250 psi (15.5×10^6 N/m^2) (tension)
Axial stress	-	8 psi (55.1×10^3 N/m^2) (tension)
Hoop stress	-	63,206 psi (436×10^6 N/m^2) (tension)

The margin of safety based on maximum stress theory was +0.107. The margin of safety based on distortional energy failure (Von Mises) theory yielded a slightly larger margin of safety (+0.127) as all principal stresses were tensile.

Two loading conditions were considered in the Part B analysis.

(1) Pressure distribution calculated from compressible isentropic ($\gamma = 1.2$) flow based on a chamber pressure of 938 psi (6.47×10^6 N/m^2) was applied on the nozzle shell surface. This pressure was found to vary from 320 psi (2.21×10^6 N/m^2) at flange A (see Figure 7) to 938 psi (6.47×10^6 N/m^2) at surface B. A load was also applied at flange A so that the resultant horizontal reaction at C would equal the design ejection force of 1,250,000 lb (5.56×10^6 N).

(2) This loading condition was similar to the first, except that an internal pressure of 938 psi (6.47×10^6 N/m^2) was added to the entire surface of area D (see Figure 7).

Condition 1 was more critical than condition 2 and therefore controlled the design. From the computer analysis, all stresses in Part B were below the allowable yield and allowable buckling of the material. For the most part, however, strain was the governing factor. The highest strain of 0.23% was at Element 29, showing a margin of safety of +0.087.

The relative movement at the bearing joint between the nozzle shell and seal forward ring is shown in Table V for loading condition 1. No joint separation existed even at full chamber pressure.

At the attachment joints between the seal and the nozzle structure, the interface load is normally in compression from the ejection force. Even with the maximum torque of 5,000,000 in.-lb (5.65×10^5 N-m) that can be applied, the separating force at the joint is small. The size and spacing of the attachment bolts were, therefore, governed by good design practices considering vibration and handling conditions.

b. Flexible Seal Assembly

(1) Stress Distribution

The stress distribution within the flexible elements of the seal assembly was also determined by means of finite element computer programs. Programs, Reference 4, that can consider completely incompressible materials as well as non-axisymmetric loading on axisymmetric solids of revolution were used. The basic analytical model used in the analysis is shown in Figure 8. This model considered the ejection force to be applied uniformly through the cross section of the seal and a fixed boundary existed at the seal aft ring. Detailed solutions were run for three specific loading conditions:

Condition 1: Ejection force applied to an undeflected seal geometry with the chamber pressurized.

Condition 2: Rotational torque applied to produce 1.95° (.034 rad) seal deflection with the chamber unpressurized.

Condition 3: Ejection force applied to a 1.95° (.034 rad) deflected seal geometry with the chamber pressurized.

From the analytical results, the stress distribution in each rubber pad and steel shim was obtained. The maximum stress levels for the three loading conditions are shown in Figures 9 through 16. In all cases the values shown represented the average stress within the indicated "element". From

the maximum predicted stress, the corresponding factors of safety for each loading condition were calculated and are shown in Table VI. The resultant safety factors met the design criteria specified in Section II.A.

To understand the behavior of the seal under the combined loads, the deflections and stress distributions obtained from the computer solutions were plotted. Figure 17 shows a plot of the normal and shear stresses acting on a typical shim-pad interface for loading condition 1. From this plot of stress distribution, it is apparent that a rotational moment is applied to the shim. The rotation of the shim results in the high compressive stress on the inner bore surface of the shim. Figures 18 and 19 indicate the deformations at the inner and outer edges of the rubber pad, respectively, for this loading condition. The total axial deflection of the seal was predicted to be 0.235 in. (0.00596 m) due to the combined loads.

(2) Elastic Stability

While the compressive stress that resulted from the twisting moment in the shim is not high in comparison to the compressive yield strength of the shim material, instability failures have been experienced on some laminated seals of this type. In order to check the possibility of buckling, the maximum compressive stress in the shim was compared to the critical buckling stress for an assumed equivalent beam on an elastic foundation.

From Reference 5, the critical buckling load for an infinitely long beam on an elastic foundation was derived as:

(1) $N_{cr} = 2\sqrt{k\ EI}$

where: N_{cr} = critical load, lb/in. (N/m)

k = foundation modulus per unit length, lb/in.^{3} (N/m^3)

E = Young's modulus, lb/in.^{2} (N/m^2)

I = Moment of inertia per unit width, in.^{3} (m^3)

For a beam of unit width and rectangular cross section, expression (1) reduced to:

(2) $\sigma_{cr} = \sqrt{\frac{k\ Eh}{3}}$ where: σ_{cr} = critical buckling stress, psi (N/m^2)
h = thickness, in. (m)

Applying equation (2) to a steel shim of 0.70 in. (.0178 m) thickness gives:

(3) $\sigma_{cr} = 2{,}600\sqrt{k}$ in psi
$= 35{,}000\sqrt{k}$ in N/m^2

The value of k for use in this expression was determined by applying a unit edge load to the model shown in Figure 20. A conservative assumption was made for the model in that the total thickness of rubber pads was supported on either side of the critical steel shim without the reinforcement of the other shims. The resultant deflection at the point of load application was used to compute a spring rate for the flexible element of the seal.

Results of this solution gave a spring constant of 9470 lb/in. (1.655×10^6 N/m). This value can be considered equivalent to the foundation modulus per unit area K of 9470 lb/in.^{3} (2.56×10^9 N/m^3), then:

$\sigma_{cr} = 2600\sqrt{9470} = 253{,}000$ psi
$= 3.5 \times 10^4\sqrt{2.56 \times 10^9} = 1.75 \times 10^9$ N/m^2

Since critical buckling stress is well above the 70,000 psi (483×10^6 N/m^2) compressive yield strength of the shim, it can be concluded that buckling of the shim will not occur and compressive stress is the criteria for design. From Figures 12 and 15, the maximum compressive stress in any shim was found to be 50,800 psi (350×10^6 N/m^2) [3900 psi (27×10^6 N/m^2) due to rotation plus 45,900 psi (323×10^6 N/m^2) due to ejection loading on the deflected geometry]. The resultant factor of safety for shim stresses is then 1.38 as shown in Table VI.

c. Elastomeric Boot

An elastomeric boot of 0.50 in. (.0127 m) thick V-45 rubber (Figure 5) was used to protect the seal from the thermal effects resulting from exposure to the motor propellant combustion products. A heat transfer analysis was performed to evaluate the thermal response of the boot and its effect on the seal for a full-length 260-in. (6.6 m) dia motor firing (approximately 140 seconds).

In order to reduce the severity of the local thermal environment to tolerable values, the boot and seal were located in a cavity separated from the main gas flow environment of the motor by a narrow gap, which was small enough to attenuate any external flow disturbances. The heat transfer in such a cavity has been treated analytically and experimentally in Reference 6. For conditions similar to the selected configuration, the heat transfer coefficients are related to the flow conditions external to the cavity and the cavity geometry by the following equation:

$$\bar{h} = .016 \left(\frac{x_w}{x_g}\right)^{-.45} Re_{xg}^{-.5} (\rho v) \bar{C}_p$$

where:

$\bar{h}$ = average heat transfer coefficient within the cavity, $\frac{Btu}{hr\ ft^2\ °F}$

x_w = length of cavity contour, in.

x_g = gap width, in.

$(Re)_{x_g}$ = Reynolds number of external flow based on gap width

(ρv) = local mass flux external to the cavity, $\frac{lb}{hr\ ft^2}$

$\bar{C}_p$ = specific heat of exhaust products, $\frac{Btu}{lb\ °F}$

Use of the above relation represents an extrapolation of the data provided in Reference 6 because the Reynolds numbers and cavity geometries for which test data were obtained were different than those in this analysis. Correlation analysis indicated the thermal model slightly over-predicts the material decomposition rates.

The input data for evaluating the average cavity heat transfer rates were as follows:

Propellant:	ANB-3254
Chamber pressure:	600 psia (4.14×10^6 N/m^2) average
Chamber temperature:	5434° (3280°K)
Aft closure Mach number:	0.3
Gap Width:	0.15 in. (.0381 m)

Substituting these parameters into equation (1), the resulting heat transfer coefficient was predicted to be 24 Btu/hr-ft^2-°F (19×10^3 joule/m^2 sec °K). As indicated by equation (1) the heat transfer rates could be reduced by either increasing the cavity volume (perimeter) or decreasing the gap width.

The thermal response of the selected design exposed to a full-length 260 in. (6.6 m) motor firing, 140 seconds, is presented in Figure 21. Material density profiles are noted at 40, 80, and 140 seconds duration, together with the predicted temperature gradient at time of burnout (140 seconds). The depth of the fully charred zone is predicted to be 0.16 in. (.00406 m) with the total thermal decomposition zone extending to a depth of 0.31 in. (.00788 m). At burnout, the maximum temperature of the flexseal, assuming the boot remained in perfect contact throughout the firing is 90°F (306°K) or 10°F (6°K) above ambient. In regions where the boot does not contact any portion of the flexseal the back-side temperature of the boot would be on the order of 250°F (394°K).

The above results indicated that the boot design was adequate to protect the flexible seal from excessive temperature even with an empty cavity between the boot and the seal. In the actual application where this cavity was filled with a low viscosity grease, the backside temperature of the boot would be substantially less than 250°F (394°K).

d. Failure Modes Analysis

An analysis was performed of three basic failure modes related to the flexible seal. These modes were: (1) structural failure of the seal, (b) the requirement of torque in excess of that available, and (c) premature burn-through of the insulation boot protecting the flexible seal surface. The details of this analysis are included in Appendix A.

Stress analysis identified failure of the seal rubber pads in shear as the most likely mode of mechanical failure. Because of the complexity of the relationship, shear forces cannot be related to the design parameters governing them by simple formulas. The only feasible method for estimating the probable distribution of the shear requirement, therefore, was to employ Monte Carlo simulation techniques in conjunction with the computer program used in the basic stress analysis. Results were obtained for eight simulation runs. From these results the probability of maximum shear exceeding the material capability was calculated. A probability of failure of 3×10^{-6} was obtained.

The calculation of the probability of occurrence of torque requirement in excess of the design capability was made using the basic relationship between requirement vs capability. The requirement average was estimated from an approximate design equation that related torque to rubber modulus and seal geometry. The variability of the required torque was estimated from the formula by the propagation of variance technique. The results indicated that an increase of the torque capability from the design nominal of 5.0×10^6 in.-lb (5.65×10^5 N-m) to 5.87×10^6 in.-lb (6.63×10^5 N-m) was required to reduce the probability of exceedence to the target value of 1×10^{-6}.

In calculating the probability of premature insulation boot burn through, the relationship between requirement and capability was also used. The capability was expressed in seconds of available protection by the ratio of the boot thickness to the erosion rate. The requirement was expressed in seconds of protection required prior to the end of action time. This analysis showed that with the nominal boot thickness of 0.45 (.0014 m), the probability of failure was 1×10^{-8}.

Based on the results of this analysis, the probability of occurrence of seal structural failure and boot burn through failure modes was less than or close to the desired value of 1×10^{-6}. An increase in torque capability was necessary to reduce the probability of exceeding the torque requirement to this value.

4. Engineering Drawings and Specifications

Detailed engineering drawings were prepared for the fabrication of the individual seal components as well as the assembly processing of the flexible seal. These drawings were:

Drawing No.	Title
1148903	Flexible Seal - 260-in.-dia Motor
1148904	End Ring, Fwd - Conical, Flexible Seal
1148905	End Ring, Aft - Conical, Flexible Seal
1148906	Shim - Conical, Flexible Seal
1148907	Pad - Conical, Flexible Seal
1148993	Boot, Elastomeric - Conical, Flexible Seal

The drawings defined the materials and dimensional tolerances of each component in accordance with design requirements. Each rubber pad was designed to be molded from a flat pattern mold. Eight pads were used to complete a circumferential layer in the seal, and dimensional tolerances were controlled so that proper interface fit between pads was obtained without machining.

The seal assembly drawing defined the interface requirements between components and the overall dimensions of the assembly. The limits of mismatch between components were specified. Adhesive materials were specified for the rubber pad interface bond, as well as the rubber pad to steel component bond. These adhesive materials were selected from results of evaluation performed under Task II of this program.

Acceptance and quality control requirements for materials and processing of the seal were delineated by specifications. These specifications were:

Spec. Number	Title
MIL-S-6758	Steel, Chrominum-Molybdenum 4130 Bars and Reforgings
AGC-34463	Compound, Natural Rubber

Spec. Number	Title
AGC-34230	Insulation, Butadiene Acrylonitrile, Unvulcanized
AGC-36590	Seal Assembly, Flexible, Fabrication of
AGC-36420	Insulation, Rubber, Butadiene Acrylonitrile, Autoclave Cure, Fabrication of

The control limits imposed by the specifications, in particular, for the natural rubber compound and for processing of the seal assembly, were derived from results of evaluation programs performed under Task II. Method of surface preparation for rubber and steel components and bond integrity determination were specified in the seal assembly specification.

Engineering drawings and specification used in this program are enclosed in Appendix B.

E. MANUFACTURING PLAN

In defining the plans for the fabrication of the seal components and assembly, well-established techniques were used wherever possible. In the case where new manufacturing and processing materials and techniques were required, the development and evaluation of these items were performed under Task II of this program.

1. End Rings and Reinforcement Shims

Fabrication of the seal steel components, i.e., reinforcement shims and end rings, followed processes that provided a high degree of finished dimensional stability and accuracy. Each component was machined from ring-rolled forgings to the final dimension. Because of the relative elasticity of the parts, final dimensional inspection was conducted while the part was on the turning lathe. Magnetic particle inspection of these components was performed prior to acceptance.

2. Rubber Pads

The selected method for the fabrication of the rubber pads was by transfer-molding the pads in a close tolerance two-cavity mold. Each mold charge produced two pads along with a quality control specimen that was used to verify the proper state of cure was achieved in the molding cycle.

Prior to initiation of production, a development effort was performed by the fabricator, General Tire and Rubber Co. (GT&R) to characterize the processes. This development phase included the following activities:

a. Design and fabricate mold and tooling.
b. Validate mold design through detailed dimensional inspection of trial parts.
c. Optimize molding parameters and cure cycle.
d. Establish acceptance test procedure and limits.

From the results of the development effort, an integrated manufacturing and inspection plan was prepared that covered all aspects of the pad fabrication process from raw material acceptance through finished part shipment. Each pad was serialized to provide traceability through the process sequence. Process documentation for each pad included:

a. Acceptance test data for the raw material lot.
b. Certification of absence of defects by visual inspection.
c. Dimensional inspection results.
d. Cure cycle records.
e. Quality Control specimen test data.

In addition to this development effort, a process demonstration task was conducted as a part of Task II to confirm the dimensional stability of the pads necessary to satisfy the seal assembly bonding process and to establish nondestructive test techniques for final acceptance of the pads.

3. Elastomeric Boot

Fabrication of the elastomeric boot employed a plan which has been extensively used in the processing of motor case insulation of the same material types. This plan consisted of molding the boot in segments, which were subsequently joined together to form the circular part. Each segment was one-sixth of the circumference. The mold was designed to match the S-shape internal configuration of the boot. Uncured rubber sheets were layed up on the mold to the designed thicknesses and cured with autoclave [100 psi (6.9×10^5 N/m^2)] pressure and 310°F (428°K) temperature.

Prior to the production of the boot segments, a development effort was performed by the fabricator to establish a technique for the splicing of the segments. From the results of this effort, the splicing procedure, as well as the splice characteristics, were obtained. Comparison of mechanical properties between the parent material and the splice was made to ascertain that the properties met the design requirements.

Radiographic inspection was used for the detection of defects in the boot. A procedure similar to that used for joining segments was established for the repair of defects.

4. Flexible Seal Assembly

The plan for the assembly processing of the flexible seal consisted of bonding the individual components together in successive steps. Room temperature curing adhesive systems were used for both the rubber pad interface bonds and the rubber pad-to-steel shim bonds. Several candidate adhesive systems were evaluated in Task II of this program prior to their selection for use. The selected adhesive systems were characterized to determine that the bond properties exceeded the design requirements.

Surface preparation, adhesive application and curing techniques were established as a part of the Task II effort. A primer that is compatible with the selected adhesive system was used for protection of steel component surfaces against corrosion. A chlorination treatment was used to prepare rubber pad surfaces for bonding. Bonding and curing procedures included mating of the bond surfaces under vacuum pressure to minimize bond voids and applying mechanical pressure to the bond interface during cure.

Prior to processing of the actual seal, the selected procedures were checked out by the fabrication of a full size process demonstration ring. Tooling and fixtures intended for fabrication of the seal assembly were employed in the process demonstration. Nondestructive techniques for detecting bond defects were established from inspection of the bondlines in the process demonstration ring. Bond strength properties were obtained from sectioning and testing of the ring.

From the results obtained in Task II, intergrated process and inspection procedures were prepared for each step in the seal assembly processing. Detailed procedures were defined for the surface preparation of the individual components and for the adhesive bonding at rubber pad interfaces and between rubber pad and steel components.

F. PROCESS TOOLING DESIGN

From the established manufacturing plan, tooling and fixtures were designed to meet the flexible seal processing and assembly criteria. Major items of tooling were:

Drawing No.	Title
T-1023775	Seal Assembly Bond Fixture
T-1023859	Inverting Fixture for the Bond Fixture
T-1023860	Lift Fixture for the Metal Shims
T-1023861	Handling Cart for the Metal Shims

Drawing No.	Title
T-1023862	Adhesive Spreader
T-1023863	Elastomeric Boot Bond Fixture
T-1024056	Primer Curing Oven

Design criteria for the assembly bond fixture were: (1) position the seal assembly with the centerline in the vertical attitude for bonding, (2) invert the seal component for adhesive application, (3) bond the seal components under vacuum pressure, and (4) apply positive pressure at the bondline during the adhesive cure cycle.

The assembly bond fixture design consisted of an annular vacuum chamber, Figure 22, in which the seal components were bonded. The chamber was separable into two parts; the top with the outside wall, and the bottom with the inside wall. The bottom of the fixture contained a stand on which the forward end ring of the seal seated. Ten air cylinders were attached to the top portion of the fixture for assembly to the seal aft end ring. Trunnions were incorporated for inverting the top portion of the fixture for adhesive application. Vacuum fittings were used to evacuate the chamber during the bonding process. Pressurization of the air cylinders provided mechanical force at the bondline during the adhesive cure cycle.

The rotating fixture design consisted of a strong-back with legs for attachment to the trunnions on the bond fixture. The height of the legs was designed to clear the top portion of the bond fixture during inverting.

Two types of fixtures were designed for lifting the metal shims. The basic fixture designs were the same consisting of a spider support with three vertical lift points. The difference was in the lifting mechanism using either the magnetic contact or the suction-cup types. Subsequent usage indicated that the fixture with the suction-cup design provided a more positive lifting capability.

The handling cart was designed with the versatility of handling and transporting the metal shim in the upright and inverted configurations, as well

as the end rings. Since the cart supported the seal components in the oven during primer cure, the cart was designed to withstand the oven temperature.

The adhesive spreader was a flat steel plate with serrations on one edge. The height of the serrations was made adjustable so that the amount of adhesive applied on the surface can be changed.

A box type oven was designed for curing of the primer. Automatic temperature control was incorporated for maintaining temperatures up to 400°F.

The fixture design for bonding the elastomeric boot to the seal consisted of mechanical ring clamps which applied bond pressure axially on each end of the seal. In addition to the clamps, steel bonding straps were used to apply radial pressure on the adhesive bondline during cure.

G. TEST PLAN

A test program was defined for structural testing of the flexible seals. The program included functional pressure proof and vectoring tests of both seals and destructive test of one seal. The plans for conducting these tests are as follows:

1. Functional Test

a. Pressure Proof Test

Initially, a leak test of the seal will be conducted at 50 psig (3.45×10^5 N/m^2) test pressure. Following this, the test pressure will be increased to a maximum of 850 psig (5.86×10^6 N/m^2). This pressure corresponded to 1.15 times both the maximum expected operating pressure (MEOP) of the motor and the maximum ejection load acting on the seal. At pressure levels of 200, 400, 600, 735, and 850 psig (1.38, 2.76, 4.14, 5.06, and 5.86×10^6 N/m^2), test data will be recorded to determine the seal axial deflection and steel shim stress.

b. Vectoring Test

Vectoring tests up to $\pm 2°$ (.0349 rad) deflection will be performed at various pressure levels. These pressure levels are equivalent to 0, 30, 60, 90, and 115% of the maximum predicted ejection load of one million pounds (4.45×10^6 N). The tests will be conducted in both the pitch and yaw planes of each seal. Test data will be measured so that the following seal performance characteristics can be determined:

(1) Actuation torque vs seal deflection angle

(2) Axial deflection vs ejection load

(3) Pivot point movement during vectoring

(4) Torque variation between ascending and descending deflection angle (hysterises effect)

(5) Null position shift

(6) Torque variation between seals and between the pitch and yaw axis for the same seal

(7) Metal shim hoop stress

2. Destructive Test

In the destructive test phase, a sequence of tests that exceed the functional test requirements will be conducted until the first evidence of seal structural failure (actual or imminent) occurs or leakage is detected.

a. Vectoring Test

The seal will be deflected to $\pm 3.5°$ (.061 rad) vector angle. This maximum deflection angle may be less if limited by the available output force of the hydraulic actuator or by the physical interference between the seal and test fixture.

b. Ejection Load Test

Test pressure will be increased to an equivalent ejection load of 1.5 million lb (6.67×10^6 N) acting on the seal. The increase will be in steps of pressure equivalent to 1.2, 1.3, 1.4, and 1.5 million lb (5.34, 5.79, 6.22, 6.67×10^6 N) ejection load. At each pressure step, the seal will be deflected to $\pm 2°$ (.0349 rad) vector angle.

c. Fatigue Test

Approximately 1000 cycles of flexible seal vectoring will be performed to evaluate the capability of the seal to survive a repetitive stress reversal condition. The duty cycle will consist of 500 cycles of $\pm 1°$ (.0175 rad) followed by 500 cycles of $\pm 2°$ (.0345) vector angle. A sinisoidal command signal will be used with the maximum slew rate that can be obtained with the hydraulic power supply unit. A test pressure of 30 psig (20.7×10^4 N/m^2) will be used throughout the fatigue test.

d. Pressure Test

In this test, chamber pressure will be increased to 1100 pisg (7.59×10^6 N/m^2), which acts on the external surface of the seal and simultaneously results in 1.5 million lb (6.67×10^6 N) ejection load acting axially on the seal. Pressure will be held at 200, 400, 600, and 880 psig (1.38, 2.76, 4.14, and 6.06×10^6 N/m^2) while seal axial deflection data are recorded. The pressure at 1100 psig (7.59×10^6 N/m^2) will be held for two minutes to monitor for leakage followed by venting of the chamber to atmospheric pressure.

At the end of destructive test, the condition of the seal will be documented. Photographs will be taken to document all failure conditions. If failure of the seal occurs, the mode of failure will be determined.

Before and after each phase of functional and destructive testing, seal flange-to-flange parallelism and concentricity measurements will be taken.

Comparison of test data will be made to evaluate the contribution of actuation torque with the elastomeric boot installed in place. One seal will be functionally tested without the elastomeric boot, while the second seal will be functionally and destructively tested with the boot in place.

H. TEST FIXTURE DESIGN

A fixture was designed to meet the requirements for functional and destructive testing of the flexible seal. Basic design criteria for the fixture were: (1) subject the seal to designed load conditions, (2) preclude its restraining or guiding movement of the seal under applied loading conditions, (3) minimum fabrication cost, and (4) adaptable for testing of flexible seals designed for nozzles having throat diameters over the range of 71.0 to 90.0 in. (1.8 to 2.28 m).

The primary load conditions that the fixture must simulate were: chamber pressure acting on the seal external surface, nozzle ejection load, and nozzle rotation (vectoring). Because a fixture cannot be designed to simulate all of these loads simultaneously without constrainting the pivot point location, a fixture design concept was selected that subjected the seal to a combination of loads in the pressure and vector tests. During pressure test, the nozzle ejection load and the external pressure load were simulated. In the vectoring test, the nozzle ejection load and shear stress in the rubber pads were produced, while the external pressure was substantially reduced. This difference in external pressure was found from stress analysis to have only slight effect on the rubber shear stress.

The selected fixture design is shown in Figure 23. Major components of the fixture consisted of: (1) tank structure, (2) piston, (3) seal support structure, and (4) actuator support structure. On the top of the tank structure, provisions were included for assembly of the seal aft ring. Two actuator

attachment lugs, 90° (1.57 rad) apart, were on the external surface of the tank. The bottom part of the tank structure was the cylinder wall which mated with the piston. The piston had O-rings for pressure seal against the cylindrical wall. In the pressure test configuration, the piston was moved upward and attached to the seal support structure (see Figure 23). Provisions were incorporated into the seal support structure for assembly of the seal forward ring on the bottom flange and the actuator support structure on the top surface. The interface was designed so that the actuator support structure can be positioned in either the pitch or yaw plane with respect to the seal support structure.

A key element of the test fixture design effort was verification of its structural adequacy. A structural analysis was completed which indicated that a minimum safety factor of 1.5 existed at a pressure level of 1125 psi (7.75 x 10^6 N/m^2) (1.5 x motor MEOP) for both the pressure and vectoring configurations. This analysis was predicated on using T-1 steel with a minimum yield strength of 90,000 psi (620 x 10^6 N/m^2) in the rolled and welded construction.

Detailed fabrication drawing T-1023498 was prepared of the test fixture design.

IV. TASK II - LABORATORY SUPPORT SERVICES

A laboratory investigation program was performed in support of the flexible seal design and fabrication effort. The objectives of this program were: (1) to define the elastomer and laminate physical properties and the effect of various environmental and loading conditions on these properties, and (2) to evaluate processing and inspection techniques proposed for seal fabrication and to determine the effect of processing variables on seal performance.

A. MATERIAL PROPERTIES

1. Rubber Pad

The natural rubber, Gen-Shear 44125, which was selected as the rubber pad material for this program was extensively evaluated in an Aerojet

Independent Research and Development Program, Reference 7, prior to the initiation of this program. The material properties determined by specimen tests conducted under this IR&D program included bulk modulus; tensile, shear, and compressive properties; and creep characteristics.

a. Bulk Modulus

In determining bulk modulus, three rubber specimens, 0.375 x 0.50 x 7 in. (.0095 x .0127 x .178 m) were tested by immersing in silicone oil and pressurizing in a pressure vessel up to 1,000 psi (6.9×10^6 N/m^2). The change in specimen length with pressure was measured with a linear variable differential transducer (LVDT) and indicated a linear variation. From the measured data, the bulk modulus was calculated to be 296,700, 296,400, and 269,250 psi (2.045, 2.043 and 1.855×10^9 N/m^2) for an average modulus of 287,000 psi (1.98×10^9 N/m^2).

b. Tensile Properties

Twelve tensile specimens with the configuration shown in Figure 24 were tested to characterize the tensile property. Rubber thicknesses for the specimens were as follows:

No. of Specimens	Rubber Thickness, in. (m)	Type	Shape Factor(1)
6	0.18 (.00457)	Bonded	2.2
3	0.10 (.00254)	Bonded	4.0
3	0.05 (.00127)	Molded	8.0

(1) Shape factor for the specimen configuration is defined as $S = D/4t$, where: D = diameter and t = rubber thickness.

In the bonded specimens, Chemlok 304 epoxy adhesive was used for bonding the rubber to the steel end plates. Molded specimens were fabricated by injecting uncured rubber between the end plates and then vulcanizing in place.

Each specimen was tested to 400% strain at two different cross-head speeds of the testing machine, 0.5 and 5.0 in./min (0.212 and 2.12 x 10^{-3} m/S), resulting in two different strain rates on the specimen. Subsequently, each specimen was tested to failure using the 5.0 in./min (2.12 x 10^{-3} m/S cross-head speed. The stress-strain relationship was obtained for each specimen and is shown in Figures 25, 26, and 27. The results indicated that for a higher strain rate on the specimen, the shear strain was increased at the same stress level. Comparison of the data for the three specimen sizes showed that the ultimate tensile strength and elongation is higher for larger shape factors.

Examination of the specimens that failed in the tension test revealed internal failure of the rubber in the form of numerous small pores (spherical indentation) as shown in Figure 28. This phenomena has been observed in previous tests by GT&R. An investigation was conducted to correlate the tensile stress level at which internal failure initiated. A series of five tensile specimens with 0.18 in. (.00457 m) rubber was loaded to a predetermined stress level and subsequently dissected for visual inspection. Internal failure was observed to start between 88 and 97 psi (6.07 and 6.7 x 10^5 N/m^2) tensile stress. This agrees with the point on the stress-strain curve where a sudden change in slope occurs (Figure 25). Since the occurrence of internal failure can substantially reduce the shear capability in the rubber, tensile loading of the rubber is best minimized in flexible seal design.

c. Shear Properties

Quadruple lap shear specimens as shown in Figure 29 were used to determine the shear properties of the rubber. Three specimens with 0.18 0.10, and 0.06 in. (.00457, .00254, and .00152 m) rubber thickness were prepared. The specimens with the 0.10 and 0.18 in. (.00254 and .00457 m) rubber thicknesses have the rubber pads bonded to the steel plates with Chemlok 305 adhesive, while the specimen with the 0.06 in. (.00152 m) rubber was fabricated by injecting uncured rubber between the steel plates and then vulcanizing in place.

The specimens were tested at different strain rates and with various compressive pressure levels to determine their effect on the shear properties. Each specimen was enclosed in a pressure vessel and pressurized to 1000 psi (6.9×10^6 N/m^2) simultaneously with the application of 200% shear strain. Results in Table VII indicated no significant difference in shear stress and modulus even with an order of magnitude difference in strain rate and with compressive pressure variation from 0 to 1000 psi (6.9×10^6 N/m^2). A plot of shear stress-vs-strain variation for the three specimens is shown in Figure 30. A low shear stress at failure for the specimen with the 0.18 in. (.00457 m) rubber resulted from excessive bond voids in the specimen. For all three specimens, the shear modulus was relatively constant [25 to 27 psi (1.72 to 1.86 x 10^5 N/m^2)] up to 400% strain.

d. Compressive Properties

Three specimens were prepared and tested to characterize the compressive property of the rubber. The configuration of the specimen is identical to the tensile specimen as shown in Figure 24. All specimens have the rubber pads bonded to end plates with Chemlok 305 adhesive. Variations of specimen diameter and rubber thickness were incorporated to produce three different shape factors:

Diameter, in. (m)	Rubber Thickness, in. (m)	Shape Factor*
1.60 (.0406)	0.19 (.00482)	2.1
1.60 (.0406)	0.10 (.00254)	4.0
2.98 (.0756)	0.10 (.00254)	7.5

*Shape factor is given as: $S = \frac{D}{4t}$ where D = diameter and t = rubber thickness

The 1.60 in. (.0406) dia specimens were tested in compression to result in approximately 4500 psi (31×10^6 N/m^2) stress, while the 2.98 in. (.0756 m) dia specimen was loaded to 1200 psi (8.28×10^6 N/m^2) which was the maximum capacity of the testing machine. A definition of the stress-strain

relationship was obtained for each specimen and is shown in Figure 31. As expected, the compressive modulus was a variable that increases with applied load. For the same stress level, the compressive modulus value was higher for a larger shape factor.

Correlation of the experimental compressive modulus with analytical results was made. Specimen geometries corresponding to the test specimens were analyzed by the finite element method, Reference 3. Since this method only considers linearity in material properties, effective compressive moduli of 843 and 2,543 psi (5.81 and 17.5 x 10^6 N/m^2) were obtained for shape factors of 2.1 and 4.0, respectively. The analytical values agreed closely with the experimental results when compared with the initial slope of the stress-vs-strain curve as shown in Figure 31.

e. Creep Characteristics

Six specimens were tested to determine the creep characteristics of rubber for shape factors of 2.0 and 7.5. Each specimen had 0.10 in. rubber (.00254 m) which was bonded to metal end plates with Chemlok 305 adhesive. Three each of the specimens were 1.60 and 3.00-in.-dia (.0406 and .0762 m-dia).

Each specimen was subjected to the following tensile stress:

Specimen	Diameter, in. (m)	Shape Factor	Tensile Stress, psi (N/m^2 x 10^{-3})
1	1.60 (.0406)	4.0	30 (207)
2	1.60 (.0406)	4.0	50 (345)
3	1.60 (.0406)	4.0	80 (552)
4	3.00 (.0762)	7.5	30 (207)
5	3.00 (.0762)	7.5	50 (345)
6	3.00 (.0762)	7.5	65 (448)

A record was made of the strain at the following time intervals after load application: 1 min, 6 min, 18 min, 36 min. 1 hr, 1 day,

3 days, 1 week, and 1 month. The static load was then removed and the change in length was recorded at the following time intervals after load removal: 1 min, 6 min, 18 min, 36 min, 1 hr, 4 hr, 1 day and 1 week.

The results (strain-vs-time) for specimens 1 through 5 are shown in Figure 32. The data, except for specimen 2, showed a continuous increase in strain even up to 1 month duration. Specimen 2 indicated a constant strain for the full test duration. Generally, the magnitude of creep was higher with a higher tensile stress for the same shape factor and with a lower shape factor for the same tensile stress. The data for specimen 6 were not usable since the high tensile load resulted in internal failure of the specimen and caused 160% strain within 1 month duration.

The creep recovery in the specimen occurred instantaneously after removal of the tensile load. Residual creep during the time interval from 1 minute to 1 week after load was removed was less than 1%.

f. Poisson's Ratio

Poisson's ratio of the rubber was calculated by the equation:

$$\nu = \frac{3K - 2G}{6G + 2G}$$

where: K = rubber bulk modulus, psi (N/m^2)
G = rubber shear modulus, psi (N/m^2)

The bulk modulus and shear modulus values are those determined from specimen tests.

g. Aging and Humidity Tests

The effects of aging and humidity on elastomer and composite properties were initially evaluated by five tensile and three quadruple lap shear test specimens. Each tensile specimen was 1.6 in. (.0406 m) dia (Figure 24) with

a 0.10 in. (.00254 m) rubber layer bonded between the steel end plates. Quadruple lap shear specimens have 4 x 4 x 0.10 in. (.102 x .102 x .00254 m) rubber pads bonded at each end of the steel plates. Two shear specimens and one tensile specimen were coated on the exposed rubber edges to evaluate a candidate protective coating material, Black-Out, a R. T. Vanderbilt product.

The specimens were subjected to environmental exposures in accordance with the schedule shown in Table VIII. Aging exposure was conducted at 80°F (300°K) temperature and ambient humidity, while humidity exposure was in an oven of 90% relative humidity and 110°F (317°K) temperature.

After three months exposure, the protective coating on the coated specimens was extensively cracked. Separation of the coating from the rubber also occurred. Therefore, the three specimens with the protective coating were removed from further tests.

At the end of each specified exposure duration, the remaining specimens were tested to determine the change in properties. Tensile specimens were tested to a stress level of 50 psi (3.45×10^5 N/m^2) while shear specimens were tested to a strain level of 300%. The test results are summarized in Table IX. A continual increase in shear modulus and decrease in tensile strain was indicated with increase in exposure time. Both of these effects are indications of increased stiffness in the rubber. At the end of nine months exposure to the high humidity environment, an increase in shear modulus from 24 to 30 psi (1.65 to 2.07×10^5 N/m^2) was noted. However, only a slight increase in modulus was observed for specimens exposed to the milder aging environment. Specimens with an additional month's humidity exposure after the nine months aging exposure showed a significant increase in shear modulus and decrease in tensile strain. This indicated that the stiffness of the rubber, as expected, was increased more rapidly under the severe humidity exposure than the ambient aging conditions.

After exposure to all the specified conditions, each specimen was tested to failure. The properties at failure are shown in Table IX. Comparison with test data of similar specimens not subjected to these environmental

exposures, Figure 33, indicated that the shear modulus was higher and the shear strength was lower. The significant difference in the data confirmed the necessity for protecting the rubber layer of the flexible seal against these types of environmental exposure.

In order to qualify a material in time for use in the environmental protection of the rubber in the flexible seal, an accelerated aging program was preformed to evaluate two candidates prior to final selection. These candidate materials were Hypalon, a DuPont synthetic rubber product, and chlorobutyl rubber sheet. In addition to their excellent protective qualities, these materials have the desired properties of low modulus and high elongation. Hypalon was applied as a surface coating, while chlorobutyl rubber sheet was bonded to the seal surface.

Twelve specimens, 1.00 x 3.75 x 0.10-in.-thick (.0254 x .0952 x .00254 m thick) rubber, with the following surface preparation and protective materials were prepared:

No. of Specimens	Surface Preparation	Protective Material
2	Untreated	None
2	Chlorinated	None
2		*Chlorobutyl rubber sheet (two surfaces)
2		*Chlorobutyl rubber sheet (all surfaces)
2		Three brush coats of Hypalon
2	Chlorinated	Six brush coats of Hypalon

*0.02 in. (5.08 x 10^{-4} m) chlorobutyl rubber sheet bonded to specimen with PR-1221 adhesive.

The specimens were mounted for test in accordance with ASTM-D518, Procedure B. The test method for accelerated ozone cracking of vulcanized rubber was in accordance with ASTM-D-1149 using the counter-current absorption column for measuring ozone concentration. The specimens were subjected to an exposure of

158°F (343°K) for 70 hours and then 7 days exposure to an ozone concentration of 50 parts per hundred million parts of air at a temperature of 140°F (333°K).

At the end of exposure time, extensive surface cracks were apparent on the specimens without a protective material, Figure 34. Specimens that were coated with either Hypalon or chlorobutyl rubber sheet showed no surface deterioration. Subsequent dissection of the specimens and examination under a seven-power magnification revealed no degradation of the underlying rubber surfaces. These results indicated that either of the candidate materials can provide adequate protection under the test conditions of aging and ozone exposure. For surface protection of the flexible seal, Hypalon was selected because of its ease of application and good adhesion to both rubber and steel surfaces.

2. Metal Shim

Normalized AISI 4130 steel was the material selected for the metal shims and end rings of the flexible seal. This steel has a 70,000 psi (4.83×10^8 N/m^2) yield strength and 29×10^6 psi (2.0×10^{11} N/m^2) tensile modulus. All properties necessary to support the flexible seal analysis are characterized through the extensive use of this material in the industry.

Because of the size and flexibility of the steel shim, dimensional stability of this material using the selected shim fabrication method must be verified. Verification of this characteristics was made in the Process Demonstration Task as discussed in Section III.B.3.

3. Elastomeric Boot

Gen-Gard V-45, an acrylonitrile-butadiene rubber with silica fiber fillers, was selected as the elastomeric boot material. This material has a minimum tensile strength of 2000 psi (1.38×10^7 N/m^2) and an elongation of 200%. Elevated temperature properties for the thermal response prediction of the boot were available through its used as motor case internal insulation, as well as in similar applications for the thermal protection of flexible seals.

B. ASSEMBLY PROCESSES

Laboratory investigations to establish processing materials and procedures for the assembly of the flexible seal were performed. Adhesive systems for the rubber pad bond and metal-to-rubber bonds were evaluated. Each step of the bonding procedure; i.e., surface preparation, adhesive application and cure cycle, was demonstrated so that a technique that resulted in minimum bond voids and maximum shear strength can be selected. Nondestructive test methods for the detection of bond defects and internal defects in the rubber were developed. The selected processing and inspection procedures were incorporated into the fabrication of a full size process demonstration ring to checkout the entire operational procedure and equipment prior to initiation of flexible seal fabrication.

1. Adhesive Evaluation

a. Metal-to-Rubber Bond

Several candidate adhesive systems were evaluated by the rubber fabricator, GT&R, for use in the bond between the rubber pads and steel shims. Results from lap shear specimen tests indicated that only Chemlok 304 and 305 adhesives (Hughson Chemical Products) consistently resulted in 100% cohesive failure in the rubber pad that had a chlorination treatment of the rubber surfaces. Both of these are two-part epoxy resin, structural adhesive systems, which cure at room temperature. The Chemlok 305 adhesive with a lower viscosity was selected for its ease of application and uniformity in wetting of the surface. Subsequent lap shear specimen tests demonstrated that the ultimate shear strength of the adhesive was in excess of 2000 psi (1.38×10^7 N/m^2). This value is substantially higher than the ultimate shear strength of the rubber and meets the seal design requirements.

b. Rubber Skive Joint Bond

To preclude premature failure, the adhesive for the rubber skive joint bond must not only have good bond strength, but also have elongation

and durometer hardness similar to Gen-Shear 44125 rubber. Several candidate adhesive systems were comparatively evaluated. These included:

Uralane 5735 (Furane Plastics, Inc.)
Uralane 8309 (Furane Plastics, Inc.)
EC-1239, Class B (3M Company)
Scotch-Grip 1300L (3M Company)
Bostik 7074 and Boscodur 5 (United Shoe Manufacturing Co.)

Quadruple lap shear specimens, as shown in Figure 35, each with four 0.30 x 2.0 x 2.0 (.0076 x .051 x .051 m) rubber pads, were prepared for evaluation. The rubber pad of each specimen contained 45° skive joints oriented parallel and perpendicular to the direction of force. The skive joints in the rubber pad were bonded with the candidate adhesives and then the pads were bonded to the steel plates with Chemlok 305 adhesive to form the specimen.

The specimen test data, Figure 36, indicated that Uralane 5735, Scotch-Grip 1300L, and Bostik 7074 adhesives resulted in the highest ultimate strength. Examination of the failure plane revealed that the physical characteristics of Uralane 5735 and Scotch-Grip 1300L adhesives were nearly similar to the Gen-Shear 44125 rubber. These specimens have no separation at the skive joint. Prior to final selection, two additional quadruple lap shear specimens were tested to confirm the reproducibility in shear characteristics of the Uralane 5735 and Scotch-Grip 1300L adhesive systems. Examination of the specimen failure plane showed, Figure 37, that the skive joint with Uralane 5735 adhesive bond was intact while substantial separation of the Scotch-Grip 1300L adhesive joint occurred. Uralane 5735 adhesive was therefore selected for use in the rubber skive joint bond of the seal.

2. Bonding Process Evaluation

a. Surface Preparation

Since the use of masking materials is a necessity in seal processing, the degradation of bond strength on steel surfaces that have been in

contact with these materials must be evaluated. In this evaluation, steel sheets were initially grit blasted and the surface of sets of two sheets were prepared as indicated in Table X. Each set of two prepared steel sheets was bonded with Chemlok 305 adhesive to form test panels in accordance with ASTM D1002. Three specimens were machined from each panel and tested to determine the bond strength. The test results showed that the bond strength of primed steel panels, in all cases, was higher than bare steel panels. Bond surface in contact with either peel coat or teflon tape, however, did not significantly degrade the bond strength. These materials were acceptable for masking of component parts and fixtures during seal processing.

Priming of the steel bond surfaces was desirable not only to attain a higher bond strength as indicated from specimen tests but also to protect the components from corrosion in the interim of seal processing. FM-47 primer was selected for the preparation of the steel component bonding surfaces using the following procedure:

(1) Abrade the surface with 100 grit zirconite abrasive to remove all traces of primer, rust, and foreign materials.

(2) Clean the abraded surface with trichloroethane solvent and rinse with methyl-ethyl ketone solvent.

(3) Apply FM-47 primer and cure at 325 $\pm$ 25°F (436 $\pm$ 14°K) for two to four hours.

Evaluation test performed by the rubber supplier, GT&R, indicated that the shear strength was substantially improved and failure occurred cohesively in the rubber when the rubber surface was treated with a chlorination solution. As part of the processing procedure in seal assembly, each rubber pad was prepared for bonding by treatment in a chlorination solution containing the following (by volume): 100 parts of distilled water, 3 parts of 5.25% sodium hypochlorite solution, and 0.5 parts of concentrated hydrochloric acid. Each rubber pad was scrubbed with hexane solvent and then submerged into the solution for five minutes. Subsequently, the pad was rinsed in distilled water and dried prior to bonding.

b. Adhesive Application

Material, equipment, and processing techniques were verified to ensure that the application of adhesive during flexible seal assembly will meet the specified requirements. Procedures for mixing, spreading, and curing of adhesive were evaluated.

The technique of adhesive mixing with the Semco mixer was demonstrated. A batch of Chemlok 305 adhesive consisting of 2000 grams each of parts -1 and -2, which is the amount required for each bonding operation of the seal, was mixed. The adhesive was dispensed into four trays, each with a varying duration of mixing. Lap shear test panels were prepared from adhesive mixed for the various durations. Specimen test results indicated that the adhesive shear strength increased from 1166 to 2813 psi (8.04 to 19.4 x 10^6 N/m^2) as a result of increasing the duration from 10 to 20 strokes of the mixer. A mixing duration equivalent to a minimum of 20 strokes of the mixer was specified for seal processing.

No evidence of exothermic reaction that would shorten the working life of the adhesive was apparent after the adhesive was dispensed into trays. The adhesive remained workable in excess of 1.5 hours after mixing. This working life is normally adequate for each bonding operation of the seal.

A fixture, Figure 38, was used to evaluate the effects of spreading technique and bonding pressure on the resultant bondline characteristics. The bond surfaces were inclined at an angle of 40 degrees (.698 rad) from the centerline to simulate the flexible seal. Prior to applying adhesive, the rubber and steel bonding surfaces were coated with a release agent so that the adhesive layer could be removed for detailed examination. After adhesive was applied, a 25 to 28 in. Hg (8.44 to 9.45 x 10^4 N/m^2) vacuum was drawn in the vacuum chamber prior to mating of the bonding surfaces. During the adhesive cure cycle, bond pressure was applied at the bond interface by means of external load.

Four sets, each containing two specimens, were processed for evaluation. From the results of this evaluation, the selected adhesive application procedure was: (1) spreading of the adhesive with a serrated trowel, (2) mating of the bond surfaces under a minimum of 25 in. Hg (8.44×10^4 N/m^2) vacuum, and (3) curing the adhesive with 5 psi (3.45×10^4 N/m^2) bondline pressure and zero vacuum pressure.

c. Nondestructive Test Method

Nondestructive test techniques were evaluated for the detection of defects in the rubber pads and bond voids at the rubber-to-steel adhesive bonds.

Generally, two types of defects occur in the rubber pad, voids or delaminations and inclusions. A pulse-echo ultrasonic (C scan) method was found to be effective in detecting voids and delaminations. In this method, each rubber pad was immersed in a fotoflow solution, removed and drained, and placed in a tray of distilled water. The ultrasonic signal is transmitted through the pad by a transducer. Any defects indicated by a change in signal is automatically recorded in a full scale map of the pad as the surface of the pad is scanned. The procedure for this inspection method is described in Appendix C. Foreign inclusions in rubber pads were detected by conventional radiographic techniques.

In the detection of bondline defects, ultrasonic and laser-speckle inspection techniques were the promising methods. The laser-speckle method was a candidate for detection of bond defects from the rubber surface. In this method, the surface of the bonded elastomer is illuminated with a laser beam, which produces a distinct speckle pattern on the surface. When the surface is deformed slightly with a probe, the pattern shifts noticeably in the area around the probe. When an unbonded area exists below the probe, the speckle pattern shift is greater. The accuracy and sensitivity of this method are related to the thickness and hardness of the elastomer. Because of the low modulus and 0.3 in. (.076 m) thickness in the seal rubber pad, the results obtained could not be readily interpreted.

A conventional contact pulse-echo ultrasonic technique was found to provide a high degree of accuracy in the detection of bond voids from both the rubber pad and the metal shim surfaces. In this method, distilled water was used to maintain acoustic coupling between the face of the transducer and the contact surface. A procedure for this inspection technique was prepared and is described in Appendix C. This technique was selected for use in the inspection of bond defects during seal processing.

3. Process Demonstration Ring

Two full scale steel shims were bonded to a prototype rubber layer to verify the process procedures and tooling intended for the fabrication of the flexible seal. Surface preparation, adhesive system, and bonding procedure duplicated those intended for seal fabrication.

Eight rubber pads were chlorinated and positioned on the seal forward flange in the assembly bond fixture. The pads were bonded with Uralane 5735 adhesive to form a circular rubber layer. Mating of the pads was found to be satisfactory without machining of the interface edges. The resultant mismatch was within acceptance limits.

A steel shim was bonded to the rubber layer with Chemlok 305 adhesive. This shim was mechanically attached to the seal aft flange on the assembly bond fixture as shown in Figure 39 to simulate conditions in the initial bonding sequence of the actual seal fabrication. Subsequently, a steel shim was bonded to the other face of the rubber layer duplicating the entire bonding process procedure.

After completion of each bond, nondestructive tests were performed to determine the bond integrity. Using the ultrasonic method, a 0.5 in. (.0127 m) unbonded area was detected by inspection through the rubber layer. Subsequent dissection of the ring confirmed the size and location of the defect. Inspection for voids in the second bondline also used an ultrasonic method. No indication of bond defects was obtained in inspection of this bond.

Visual inspection of the completed process demonstration ring revealed a 90° (1.57 rad) arc of mismatch between the rubber layer and the steel shims. The mismatch resulted from displacement of the rubber layer by inadvertent contact with the bond fixture during the bonding process. Modifications of the assembly tooling were made, as discussed in Section IV.B, to prevent recurrence of this problem and to provide more positive alignment of the parts during bonding.

Ten lap shear specimens were machined from the process demonstration ring and tested to determine the adhesive bond strength and rubber characteristics. Three specimens have axial skive joints. Each specimen was 2 in. (.051 m) wide and was machined from the cross-section of the ring as shown in Figure 40. The specimen deformation during test is shown in Figure 41. Six specimens failed in a shear plane through the rubber with ultimate shear stress and strain levels in excess of 600 psi and 700%, respectively, Table XI. However, four specimens which were from the same quadrant of the ring exhibited low ultimate shear properties. Visual inspection of these specimens revealed adhesive failure at the interface between the steel and the FM-47 primer. The cause of this was apparently from contamination of the surface by use of impure solvent combined with insufficient covering with FM-47 primer. Procedures for processing of the flexible seal were changed to incorporate the use of reagent grade methyl-ethyl-ketone solvent and the application of two spray coats of FM-47 primer with an intermediate drying cycle between coats on all steel components.

V. TASK III - FABRICATION

A. FLEXIBLE SEALS

1. Metal Parts

A total of ten metal shims and two sets of end rings were fabricated by Oakland Machine Works. In addition to the eight metal shims required for the two flexible seals, two shims were used in fabrication of the process demonstration ring of Task II.

All of the metal components were machined from rolled-ring forgings of AISI 4130 steel. The steel forgings were heat treated to a minimum yield strength of 70,000 psi (4.83×10^8 N/m^2) at 0.2% offset.

Because the components were comparatively flexible, dimensional inspection was performed while the part was held rigidly on the turning lathe after completion of final machining. In the case of the metal shim, the part was completely machined except for a holding tab, which was parted after completion of inspection. The completed metal shim is shown in Figure 42. Dimensional inspection data indicated no discrepancies from the designed tolerance specified in the engineering drawing.

Prior to acceptance, each completed part was inspected by the fabricator using the magnetic particle method. No surface defects were observed and all the parts were accepted for use in fabrication of the seals.

2. Rubber Pads

Fabrication of rubber pads was performed by General Tire and Rubber Company at the Wabash, Indiana facilities. Prior to initiation of production, two tasks were completed by the fabricator in support of the fabrication effort. These tasks were to establish the curing procedure and the quality control acceptance criteria, and to design and fabricate the production mold.

Two lots of Gen-Shear 44125 rubber were characterized to establish the optimum cure time for fabrication of the 0.3 in. (.0076 m) thick rubber pads. In determining the optimum cure time, Rheometer tests were initially used to obtain the degree of cure with time for a selected cure temperature of 280°F (411°K). Full cure was found to develop between 60 to 90 minutes for the Lot 21 material and 45 to 70 minutes for the Lot 23 material. Subsequently, 4 x 4 x 0.3 in. (.102 x .102 x .0076 m) slabs of rubber were cured at these durations and tested in compression in accordance with the procedure specified in Table XII. Compressive load at 25% strain versus cure time was plotted as shown in Figure 43. Optimum cure time which corresponds to maximum load was 70 and 60 minutes for material Lots 21 and 23, respectively.

The test slabs cured at the optimum duration were tested to obtain compression-deflection curves for each lot of material. Acceptance limits, Figure 44, were established which are ±10% of the average values for the two lots of materials tested. When compression test results of the quality control specimen which were cured along with the seal rubber pads, are within these limits, the seal pads are considered correctly cured and acceptable.

Production of the rubber pads used a two-cavity mold, which consists of three separate plates. The bottom plate has cavities for molding two pads and the 4 x 4 in. (.102 x .102 m) quality control specimen. The center plate has 24 sprues for transferring the raw material from the pot on top of the center plate into the cavities. The center plate is rigidly attached to the bottom plate by bolts. The top plate has a ram to force the uncured stock from the pot through the sprues. During the molding operations, the three plates are positioned between heated platens of a hydraulic press which exerts the molding pressure.

Initially, ten rubber pads were fabricated to checkout the processing procedure and to determine dimensional conformance of the cured part. Subsurface blisters were evident in each of these pads. Most of the blisters were 0.06 to 0.12 in. (.0015 to .0030 m) with an occassional one as large as 0.5 in. (.0127 m). The blisters were caused by the swirling action of the raw stock being injected into the cavities which resulted in air entrapment. The mold was reworked to remedy this problem. Pressure seals were incorporated so that a 26-in. Hg (8.78×10^4 N/m^2) vacuum pressure can be applied to the mold cavities during cure. Some of the sprues were closed to change the swirl pattern of the material entering the cavities. The ram pressure was increased to 900 psi (6.21×10^6 N/m^2). Incorporation of these changes greatly reduced the frequency of occurrence of the blisters.

Prior to acceptance of the rubber pads for use in the flexible seal, each individual pad was subjected to ultrasonic and radiographic inspections. Internal defects, such as voids, inclusion, and undispersed carbon black that may

adversely affect the performance of the seal were the criteria for rejection. Twenty-six pads were found to have undispersed carbon black and voids greater than 0.20 in. (.0051 m). These pads were rejected and were used for the process demonstration task only. Replacements were fabricated to obtain sufficient pads for the two production seals.

3. Elastomeric Boot

The fabrication of the elastomeric boot consisted of hand layup and autoclave cure of Gen-Gard V-45 rubber on quarter section mandrels. The cured quarter sections were spliced with a layup of a cushion of uncured V-45 on the splicing surfaces. The parts were positioned in a splicing jig, and the splice was cured at 300°F (422°K) temperature and 500 psig (3.45×10^6 N/m^2) pressure.

Tests were performed by the fabricator, Holz Rubber Company, to evaluate the mechanical properties of V-45 material spliced by this procedure. Three specimens of V-45 incorporating the splice joints and three specimens without joints were prepared and tested in accordance with Federal Standard 601, Methods 4111 and 4121, Die #3 to determine the tensile properties. Minimum tensile strength and elongation of 1275 psi (8.79×10^6 N/m^2) and 500%, respectively, were obtained for specimens with the splice joint, as shown in Table XIII. These values met the design requirements of the elastomeric boot with a high margin of safety.

The completed boot was inspected dimensionally and radiographically prior to acceptance. Dimensional inspection of both boots revealed that all dimensions were within designed tolerances. Radiographic inspection of the boots indicated that some delaminations existed at the ends of the boot and at the S-section. Since these delaminations were generally in a plane parallel to the surface, failure of the boot resulting from them is unlikely. Because of the difficulty in repairing the defects, only the defects that may impair the performance of the boot were repaired. In the second boot, five void areas were repaired by: (1) removing the void by grinding, (2) filling the area with uncured V-45 rubber, and (3) locally vulcanizing the rubber in the repair area.

4. Seal Assembly

In assembly of the flexible seal, each component was successively bonded to the other starting at the aft end ring. The aft end ring was attached to the top portion of the assembly bond fixture by the shafts of the air cylinder. The forward end ring was positioned on the base of the fixture. A steel shim was placed on the forward ring as shown in Figure 45 to serve as a guide for the bonding of the rubber pads. Eight pads, previously prepared with the chlorination treatment, were positioned on the steel shim and bonded at the skive joint with the Uralane 5738 urethane resin. After cure, each skive joint was visually inspected to determine the mismatch at the joint and the voids on the surface. All voids were repaired by filling with the urethane resin.

Subsequently, Chemlok 305 epoxy adhesive was applied on the mating surface of the aft end ring and the rubber layer. A typical procedure for applying and spreading adhesive on the surface of the component that rests on the base of the fixture is depicted in Figures 46 and 47. Similarly, the applying and spreading of adhesive on the mating surface of the component that is attached to the top half of the fixture is shown in Figures 48 and 49. A serrated spreader was used to regulate the amount of adhesive to be deposited on the surface. After completion of adhesive application, the top half of the bond fixture was inverted and mated with the bottom half as shown in Figures 50, 51, and 52. Finally, the fixture was positioned for adhesive cure under vacuum pressure and mechanical load, Figure 53.

Visual and ultrasonic inspection of each bondline was performed after completion of cure. Flat panels that were bonded with each adhesive bond cycle were machined into lap shear specimens and tested to evaluate the adhesive curing characteristics. Adhesive cure characteristics and ultrasonic inspection results for both seals are summarized in Table XIV.

Some discrepancies from specified requirements were noted in the first seal to be fabricated. A mismatch of 0.080 in. (0.002 m) occurred at the inside diameter between the seal upper flange and the first rubber layer. This

problem was remedied by rework of the assembly fixture to provide for more accurate alignment in the centering of the parts during bonding. Ultrasonic inspection of the first bond indicated seven unbonded areas, each approximately 0.5 in. (.0127 m) dia and located 0.5 to 1.0 in. (.0127 to .0254 m) from the inside diameter edge. This condition resulted from inadequate filling of the voids due to the rapid release of vacuum pressure. The process procedure was subsequently revised to allow for a slow release of vacuum pressure and to apply a thicker coating of adhesive on the bond surfaces. With the incorporation of the revised procedures, only one other unbonded area, 0.5 in. (.0127 m) by 2.0 in. (.051 m) was observed from ultrasonic inspection on the remaining bonds. This unbonded area, which was at the edge of the rubber layer, was repaired by filling with Chemlok 305 adhesive.

Results of adhesive curing characteristics indicated that the adhesive strengths of bond sequence No. 2 and 3 for seal No. 1 were lower than expected (see Table XIV). Although the lowest bond strength still provided a safety factor greater than 2.0 on the seal design, the lot of Chemlok 305 adhesive with which the low strength was obtained was isolated. This lot of adhesive was removed from further use in seal fabrication.

After completion of the adhesive bond operations, both seals were cleaned by gritblasting to remove extruded adhesive. The completed seal is shown in Figures 54 and 55. Measurements were taken at 10 locations equally spaced around the seal circumference to determine the variation of seal height and concentricity between the end flange rings. The measurements are tabulated in Table XV for both seals. Seal No. 1 had a maximum height variation of 0.085 in. (.00216 m) and a concentricity variation of 0.041 in. (.00104 m), while seal No. 2 had a maximum height variation of 0.005 in. (.000127 m) and a concentricity variation of 0.072 in. (.00183 m). This magnitude of variation can be expected for a seal of this size and will not affect the seal performance.

The elastomeric boot was installed on the seals to complete the flexible seal assembly (Figure 56). The boot was not installed on seal No. 2

until after completion of functional tests conducted under Task IV to facilitate visual inspection of the seal after test. On seal No. 1, however, the boot was installed prior to the start of testing to determine comparatively the effects of the boot on seal performance. The processing procedure for the installation of the boot was as follows:

a. Clean bare steel surfaces by light sandblasting and wipe with MEK solvent.

b. Prime steel surfaces with GACO N-11 primer except rubber surfaces and areas for bonding to the boot.

c. Apply a minimum of two coats of GACO Flexmarine (Hypalon), material on the O.D. and I.D. surfaces except bonding areas.

d. Install and bond the elastomer boot to both ends of the flexible seal with adhesive.

e. Fill the cavity between the boot and the seal with a low viscosity silicone grease.

B. ASSEMBLY TOOLING

Five principal tool items were fabricated for use in the assembly processing of the flexible seals. These tools were:

1. Lift and rotate fixture
2. Shim lift fixture
3. Handling cart
4. Boot bonding fixture
5. Vacuum bonding fixture

The largest tool item was the vacuum bonding fixture, which was fabricated by Conseco Division of Whittaker Corporation, San Leandro, California.

All of the tooling performed satisfactory for the intended application except some rework was done on the bonding fixture. Rework on the assembly bonding fixture was made to remedy problems observed during fabrication of the process demonstration ring. This rework included: (a) increase the number of alignment adapters from 4 to 8 and structurally reinforce the adapters, (b) replace the air cylinder extension shafts, (c) provide supports to prevent shifting of the seal end flange during inverting, and (d) incorporate mechanical clamps for sealing of the fixture and reacting the force applied during the adhesive bond cure cycle. The rework was completed prior to the start of seal fabrication.

The shim lift fixture was initially designed using magnetic pads for the lifting force. Because of the high angle on the shim surface, however, the pads have a tendency to slide on the shim surface. To provide a more positive means of holding at the lift points, the fixture was redesigned using the suction-cup concept. Three segments, approximately 14- in. (.355 m) long were machined from the process demonstration ring for this purpose. Vacuum fittings and gaskets were incorporated on each segment to form a surface seal. Vacuum was drawn at the interface between the segment and the shim. This revised fixture performed well in lifting the shim throughout processing.

C. TEST FIXTURE

The seal test fixture was fabricated by Oakland Machine Works using rolled and welded T-1 steel plates. Pressure vessel grade steel in 4.0 in. (.102 m) thickness was used for the tank and base structure of the fixture, while structural grade steel was used for all unpressurized components. All welds were inspected by radiographic and magnetic particle methods. A repair weld was made after a crack was detected on the weld between parts -204 and -205 (see Figure 23).

All mating surfaces were machined to meet the designed dimensions. Because of the close tolerance requirement for sealing between the piston and the cylinder components of the fixture, a trial assembly of these components was performed by the fabricator. The diametral clearance between the piston and

cylinder components was 0.009 to 0.012 in. (2.28 to 3.05 x 10^{-4} m). This clearance was acceptable for the O-ring seal.

During preparation of the test fixture for seal testing, cracks were visually detected on the surface of the welds between the actuation lug and the tank structure and at the cylindrical wall of the tank structure as shown in Figure 57. Longitudinal and transverse cracks were observed on the actuation lug welds. A longitudinal weld crack, Figure 58, was observed in the region of the cylindrical wall where repair welding had been accomplished. None of these weld cracks was indicated on X-ray films from radiographic inspection. Because of the uncertainty on the depth of the weld cracks, the test fixture was returned to the fabricator for further examination and rework.

After the test fixture had been returned to the fabricator a complete radiographic inspection was made of the circumferential weld in which cracks had been visually observed. All detectable weld cracks from both visual and radiographic inspections were removed by grinding. Weld repairs were made in these areas under conditions of stringent control on preheat and welding techniques. Subsequent radiographic inspection indicated excellent penetration of the repair welds and no additional cracks in the weld.

To provide an indication of the stress level within each weld in the test fixture, a stress analysis was conducted using the finite element method. Stress levels for both the high pressure and vectoring conditions were obtained. The results are summarized in Table XVI and indicated a varying stress of 20,282 psi (1.4 x 10^8 N/m^2) occurred at the weld between parts -204 and -205. This stress level is substantitally below the anticipated weld strength of 70,000 psi (4.83 x 10^8 N/m^2).

Dimensional inspection of the test fixture after weld repair indicated that an ovality existed on the inside diameter of part -205. Diameter measurements varied between 108.256 in. to 108.285 in. (2.7497 to 2.7504 m) at the area where the O-ring seals. To eliminate possible interference with the piston, the diameter of the bore was machined to a minimum of 108.268 in. (2.7500 m). Further dimensional tolerance

analysis revealed that the sealing capability of the O-ring was inadequate under the worst tolerance condition. Therefore, O-rings with an increased cross sectional diameter to provide the proper squeeze were used with the reworked fixture.

VI. TASK IV - TESTING

A. TEST SETUP

The flexible seal test program was conducted in the Structural Test Laboratory using the Universal Test Cell and the Instrumentation and Control Center. The seal test fixture was installed in the test cell and the base cylinder of the fixture was leveled and welded to the floor plate of the test cell. A hydraulic jack for lifting and lowering the piston of the test fixture was bolted to the floor plate.

The flexible seal was assembled to the test fixture as depicted in Figure 59. With the seal properly assembled, motor loads on the seal were simulated by pressurizing the fixture with nitrogen gas. A pressurized area of the fixture was selected to provide the required ejection force on the seal. Simultaneously, the same gas pressure acted on the outside diameter of the seal. To obtain the seal behavior that is directly applicable to the expected performance on the 260 in. (6.6 m) motor nozzle, the actuator attachment points on the fixture were located identically to the nozzle design.

1. Proof Pressure Test

For the proof pressure test, the -301 lower platen, or piston, of the test fixture was bolted to the bottom of the -401 upper platen assembly, as shown on the right hand side of Figure 59. In this configuration, the motor loads of ejection force and chamber pressure acting on the seal were both simulated by pressurization of the fixture. A schematic diagram of the gas pressure system for this test is shown in Figure 60.

Instrumentation was installed to determined the shim compressive stress and axial deflection of the seal at various pressure levels. Four biaxial strain gages were placed 90° (1.57 rad) apart on the inner circumference of the middle shim as shown in Figure 61. Strain data were recorded manually using BLH SR-4 strain indicators. Axial deflections of the seal were obtained using dial indicators at 90°(1.57 rad) locations, Figure 62. Reading of the indicators was done remotely utilizing closed circuit television. The equipment for monitoring the instruments and recording the data is shown in Figure 63. Test pressure was measured with two 0-1500 psi pressure transducers. The output from the transducers was continuously recorded on an oscillograph. Control of the test pressure was accomplished manually using a hand valve and the pressure gage for reference, Figure 64.

The test setup for the seal proof pressure test is shown in Figure 65.

2. Vectoring Tests

The test fixture configuration for the seal vectoring test is depicted on the left hand side of Figure 59. In this configuration, the -301 piston was lowered away from the upper platen and the bolt holes were sealed with pipe plugs. To eliminate the possibility of loading the seal in tension in this configuration, the fixture was equipped with three adjustable support arms, which transferred the weight of the upper platen assembly to the tank structure of the fixture and bypassed the seal.

In the vectoring configuration, the increase in pressurized area required that the test pressure be reduced to attain the proper ejection force on the seal. Thus, while ejection force was of the correct magnitude during vectoring test, the chamber pressure on the seal external surface was necessarily low.

An 8 in. (.203 m) dia hydraulic cylinder with servovalve control capability was used to deflect the seal during vectoring test. Operating at 3000 psi (2.07×10^7 N/m^2) hydraulic pressure, the actuator has a 120,000 lb (5.35×10^5 N) force capability and a $\pm$12 in. (.305 m) stroke. A Dennison hydraulic pump having a flow capability of 20 gpm (.00126 m^3/sec) at 3000 psig (2.07×10^7 N/m^2) pressure supplied the actuator. A schematic diagram of the actuation system is depicted in Figure 66.

The desired deflection angle/actuator stroke program was plotted on R-I Controls Type MCR48-1010 graph paper. This paper was placed on the drum of a Model FGE 5048 Data-Trak Programmer (Research Incorporated). The output from the programmer was fed into a Model LC 5131 Servac servo-controller (Research Incorporated), which controlled a Raymond Atchley, Inc., Model 425, 25 gpm servovalve. One of the R-I Controls Model 7101-16 displacement transducers on the actuator was connected to supply feedback signal to the servo-controller.

In addition to strain gages for measurement of shim stresses, other instrumentation was incorporated for the vectoring test. Deflection potentiometers were used to measure the actuator stroke position. Actuation load was measured by a Morehouse-ring load cell, which was integrally assembled to the actuator. Supply and return line pressure and the differential pressure across the hydraulic actuator, as well as gas pressure on the test fixture were measured by Tabor pressure transducers. A tabulation of the type and range of instrumentation used is shown in Table XVII.

To obtain the seal performance characteristics, movement of two selected points on the test fixture was measured. These points are denoted as E and F on Figure 59. Two deflection potentiometers were connected to each point and attached to a fixed bracket on the other end at a predetermined angle as shown in Figure 67. During vectoring, the change in length of each potentiometer was measured and the X and Y coordinates of these points were calculated. From the calculated positions of these two points, the axial and lateral deflection, rotation angle, pivot point location, and rotational torque of the seal were

analyzed by the procedure outlined in Appendix D. This procedure was programmed into the computer for solution.

A photograph of the test setup for conducting the seal vectoring test is shown in Figure 68.

B. TEST PROCEDURE

1. Seal Measurement

Height and lateral measurements of the seal were taken as shown in Figure 69, at specified steps of the test procedure to determine if the free-state configuration of the seal was significantly changed during test. The height measurements were made with a vernier height gage at 45° (.785 rad) intervals, while lateral measurements were taken with a micrometer at four places, 90° (1.57 rad) apart. The initial measurements, which were used as a reference, were made with the seal bolted to the -401 upper platen of the test fixture. After assembly of the seal to the fixture, the setscrews in the three support arms of the fixture were adjusted to obtain a satisfactory match to the referenced height measurements. Subsequently, seal measurements were taken after completion of the proof pressure and vectoring tests and after each phase of the destructive tests.

In addition, the inside diameters of the seal at locations that corresponded to the above lateral measurements were measured before and after completion of all the tests to verify the free-state configuration of the seal.

2. Leak Test

Leak test on the seal was conducted prior to functional test and after each step of pressure and vectoring tests. Prior to the start of pressure test, a mixture of nitrogen and helium gas was used to pressurize the test fixture to 100 psig (6.9×10^5 N/m^2). After holding at this pressure for 2 min. the pressure was reduced to 30 psig (2.07×10^5 N/m^2). At this pressure, a CEC Model 24-120A Helium Leak Detector was used to inspect the inside diameter of the seal for

leakage. In both pressure and vectoring test sequences, leak tests were performed using a helium leak detector.

3. Functional Test

Functional tests were performed on both flexible seals, Seal SN 01 with the elastomer boot in place and Seal S/N 02 without the boot.

a. Pressure Proof Test

Following a satisfactory leak test, the pressure in the fixture was incrementally increased to 200, 400, 600, 735, and 850 psig (1.38, 2.76, 4.14, 5.06, and 5.86 x 10^6 N/m^2). The pressure was maintained at each level to record strain gage and seal deflection data. At the 850 psig (5.86 x 10^6 N/m^2) pressure level, both the ejection force and pressure load acting on the seal were equivalent to 115% of the 260-in. (6.6 m) motor MEOP loads.

b. Vectoring Test

In the vectoring configuration of the fixture, a 2.2 psig (1.52 x 10^4 N/m^2) pressure was maintained to balance the weight of the fixture upper platen prior to removal of the support arms in preparation for vectoring test. This pressure was considered the reference "zero" condition, and seal height and lateral measurements were taken in this condition during vectoring tests.

A series of vectoring tests to a $\pm 2°$ (.0349 rad) deflection angle was conducted on the pitch and yaw planes of the two seals as indicated in Table XVIII. In the 0-180° (0-3.14 rad) plane, duty cycle A tests were performed at pressure levels of 2.2, 30, 58, 87, and 111 psig (1.52, 20.7, 40.0, 60.0, and 76.5 x 104 N/m^2). At the 111 psig (76.5 x 10^4 N/m^2) pressure level, the ejection force acting on the seal was equivalent to 115% of the motor MEOP load. In addition, duty cycle B tests were performed at pressure levels of 40 and 2.2 psig (27.6 and

1.52 x 10^4 N/m^2). The tests on the 90-270° (1.57-4.71 rad) plane were identical except that the duty cycle A tests with 30 and 87 psig (20.7 and 60 x 10^4 N/m^2) pressure were omitted.

The duty cycles and the points at which data were subsequently reduced are shown in Figure 70. Duty cycle A consisted of a series of 0.5° (.00873 rad) incremental steps through plus and minus 2° (.0349 rad) with a hold of approximately 3 seconds at each level. The vectoring rate between levels was approximately 0.25° (.00436 rad) per second. Duty cycle B contained 10 cycles of ±1° (.0175 rad) followed by 10 cycles of ±2° (.0349 rad) deflection angle. The maximum vectoring rate attained was 0.5° (.00873 rad) per second, and the rate was normally between 0.4° (.00698 rad) and 0.5° (.00873 rad) per second.

Since the seal deflection angle was controlled by the actuator stroke, a vectoring test was initially performed to establish the relationship of deflection angle and actuator stroke. A test cycle at 2.2 psig (1.52 x 10^4 N/m^2) pressure and a predicted 1.5° (.0262 rad) deflection angle was performed. The calculated deflection angle by computer analysis was obtained to correlate with the measured actuator stroke. From this relationship, the stroke for a 2° (.0349 rad) angle was predicted for use in the subsequent vectoring tests.

The actuator null position changed with chamber pressure as a result of the axial deformation of the seal. To determine the null position of the actuator at each test pressure level, an additional test was performed by pressurizing the chamber to the required pressure level with both sides of the actuator vented to atmosphere. The average actuator stroke position from ascending and descending pressure tests was taken as the null position for that pressure level.

4. Destructive Test

Destructive test was performed on Seal S/N 01 with the elastomeric boot installed and following completion of the functional tests. Three types of tests were included: vectoring, fatigue, and pressure tests.

a. Vectoring Test

The seal was deflected to $\pm 3°$ (.0524 rad) and $\pm 3.5°$ (.061 rad) at two test pressures, 30 and 87 psig (20.7 and 60.0 x 10^4 N/m^2). The 87 psig (60.0 x 10^4 N/m^2) pressure resulted in an ejection force which was equivalent to 90% of the 260-in. (6.6 m) dia motor MEOP load. A duty cycle A program was used in each test sequence. In the preparation of the Data-Trak trace for these tests, the nonlinearity in the relationship between deflection angle and actuator stroke revealed from functional test data was incorporated.

b. Fatigue Test

Approximately 1000 cycles of flexible seal rotation at a chamber pressure of 30 psig (20.7 x 10^4 N/m^2) was performed during this test. The duty cycle consisted of 500 cycles of $\pm 1°$ (.0175 rad) followed by 500 cycles of $\pm 2°$ (.0349 rad) deflection. During fatigue test only the actuator stroke, load, and hydraulic pressure were recorded on the oscillograph trace.

c. Pressure Test

The test fixture was reconfigured to the proof pressure test position prior to the initiation of this test. A turbine oil was used as the pressurizing medium to minimize the amount of stored energy to be dissipated in the event of rupture. In this test, the chamber pressure was increased from zero to 1140 psig (7.86 x 10^6 N/m^2), held for 2 minutes, and then reduced to zero. The maximum pressure is equivalent to 150% of the MEOP ejection force and chamber pressure for the 260 in. (6.6 m) motor. During the hold period, the pressure gage was monitored for evidence of leakage.

C. TEST RESULTS AND ANALYSIS

1. Seal Measurements

Height and lateral measurements of the seal are tabulated in Tables XIX and XX. The data indicated no significant change occurred in the seal dimensions

even after completion of destructive tests. The variation in the measurements was generally less than 0.01 in. (.000254 m). This magnitude of variation is not expected to have any effect on the seal performance.

Pretest and posttest measurements at the inside diameter of the seal are shown in Table XXI. The maximum difference between the measurements was 0.03 in. (.00076 m) which is extremely small in proportion to the diameter of the seal.

2. Leak Test

No evidence of gas leakage through the seal was observed during all phases of testing. In the high pressure tests, no pressure drop was noted from visual observation of the pressure gages during the hold period. Also, helium leak detection at pressures below 30 psig (20.7×10^4 N/m^2) indicated no leakage.

3. Functional Test

a. Proof Pressure Test

(1) Axial Deflection

Both seals were proof tested at loads up to 1.15 times MEOP [850 psig (5.85×10^6 N/m^2) external pressure and 1.15×10^6 lb (5.11×10^6 N) ejection force]. Axial deflection of the seals obtained from dial gage measurements are tabulated in Table XXII. The average deflection is plotted versus ejection load in Figure 71. Comparison of seals S/N 01 and S/N 02 data indicated a close agreement in the magnitude of deflection and the hysteresis characteristics. Deflections of 0.140 and 0.148 in. (.00356 and .00376 m) occurred at maximum ejection load which is substantially lower than the predicted deflection of 0.235 in. (.00597 m). Comparison of deflections between increasing and decreasing pressure cycles indicated that the hysteresis characteristic is the reverse of that normally expected. This reverse hysteresis characteristic apparently resulted from a change in the frictional force of the test fixture O-ring seals.

(2) Shim Compressive Stress

From the recorded strain gage data, the compressive hoop stress of the steel shim was calculated and is tabulated in Table XXIII. A plot of the average stress versus ejection load is shown in Figure 72. The values of stress were identical for the two seals. A linear relationship of stress versus ejection force was obtained, and a maximum compressive stress of 40,000 psi (2.76×10^8 N/m^2) occurred at 1.15×10^6 lb (5.11×10^6 N) ejection force. This magnitude was slightly lower than the predicted compressive stress of 42,800 psi (2.95×10^8 N/m^2) for a one million pound (4.45×10^6 N) ejection force.

b. Vectoring Test

(1) Axial Deflection

The axial deflection of the seals in the vectoring configuration was obtained as computer output data from the seal performance analysis. As shown in Figure 71, the axial deflection was twice that obtained from proof pressure test for equivalent ejection loads. This fact was substantiated by direct dial gage measurements in both test configurations. The difference in deflection was apparently due to a lower external pressure acting on the seal in the vector test configuration. As depicted in Figure 17, a lower external pressure results in a higher shim rotation and effectively "flatens" the shim. This effect reduces the equivalent shim thickness and decreases the distance between the end flanges of the seal. From this standpoint, the axial deflection of the seal obtained from pressure test is more realistic and should be used in nozzle design.

(2) Shim Compressive Stress

The higher shim rotation that occurred during vectoring test was confirmed by a higher shim compressive stress as compared with the proof pressure test data for the same ejection load. Comparison of the compressive stresses in Figure 72 indicates that a 20% higher stress existed for the vector test condition. The data also showed a slight deviation from a linear relationship

with ejection load. The stresses calculated from strain gage data for the null position of both seals are tabulated in Table XXIV. Close agreement between the two sets of stress values was obtained.

During a $\pm 2°$ (.0349 rad) seal deflection with 1.15 million lb (5.11×10^6N) ejection load, approximately 25,500 psi (1.76×10^8 N/m^2) hoop compressive stress is either added to or subtracted from the neutral position stress. This value of stress, which is due to seal rotation alone, is substantially higher than the 8,000 psi (5.52×10^7 N/m^2) predicted. As a result, the total hoop stress in the shim with the combined maximum vectoring and ejection loads, was at the limit of the allowable material yield strength of 70,000 psi (4.82×10^8 N/m^2). However, with a higher external pressure acting on the seal in the actual motor condition, the maximum shim stress would be reduced to 65,600 psi (4.52×10^8 N/m^2) for the 115% MEOP loads.

The variation of compressive hoop stress in the steel shim with test pressure is shown in Figure 73. This hoop stress resulted from the combined pressure and vectoring loads at 2° (.0349 rad) seal deflection angle. The stress level at $\pm 2°$ (+.0349 rad) deflection was approximately 8,000 psi (5.52×10^7 N/m^2) higher than -2° (-.0349 rad) deflection. The difference resulted from the actuation force. In the case of a +2° (+.0349 rad) deflection, the actuation force is additive to the ejection load and causes a higher shim rotation. The reverse is true of a -2° (-.0349 rad) deflection. Comparison of the data between the two seals indicated that the hoop stress was approximately the same and not significantly affected by the elastomeric boot.

(3) Actuation Torque

The variation of actuation torque with deflection angle is shown in Figures 74 and 75 for seals S/N 01 and 02, respectively. The actuation torque was for an ejection load of 1.15×10^6 lb (5.11×10^6 N). The variation was nearly linear and the hystersis characteristic was normal. The torque for $\pm 2°$ (.0349 rad) deflection of seal S/N 02 was 4.98×10^6 in.-lb (5.62×10^5 N-m), which is in good agreement with the design torque of 5.0×10^6 in.-lb (5.65×10^5 N-m) for a one million lb (4.45×10^6 N) ejection load.

The torque for a given deflection angle was not a constant, but varied with ejection load. For $\pm 2°$ (.0349 rad) deflection, the variation of torque with ejection load is plotted in Figure 76. Although generally the variation is similar, indicating the torque is maximized and then decreased with further increase in ejection load, the magnitude of torque was slightly different for the plus and minus directions of actuation, as well as for the two planes of actuation. The variation in torque for a given ejection load was approximately 10% for seal S/N 02 and 4% for seal S/N 01. The difference was attributed to the null angle that existed in the seals. As expected, the actuation torque for seal S/N 01 was higher than for S/N 02 at the same ejection load because of the added stiffness of the elastomeric boot. Using an average torque for comparison, the increase in torque resulting from the boot was 11 to 15%.

(4) Pivot Location

Movement of the seal pivot point during vectoring was obtained. Figure 77 shows the typical pivot point excursion for $\pm 2°$ (.0349 rad) deflection at zero, 0.6, and 1.15 million lb (0, 2167, and 5.11×10^6 N) ejection load. Although a clear trend in movement of the pivot point as a function of deflection angle can not be established, the grouping of the points occurred within a relatively small area, especially for higher ejection loads. It is recognized that the method of pivot point calculation is highly sensitive to any small change in seal configuration as reflected by the measured input data.

Using an average value for comparison, the pivot point location was observed to progress away from the seal aft face with increased ejection loads as shown in Figure 78. This fact is consistent with the expected increase in steel shim rotation with ejection load. The pivot point distance changed from 52.0 to 58.4 in. (1.32 to 1.48 m) when the ejection load increased from zero to 1.15 million lb (5.11×10^6 N). The theoretical pivot point location of the seal is at 53.4 in. (1.35 m). Comparison of the data for the two seals indicated that the variation was more linear for seal S/N 01 than for S/N 02.

4. Destructive Test

Prior to initiation of the destructive tests, visual inspection of the seal revealed that the inside edge of some of the rubber pads were locally unbonded from the steel shims. The unbonded areas were generally in line with the actuation planes where maximum shear stresses occurred. Maximum areas of unbondedness occurred at the forward rubber pad-to-shim bond. The separation depth of this bondline was 0.10 to 0.25 in. (.0025 to .0064 m) with some local areas extending to 0.50 in. (.0127 m) as shown in Figure 79. Subsequent destructive tests did not significantly increase the unbonded depths and leakage or pressure drop was not detected.

a. Vectoring Test

In the vectoring test, a maximum deflection angle of 3.3° (.0575 rad) was indicated from the test data. The deflection angle was limited to this value by the interference of the seal with the wall of the test fixture. Prior to this test cycle, the seal was deflected to ±3.0° (.0524 rad) with 0.3 and 0.9 million lb (1.335 and 4.0 x 10^6 N) ejection load.

The test data for both vectoring cycles with 0.9 million lb (4.0 x 10^6 N) are shown in Figure 80. The variation of actuation torque with deflection angle was generally linear up to ±2° (.0349 rad) deflection. Beyond this point, the increasing torque with deflection angle was apparent. At the deflection angle of 3.3° (.0575 rad), the actuation torque was approximately 10 million in.-lb (1.13 x 106 N-m). One set of data indicated a torque substantially higher than this value, which apparently resulted from a shift in the pivot point location when the seal contacted the wall of the fixture.

b. Fatigue Test

The seal was tested at 455 cycles of ±1° (.0175 rad) and 500 cycles of ±2° (.0349 rad). The number of cycles at ±1° (.0175 rad) was reduced from the planned 500 cycles because of a malfunction of the cycle counter on the Data Trak

programmer. The actuation load and stroke were recorded during test and are summarized in Table XXV. Although some slight differences in these values occurred, the magnitude of the difference is less than 5% and is within the measurement accuracy obtainable from the oscillograph trace.

c. Pressure Test

Axial deflection of the seal was obtained from dial gage measurements at four locations 90° (1.57 rad). The average deflection is plotted versus ejection load in Figure 81. A maximum deflection of 0.217 in. (.00551 m) was obtained at 1.5 million lb (6.67×10^6 N) ejection load. Comparison of this data with the functional test results indicated some difference. At the ejection load of 1.15 million lb (5.11×10^6 N), the axial deflection of 0.18 in. (.00457 m) from this test was higher than the 0.14 in. (.00356 m) obtained from functional proof pressure test (see Figure 71) for the same seal. The hystersis characteristic was as normally expected, but was the reverse of that indicated from the functional test results. Although no conclusion can be made on the cause of these differences, the effect on seal performance is not expected to be significant.

The compressive hoop stress of the steel shim was calculated from the strain gage data. A maximum stress of 53,100 psi (3.67×10^8 N/m^2) existed under the combined loads of 1.5 million lb (6.67×10^6 N) ejection load and 1120 psig (7.72×10^6 N/m^2) test pressure. This is in close agreement with a stress level of 52,100 psi (3.60×10^8 N/m^2) obtained by proportioning the results from the functional test to the same pressure of this test.

After completion of the destructive test series, seal S/N 01 was disassembled from the test fixture. Visual inspection revealed no physical damage to the elastomeric boot. The ends of the boot remained securely bonded to the seal.

VII. CONCLUSIONS AND RECOMMENDATIONS

A. CONCLUSIONS

Major conclusions derived from this program are:

1. An omnidirectional flexible seal has been demonstrated to meet the program objective. The seal performance characteristics were satisfactory for the intended application.

2. Existing analytical techniques can be applied to the flexible seal design to predict its performance with acceptable accuracy.

3. A seal design with conical metal shims of uniform configuration can be designed to meet rotational angle requirements in excess of $\pm 3°$.

4. Large flexible seals can be successfully manufactured by sequential assembly using ambient cure, secondary bonding techniques.

B. RECOMMENDATIONS

The following recommendations are made:

1. Further develop the analytical technique to provide a more accurate method for the prediction of elastic stability and compressive stress in the metal shim.

2. Conduct thrust vector control system test to investigate the interplay between flexible seals and flight configured actuation system.

3. Incorporate the seal into a 260-in.-dia motor static firing test to confirm the seal performance characteristics.

REFERENCES

1. "260-SL-3 Motor Nozzle and Exit Cone Design, Fabrication and Assembly, Final Phase Report, Vol. III," NASA CR-72283, Contract NAS3-7998, dated 14 June 1967.

2. Bartz, D. R., "A Simple Equation for Rapid Estimation of Rocket Nozzle Convection Heat Transfer Coefficients", JPL, California Institute of Technology, January 1957, pages 49-51.

3. Wilson, E. L., "Finite Element Analysis of Two-Dimensional Structures", Structures and Material Research Dept. of Civil Engineering, Report No. 63-2, University of California, Berkeley, California, June 1963.

4. Becker, E. B., and Brisbane, J. J., "Application of the Finite Element Method to Stress Analysis of Solid Propellant Rocket Grains," Vols I and II, Report No. S-76, Rohm and Haas Company, Huntsville, Alabama, 18 November 1965.

5. Hetenyi, M., "Beams on Elastic Foundations," University of Michigan Press, Ann Arbor, Michigan, 1946.

6. Korst, H. H., "Dynamics and Thermodynamics of Separate Flows," AGARD Conf. Proc. #4 Separated Flows, Part 2, May 1966.

7. Final Report, Flexible Seal Nozzle, Independent Research Work Order 8716-41, Aerojet-General Corp., November 1969. (Aerojet Official Use Only)

TABLE I. - NOZZLE THERMAL GRADIENT SUMMARY

Area Ratio	Depth Below Original Surface at Motor Burnout, in. ($m \times 10^2$)		
	Erosion	Char	Isotherm 100°F-(311°K)
2.00 (Entrance)	0.83 (2.11)	1.68 (4.26)	2.12 (5.39)
1.50 (Entrance)	0.87 (2.21)	1.72 (4.36)	2.16 (5.50)
1.06 (Entrance)	1.10 (2.80)	1.95 (4.95)	2.42 (6.15)
1.00 (Throat)	0.92 (2.34)	1.77 (4.50)	2.23 (5.66)
1.10 (Exit)	0.37 (0.94)	1.22 (3.10)	1.80 (4.56)
2.00 (Exit)	0.20 (0.51)	0.95 (2.41)	1.55 (3.94)

TABLE II. - COMPARISON OF PRELIMINARY FLEXSEAL ANALYSIS RESULTS

Parameter	Fwd Pivot		Aft Pivot	
Maximum compressive stress, psi ($N/m^2 \times 10^{-6}$)	48,000	(331)	48,000	(331)
Allowable critical buckling stress, psi ($N/m^2 \times 10^{-6}$)	60,400	(416)	60,400	(416)
Seal rotation torque, in.-lb $\times 10^{-6}$ ($N-m \times 10^{-6}$)	4.73	(.535)	4.17	(.471)
Maximum elastomer shear stress, psi ($N/m^2 \times 10^{-3}$)	82	(565)	82	(565)
Maximum elastomer tensile stress, psi ($N/m^2 \times 10^{-3}$)	66	(455)	66	(455)

TABLE III. - FLEXIBLE SEAL WEIGHT COMPARISON

Component Weight, lb (Kg)	Fwd Pivot	Aft Pivot	Difference
Nozzle Shell	625 (283)	820 (371)	-195 (-88)
Nozzle Closure	6270 (2840)	6590 (2985)	-320 (-145)
Backup Insert	1210 (548)	1450 (657)	-240 (-109)
Closure Insert	1980 (897)	1990 (902)	- 10 (-5)
Closure Insulation	2670 (1210)	2300 (1042)	+370 (+168)
Flexseal Assembly	4425 (2004)	4595 (2081)	(-170) (-77)
Fwd Flange	1215 (550)	1400 (634)	-185 (-84)
Aft Flange	1160 (525)	1130 (511)	+ 30 (+14)
Laminate	1890 (856)	1890 (856)	0
Boot	160 (72)	175 (79)	- 15 (-7)

The fwd pivot seal design is 565 lb (256 kg) less than the aft pivot seal design.

TABLE IV. - FLEXIBLE SEAL TVC SYSTEM COMPARISON

Torque, in./lb x 10^{-6} (N-m x 10^{-6})	Fwd Pivot		Aft Pivot	
Seal Rotation	4.73	(.534)	4.17	(.471)
Internal Aerodynamic	1.21	(.137)	0	
Jet Damping[1]	0.40	(.045)	0.40	(.045)
Axial Acceleration	1.21	(1.37)	0.28	(.032)
Inertia	0.42	(.047)	0.42	(.047)
Total Torque	7.57	(.855)	4.87	(.550)
Design Torque[2]	9.45	(1.068)	6.10	(.689)
System Requirement				
Moment Arm, in. (m)	96.5	(2.45)	59.2	(1.50)
Actuation Force, lb (N x 10^{-3})	98,100	(436)	103,000	(458)

(1) Jet damping torque is assumed equal to zero at maximum torque requirement
(2) Design torque includes 1.25 safety factor

TABLE V. - DEFLECTION OF FLEXIBLE SEAL AND NOZZLE SHELL JOINT

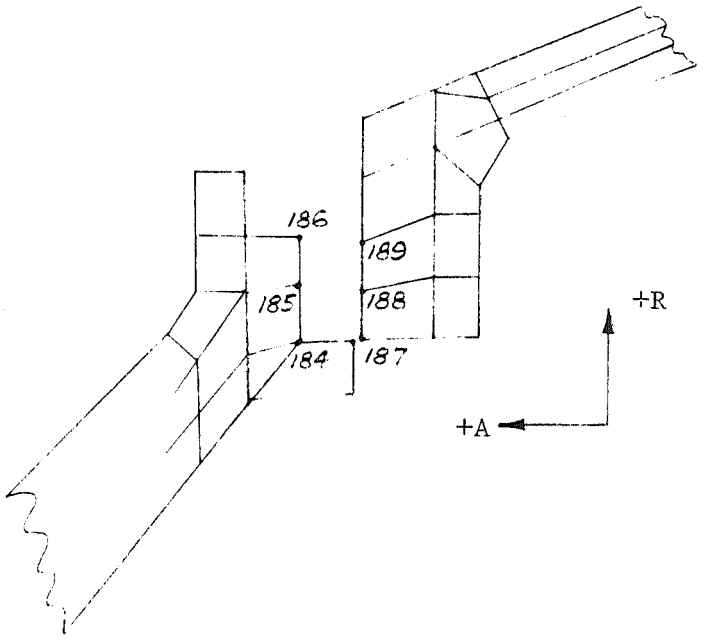

Nodal Point	Radial Displacement inch	Radial Displacement ($m \times 10^3$)	Axial Displacement inch	Axial Displacement ($m \times 10^3$)
184	-.005091	(-.129)	-.00248	(-.063)
187	-.007573	(-.192)	-.00248	(-.063)
185	-.00518	(-.131)	-.00445	(-.113)
188	-.007878	(-.200)	-.00445	(-.113)
186	-.005284	(-.134)	-.00643	(-.163)
189	-.007987	(-.202)	-.00643	(-.163)

TABLE VI. - SUMMARY OF MAXIMUM STRESS IN FLEXIBLE SEAL

Loading Condition	Type of Stress and Location	Stress Level psi	Stress Level ($N/m^2 \times 10^{-6}$)	Allowable Strength psi	Allowable Strength ($N/m^2 \times 10^{-6}$)	Factor of Safety
1	Shear stress at inside edge of P5 pad	104	(.717)	403	(2.78)	3.88
1	Compressive hoop stress at inside edge of S2 shim	42,800	(295)	70,000	(482)	1.63
2	Shear stress at outside edge of P5 pad	53	(.366)	403	(2.78)	7.59
2	Tension stress near outside edge of P5 pad	149	(1.028)	500	(3.45)	3.36
2	Compressive hoop stress at edge of S2 shim	3,900	(26.9)	70,000	(482)	High
3	Shear stress near inside edge of P5 pad	103(1) 98(2)	(.710) (.675)	403	(2.78)	3.91 4.11
3	Compressive hoop stress at inside edge of S3 shim	46,900(1) 29,300(2)	(323) (202)	70,000	(482)	1.49 2.39
2 + 3	Shear stress near inside edge of P5 pad	147	(1.012)	403	(2.78)	2.74
2 + 3	Compressive hoop stress at inside edge of shim	50,800(1)	(350)	70,000	(482)	1.38

(1) 2° clockwise rotation.
(2) 2° counterclockwise rotation.

TABLE VII. - QUADRUPLE LAP SHEAR SPECIMEN TEST RESULTS

Pressure, psig ($N/m^2 \times 10^{-6}$)	Rate, in./min. ($m/s \times 10^3$)	100% Strain: Stress, psi ($N/m^2 \times 10^{-4}$)	100% Strain: Modulus, psi ($N/m^2 \times 10^{-4}$)	200% Strain: Stress, psi, ($N/m^2 \times 10^{-4}$)	200% Strain: Modulus, psi, ($N/m^2 \times 10^{-4}$)
A. Specimens with 0.10-in. (.00254 m) Rubber					
0	.218 (.092)	28.7 (19.8)	28.7 (19.8)	53.0 (36.5)	26.5 (18.3)
0	3.14 (1.33)	28.8 (19.9)	28.8 (19.9)	53.5 (36.9)	26.8 (18.5)
250 (1.72)	.411 (.174)	28.2 (19.4)	28.2 (19.4)	52.0 (35.8)	26.0 (18.0)
250 (1.72)	4.00 (1.69)	28.6 (19.7)	28.6 (19.7)	53.0 (36.5)	26.5 (18.3)
500 (3.45)	5.67 (2.40)	29.5 (20.3)	29.5 (20.3)	53.5 (36.9)	26.8 (18.5)
500 (3.45)	.533 (.225)	28.6 (19.7)	28.6 (19.7)	52.2 (36.0)	26.1 (18.0)
750 (5.17)	.390 (.165)	28.8 (19.9)	28.8 (19.9)	52.0 (35.8)	26.0 (18.0)
750 (5.17	4.83 (2.04)	29.2 (20.1)	29.2 (20.1)	53.6 (37.0)	26.8 (18.5)
1000 (6.90)	5.38 (2.28)	29.8 (20.5)	29.8 (20.5)	54.1 (37.3)	27.1 (18.7)
1000 (6.90)	.431 (.182)	29.0 (20.0)	29.0 (20.0)	53.0 (36.5)	26.5 (18.3)
B. Specimens With 0.18-in. (.00456 m) Rubber					
0	.166 (.070)	27.0 (18.6)	27.0 (18.6)	46.0 (31.7)	23.0 (15.9)
0	9.38 (3.96)	29.0 (20.0)	29.0 (20.0)	52.0 (35.8)	26.0 (18.0)
500 (3.45)	.96 (.405)	28.0 (19.3)	28.0 (19.3)	51.0 (35.2)	25.5 (17.6)
980 (6.75)	1.34 (.566)	28.4 (19.6)	28.4 (19.6)	51.5 (35.5)	25.8 (17.8)
C. Specimens with 0.06-in. (.00152 m) Rubber					
0	.185 (.078)			52.2 (36.0)	26.1 (18.0)
0	2.52 (1.07)			54.2 (37.4)	27.1 (18.7)
250 (1.72)	.211 (.089)			53.2 (36.7)	26.6 (18.3)
250 (1.72)	2.98 (1.26)			53.8 (37.1)	26.9 (18.5)
500 (3.45)	.166 (.070)			53.2 (36.7)	26.6 (18.3)
500 (3.45)	2.88 (1.22)			53.8 (37.1)	26.9 (18.5)
750 (5.17)	.240 (.101)			53.4 (36.8)	26.7 (18.4)
750 (5.17)	3.05 (1.29)			55.0 (37.9)	27.5 (19.0)
1000 (6.90)	.324 (.137)			54.2 (37.4)	27.1 (18.7)
1000 (6.90)	4.56 (1.93)			55.0 (37.9)	27.5 (19.0)

TABLE VIII. - AGING AND HUMIDITY TEST SCHEDULE

Specimen		Aging (80°F/300°K, Uncontrolled R.H.)				Humidity Exposure (95% R.H. 110°F/317°K)			
		1 Mo.	3 Mo.	6 Mo.	9 Mo.	1 Mo.	3 Mo.	6 Mo.	9 Mo.
Shear Tests	1	x	x	x	x	x			
	2					x	x	x	x
	3			x			x		
	4*	x	x	x	x	x			
	5*					x	x	x	x
Tensile Tests	1	x	x	x	x	x			
	2					x	x	x	x
	3*	x	x	x	x	x			

*The exposed rubber edges of these specimens were treated to evaluate retardation of the aging process.

TABLE IX. - AGING AND HUMIDITY EXPOSURE TEST RESULTS

	INITIAL CONDITION	ONE-MONTH EXPOSURE	THREE-MONTH EXPOSURE	SIX-MONTH EXPOSURE	NINE-MONTH EXPOSURE	ONE-MONTH EXPOSURE*	PROPERTY AT FAILURE
Aging (80°F/300°K, Uncontrolled R.H.)							
Shear Stress @ 300%	67.5	69	62.5	66.7	68.1	78.2	Stress - 175 psi (121 x 10^4 N/m^2)
Strain, psi (N/m^2 x 10^{-4})	(46.5)	(47.5)	(43.0)	(46.0)	(47.0)	(54.0)	Strain - 520%
	69.0			62.8	81.2		Stress - 150 psi (10^3 x 10^4 N/m^2)
	(47.5)			(43.2)	(56.0)		Strain - 485%
Tensile Strain @ 50 psi	23.0	25.6	24.2	22.5	21.6	18.4	Stress - 363 psi (250 x 10^4 N/m^2)
(34.5 x 10^4 N/m^2) Stress, %	(15.8)	(17.6)	(16.7)	(15.5)	(14.9)	(12.7)	Strain - 528%
Humidity (95% R.H., 110°F/317°K)							
Shear Stress, @ 300%	72.5	72	73.3	85.7	92.2		Stress - 191 psi (132 x 10^4 N/m^2)
Strain, psi (N/m^2 x 10^{-4})	(50.0)	(49.6)	(50.5)	(59.0)	(63.6)		Strain - 497%
Tensile Strain @ 50 psi	24.0	26.3	19.8	19.2	22.5		Stress - 240 psi (165 x 10^4 N/m^2)
Stress, % (34.5 x 10^4 N/m^2)	(16.5)	(18.1)	(13.6)	(13.2)	(15.5)		Strain - 663%

*Exposure at 110°F/317°K temperature and 95% relative humidity.

TABLE X. - EVALUATION OF SURFACE EFFECTS ON ADHESIVE BOND STRENGTH

	Specimen Description	Avg. Shear Stress, psi, ($N/m^2 \times 10^{-6}$)	
B -	Bare steel	1820	(12.55)
U -	Primed with FM-47	3732	(25.75)
P -	Bare steel in contact with peel coat for 1 day	2775	(19.13)
K -	Primed steel in contact with peel coat for 1 day	3419	(23.6)
PA -	Bare steel in contact with peel coat for 7 days	3092	(21.3)
KA -	Primed steel in contact with peel coat for 7 days	3500	(24.1)
BT -	Bare steel in contact with teflon tape for 1 day	2535	(17.5)

TABLE XI. - LAP SHEAR SPECIMEN TEST RESULTS
FROM PROCESS DEMONSTRATION RING

Specimen	Shear Stress at 300% Strain, psi ($N/m^2 \times 10^{-3}$)	Ultimate Shear Stress, psi ($N/m^2 \times 10^{-6}$)	Ultimate Shear Strain, %
F	73.4 (506)	745 (5.14)	809
G	78.4 (540)	595 (4.10)	734
M_1	68.5 (471)	268[1] (1.85)	635
M_2	77.8 (536)	222[1] (1.53)	555
O_1	77.6 (535)	225[1] (1.55)	550
O_2	73.0 (503)	97.5[1] (.67)	400
P	76.7 (529)	625 (4.31)	745
R_1	75.0 (516)	698 (4.81)	808
R_2	73.1 (505)	777 (5.35)	830
R_3	71.8 (495)	806 (5.55)	833

(1) Adhesive failure at interface plane between the bare steel and the FM-47 primer.

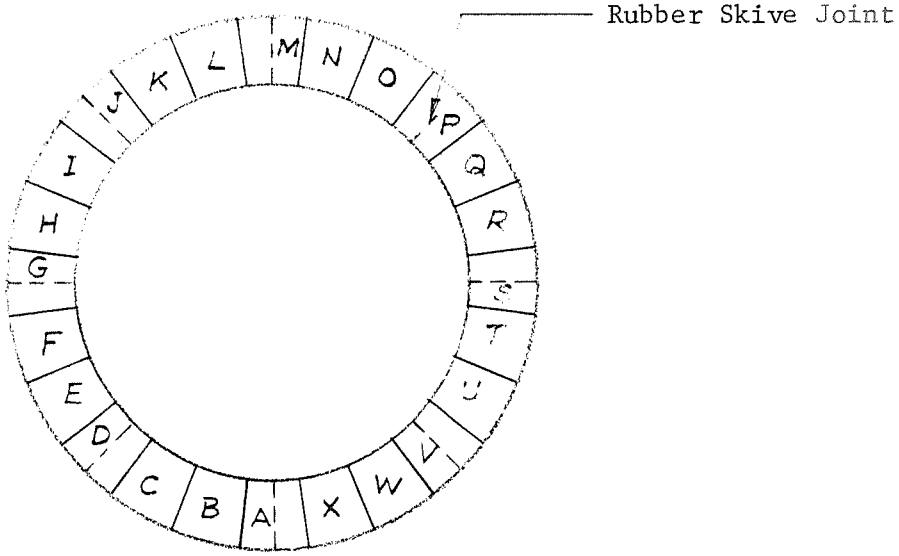

TABLE XII. - COMPRESSION DEFLECTION TEST PROCEDURE
TABLE XII

1. EQUIPMENT

   a. Instron Model TTC or equivalent.

   b. 10,000 lb capacity load cell.

   c. 2 - 6 x 6 x 1/4 CRS plates abraded on one side with aluminum oxide.

2. PROCEDURE

   a. Calibrate equipment according to manufacturers instructions.

   b. Set cross head at 0.20 in./min and chart at 10. in./min.

   c. Gauge slab in five places (4 corners plus center) and record.

   d. Center 4 x 4 x .3-in. slab between the abraded surfaces of the steel plates.

   e. Center assembly on load cell and balance.

   f. Preflex two times to 25% compression (approximately .075 in.) Load and unload at 0.2 in./min.

   g. Preload assembly to 0.5% of load at 25% compression (32-36 lb range) - balance to zero.

   h. Record third flex and plot load at .010, .020, .050, and .075 in.

TABLE XIII. - TENSILE PROPERTIES OF GEN-GARD V-45 RUBBER

Specimen	Tensile Strength, psi ($N/m^2 \times 10^{-6}$)		Elongation at Break, %
A. SPECIMENS WITHOUT SPLICE JOINT			
1	2200	(15.2)	775
2	2250	(15.5)	750
3	2250	(15.5)	775
B. SPECIMENS WITH SPICE JOINT			
1	1340	(9.25)	575
2	1275	(8.80)	500
3	1325	(9.14)	500

TABLE XIV. - FLEXIBLE SEAL COMPONENT BOND DATA

Bond Sequence	Component	Flexible Seal S/N 01 Avg. Bond Strength psi ($N/m^2 \times 10^{-6}$)	Flexible Seal S/N 01 Ultrasonic Inspection	Flexible Seal S/N 02 Avg. Bond Strength psi ($N/m^2 \times 10^{-6}$)	Flexible Seal S/N 02 Ultrasonic Inspection
1	Aft Ring/ Rubber No. 1	2970 (20.45)	7 Defects	2416 (16.65)	No Defect
2	Rubber No. 1/Shim No. 1	411 (2.84)	No Defects	2547 (17.56)	
3	Shim No. 1/Rubber No. 2	980 (6.75)	No Defects	2746 (18.95)	
4	Rubber No. 2/Shim No. 2	2142 (14.80)	No Defects	2740 (18.90)	
5	Shim No. 2/Rubber No. 3	1803 (12.44)	No Defects	2373 (16.35)	
6	Rubber No. 3/Shim No. 3	1715 (11.82)	1 Defect	2320 (16.00)	
7	Shim No. 3/Rubber No. 4	2556 (17.62)	No Defect	2667 (18.40)	
8	Rubber No. 4/Shim No. 4	2598 (17.92)	No Defect	2700 (18.62)	
9	Shim No. 4/Rubber No. 5	2108 (14.54)	No Defect	2708 (18.69)	
10	Rubber No. 5/Fwd Ring	1500 (10.35)	No Defect	2808 (19.38)	No Defect

TABLE XV. - FLEXIBLE SEAL HEIGHT AND CONCENTRICITY MEASUREMENTS

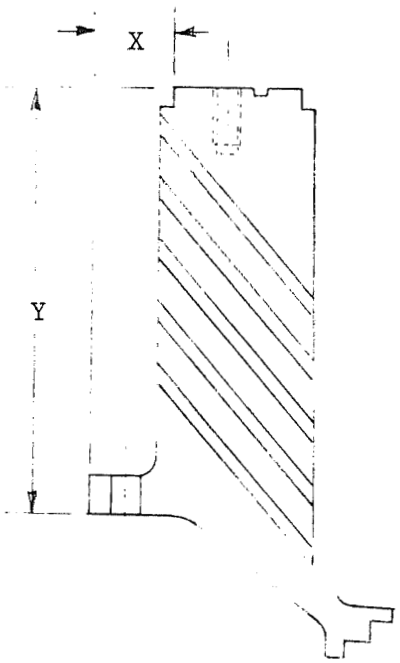

Circum. Location	Seal S/N 01, inch (m)				Seal S/N 02, inch (m)			
	X		Y		X		Y	
1	2.114		10.926		2.143		10.895	
2	2.114		10.965		2.120		10.875	
3	2.073		10.966		2.154		10.867	
4	2.093		10.920		2.128		10.890	
5	2.102		10.915		2.102		10.865	
6	2.099		10.945		2.082		10.885	
7	2.104		10.970		2.103		10.850	
8	2.099		10.945		2.086		10.855	
9	2.108		10.895		2.100		10.840	
10	2.104		10.885		2.110		10.851	
Max.	2.114	(.0536)	10.970	(.2782)	2.154	(.0547)	10.895	(.2767)
Min.	2.073	(.0526)	10.885	(.2760)	2.082	(.0529)	10.840	(.2753)
Range	0.041	(.0010)	0.085	(.0022)	0.072	(.0018)	0.055	(.0014)

TABLE XVI. - TEST FIXTURE WELD STRESS

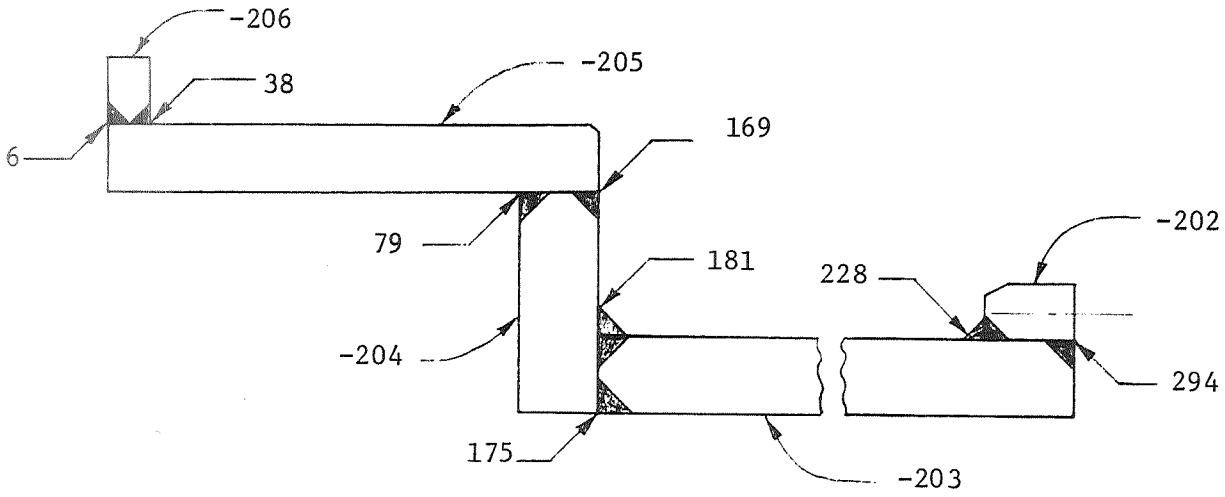

-202 to -203 Weld Stress, psi ($N/m^2 \times 10^{-6}$)

Element No.	Pressure Condition		Vector Condition	
228	7920	(54.5)	7510	(51.8)
234	4314	(29.8)	3691	(25.4)
242	3197	(22.0)	1998	(13.8)
250	2043	(14.1)	1060	(7.31)
261	1545	(10.6)	1036	(7.15)
272	1003	(6.91)	747	(5.15)
283	270	(1.86)	208	(1.43)
294	118	(.81)	81	(.56)

-203 to -204 Weld Stress, psi ($N/m^2 \times 10^{-6}$)

Element No.	Pressure Condition		Vector Condition	
175	-0.6		46	(.32)
176	107	(.74)	200	(1.38)
177	1009	(6.95)	867	(5.98)
178	2787	(19.2)	1857	(12.8)
179	4142	(28.5)	2908	(20.0)
180	4979	(34.3)	3479	(24.0)
181	6423	(44.2)	4564	(31.5)

-204 to -205 Weld Stress, psi ($N/m^2 \times 10^{-6}$)

Element No.	Pressure Condition		Vector Condition	
79	20,282	(140)	15,450	(106.5)
97	11,144	(76.9)	8093	(55.7)
115	4,887	(33.6)	3895	(26.9)
133	900	(6.20)	1289	(8.89)
151	-471	(-3.25)	189	(1.30)
169	-880	(-6.06)	-116	(-.80)

-205 to -206 Weld Stress, psi ($N/m^2 \times 10^{-6}$)

Element No.	Pressure Condition		Vector Condition	
6	0.3		22.8	(.16)
14	7.3	(.05)	774	(5.33)
22	16.8	(.12)	2525	(17.4)
30	33.5	(.23)	4618	(31.8)
38	76.9	(.53)	9552	(65.9)

Pressure Condition - 850 psi (5.85×10^6 N/m^2)

Vector Condition - 115 psi (7.93×10^5 N/m^2)

TABLE XVII. - INSTRUMENTATION SUMMARY

Parameter	No. of Channels	Location	Type Instrument	Recording Method	Max. Instr. Ranging		
					Proof	Vector	Destruct
Applied Force	1	Actuator Assy	Load-Cell	Oscillograph	N.A.	125K	150K
Actuator Position	2 (1)	Actuator Arm	Lin. Potentiometer	Oscillograph	N.A.	±4 in.	±8 in.
Chamber Pressure	2	Test Fixture	Pressure Transducer	Oscillograph	1000 psig	200 psig	200/1500 psig
Seal Deflection	8	Pitch & Yaw Planes (90° Apart)	Lin. Potentiometer	Oscillograph	1/2 in.	±3 in.	±4 in.
Hydraulic Pressure	2	Supply and Return Line	Pressure Transducer	Oscillograph	N.A.	3000 psig	3000 psig
Actuator ΔP	1	Hydraulic Cylinder	ΔP Transducer	Oscillograph	N.A.	3000 psig	3000 psig
Metal Shim Strain	8	Shim S3 at Pitch & Yaw Planes (90° Apart)	Biaxial Strain Gage	Oscillograph			

(1) One actuator position potentiometer used for feedback to the servocontroller

SI units omitted for clarity.

TABLE XVIII. - SEAL VECTORING TEST SEQUENCE

0°-180° Plane

1. Cycle A, ± 2° at 2.2 psig
   (± .0349 rad @ 15.18 x 10^3 N/m^2)

2. Cycle A, ± 2° @ 30 psig
   (± .0349 rad @ 207 x 10^3 N/m^2)

3. Cycle A, ± 2° @ 58 psig
   (± .0349 rad @ 400 x 10^3 N/m^2)

4. Cycle A, ± 2° @ 87 psig
   (± .0349 rad @ 600 x 10^3 N/m^2)

5. Cycle A, ± 2° @ 111 psig
   (± .0349 rad @ 765 x 10^3 N/m^2)

6. Cycle B, ± 1° and ± 2° @ 40 psig
   (± .01745 and ± .0349 rad @ 276 x 10^3 N/m^2)

7. Cycle A, ± 2° @ 2.2 psig
   (± .0349 rad @ 15.8 x 10^3 N/m^2)

8. Cycle B, ± 1° and ± 2° @ 2.2 psig
   (± .01745 and ± .0349 rad @ 15.18 x 10^3 N/m^2)

90°-270° Plane

1. Cycle A, ± 2° @ 2.2 psig
   (± .0349 rad @ 15.18 x 10^3 N/m^2)

2. Cycle A, ± 2° @ 58 psig
   (± .0349 rad @ 400 x 10^3 N/m^2)

3. Cycle A, ± 2° @ 111 psig
   (± .0349 rad @ 765 x 10^3 N/m^2)

4. Cycle B, ± 1° and ± 2° @ 40 psig
   (±.01745 and ± .0349 rad @ 276 x 10^3 N/m^2)

5. Cycle A, ± 2° @ 2.2 psig
   (± .0349 rad @ 15.18 x 10^3 N/m^2)

6. Cycle B, ± 1° and ± 2° @ 2.2 psig
   (± .01745 and ± .0349 rad @ 15.18 x 10^3 N/m^2)

TABLE XIX. - FLEXIBLE SEAL HEIGHT MEASUREMENTS

FLEXIBLE SEAL HEIGHT MEASUREMENTS

SEAL S/N 01	0°	45°	90°	135°	180°	225°	270°	315°
Seal Bolted to -401 Platen	10.421	10.428	10.402	10.408	10.432	10.427	10.386	10.373
After Proof & Leak Test	10.420	10.433	10.438	10.447	10.445	10.428	10.410	10.400
Before Vector Test (90°-270°)	10.404	10.416	10.409	10.416	10.428	10.431	10.420	10.408
After Vector Test (90°-270°)	10.409	10.415	10.418	10.416	10.433	10.435	10.426	10.409
Before Vector Test (0°-180°)	10.414	10.419	10.427	10.425	10.425	10.420	10.414	10.415
After Vector Test (0°-180°)	10.435	10.436	10.433	10.425	10.422	10.414	10.411	10.417
Before Fatigue Test	10.430	10.418	10.421	10.412	10.415	10.408	10.406	10.405
After Fatigue Test	10.431	10.419	10.420	10.415	10.419	10.404	10.405	10.403
After ±3.5° Vector Test	10.427	10.419	10.425	10.412	10.413	10.402	10.403	10.407
Before 1140 psig Pressure Test	10.432	10.430	10.431	10.428	10.433	10.428	10.416	10.417
After 1140 psig Pressure Test	10.425	10.436	10.433	10.438	10.432	10.420	10.423	10.415
At Disassy., Bolted to -401 Platen	10.434	10.440	10.425	10.422	10.448	10.433	10.404	10.392
SEAL S/N 02								
Seal Bolted to -401 Platen	10.384	10.411	10.415	10.428	10.458	10.436	10.377	10.350
After Proof & Leak Test	10.369	10.391	10.428	10.455	10.446	10.417	10.390	10.367
Before Vector Test (0°-180°)	10.379	10.394	10.413	10.428	10.435	10.405	10.378	10.355
After Vector Test (0°-180°)	10.360	10.393	10.417	10.416	10.436	10.408	10.380	10.378
Before Vector Test (90°-270°)	10.367	10.378	10.400	10.423	10.439	10.417	10.384	10.353
After Vector Test (90°-270°)	10.333	10.349	10.385	10.414	10.433	10.418	10.406	10.345
At Disassy, Bolted to -401 Platen	10.347	10.387	10.387	10.395	10.437	10.420	10.351	10.328

All dimensions in inches, SI units omitted for clarity.

TABLE XX. - FLEXIBLE SEAL LATERAL MEASUREMENTS

FLEXIBLE SEAL LATERAL MEASUREMENTS

SEAL S/N 01		A	B	C	D	E
Before Proof & Leak Test	0°	29.430	29.429	29.425	29.414	29.441
	90°	29.707	29.693	29.691	29.659	29.678
	180°	29.556	29.532	29.519	29.543	29.527
	270°	29.077	29.102	29.081	29.081	29.005
After Proof & Leak Test	0°	29.415	29.432	29.426	29.413	29.436
	90°	29.697	29.687	29.685	29.655	29.677
	180°	29.558	29.533	29.520	29.546	29.525
	270°	29.075	29.103	29.082	29.082	29.003
Before Vector Test (90°-270°)	0°	29.412	29.431	29.426	29.415	29.436
	90°	29.716	29.705	29.696	29.656	29.669
	180°	29.555	29.532	29.520	29.543	29.518
	270°	29.059	29.088	29.070	29.077	29.002
After Vector Test (90°-270°)	0°	29.412	29.430	29.426	29.415	29.436
	90°	29.715	29.705	29.698	29.657	29.669
	180°	29.556	29.532	29.519	29.542	29.519
	270°	29.059	29.088	29.070	29.077	29.004
After Vector Test (0°-180°)	0°	29.402	29.423	29.422	29.415	29.437
	90°	29.706	29.696	29.691	29.656	29.670
	180°	29.569	29.545	29.530	29.549	29.520
	270°	29.075	29.099	29.079	29.084	29.007
After Fatigue Test	0°	29.404	29.421	29.419	29.413	29.436
	90°	29.705	29.695	29.690	29.654	29.668
	180°	29.570	29.546	29.531	29.549	29.521
	270°	29.070	29.098	29.075	29.081	29.005
After $\pm$3.5° Vector Test	0°	29.410	29.421	29.420	29.415	29.438
	90°	29.707	29.696	29.691	29.655	29.669
	180°	29.571	29.546	29.531	29.549	29.523
	270°	29.077	29.098	29.079	29.081	29.006
Before 1140 psig Pressure Test	0°	29.408	29.423	29.421	29.415	29.438
	90°	29.696	29.691	29.687	29.654	29.669
	180°	29.562	29.544	99.530	29.548	29.522
	270°	29.071	29.100	29.080	29.082	29.006
After 1140 psig Pressure Test	0°	29.405	29.424	29.423	29.417	29.440
	90°	29.698	29.696	29.693	29.656	29.670
	180°	29.559	29.545	29.532	29.552	29.523
	270°	29.069	29.100	29.081	29.085	29.008

Table XX. - FLEXIBLE SEAL LATERAL MEASUREMENTS (cont.)

SEAL S/N 02		A	B	C	D	E
Before Proof & Leak Test	0°	29.446	29.431	29.424	29.423	29.459
	90°	29.685	29.667	29.664	29.668	29.672
	180°	29.518	29.562	29.554	29.540	29.536
	270°	29.081	29.075	29.070	29.053	29.006
After Proof & Leak Test	0°	29.448	29.434	29.427	29.423	29.455
	90°	29.684	29.670	29.665	29.669	29.672
	180°	29.517	29.541	29.557	29.548	29.534
	270°	29.079	29.074	29.070	29.055	29.007
After Vector Test (0°-180°)	0°	29.435	29.419	29.412	29.413	29.437
	90°	29.692	29.712	29.730	29.702	29.697
	180°	29.547	29.579	29.565	29.545	29.531
	270°	29.100	29.074	29.069	29.057	29.013
After Vector Test (90°-270°)	0°	29.446	29.435	29.425	29.416	29.437
	90°	29.709	29.685	29.672	29.672	29.671
	180°	29.513	29.559	29.552	29.539	29.530
	270°	29.044	29.058	29.058	29.052	29.011

All dimensions in inches; SI units omitted for clarity.

TABLE XXI. - MEASUREMENTS OF SEAL INSIDE DIAMETERS

Location	0°-180° Plane		90°-270° Plane	
	Pretest	Posttest	Pretest	Posttest
Flexible Seal S/N 02				
A	107.939	107.960	108.080	108.051
B	107.982	108.001	108.048	108.019
C	107.980	107.993	108.040	108.010
D	107.968	107.980	108.050	108.021
E	107.997	108.011	108.019	107.992
Flexible Seal S/N 01				
A	108.000	107.987	108.013	108.018
B	108.009	107.997	108.031	108.034
C	108.000	107.991	108.012	108.012
D	108.011	108.003	108.011	108.017
E	108.014	108.007	107.971	107.980

All dimensions in inches, SI units omitted for clarity.

TABLE XXII. - SEAL AXIAL DEFLECTION - PROOF PRESSURE TEST

Pressure, psig	FLEXIBLE SEAL S/N 01				FLEXIBLE SEAL S/N 02			
	0°	90°	180°	270°	0	90°	180°	270°
0	0	0	0	0	0	0	0	0
50	.010	.009	.010	.010	.010	.012	.008	.006
100	.019	.019	.021	.021	.019	.022	.019	.016
50	.013	.012	.013	.014	.013	.012	.012	.013
200	.039	.042	.041	.039	.040	.044	.040	.036
400	.077	.083	.089	.085	.077	.086	.078	.065
600	.106	.108	.122	.125	.107	.113	.102	.092
735	.125	.124	.140	.144	.131	.131	.119	.112
850	.139	.139	.155	.158	.149	.149	.134	.127
600	.099	.097	.110	.114	.108	.102	.094	.090
400	.060	.060	.067	.069	.066	.059	.054	.051
200	.025	.021	.023	.023	.029	.021	.017	.020
50	.013	.012	.010	.014	0	-.006	-.011	-.004
0	-.011	-.016	-.019	-.016	-.007	-.016	-.019	-.011

All dimensions in inches, SI units omitted for clarity.

TABLE XXIII.- SHIM COMPRESSIVE STRESS - PROOF PRESSURE TEST

Ejection Force, K lb ($N \times 10^{-3}$)	Pressure, psig ($N/m^2 \times 10^{-6}$)	Flexible Seal S/N 01					Flexible Seal S/N 02				
		Avg. Stress	0°	90°	180°	270°	Avg. Stress	0°	90°	180°	270°
67.5 (.30)	50 (.345)	2.30 (15.9)	2.36 (16.3)	2.26 (15.6)	2.28 (15.7)	2.28 (15.7)	2.21 (15.2)	2.17 (15.0)	2.07 (14.3)	2.52 (17.4)	2.07 (14.3)
135 (.60)	100 (.69)	4.62 (31.9)	4.71 (32.5)	4.45 (30.8)	4.65 (32.0)	4.65 (32.0)	4.44 (30.6)	4.52 (31.2)	4.30 (29.6)	4.62 (31.9)	4.30 (29.6)
67.5 (.30)	50 (.345)	2.41 (16.6)	2.42 (16.7)	2.26 (15.6)	2.44 (16.8)	2.52 (17.4)	2.14 (14.7)	2.17 (15.0)	2.07 (14.3)	2.26 (15.6)	2.07 (14.3)
270 (1.20)	200 (1.38)	9.01 (62.1)	8.93 (61.5)	9.02 (62.1)	9.20 (63.5)	8.90 (61.4)	9.04 (62.2)	8.85 (61.0)	9.12 (62.9)	9.25 (63.8)	8.94 (61.5)
541 (2.41)	400 (2.76)	18.8 (130)	18.6 (128)	18.4 (127)	19.1 (132)	19.0 (131)	18.6 (128)	18.2 (125)	18.5 (128)	18.9 (130)	18.6 (128)
811 (3.61)	600 (4.14)	28.3 (195)	27.6 (190)	27.8 (192)	28.7 (198)	29.0 (200)	28.0 (193)	27.5 (190)	27.8 (192)	28.6 (197)	28.0 (193)
995 (4.42)	735 (5.06)	34.8 (240)	34.0 (234)	34.2 (236)	35.4 (244)	35.5 (245)	34.4 (237)	33.4 (230)	34.0 (234)	35.2 (242)	34.8 (240)
1150 (5.11)	850 (5.86)	40.0 (276)	39.1 (270)	39.6 (273)	40.5 (279)	41.0 (283)	40.0 (276)	39.7 (274)	39.4 (272)	40.4 (278)	40.4 (278)
811 (3.61)	600 (4.14)	28.5 (197)	28.0 (193)	28.7 (198)	28.5 (197)	28.9 (199)	28.5 (196)	27.5 (190)	27.8 (192)	29.3 (202)	29.2 (201)
541 (2.41)	400 (2.76)	19.7 (136)	19.5 (134)	20.0 (138)	19.7 (136)	19.7 (136)	19.0 (131)	18.5 (128)	19.1 (132)	19.2 (132)	19.1 (132)
270 (1.20)	200 (1.38)	10.4 (71.6)	11.3 (77.9)	11.6 (80.0)	9.5 (65.5)	9.3 (64.0)	9.6 (66.1)	9.2 (63.5)	10.0 (69.0)	9.9 (68.2)	9.1 (62.7)
67.5 (.30)	50 (.345)	2.0 (13.8)	2.49 (17.2)	2.70 (18.6)	1.5 (10.3)	1.5 (10.3)	2.17 (15.0)	1.75 (12.1)	2.68 (18.5)	2.16 (14.9)	2.07 (14.3)
0	0	+.5 (3.5)	0	0	.92 (+6.3)	+1.05 (+7.2)	+.4 (+2.7)	1.0 (+6.9)	.10 (.7)	+.10 (+.7)	+.60 (+4.1)

Stress values in Ksi ($N/m^2 \times 10^{-6}$)

TABLE XXIV. - SHIM COMPRESSIVE STRESS, VECTOR TEST (NULL POSITION)

Test Pressure psig	($N/m^2 \times 10^{-3}$)	Ejection Load lb x 10^{-3}	(N x 10^{-6})	Seal S/N 01 0°		Seal S/N 01 90°		Seal S/N 02 0°		Seal S/N 02 90°	
2.2	(15.2)	0		0		0		0		0	
30	(207)	300	(1.34)	14.4	(99.3)			14.2	(97.9)		
58	(400)	600	(2.67)	27.0	(186)	27.3	(188)	27.0	(186)	28.3	(195)
87	(600)	900	(4.01)	38.9	(268)			38.1	(262)		
111	(765)	1150	(5.11)	46.9	(323)	46.1	(318)	45.6	(314)	48.0	(331)
40	(276)	400	(1.78)	19.7	(136)	20.2	(139)	19.0	(131)	21.0	(145)
2.2	(15.2)	0		0		0		0		0	

Stress values in ksi ($N/m^2 \times 10^{-6}$)

TABLE XXV. - FATIGUE TEST LOAD - DEFLECTION CHARACTERISTICS

Cycle No.	Counterclockwise Deflection		Clockwise Deflection	
	Load, lb	Deflection, in.	Load, lb	Deflection, in.
± 1° Deflection				
1	32,307	1.738	33,630	1.934
50	32,307	1.709	33,630	1.934
100	31,697	1.709	33,630	1.934
150	31,697	1.709	33,630	1.934
200	32,307	1.709	33,630	1.934
250	32,307	1.709	33,630	1.934
300	32,307	1.709	33,030	1.905
350	32,307	1.709	33,030	1.905
400	32,307	1.709	33,030	1.905
450	32,916	1.709	33,030	1.905
455	32,916	1.709	33,030	1.905
± 2° Deflection				
1	60,346	3.528	60,655	3.924
50	59,127	3.442	59,453	3.924
100	59,127	3.442	58,853	3.924
150	59,127	3.442	58,252	3.924
200	59,127	3.442	57,651	3.924
250	59,127	3.442	57,651	3.953
300	59,127	3.470	57,651	3.924
350(1)	59,127	3.447	58,252	3.838
400	59,127	3.447	58,252	3.809
450	59,127	3.447	58,252	3.809
500	59,127	3.476	58,252	3.809
Reading Accuracy(2)	610	0.029	601	0.030

(1) Cycles 326 through 500 were performed the following day.
(2) The oscillograph traces were measured to the nearest 0.01 inch. A variation of data corresponding to 0.01 inch is as shown

SI units omitted for clarity.

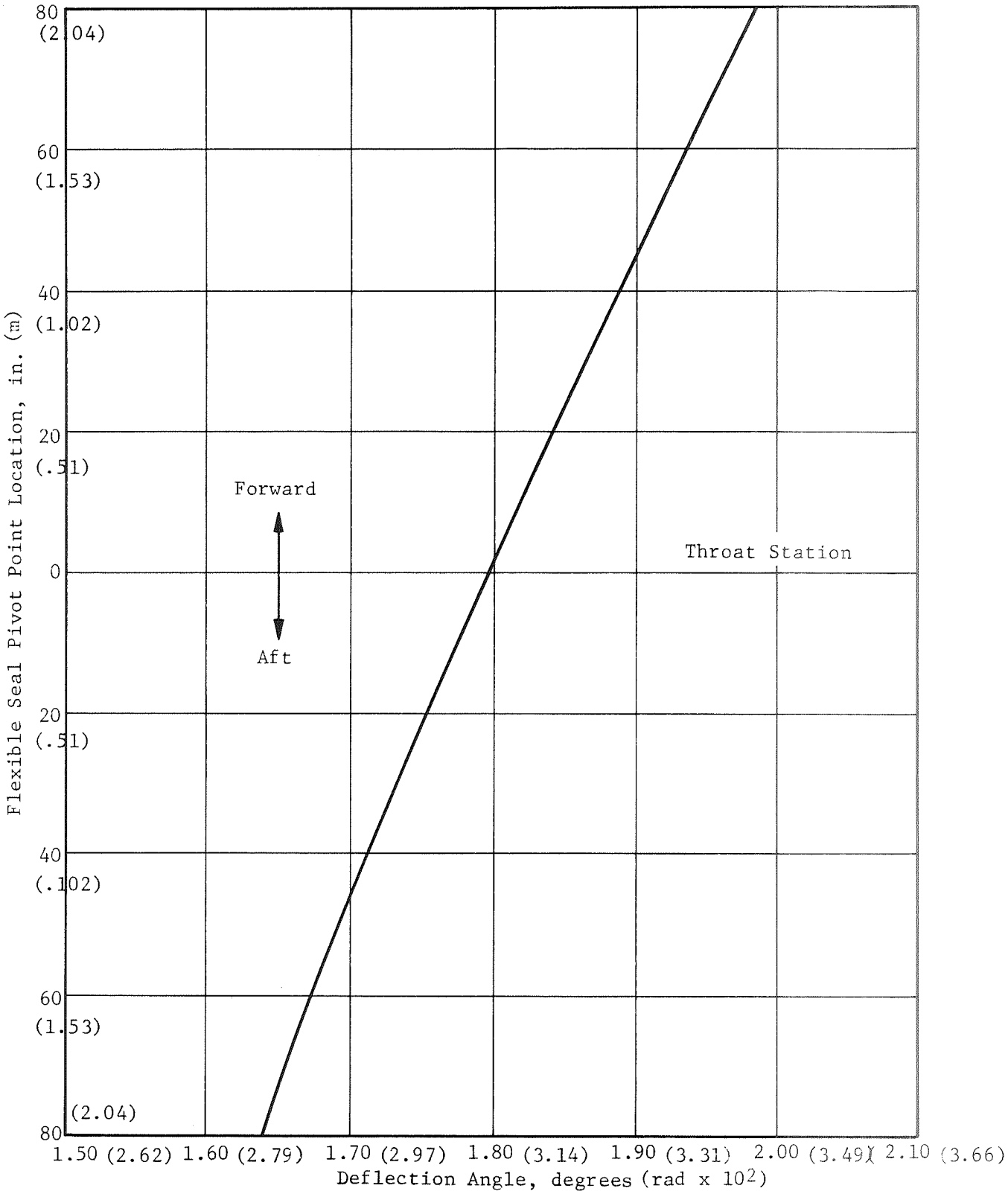

Figure 1. - Variation of Deflection Angle vs Pivot Point Location

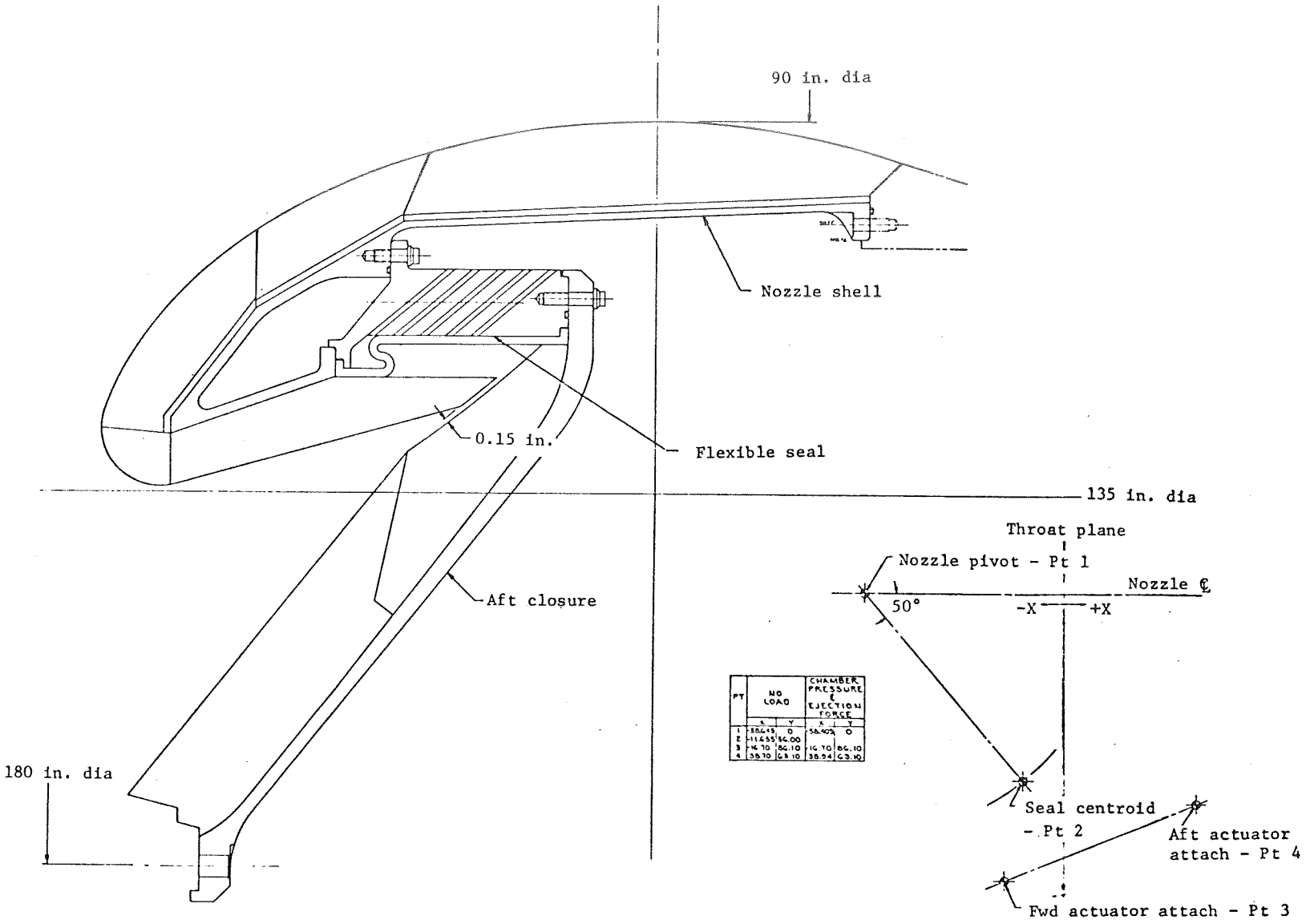

Figure 2. - Nozzle Design for 260-in.-dia Motor

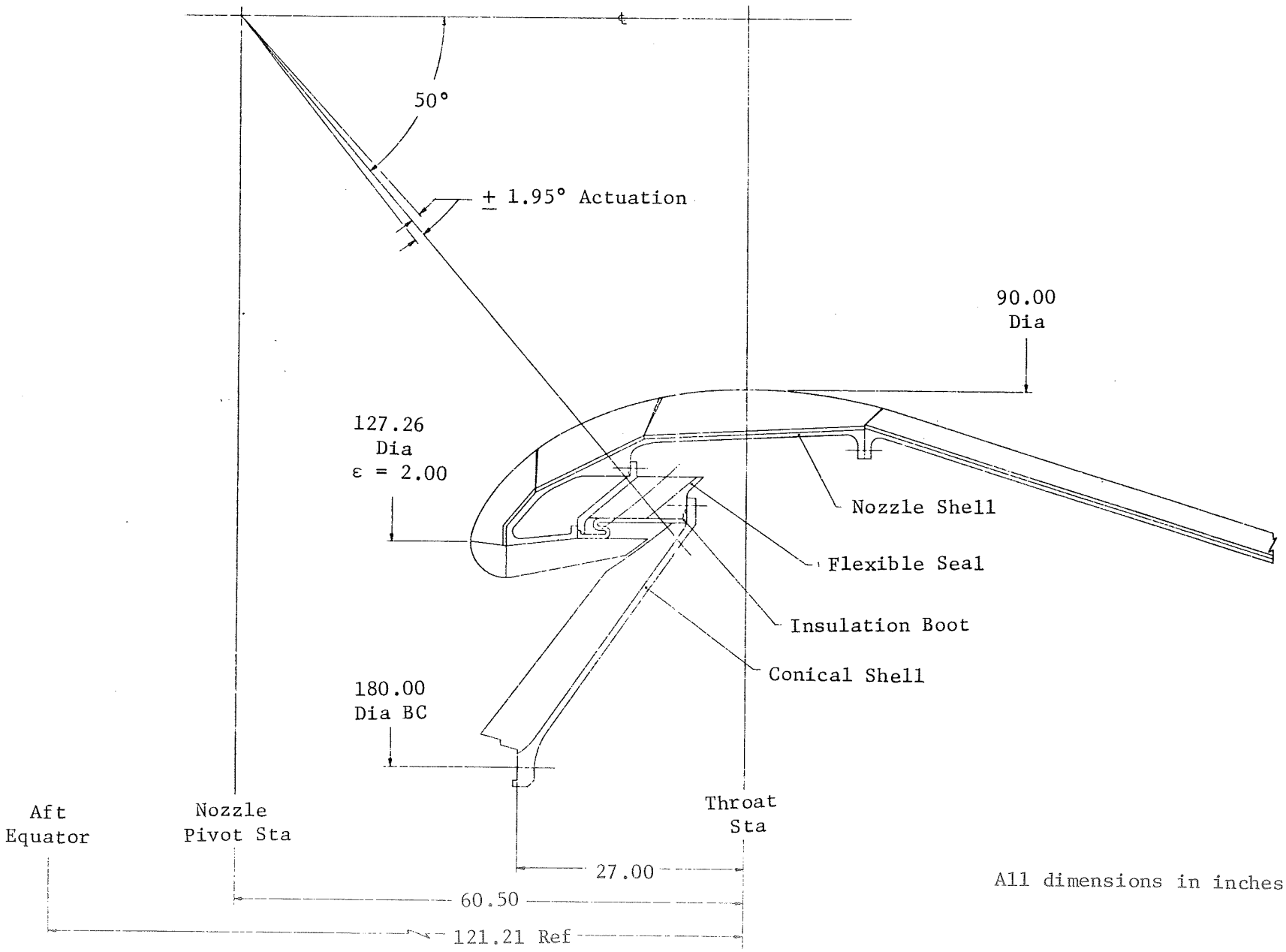

Figure 3. - Nozzle Design with Forward Pivot Flexible Seal

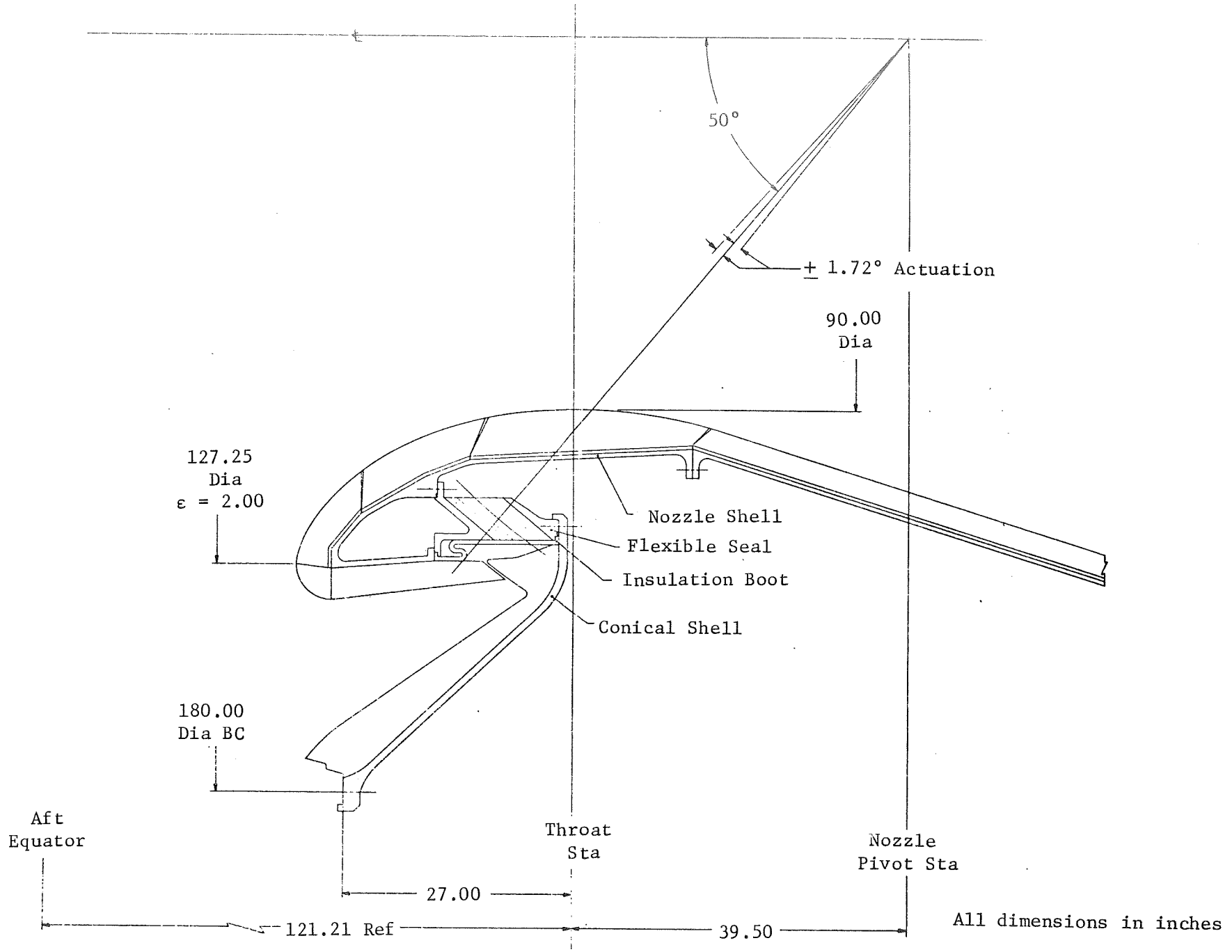

Figure 4. - Nozzle Design with Aft Pivot Flexible Seal

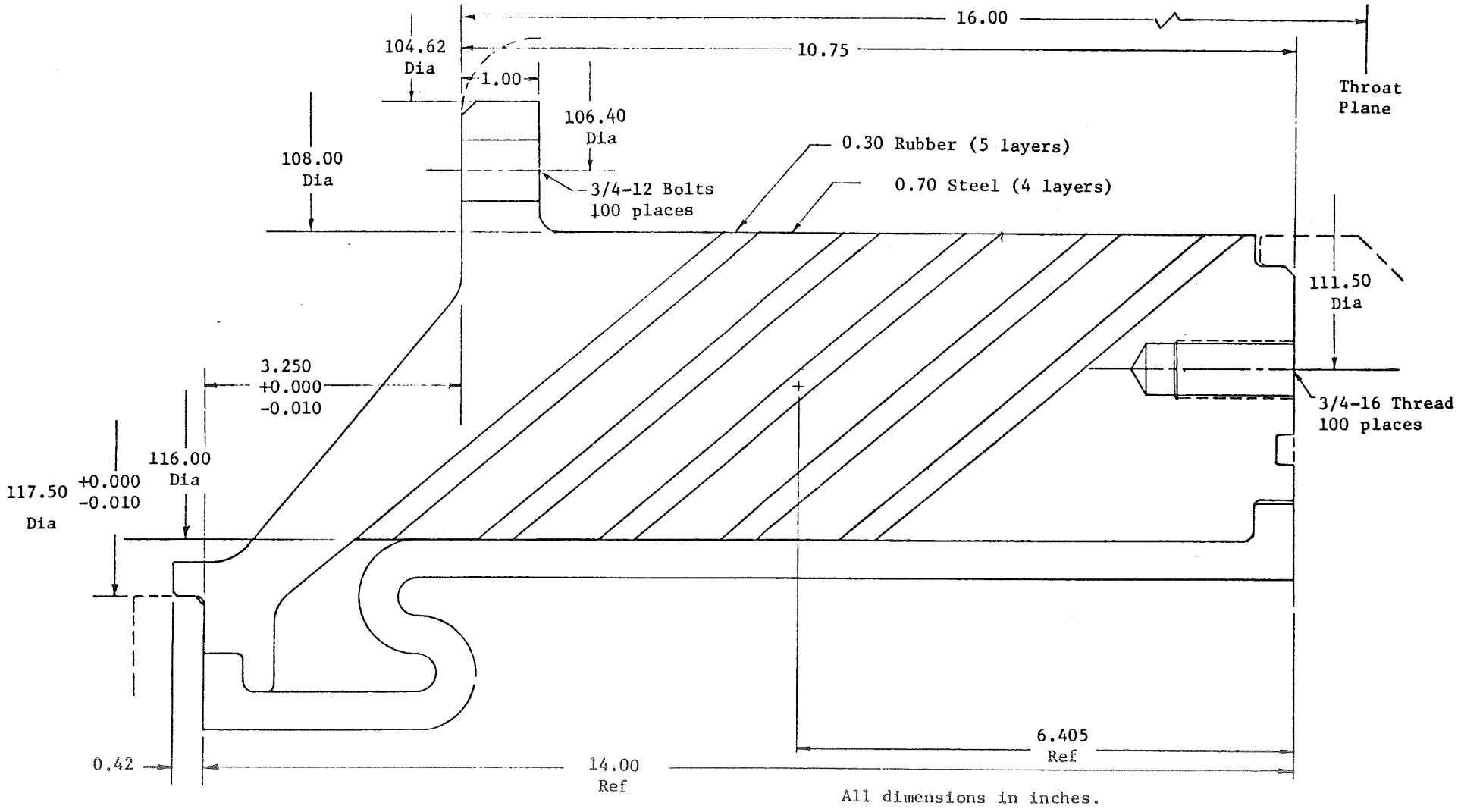

Figure 5. - Flexible Seal Design

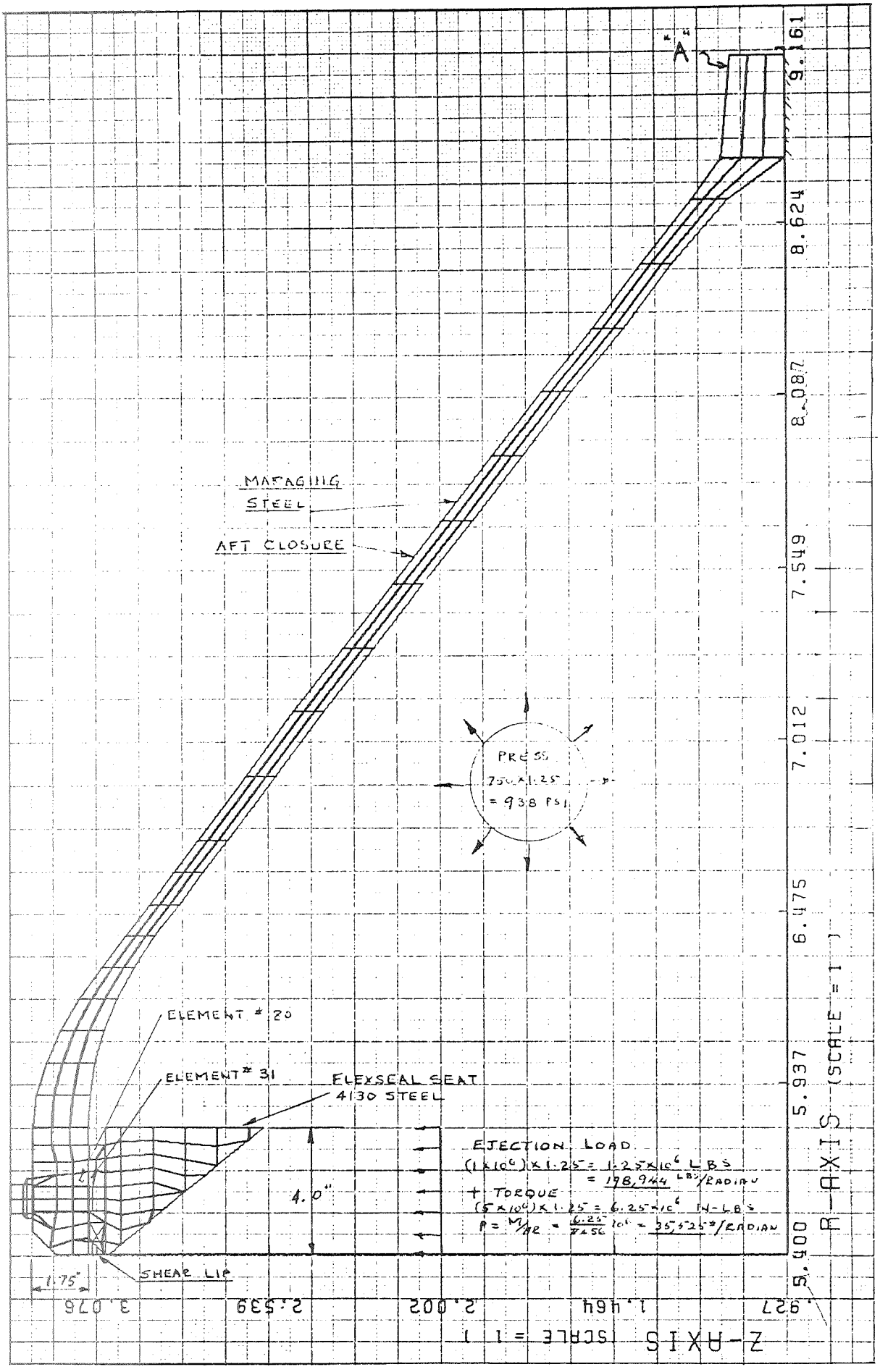

Figure 6. - Structural Analysis Grid for Flexible Seal and Aft Closure

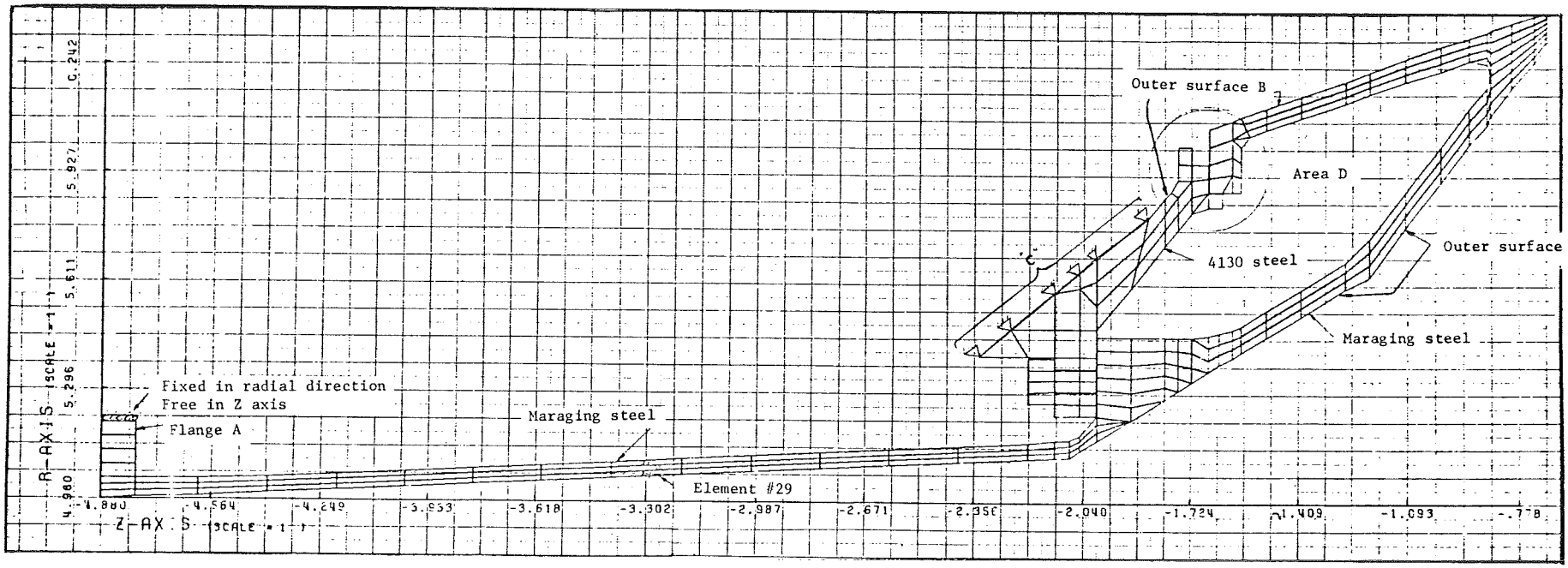

Figure 7. - Structural Analysis Gird for Flexible Seal and Nozzle Shell

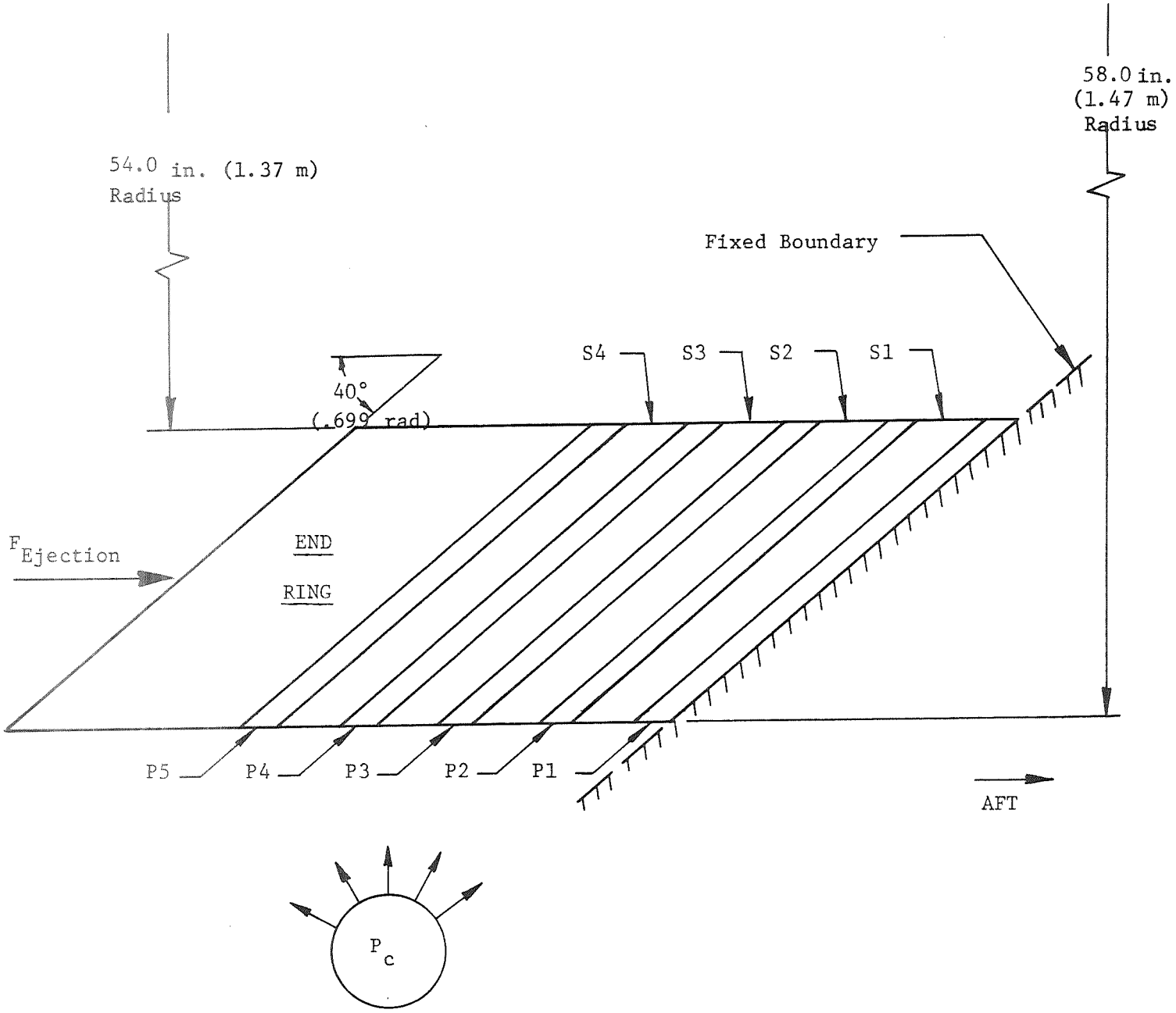

Shim (S) Thk. = 0.7 in. (.0178 m)

Pad (P) Thk. = 0.3 in. (.0076 m)

Figure 8. - Flexible Seal Analytical Model

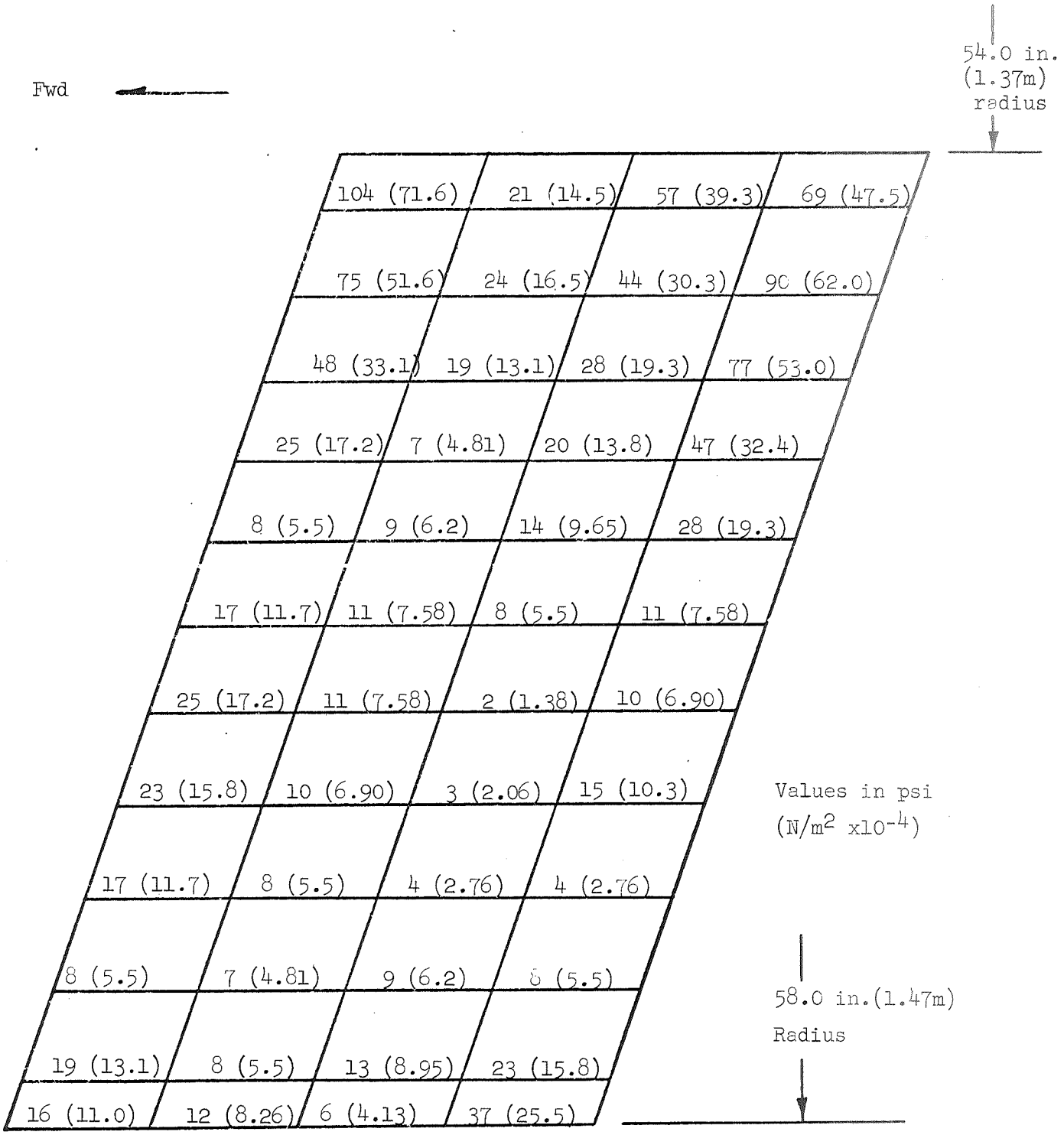

Figure 9. — Maximum Shear Stress in Pad P5 for Load Condition (1)

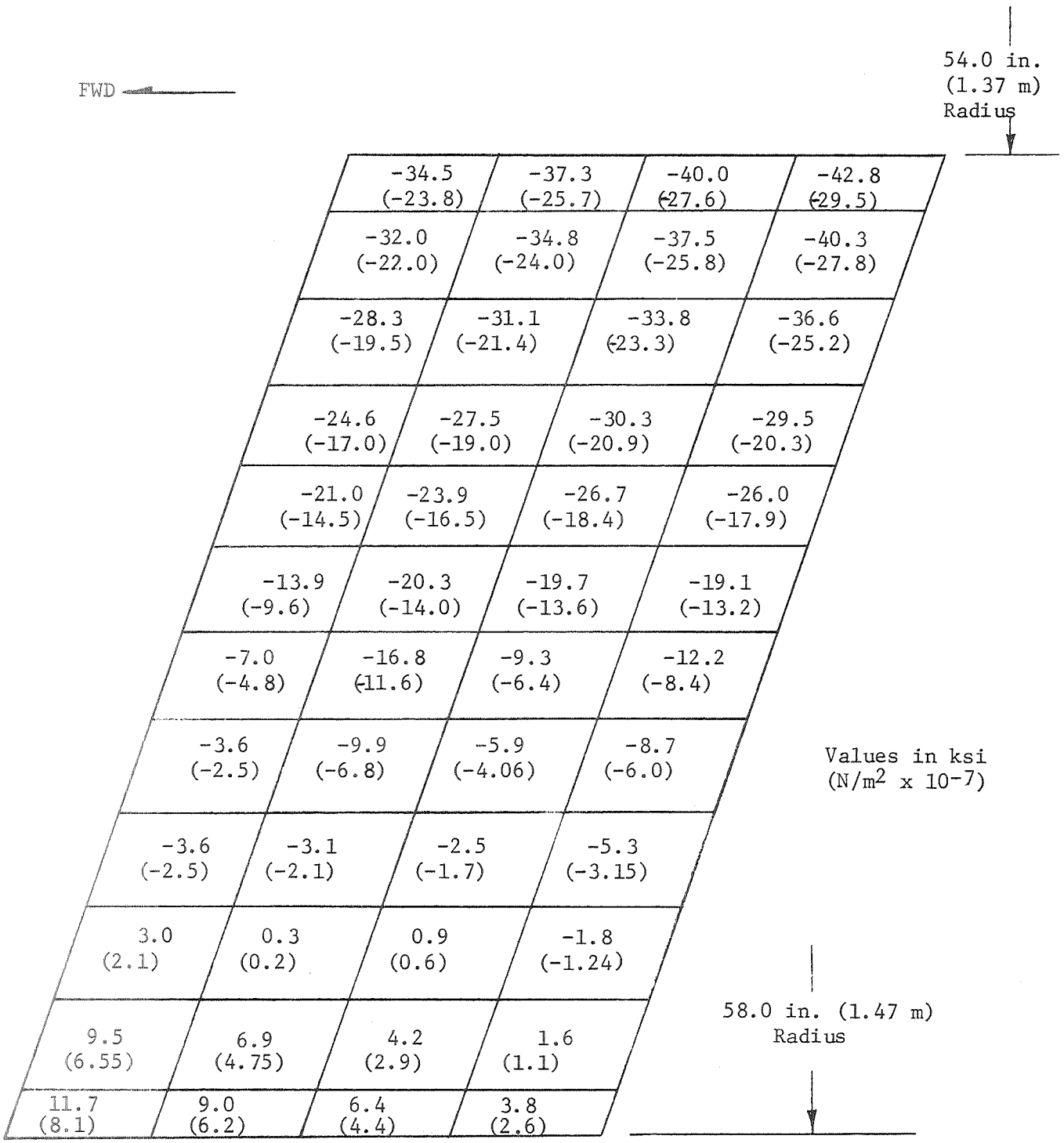

Figure 10. - Maximum Hoop Stress in Shim S2 for Load Condition (1)

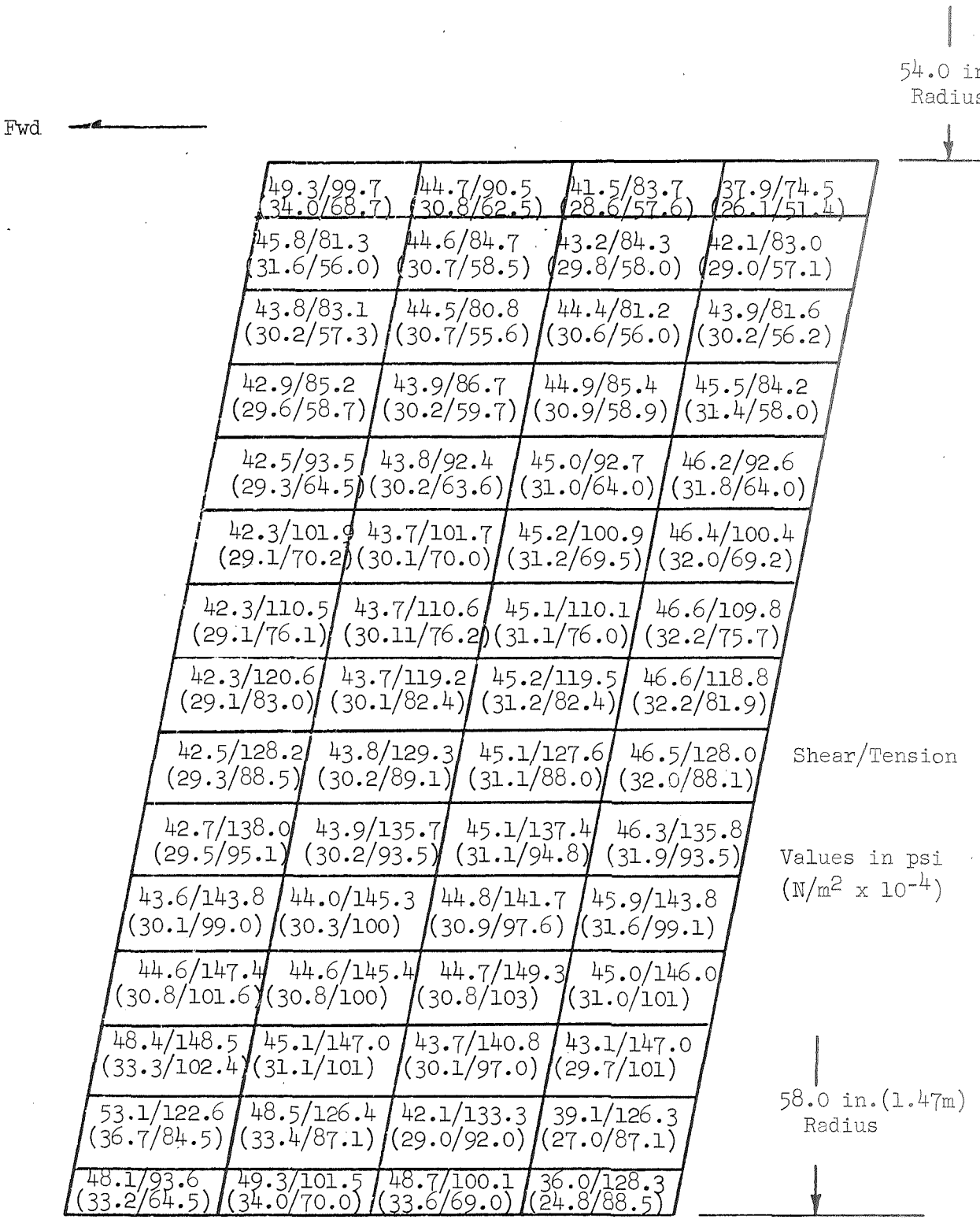

Figure 11.- Maximum Tension and Shear Stress in Pad P5 for Load Condition (2)

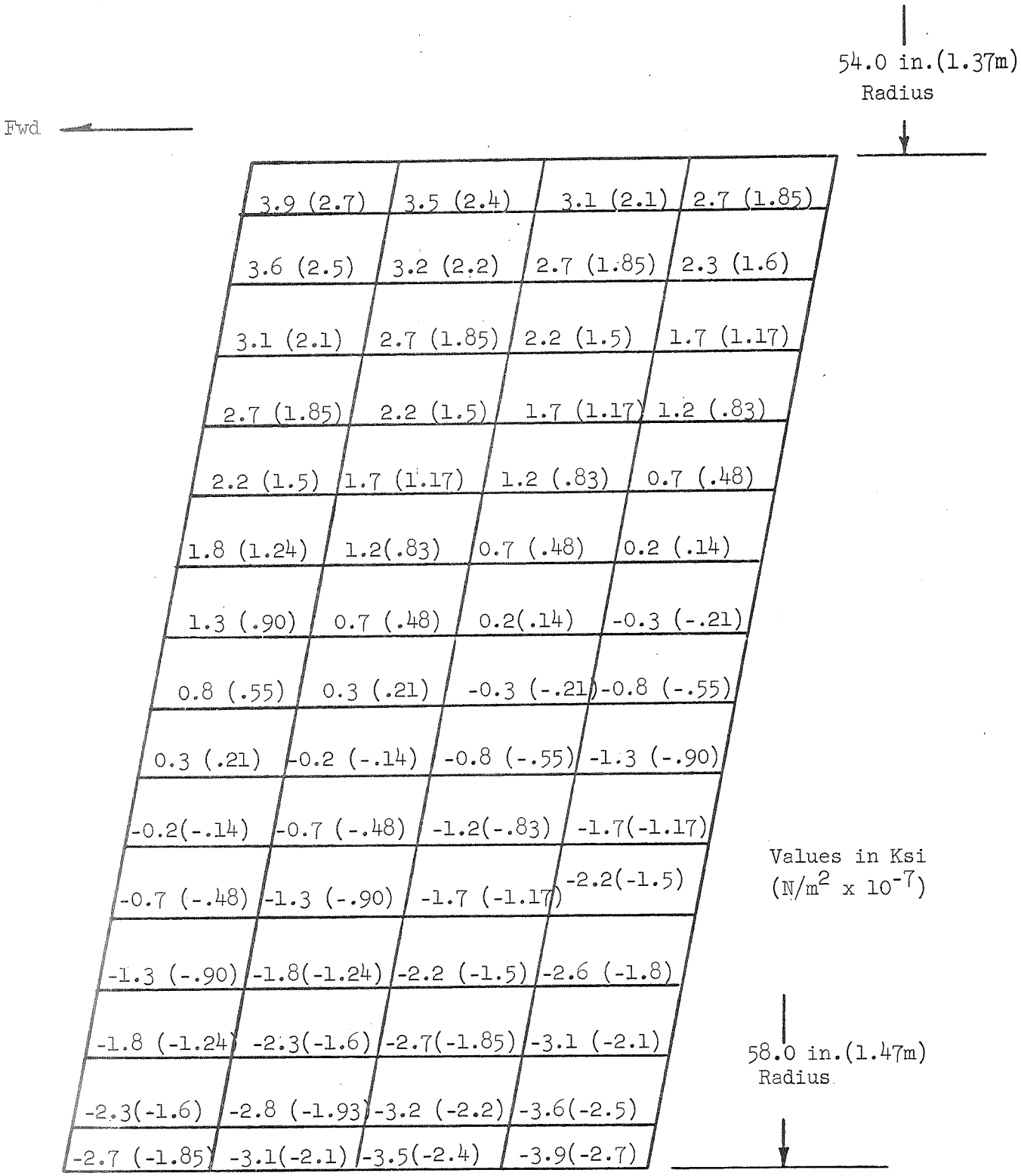

Figure 12.- Maximum Hoop Stress in Shim S2 for Load Condition (2)

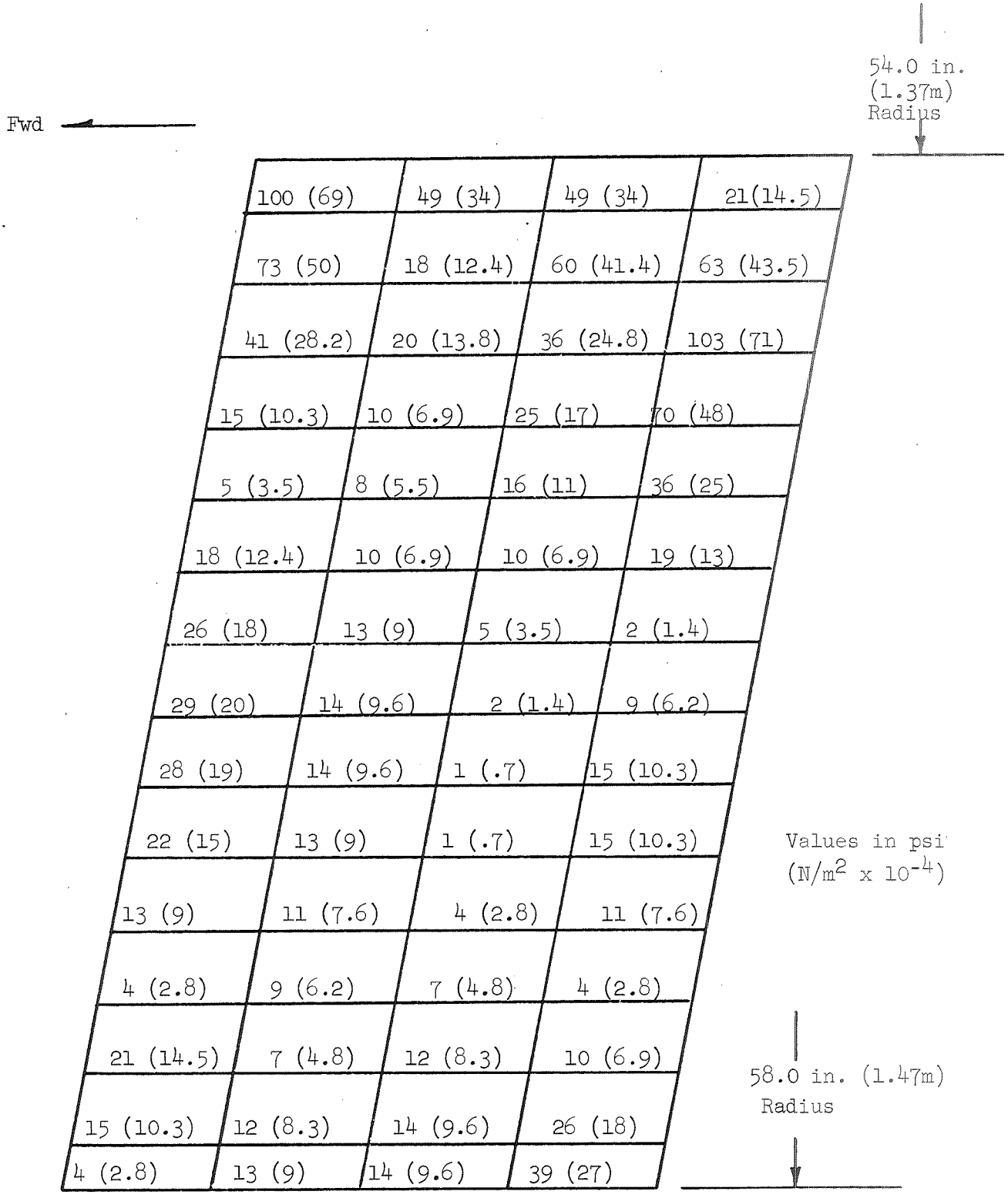

Figure 13.- Maximum Shear Stress in Pad P5 for Load Condition (3) and Clockwise Rotation

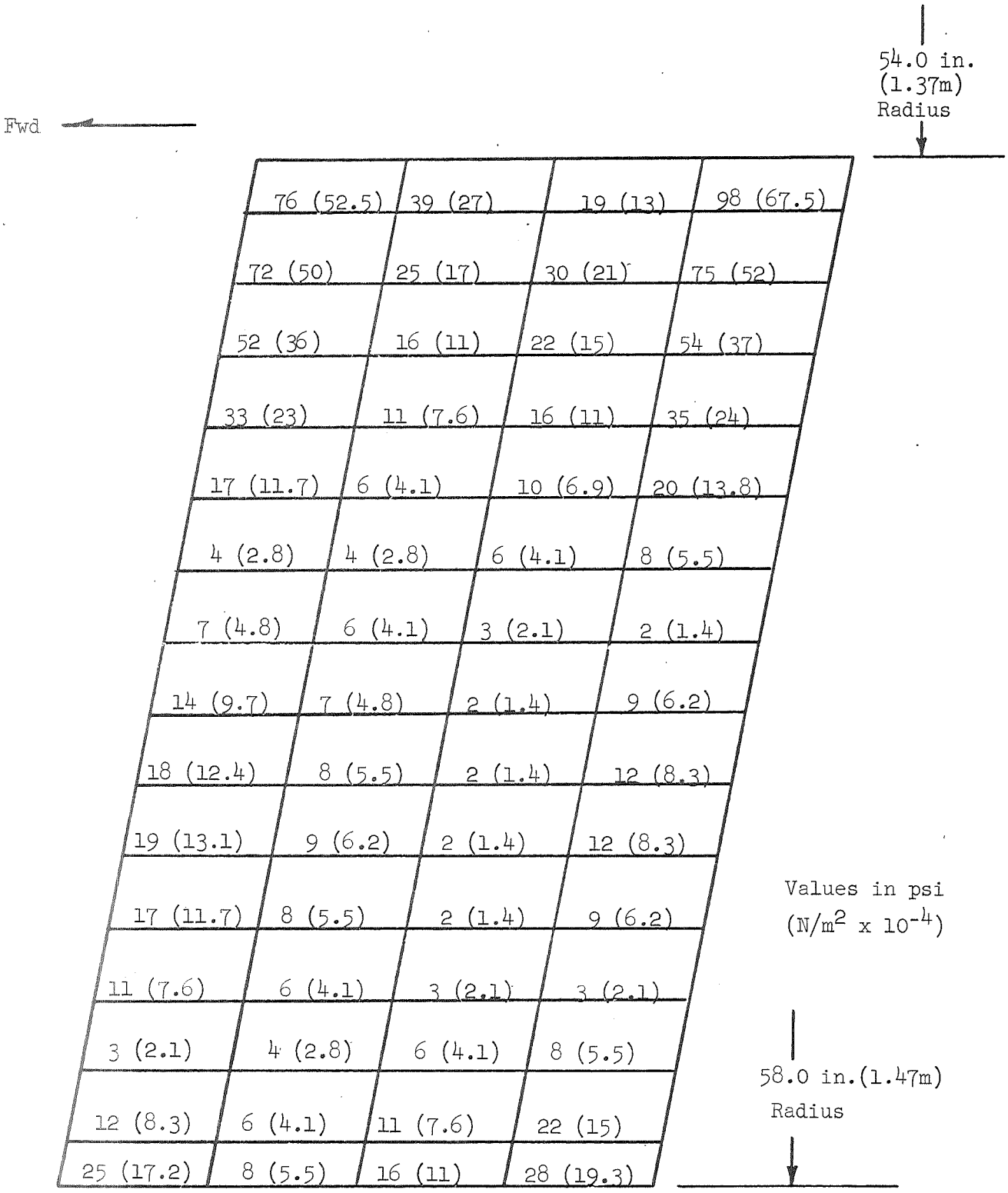

Figure 14.- Maximum Shear Stress in Pad P5 for Load Condition (3) and Counterclockwise Rotation

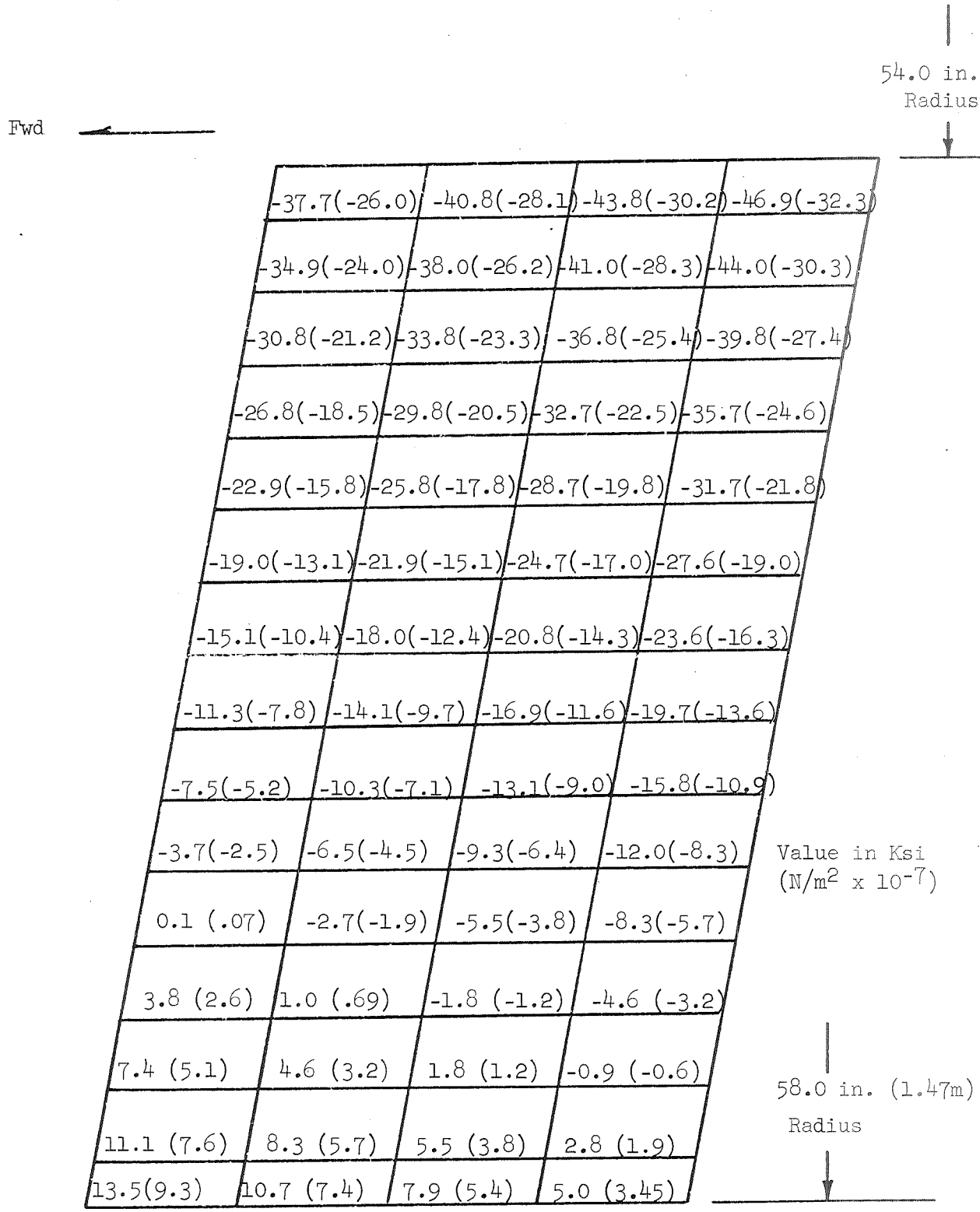

Figure 15.- Maximum Hoop Stress in Shim S3 for Load Condition (3) and Clockwise Rotation.

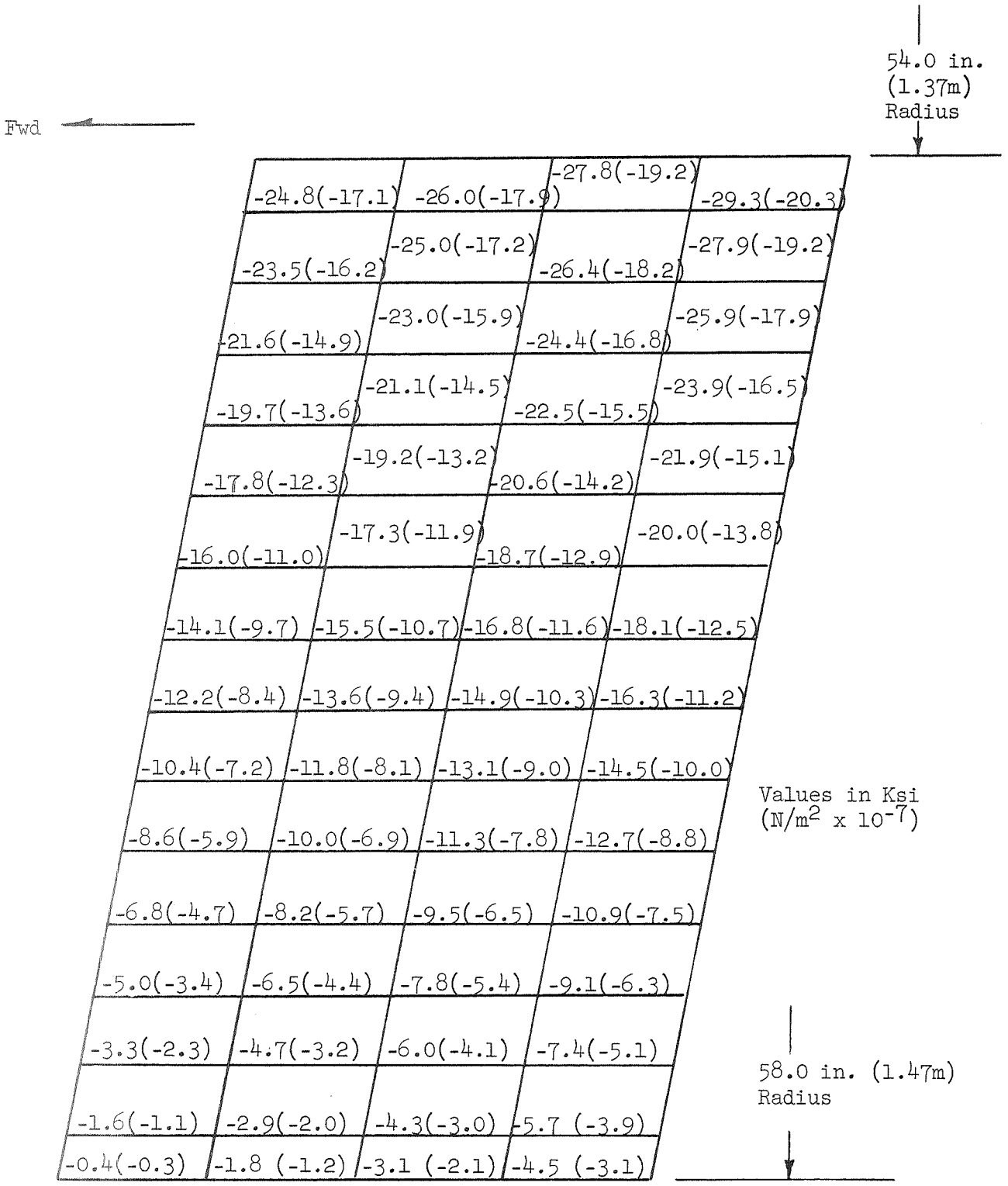

Figure 16.- Maximum Hoop Stress in Shim S3 for Load Condition (3) and Counterclockwise Rotation.

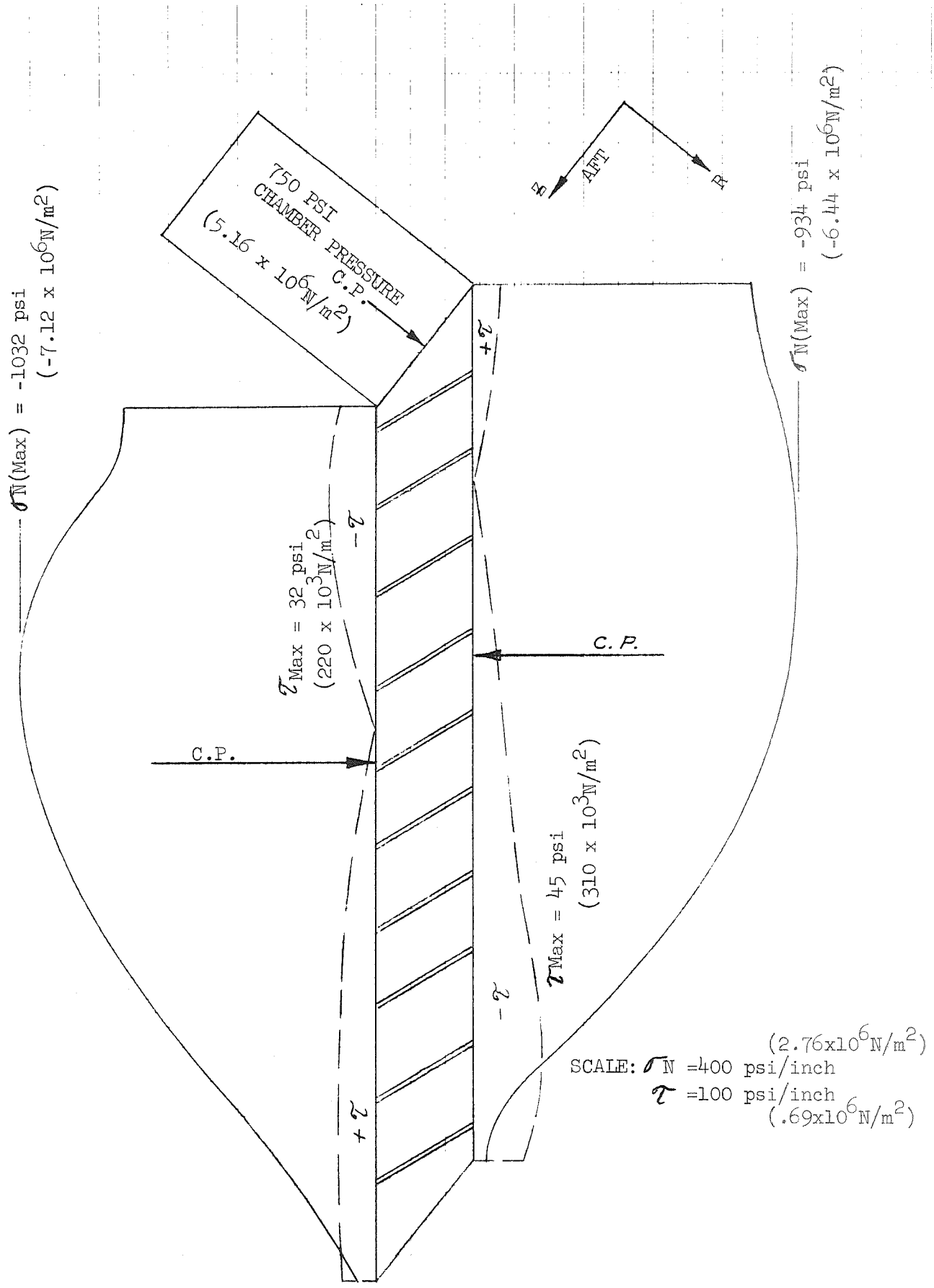

Figure 17. - Typical Stress Distribution at Metal Shim Interface

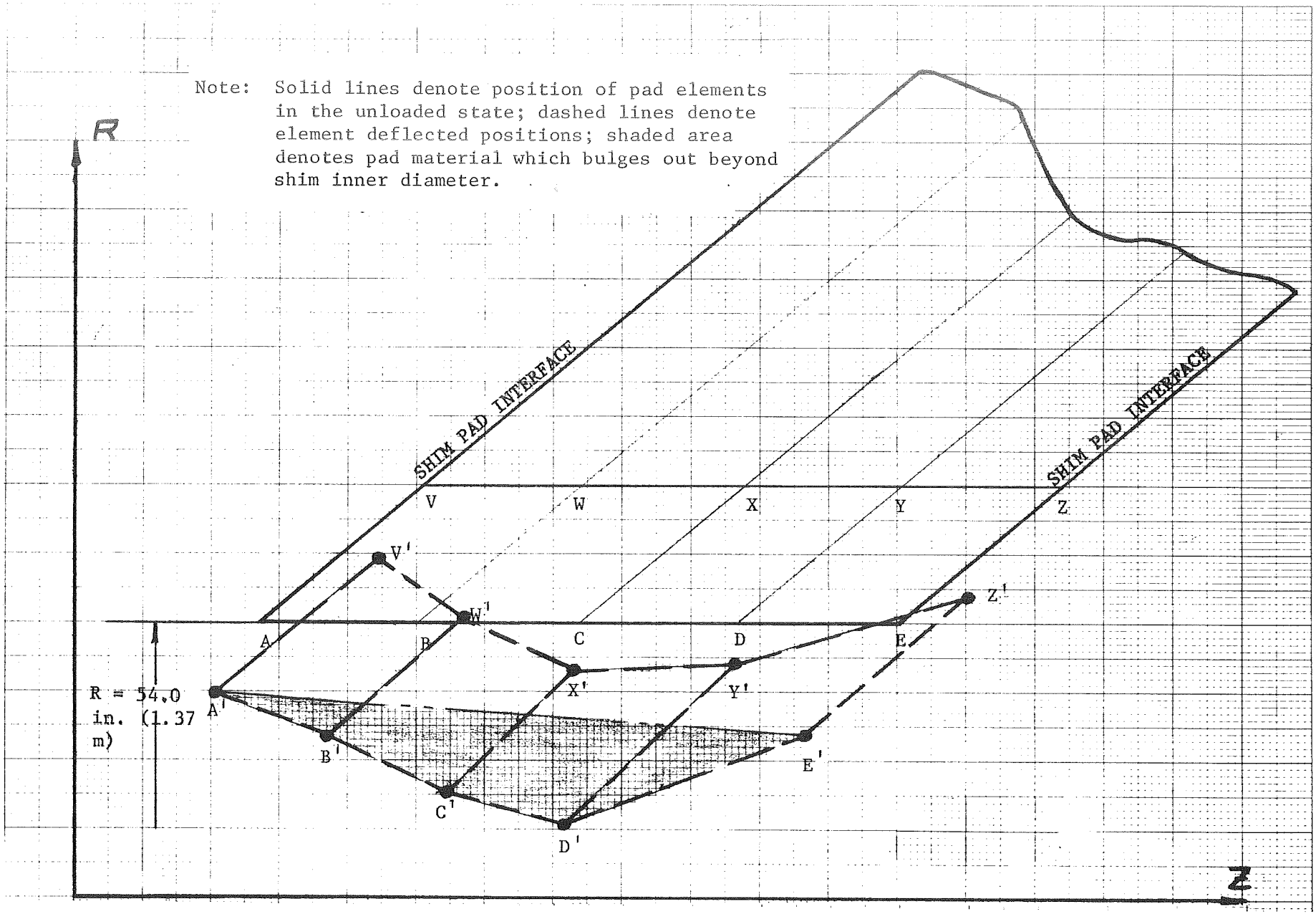

Figure 18. - Local Deformation at Inner Edge of Elastomer Pad Under Pressure and Ejection Loads

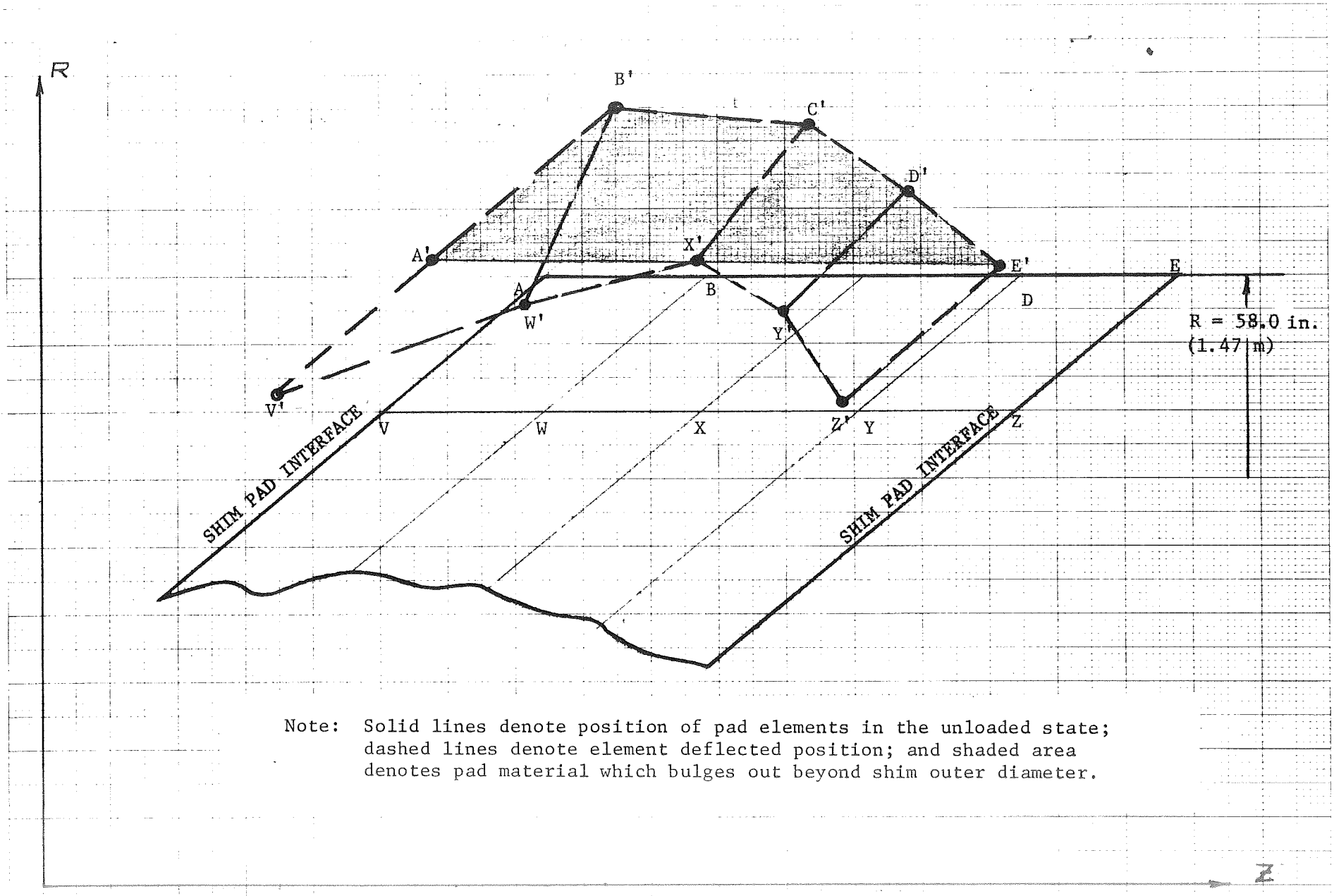

Note: Solid lines denote position of pad elements in the unloaded state; dashed lines denote element deflected position; and shaded area denotes pad material which bulges out beyond shim outer diameter.

Figure 19. - Local Deformation at Outer Edge of Elastomer Pad Under Pressure and Ejection Loads

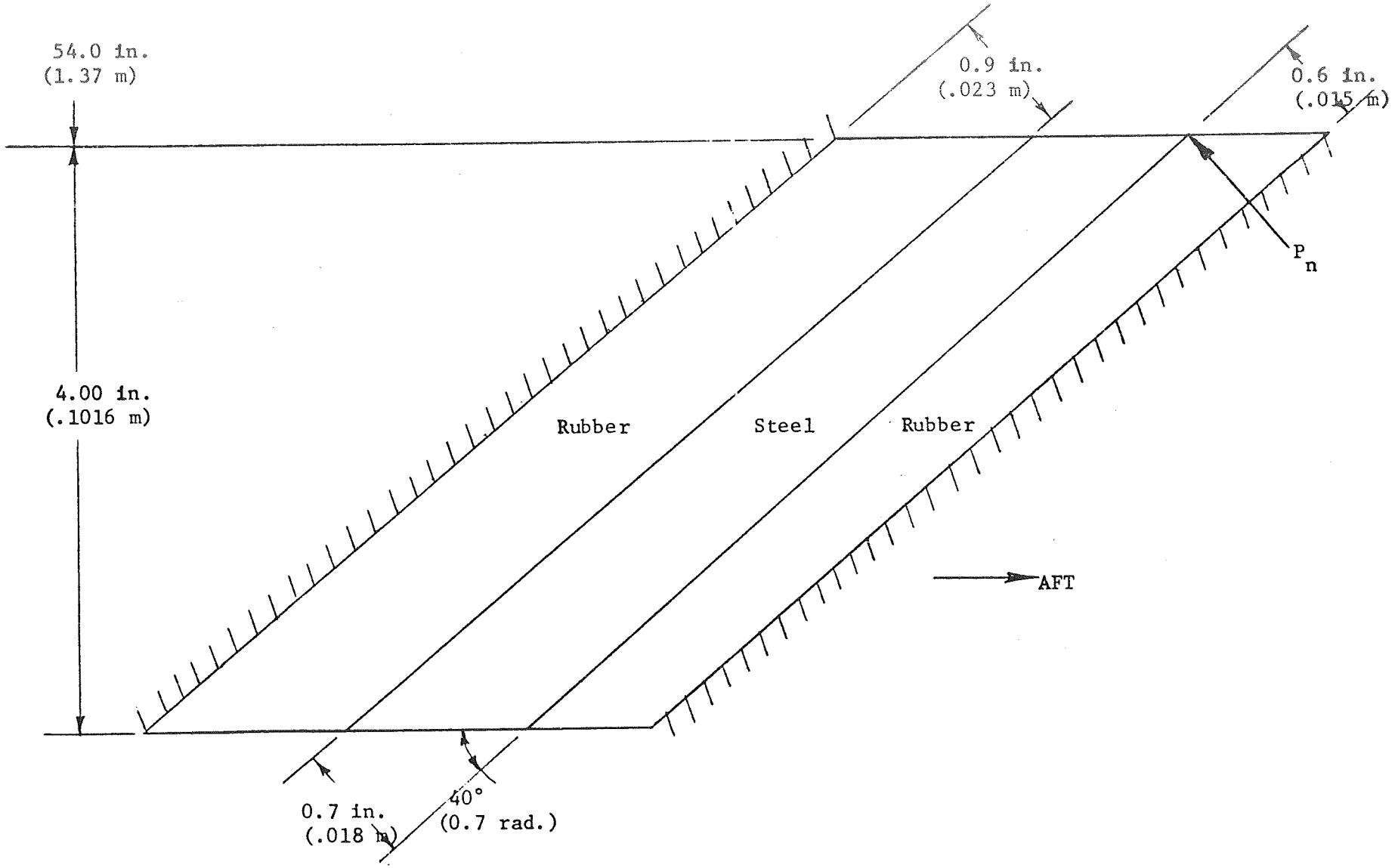

Figure 20. - Analytical Model for the Elastic Stability Analysis of the Steel Shim

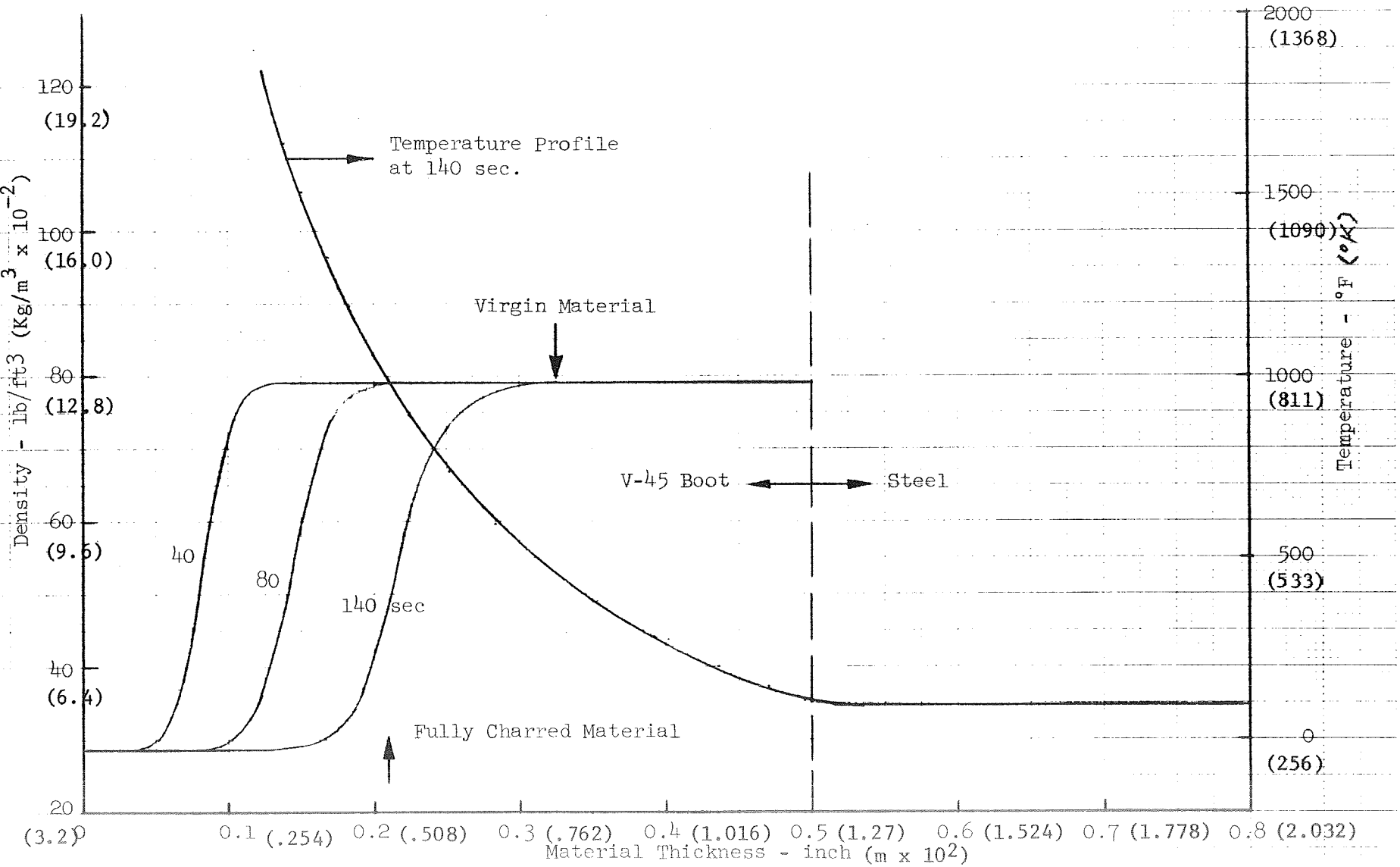

Figure 21. - Thermal History - Elastomer Boot and Flexible Seal

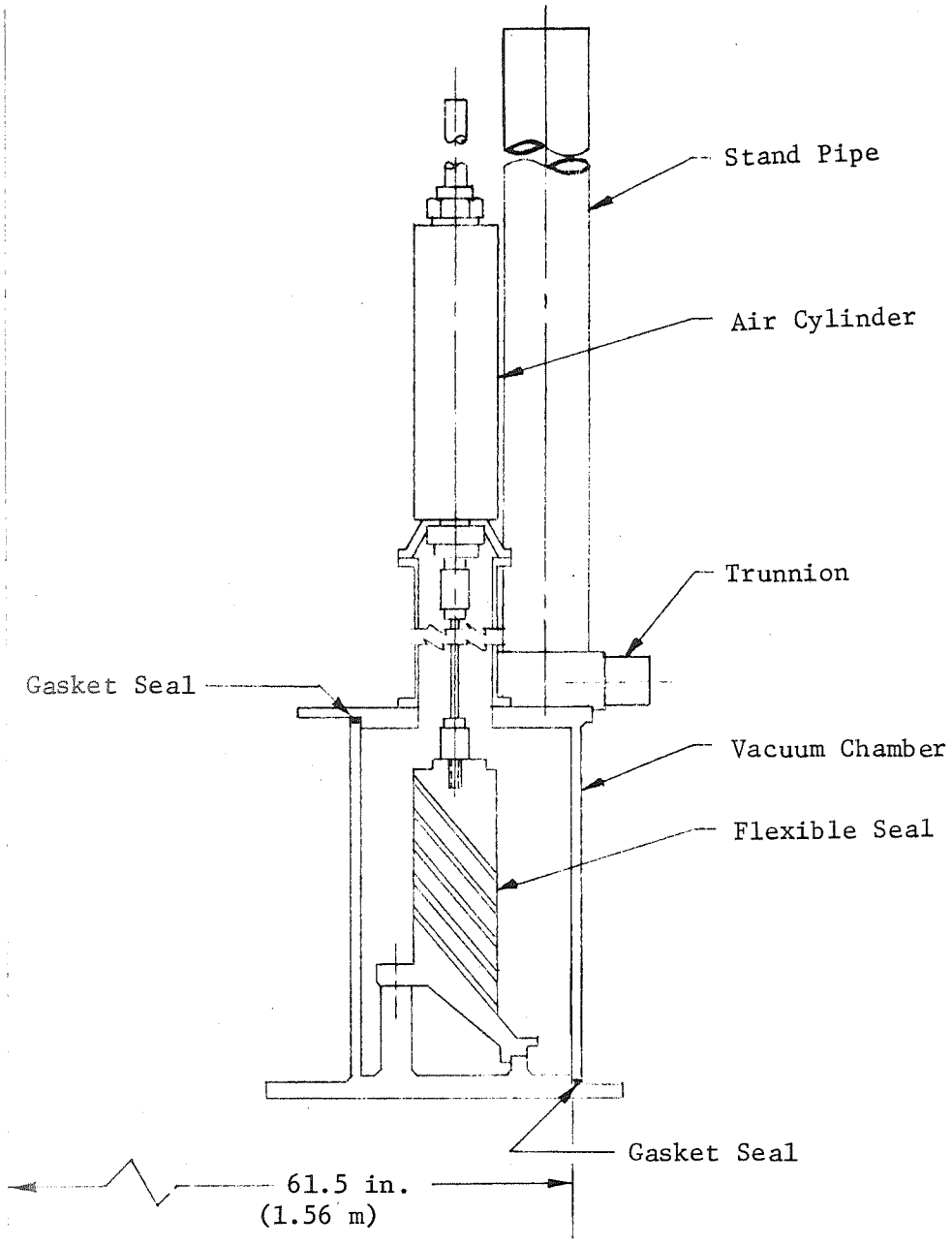

Figure 22. - Flexible Seal Assembly Fixture

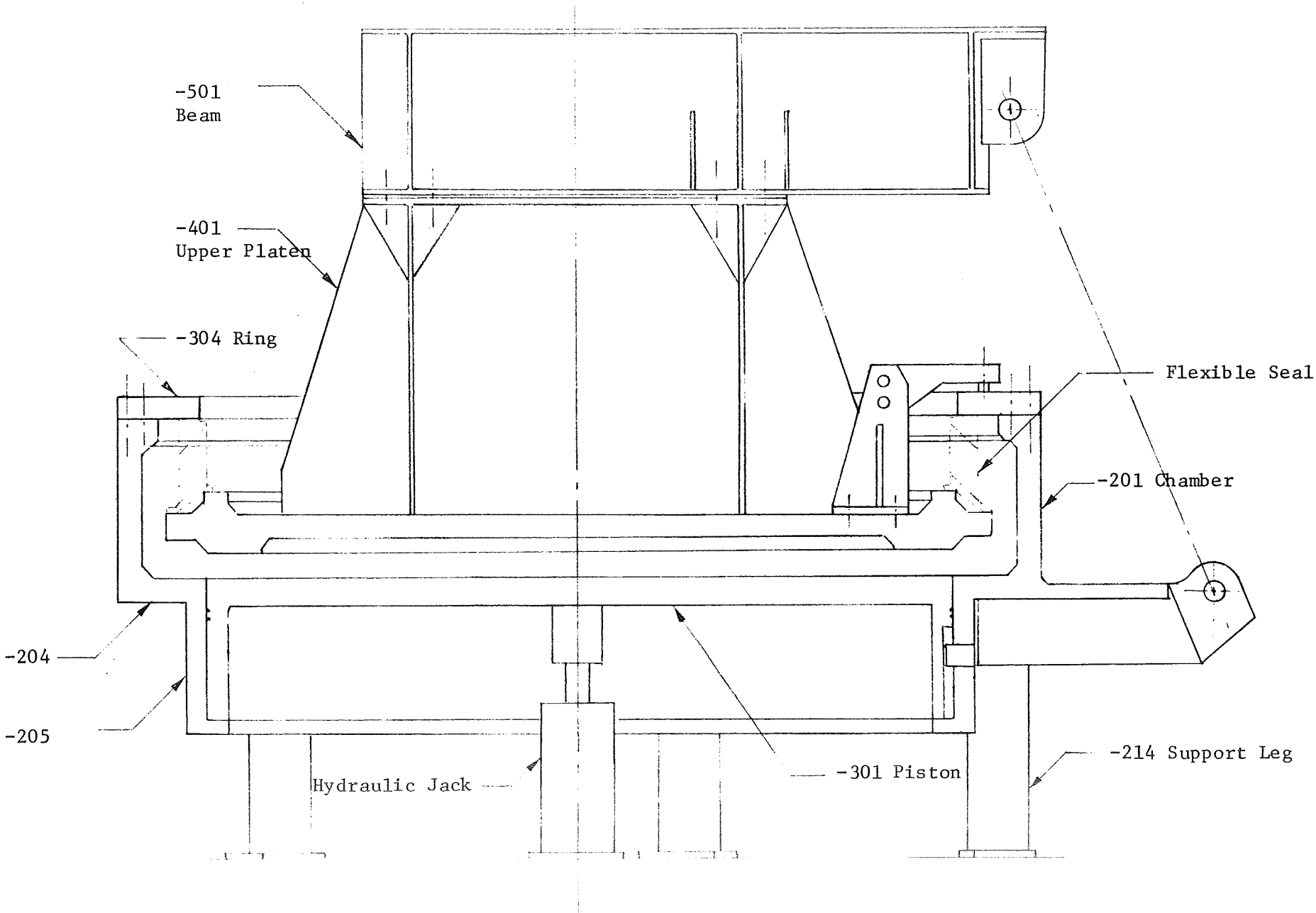

Figure 23. - Flexible Seal Test Fixture

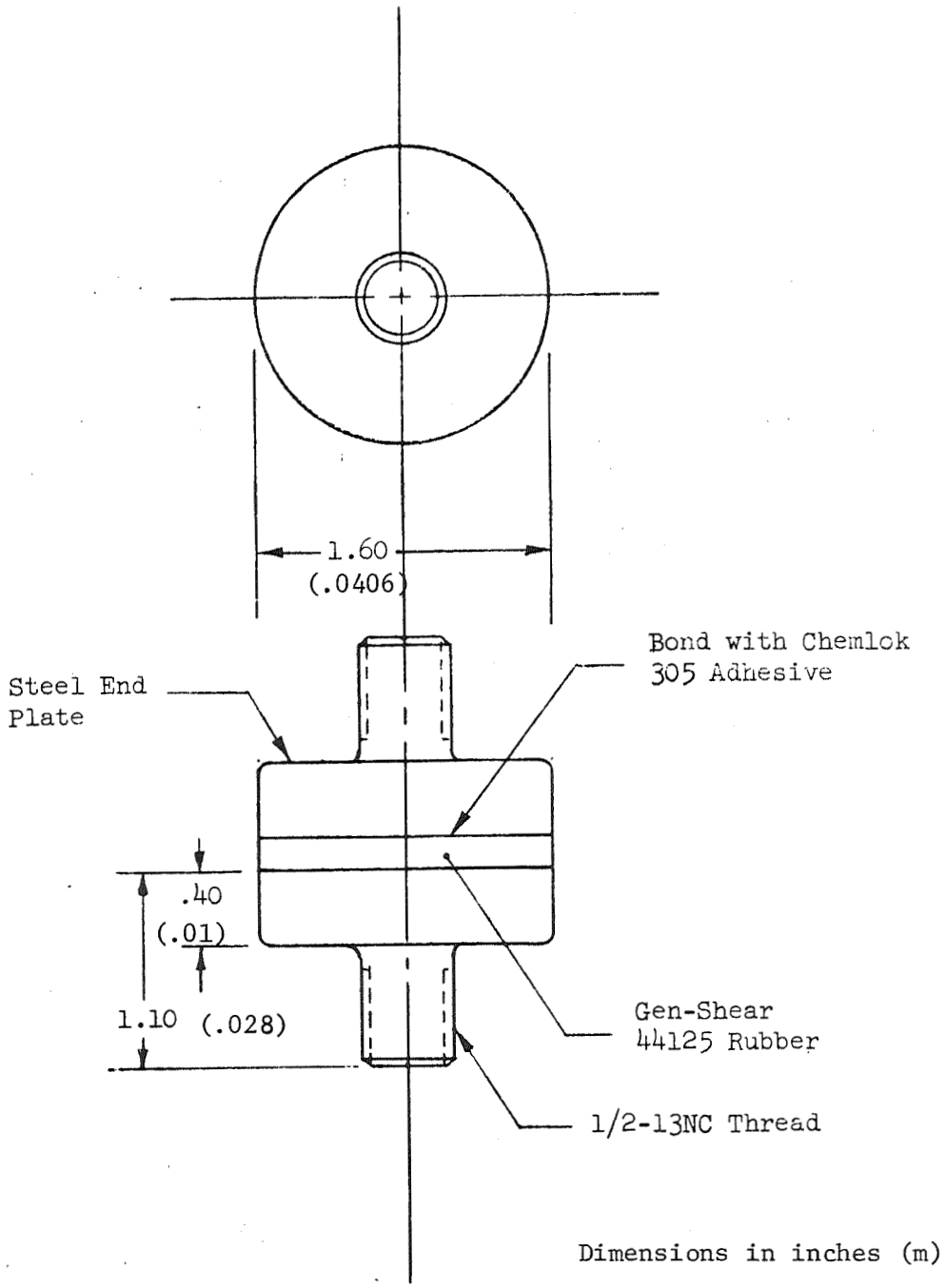

Figure 24. - Tensile Test Specimen

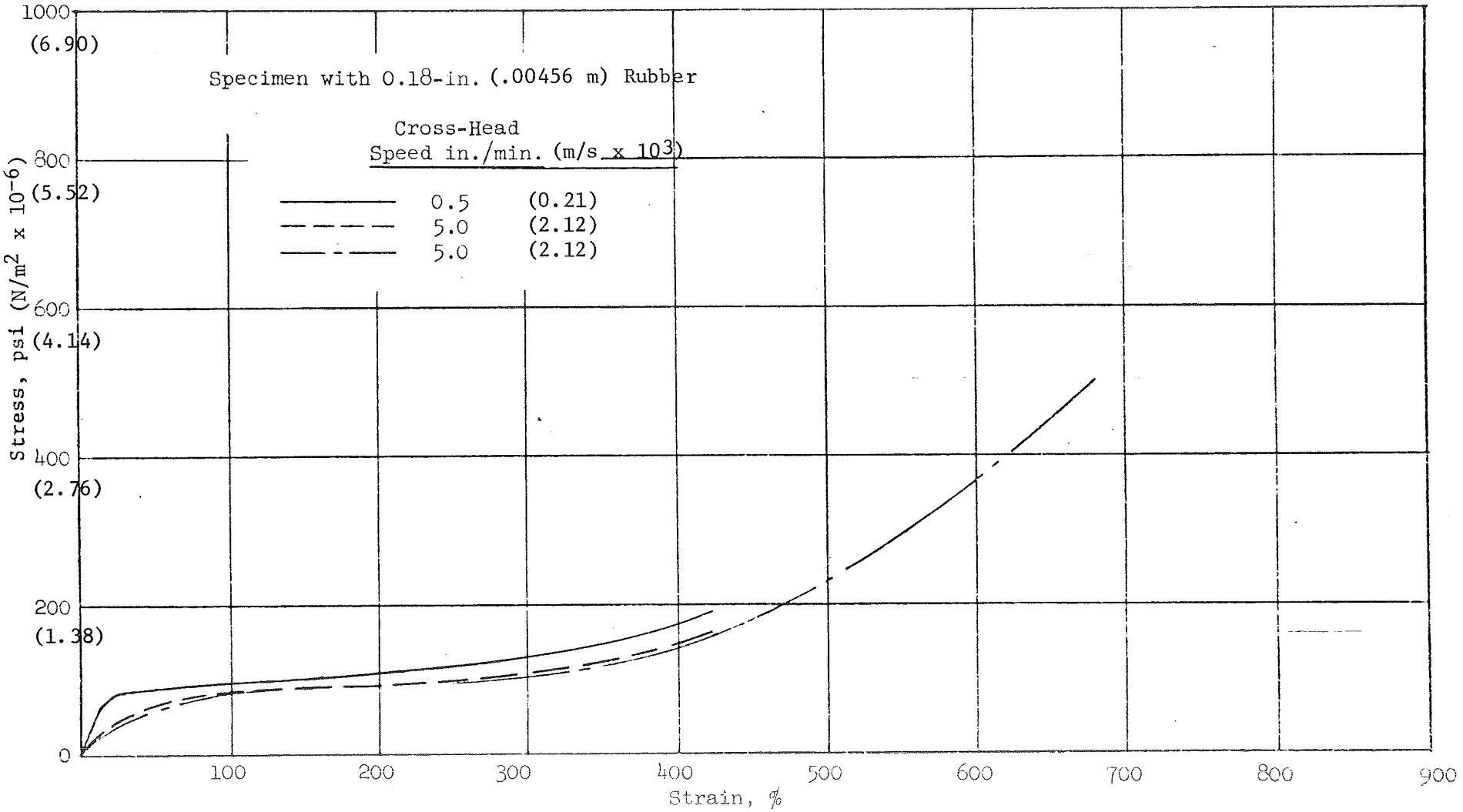

Figure 25. - Tensile Stress vs Strain, 0.18-in. Rubber

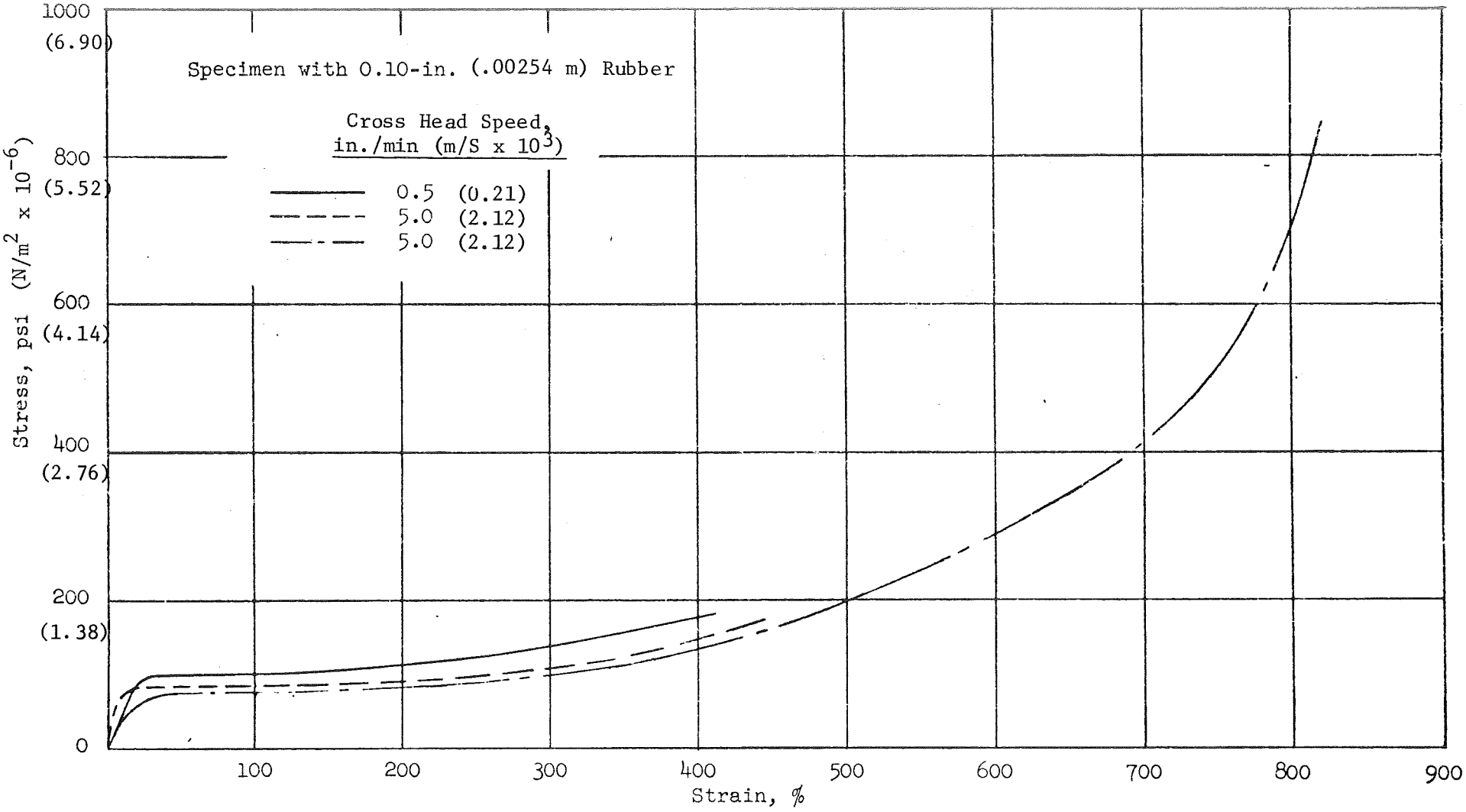

Figure 26. - Tensile Stress vs Strain, 0.10-in. Rubber

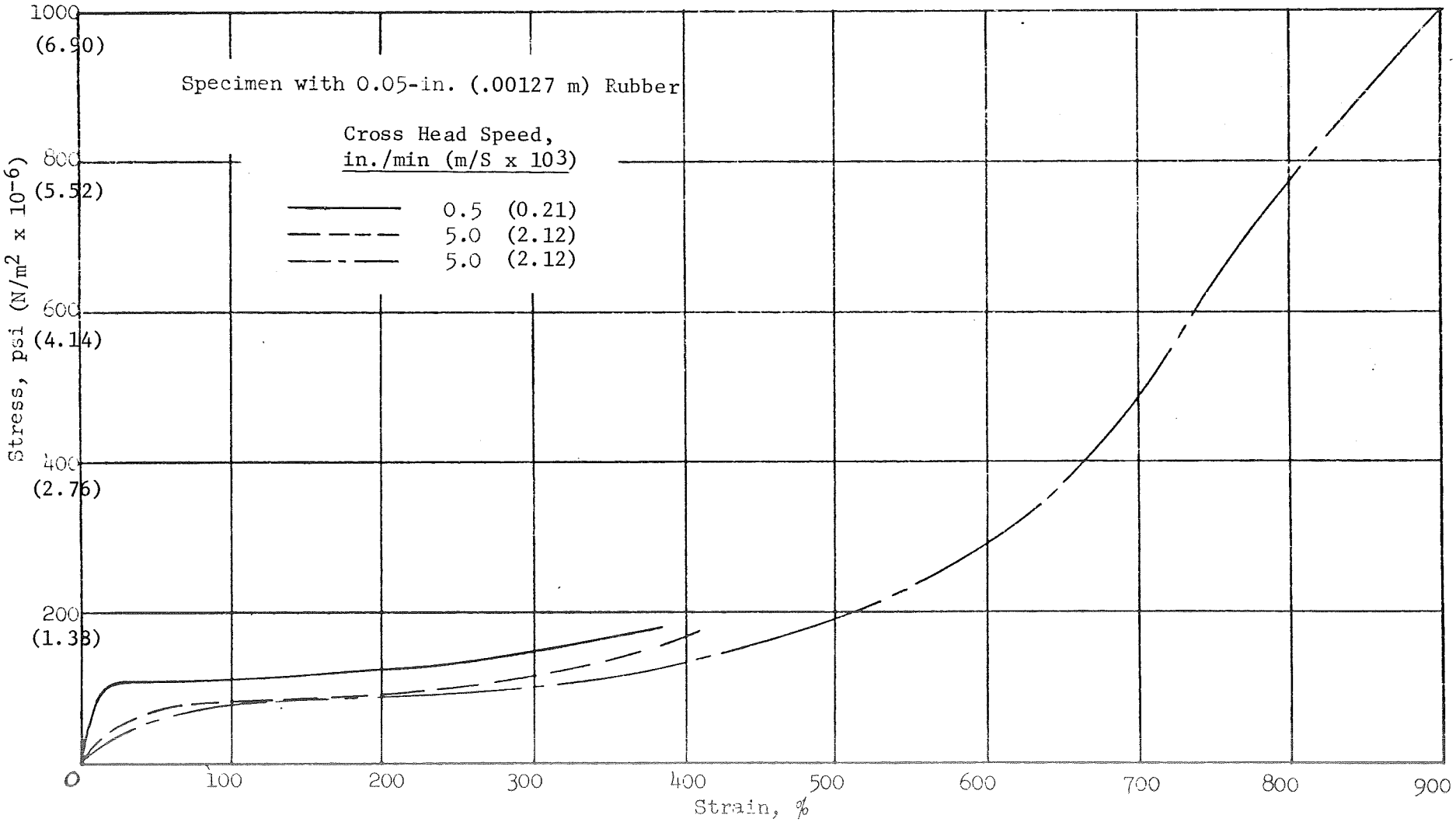

Figure 27. - Tensile Stress vs Strain, 0.05-in. Rubber

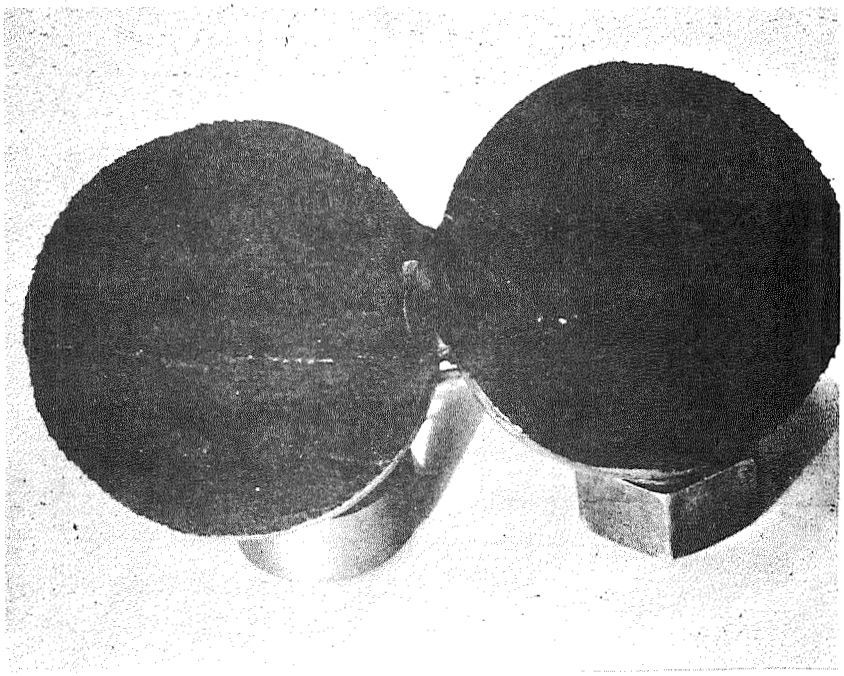

(a) start of internal failure

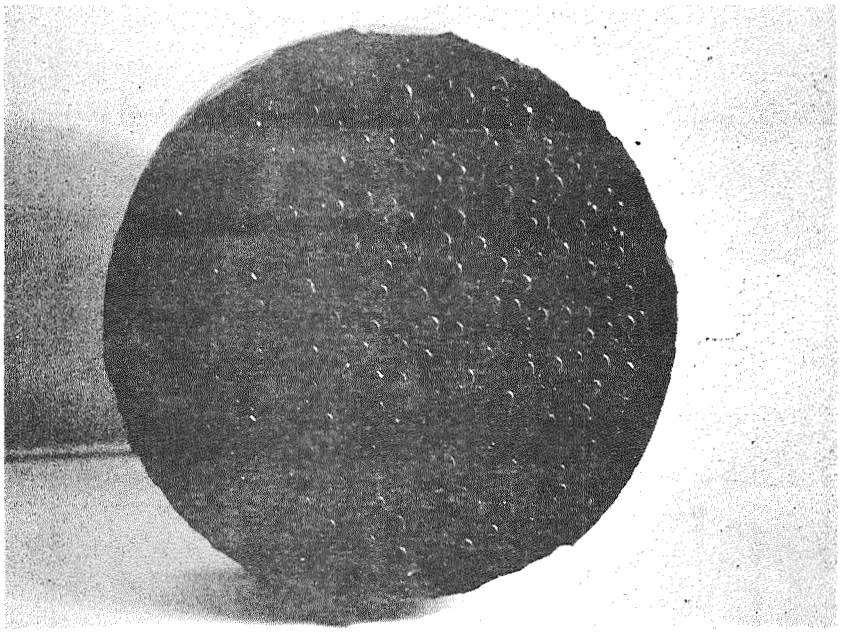

(b) internal failure at ultimate strain

Figure 28. - Internal Failure of Rubber in Tension

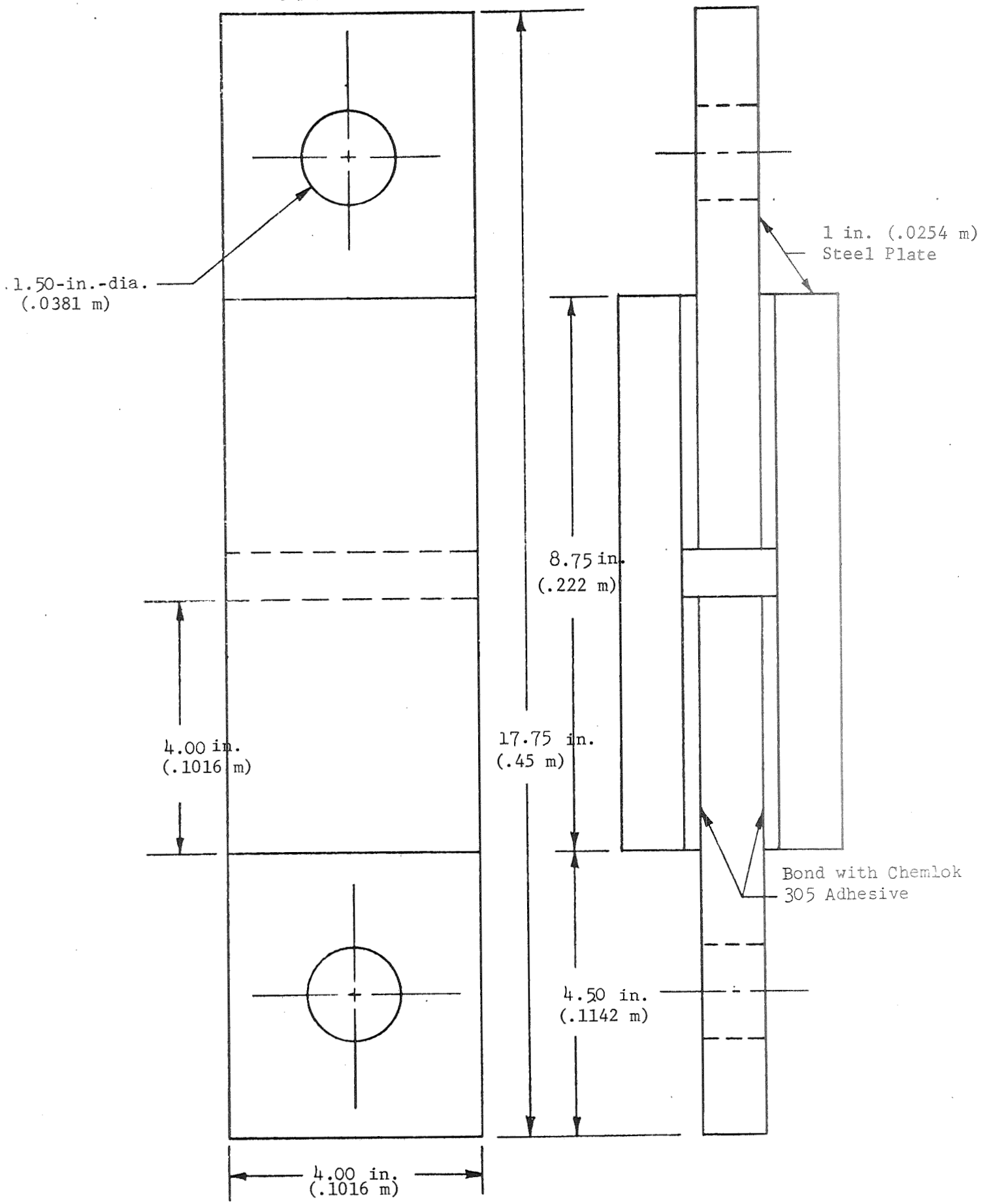

Figure 29. - Quadruple Lap Shear Specimen (4 x 4 Pad)

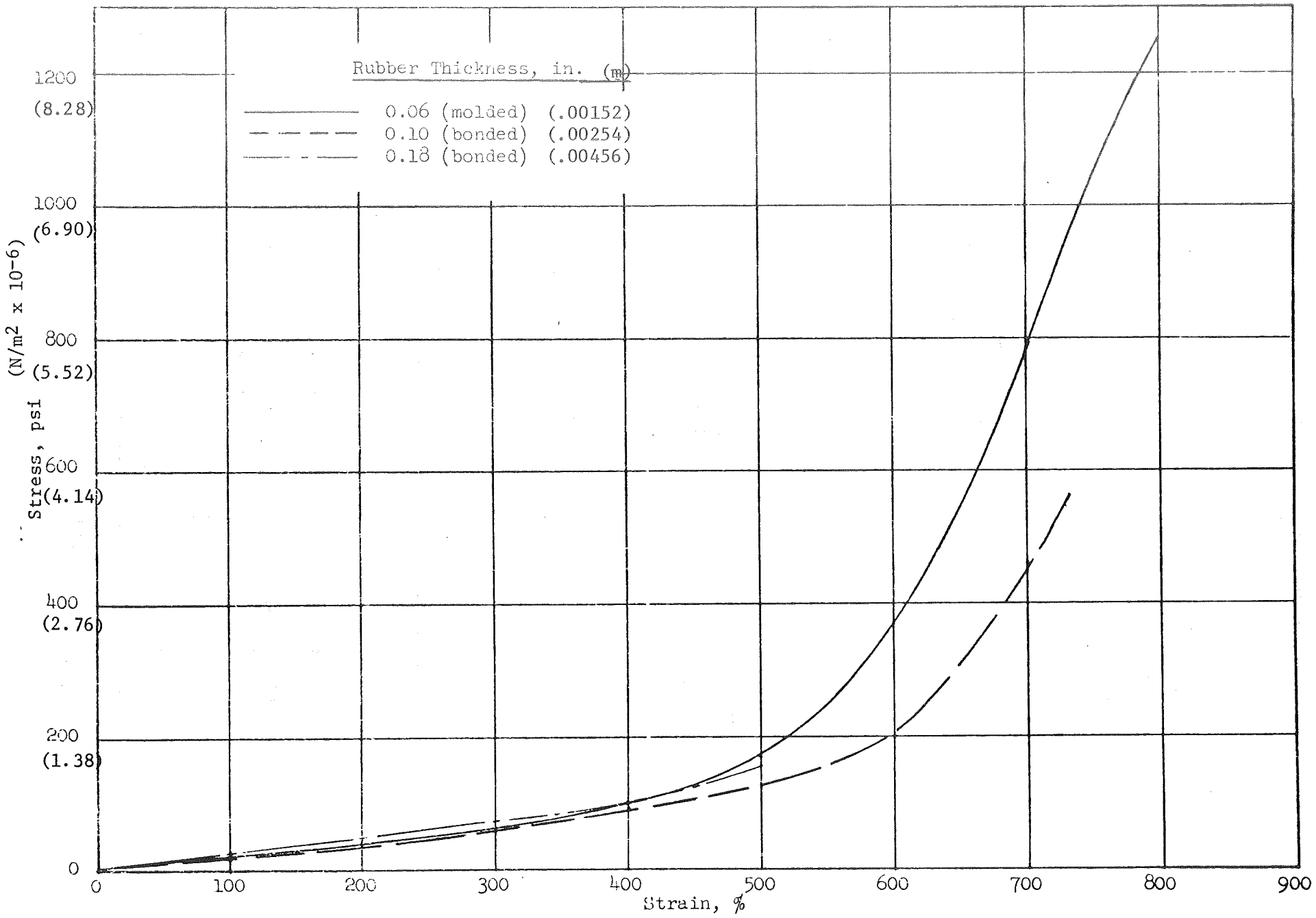

Figure 30. - Variation of Shear Stress vs Strain

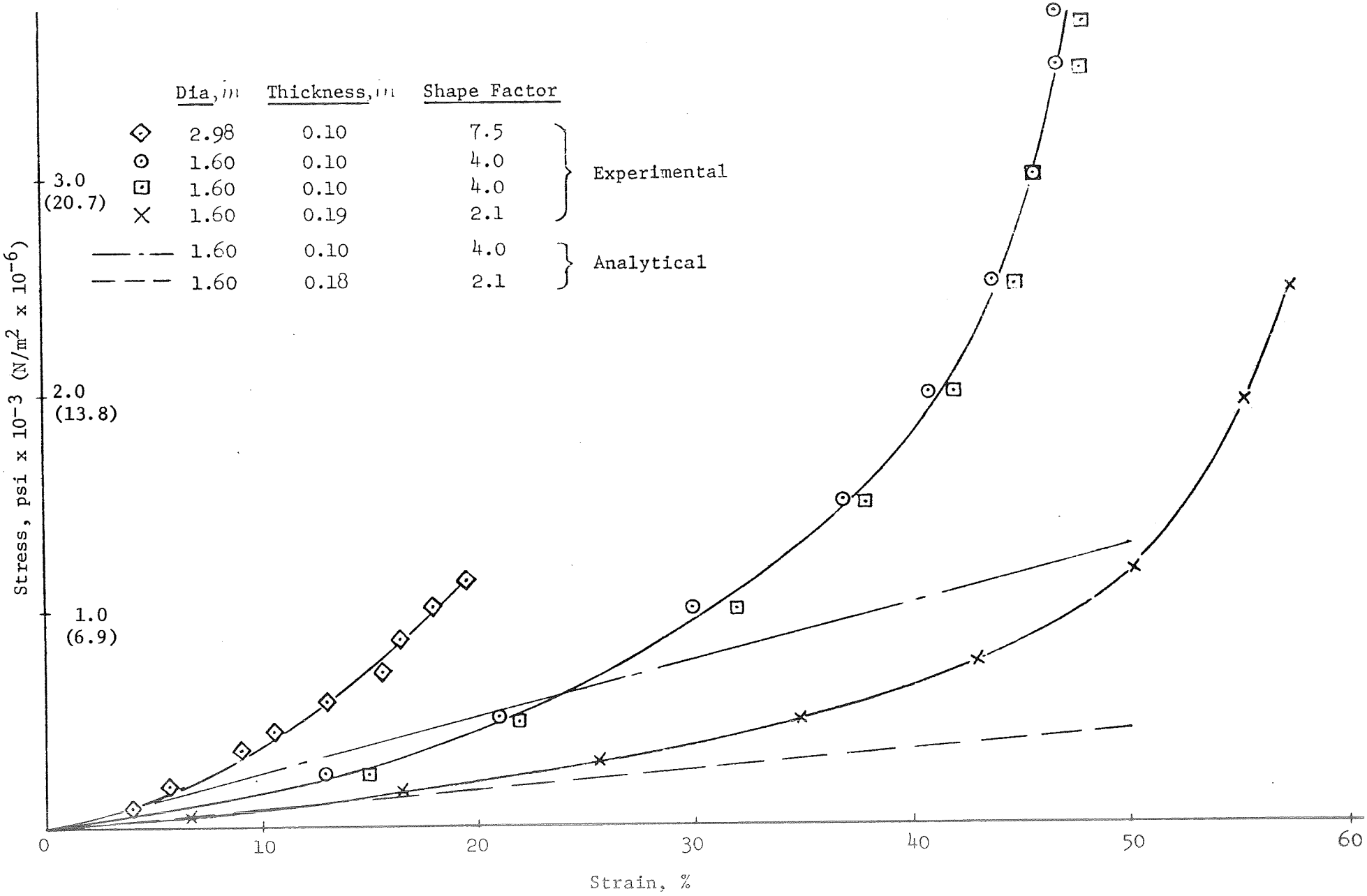

Figure 31. - Variation of Compressive Stress vs Strain

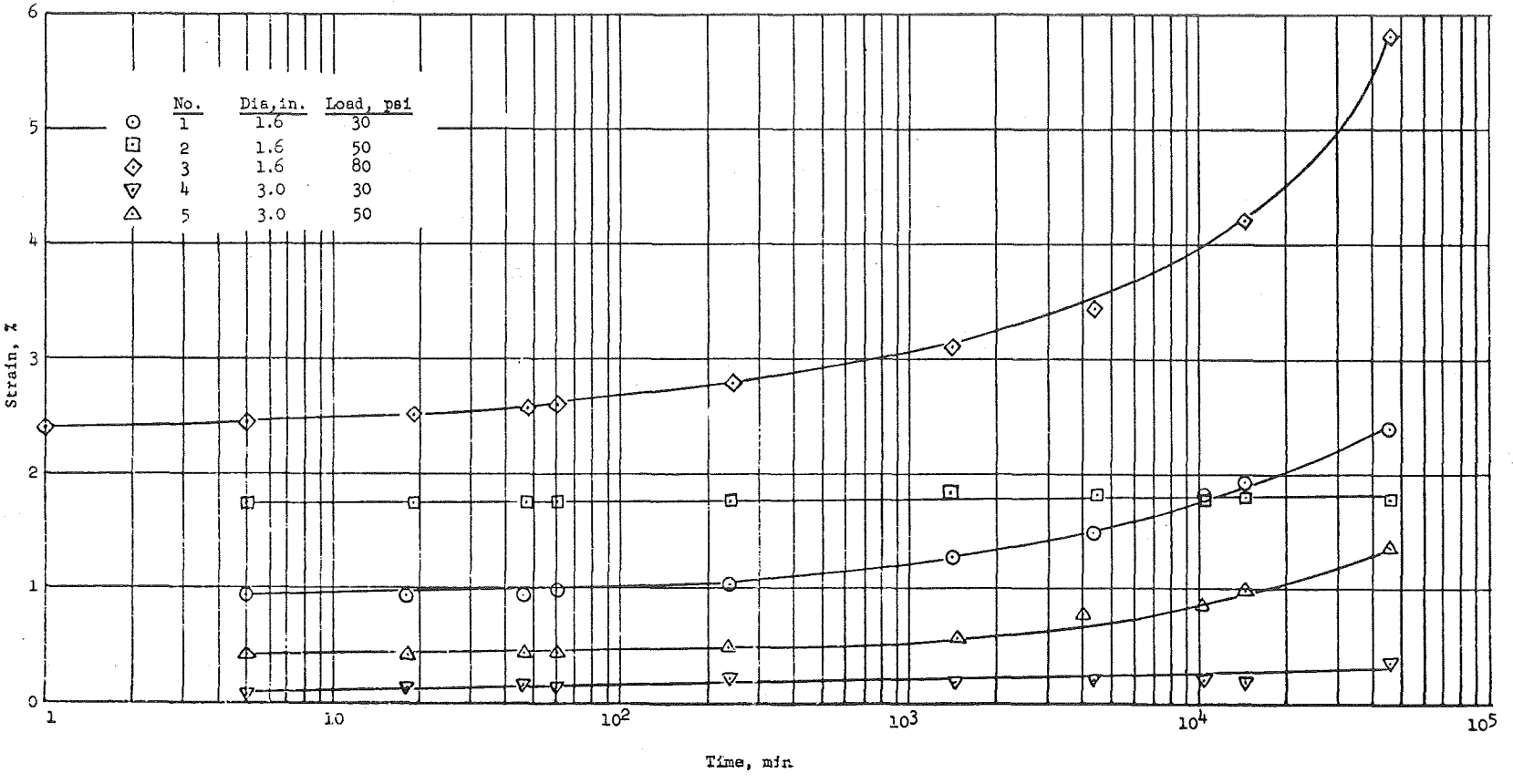

Figure 32. - Creep Strain-vs-Time Duration

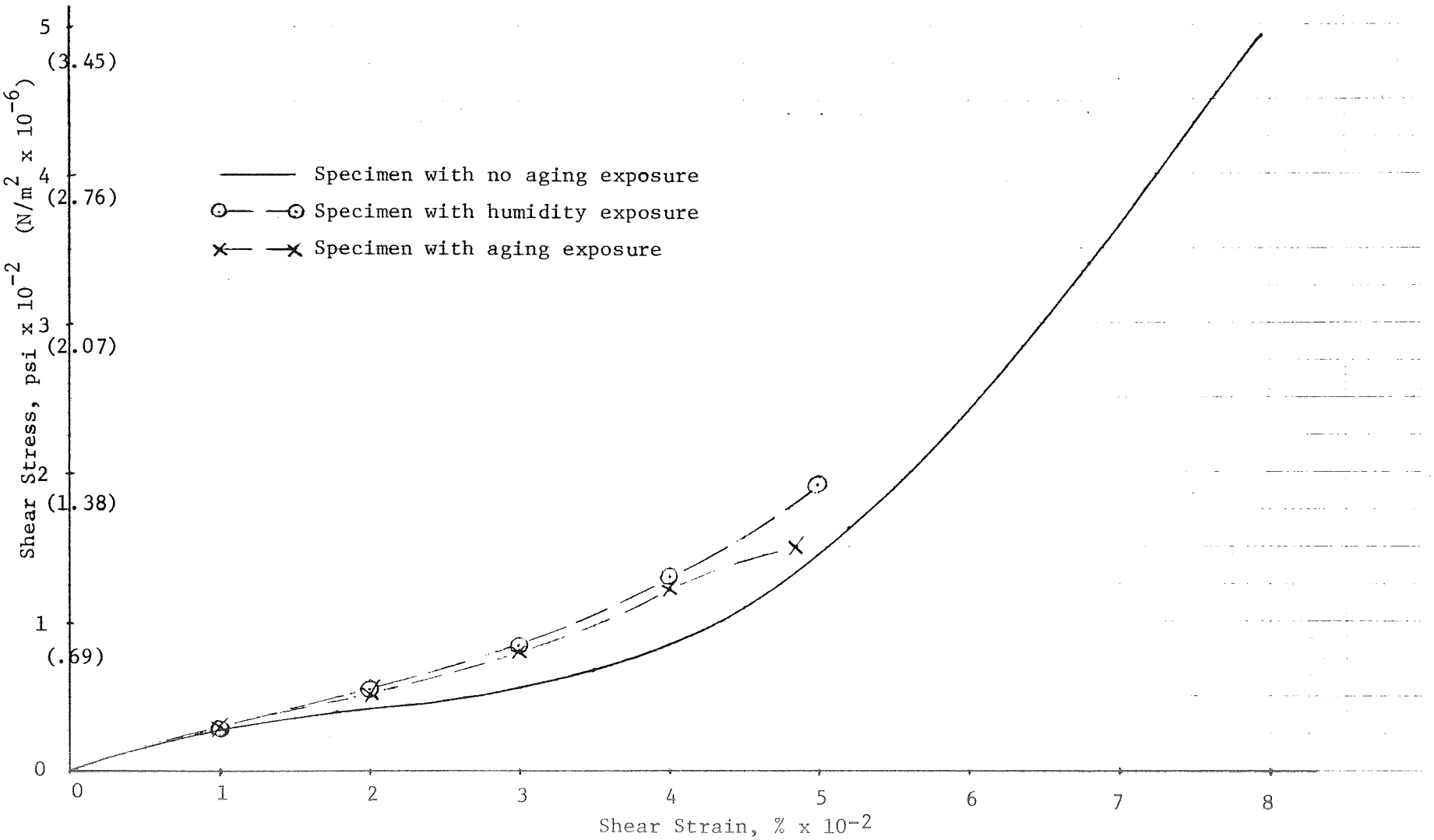

Figure 33. - Comparison of Aged and Unaged Shear Specimen Properties

Figure 33

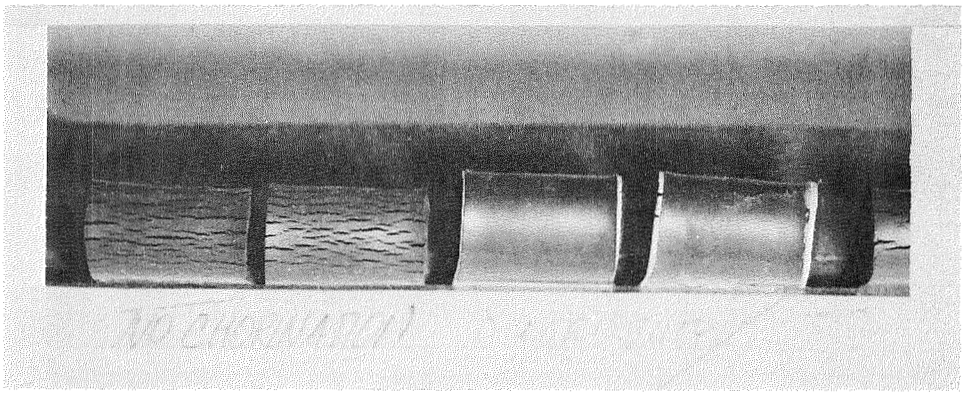

(a) Specimens without Chlorination Treatment

(b) Chlorobutyl Rubber Covered Specimens

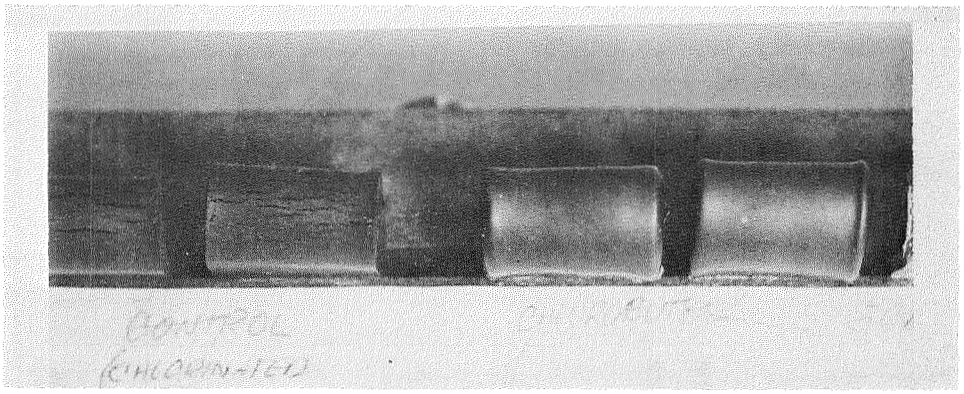

(c) Specimens with Chlorination Treatment

(d) Chlorobutyl Rubber Wrapped Specimens

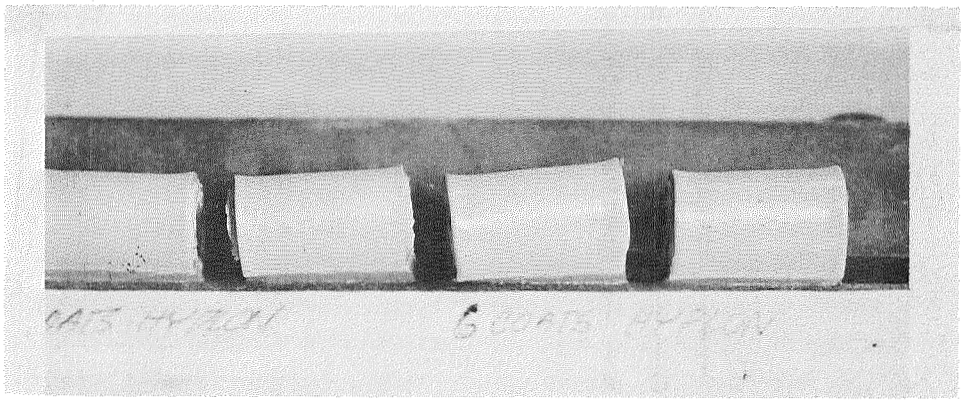

(e) Specimens with 3 Coats of Hypalon

(f) Specimens with 6 Coats of Hypalon

Figure 34. - Accelerated Aging and Ozone Exposure Test

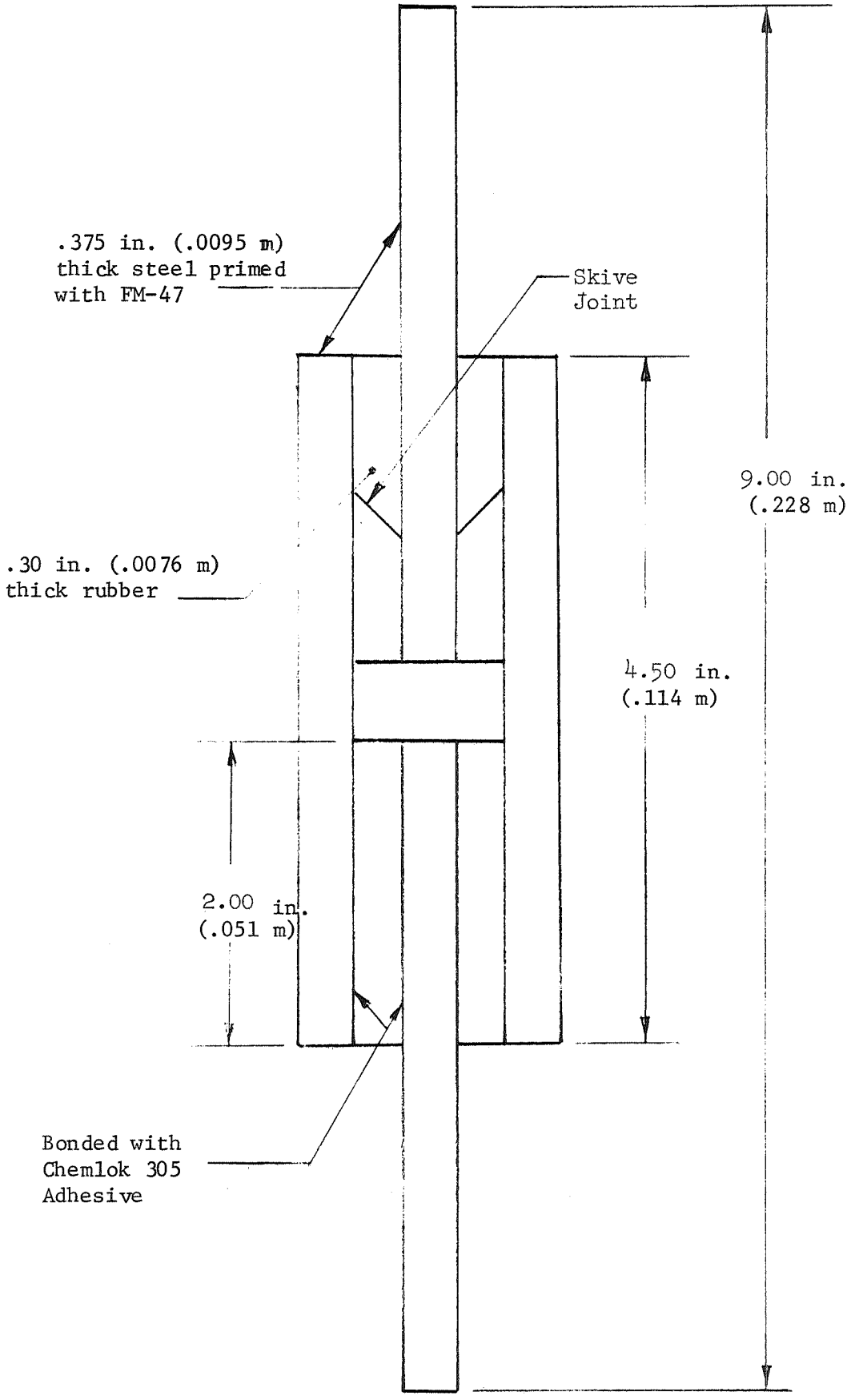

Figure 35. - Quadruple Lap Shear Specimen (2 x 2 Pad)

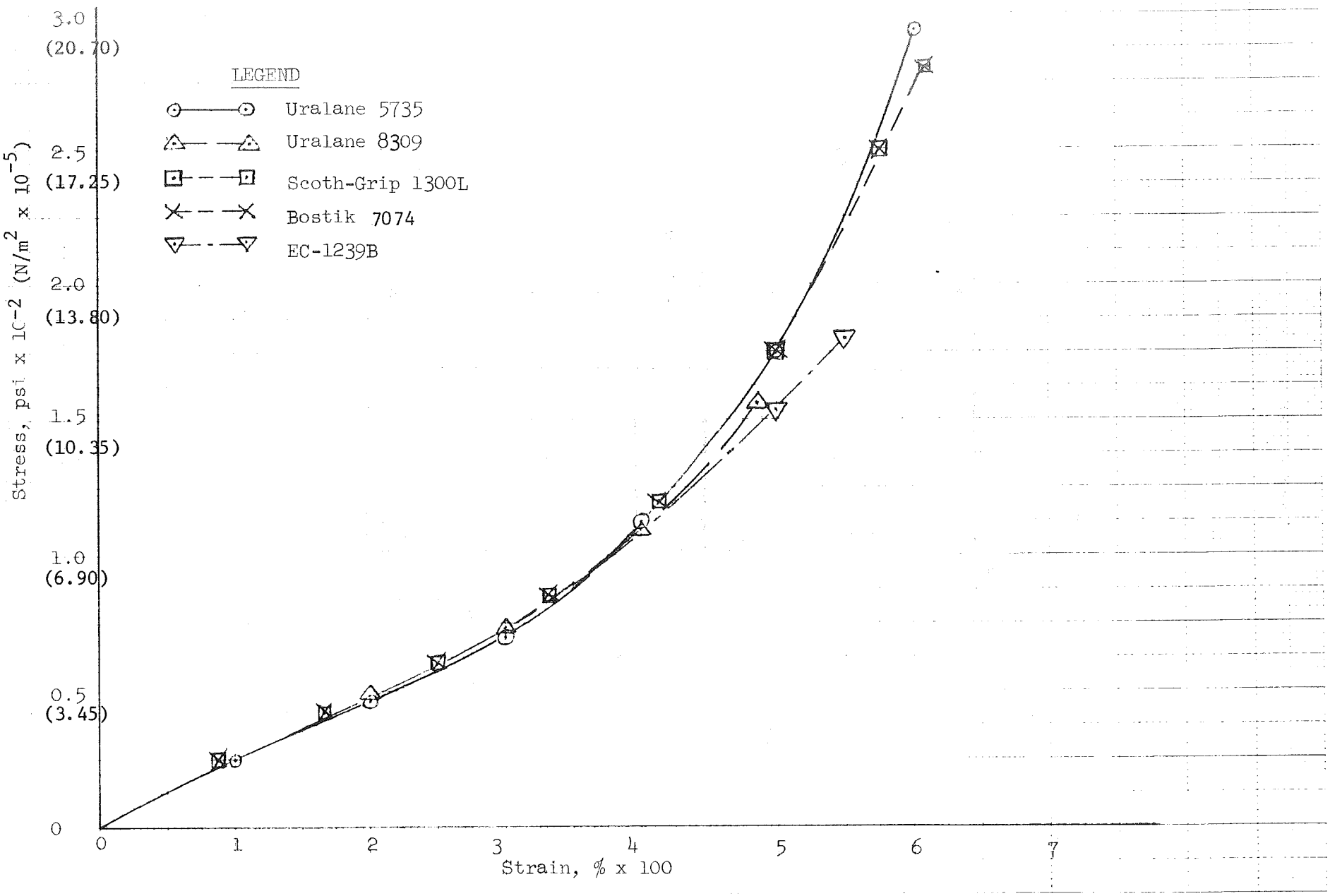

Figure 36. - Shear Stress vs Strain for Various Skive Joint Adhesive Systems

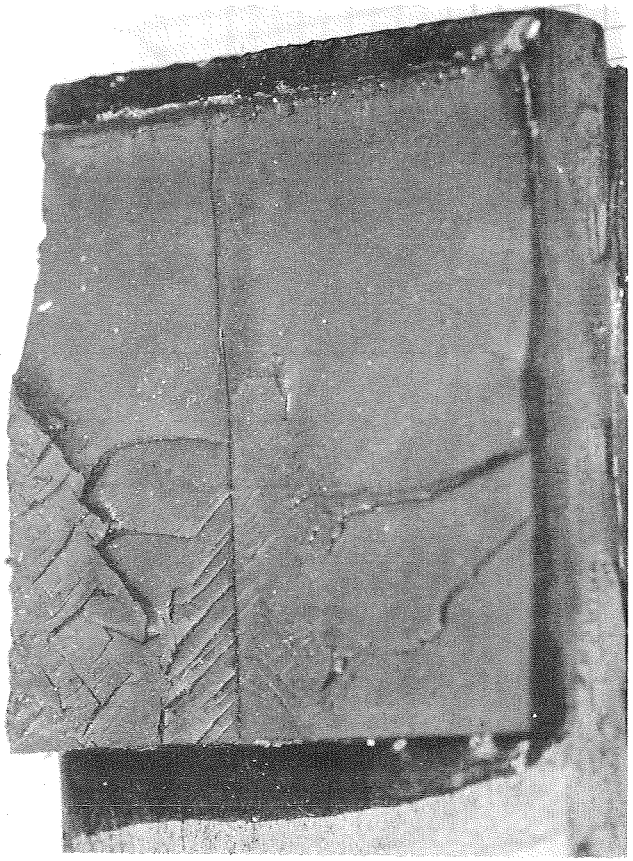

(a) Uralane 5735 Adhesive

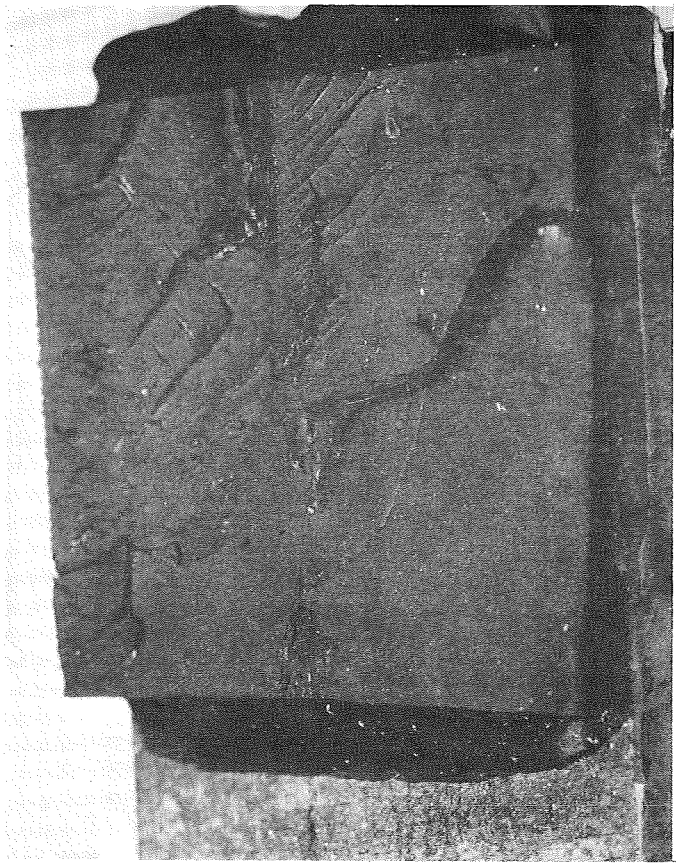

(b) Scotch-Grip 1300L Adhesive

Figure 37. - Failure Surface of Quadruple Lap Shear Specimens with Skive Joints

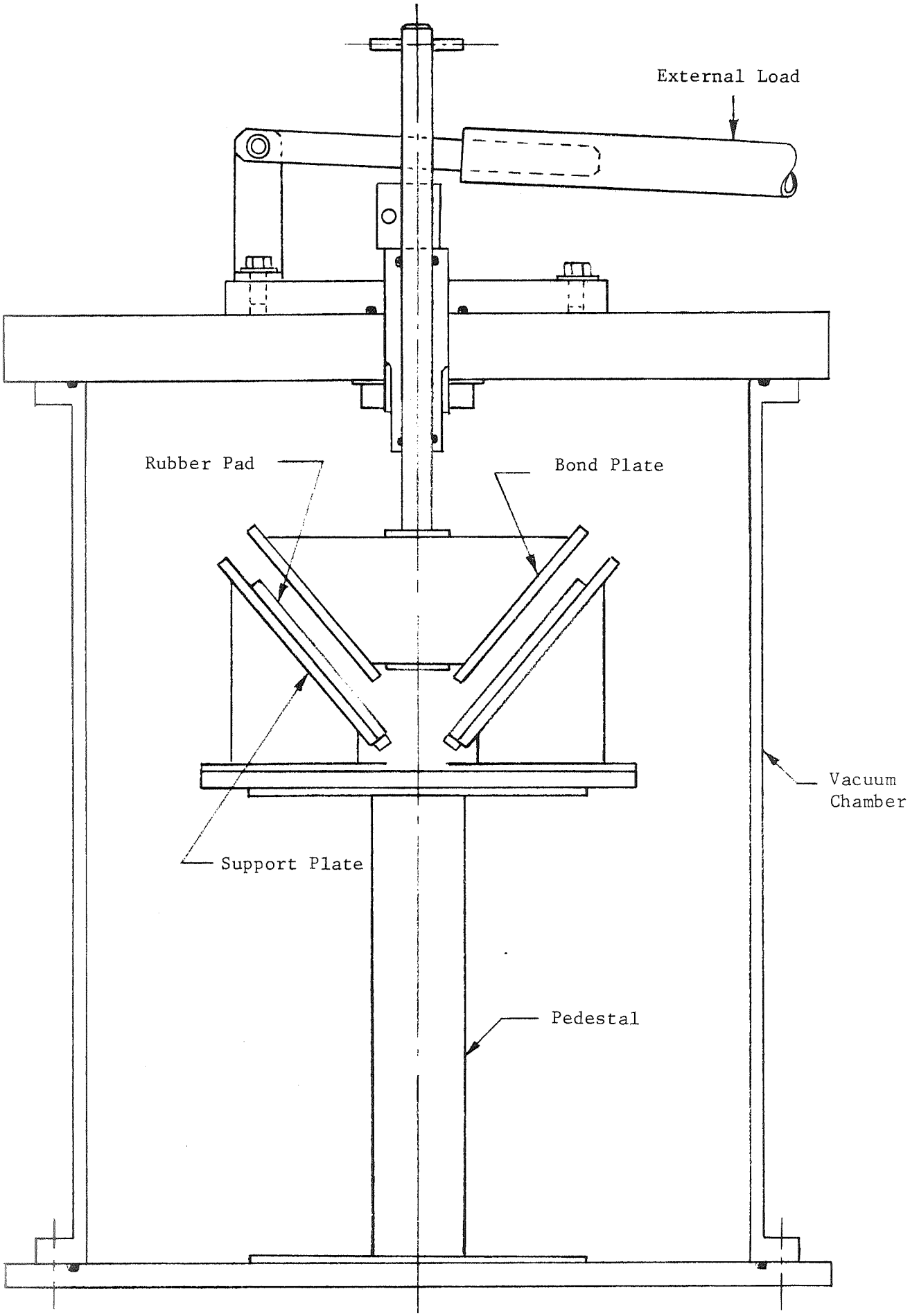

Figure 38. - Adhesive Application Evaluation Fixture

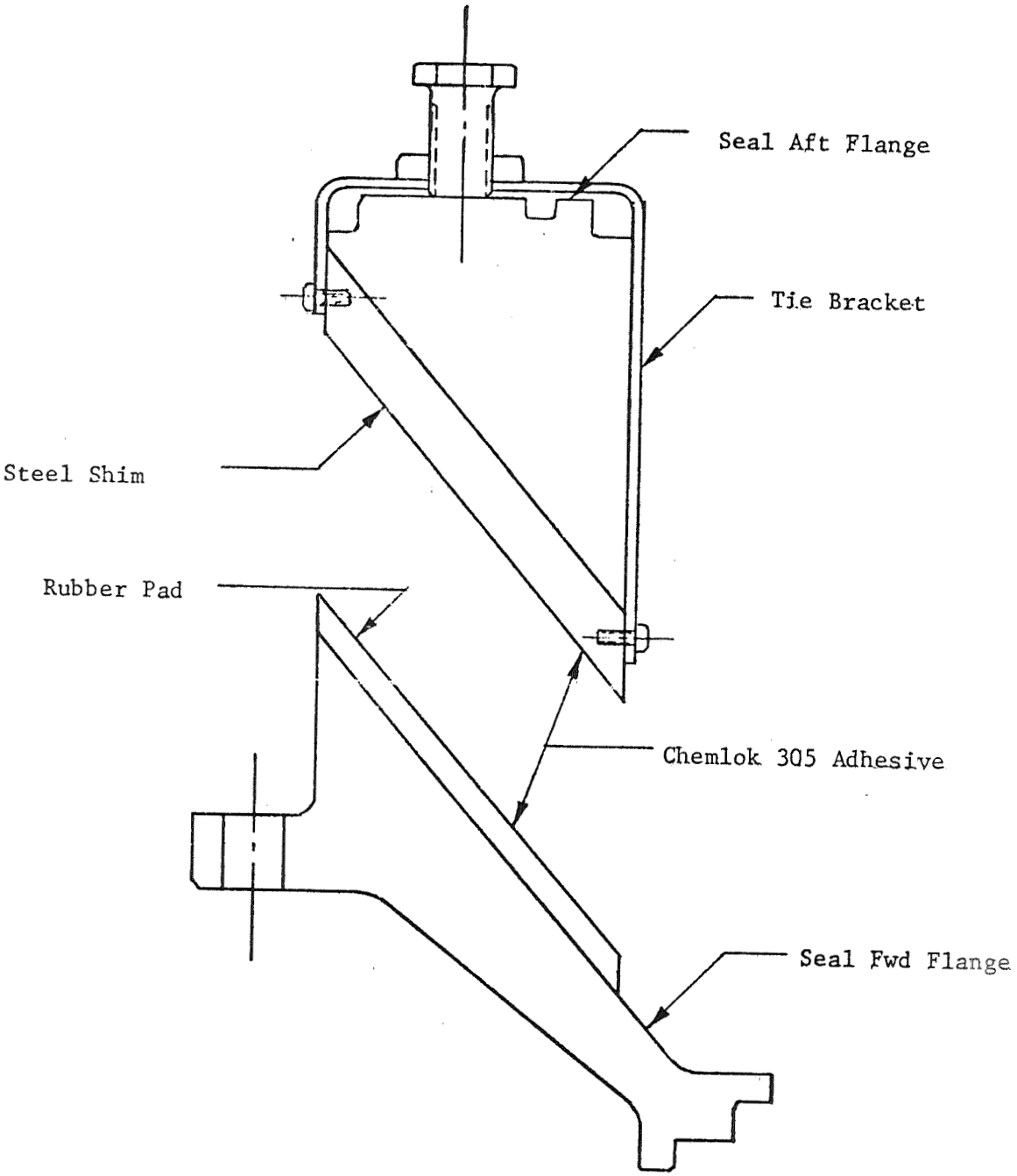

Figure 39. - Process Demonstration Bonding Setup

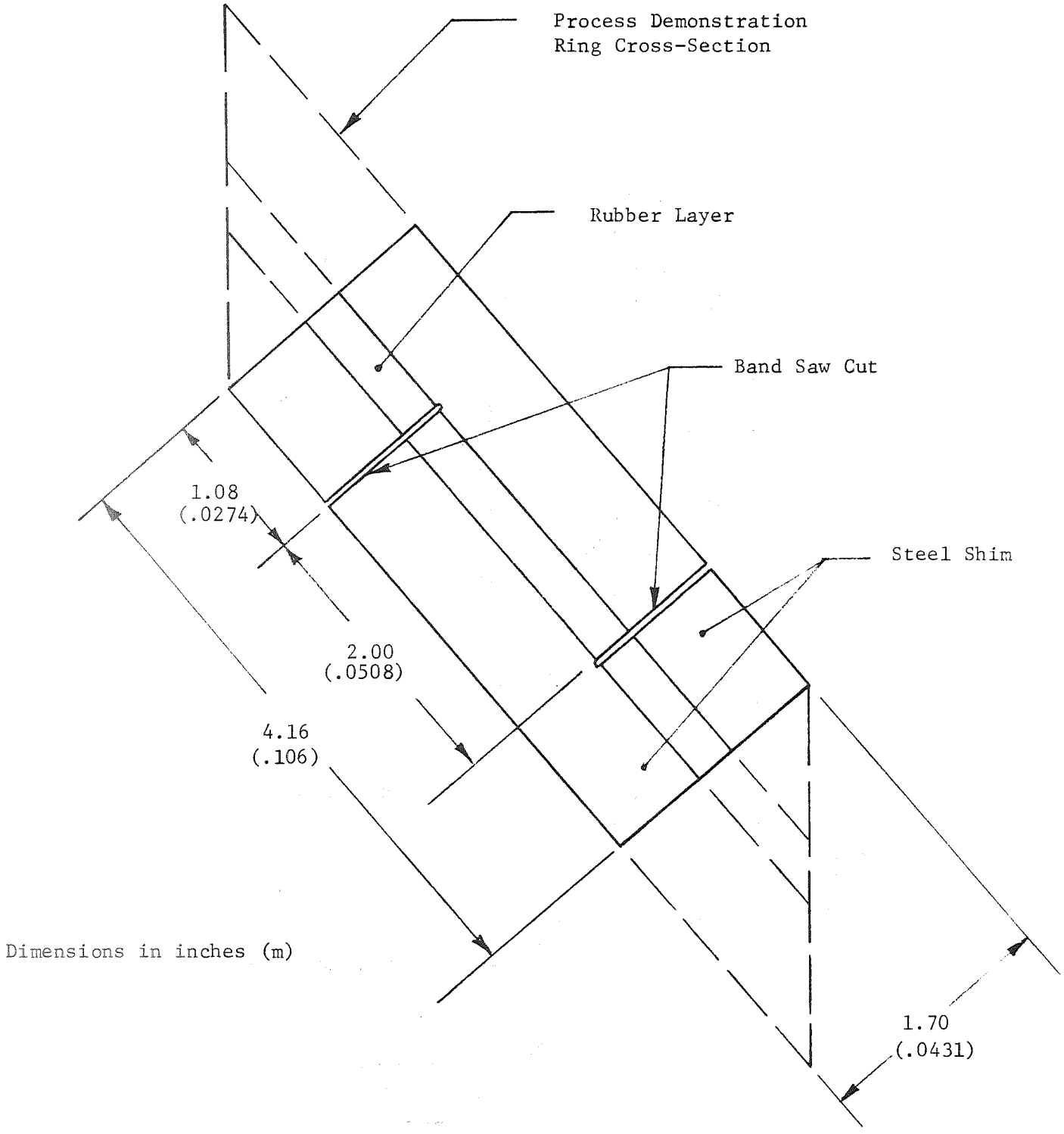

Figure 40. - Lap Shear Specimen Configuration

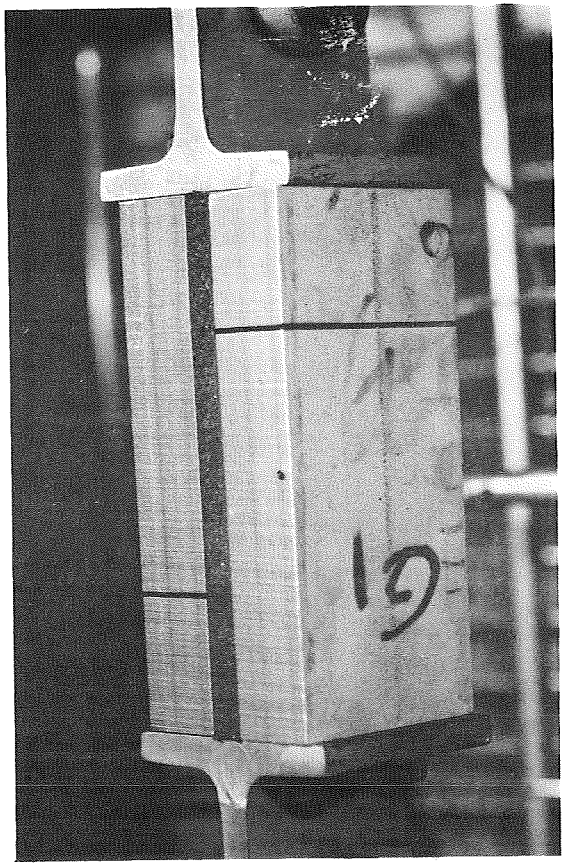

(a) 0% Strain

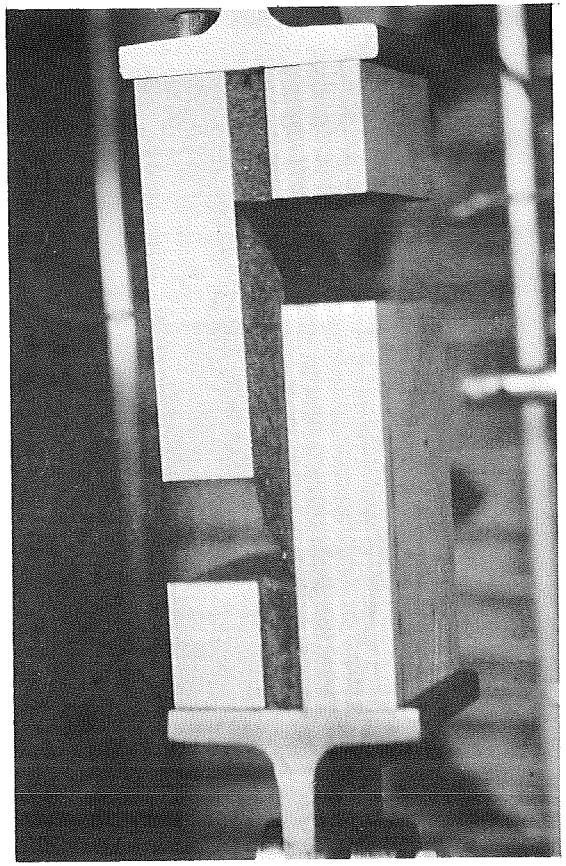

(b) 300% Strain

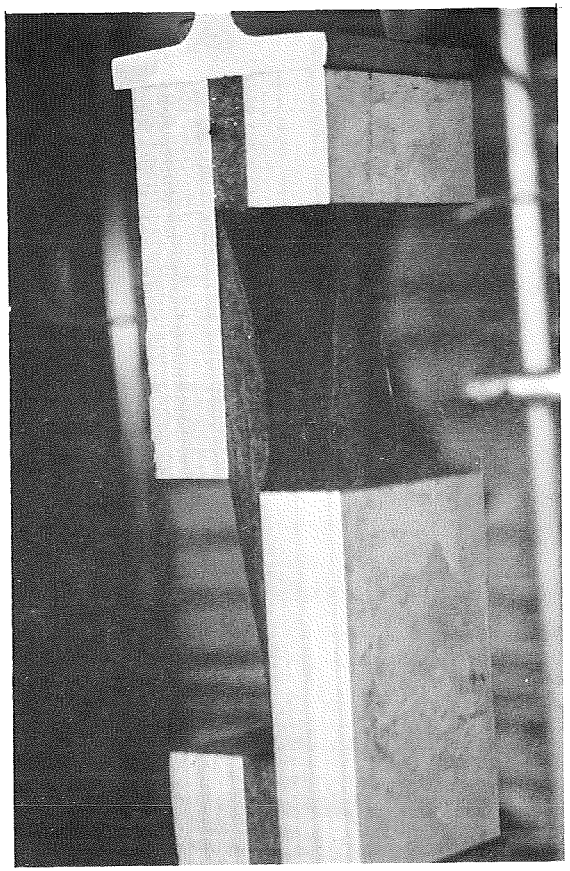

(c) >700% Strain

Figure 41. - Lap Shear Specimen Behavior During Test

Figure 42. - Flexible Seal Metal Shim

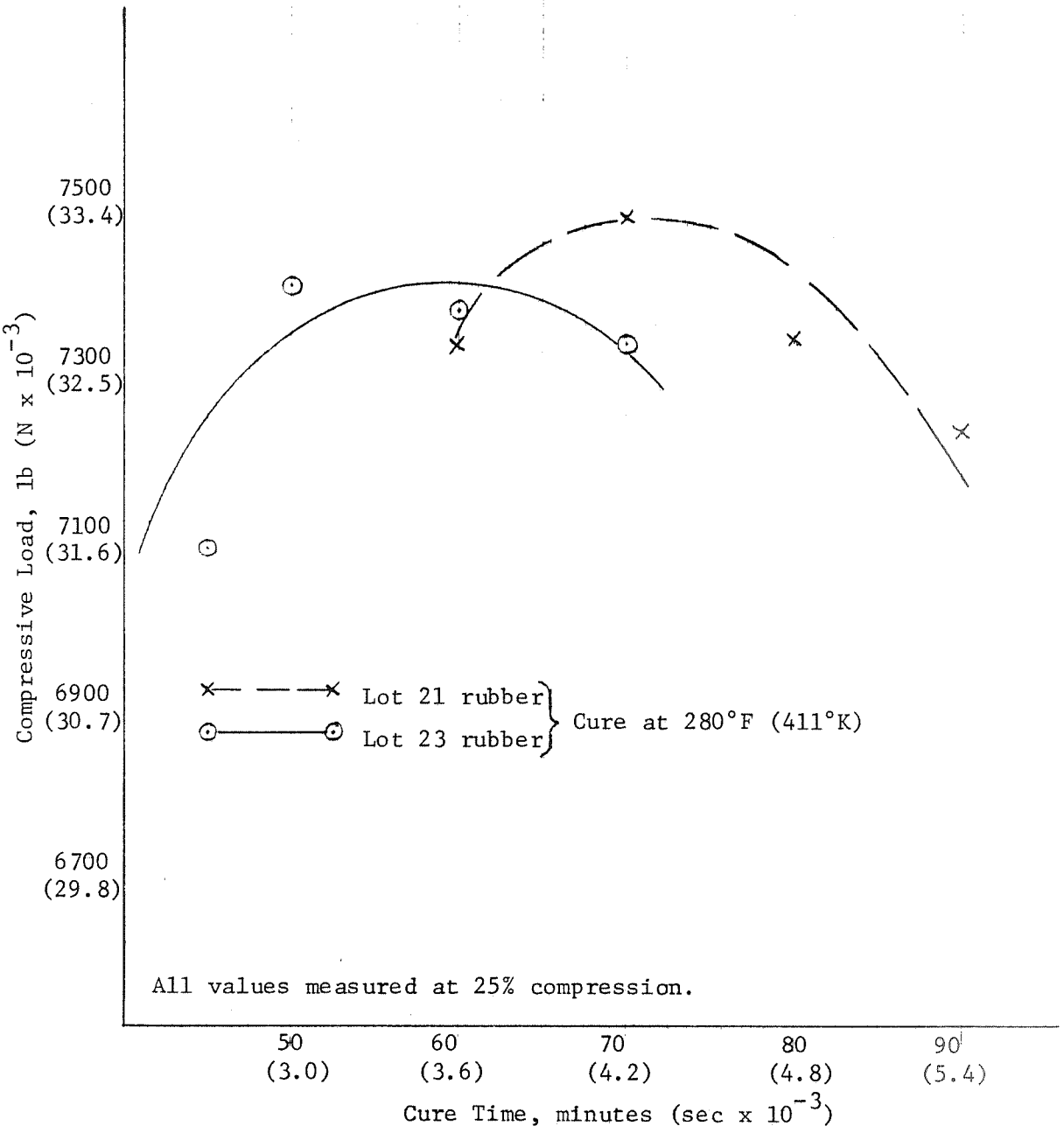

Figure 43. - Compressive Load vs Cure Time of Rubber Pad

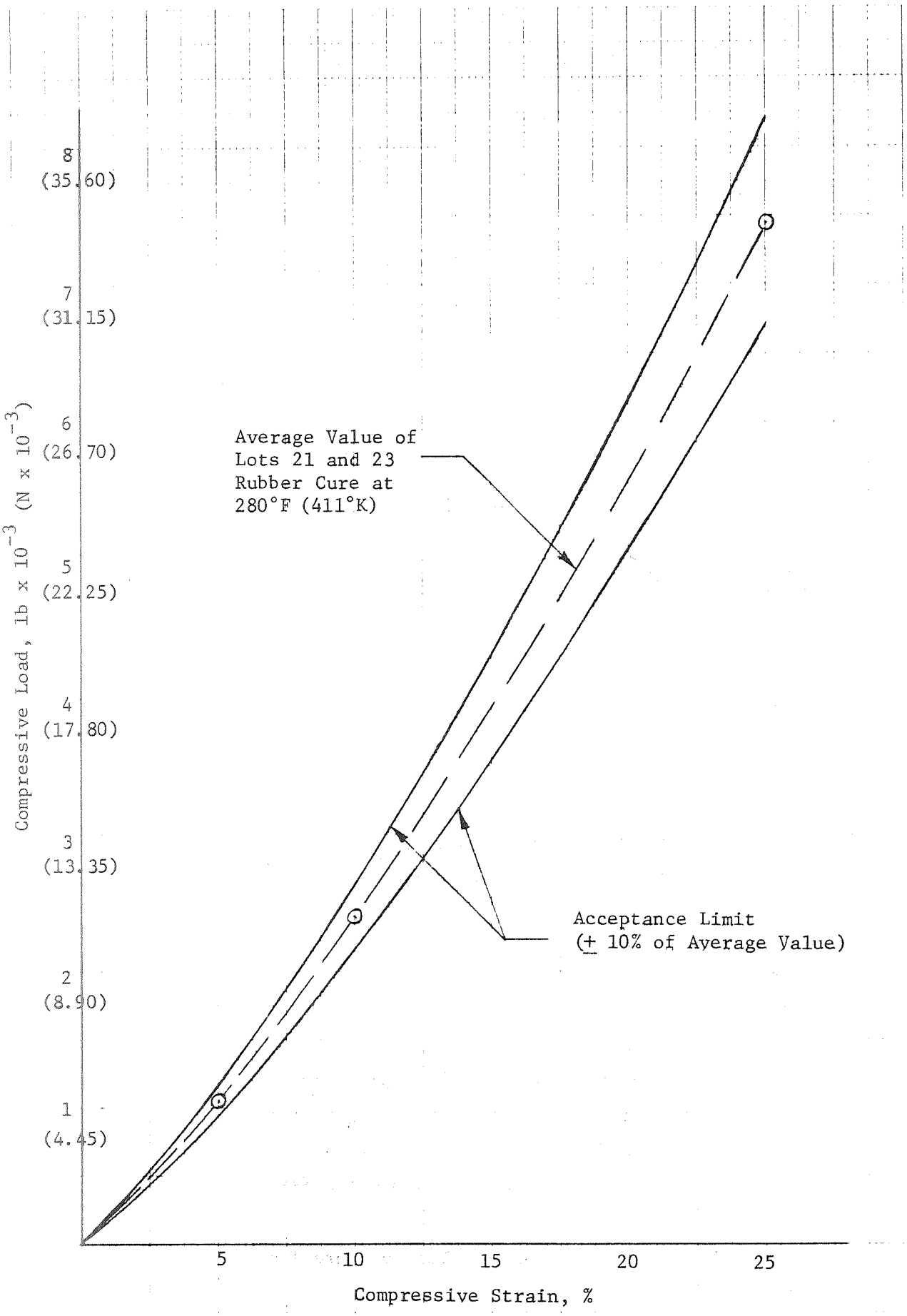

Figure 44. - Rubber Pad Compression - Deflection Acceptance Limit

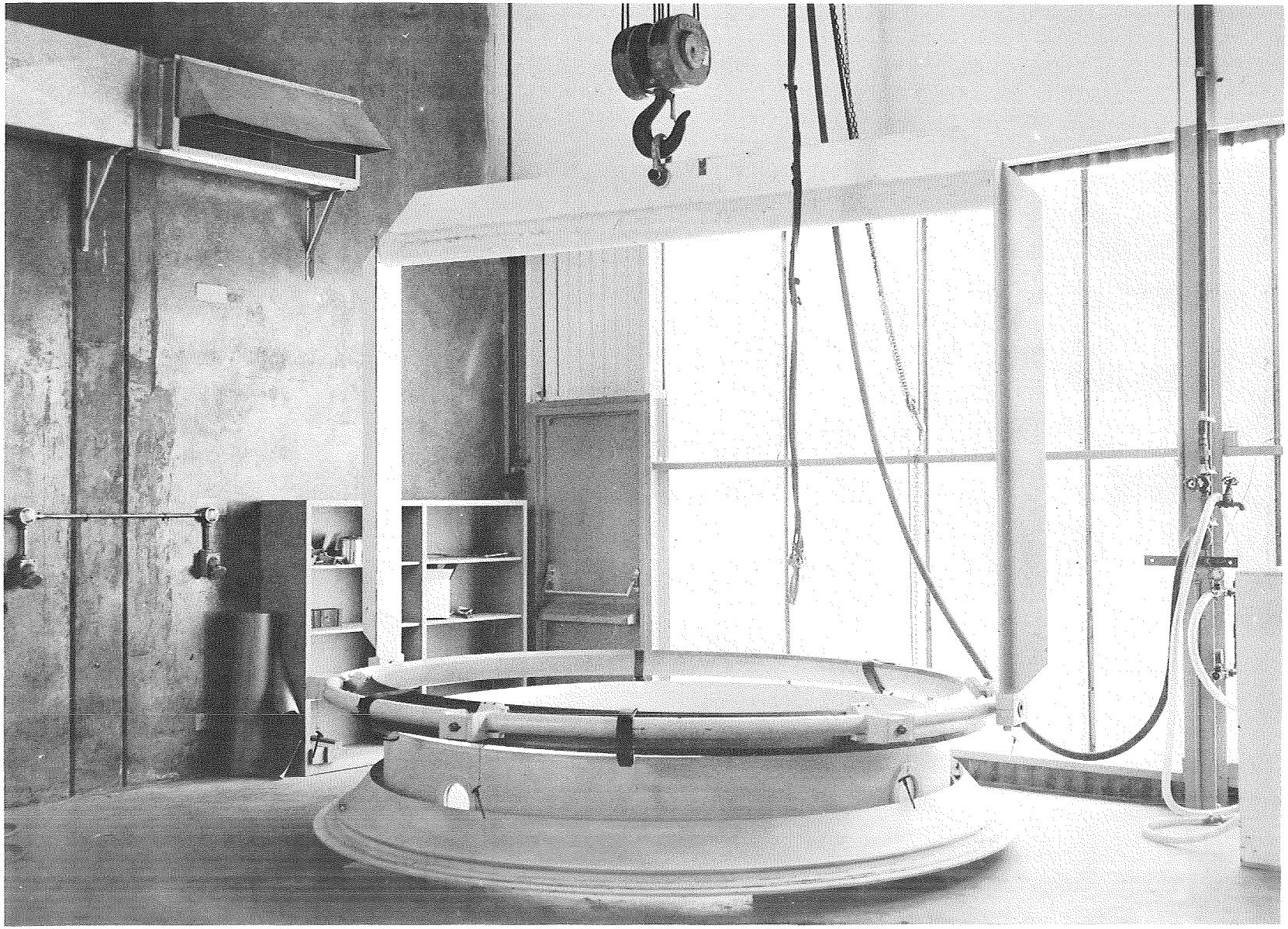

Figure 45. - Position Steel Shim on Assembly Bond Fixture

F'igure 46. - Apply Adhesive on Base Component

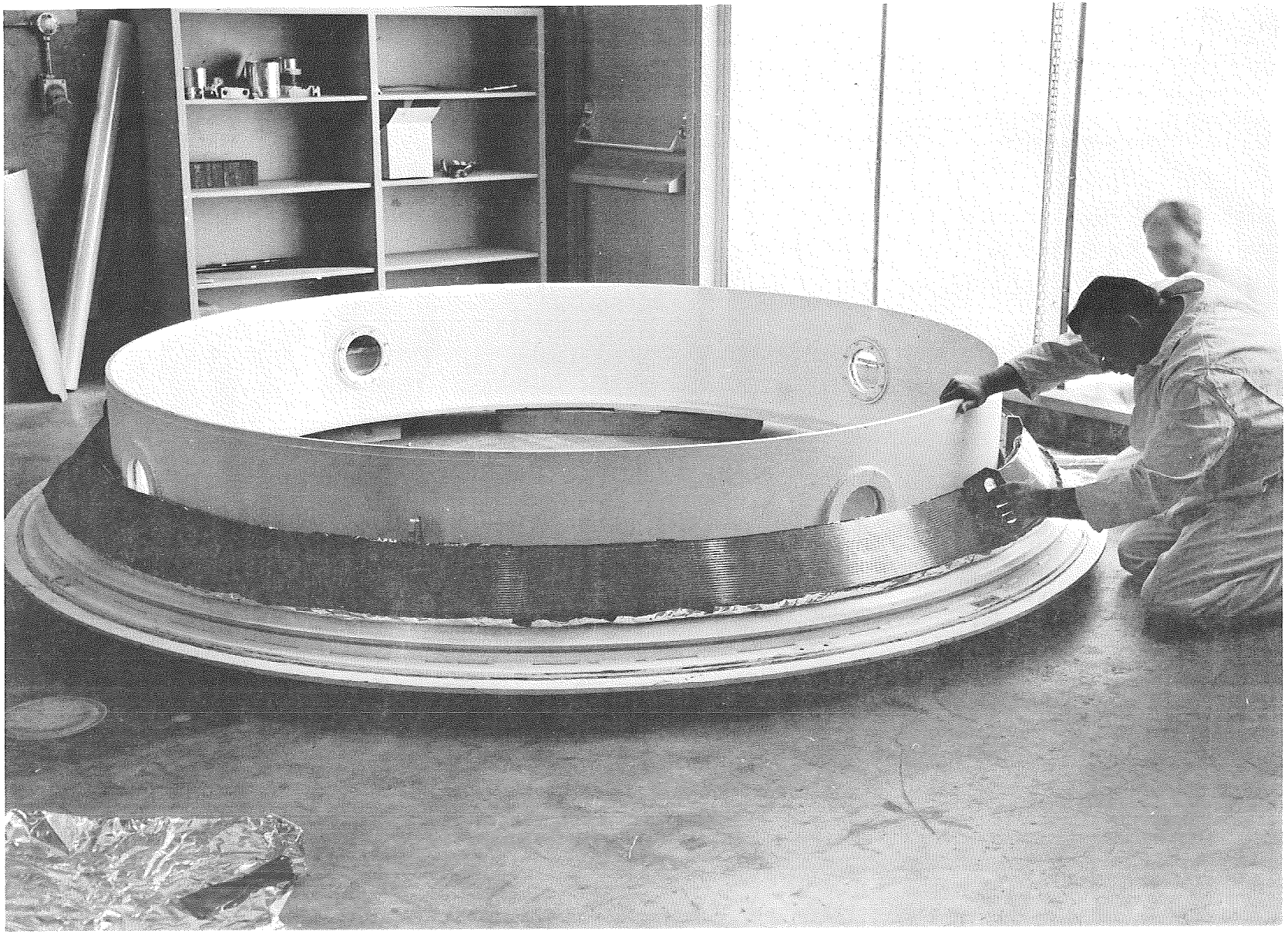

F'igure 47. - Spread Adhesive on Base Component

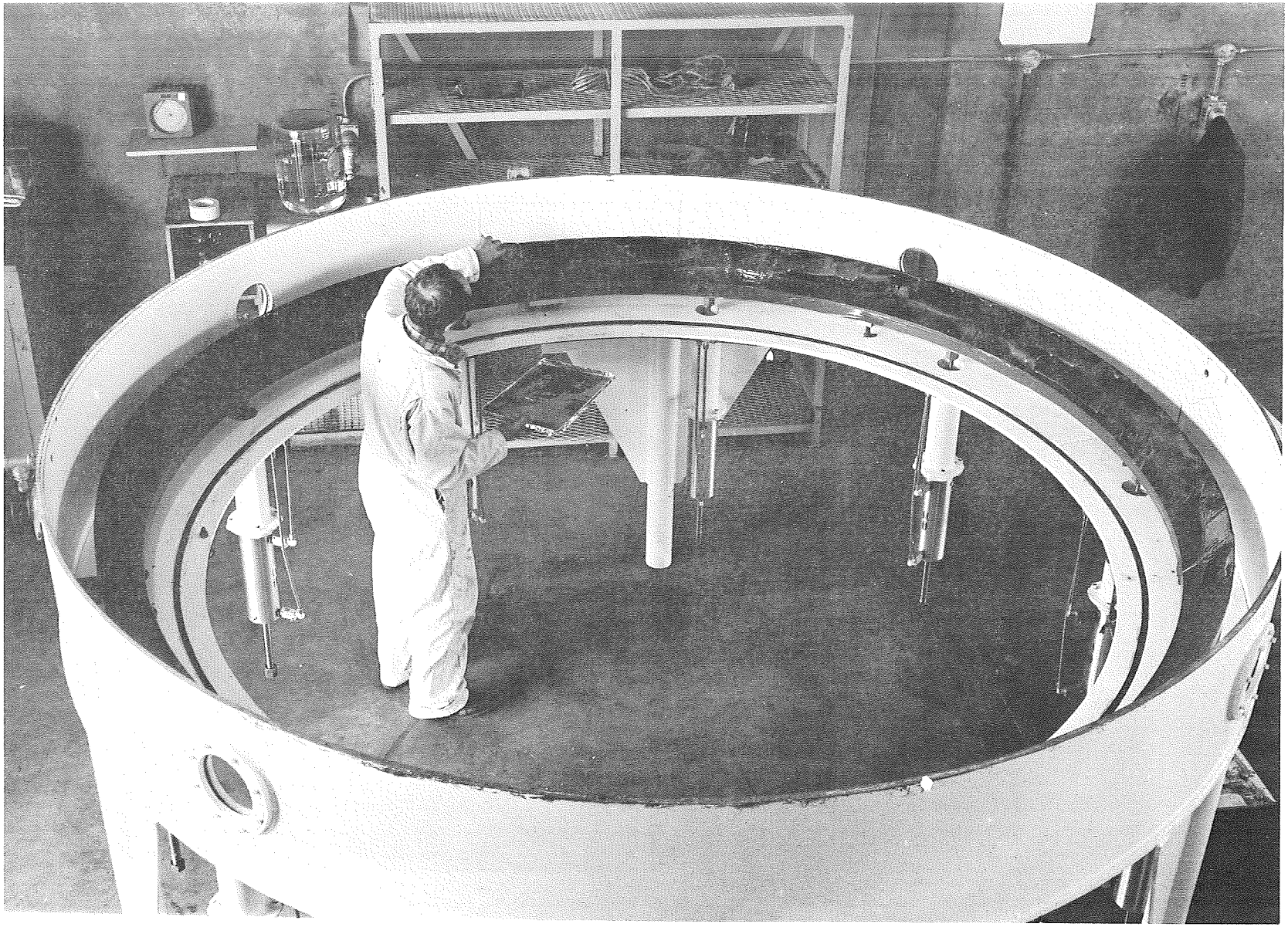

F'igure 48. - Apply Adhesive on Top Component

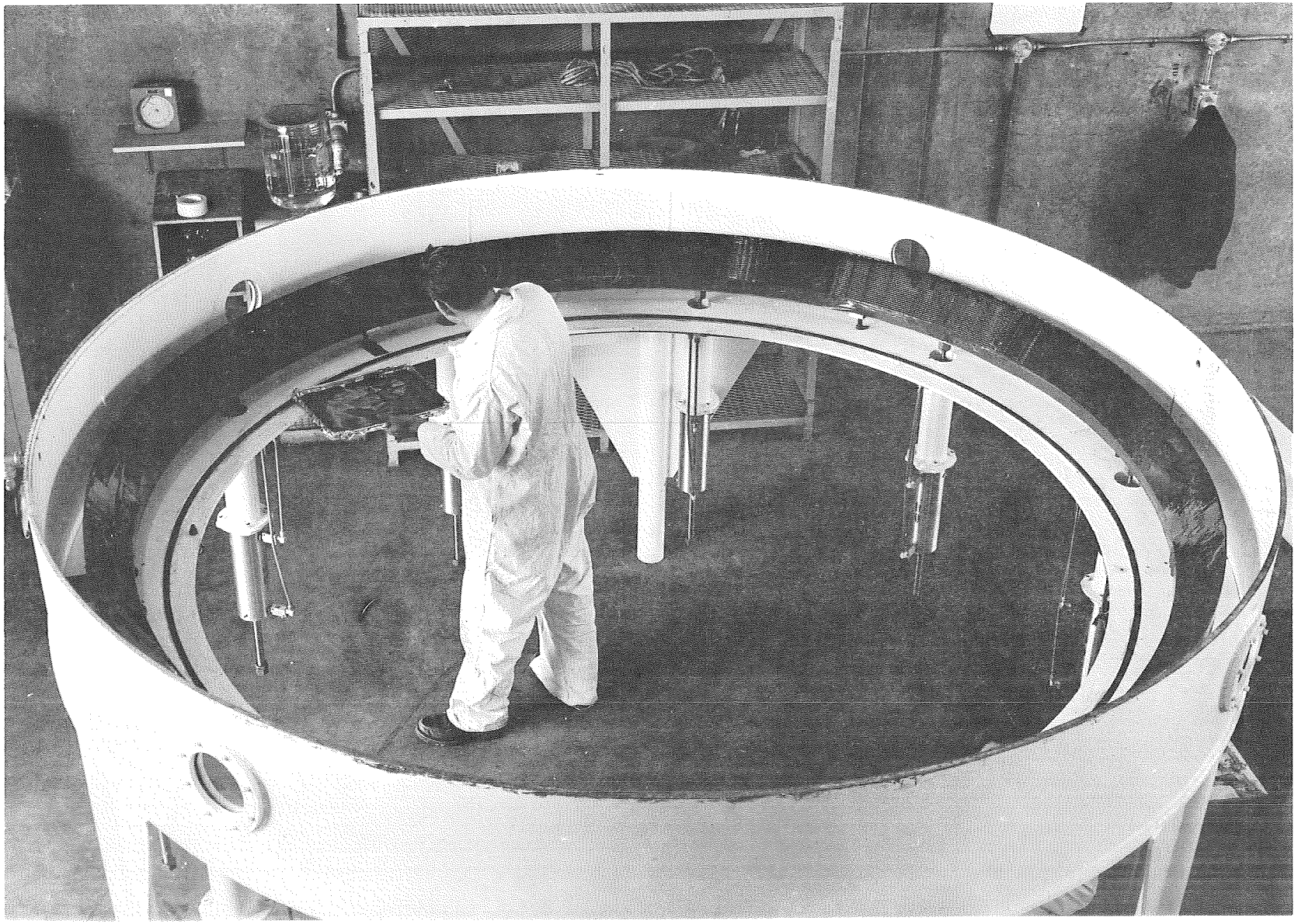

Figure 49. - Spread Adhesive on Top Component

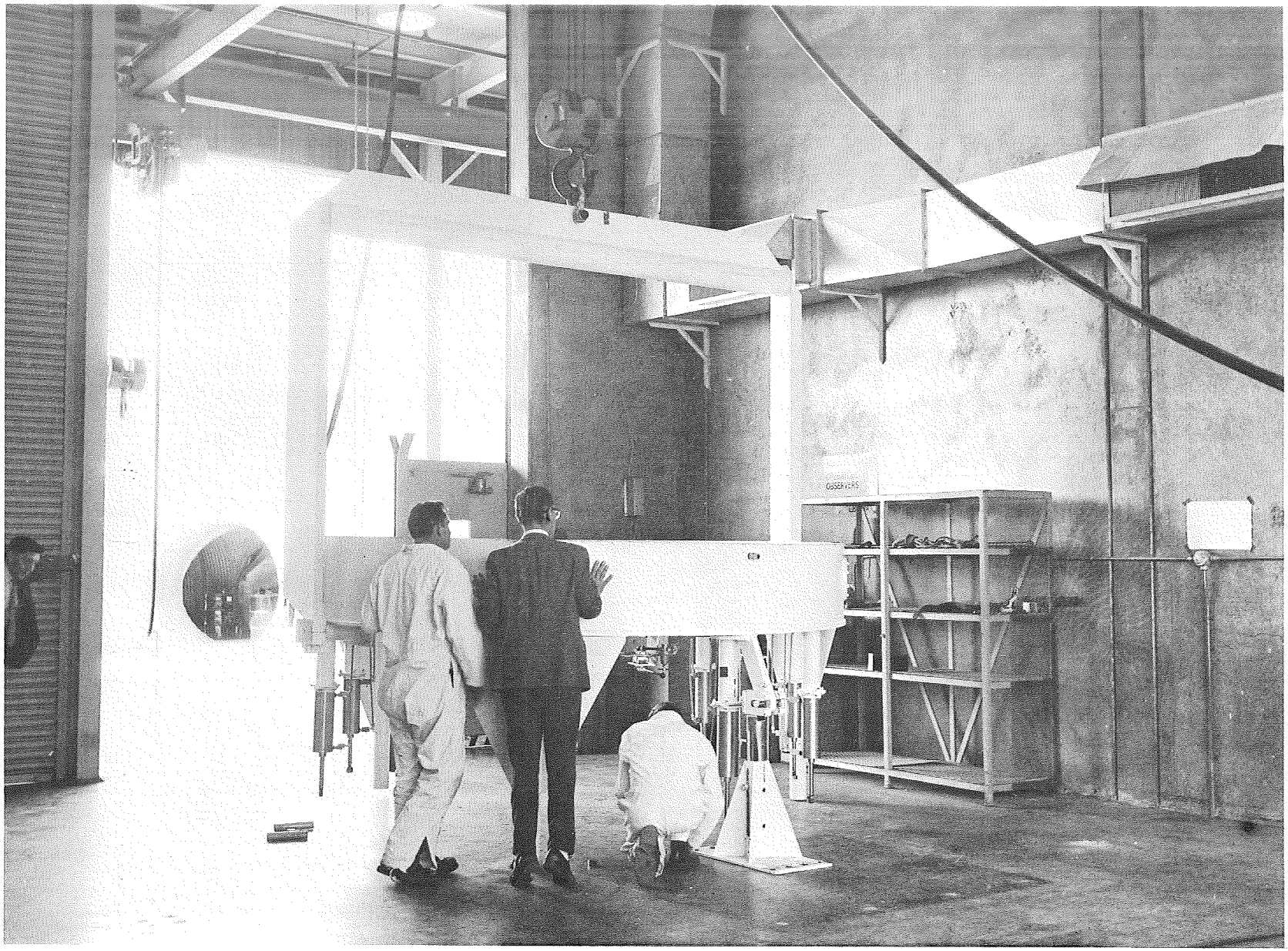

F'igure 50. - Prepare to Invert the Assembly Bond Fixture

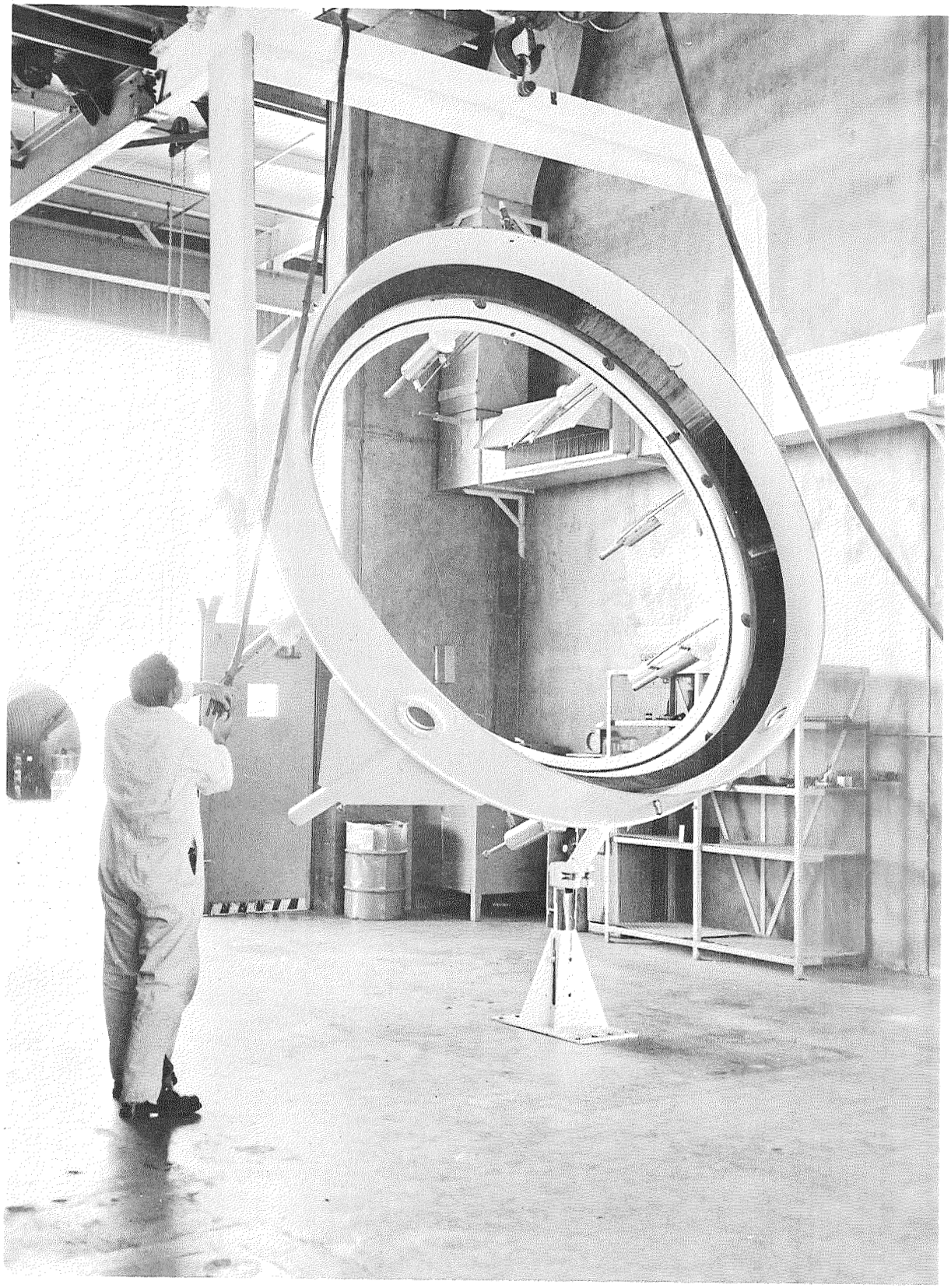

Figure 51. - Invert the Top Portion of the Bond Fixture

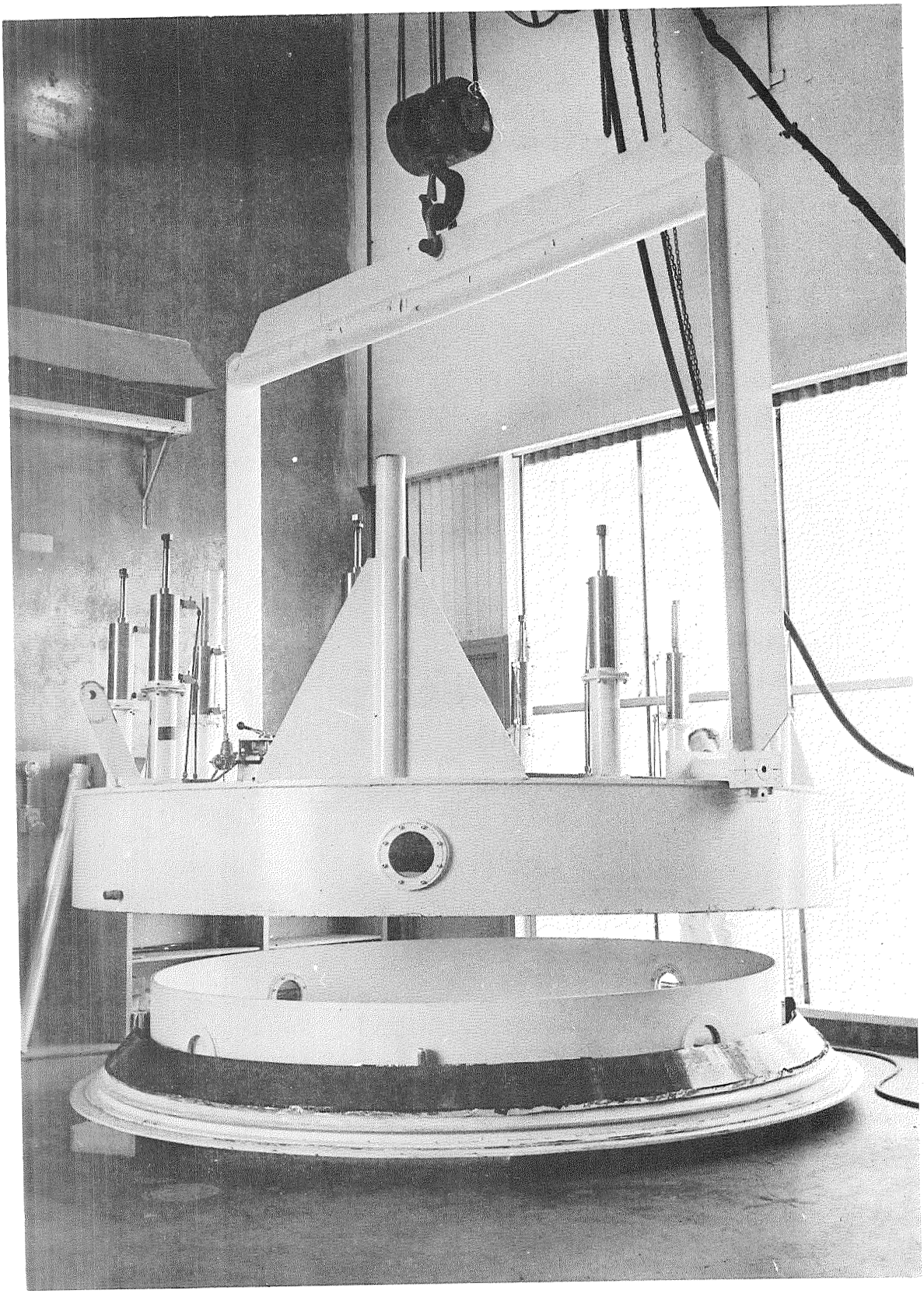

Figure 52. - Assemble the Bond Fixture

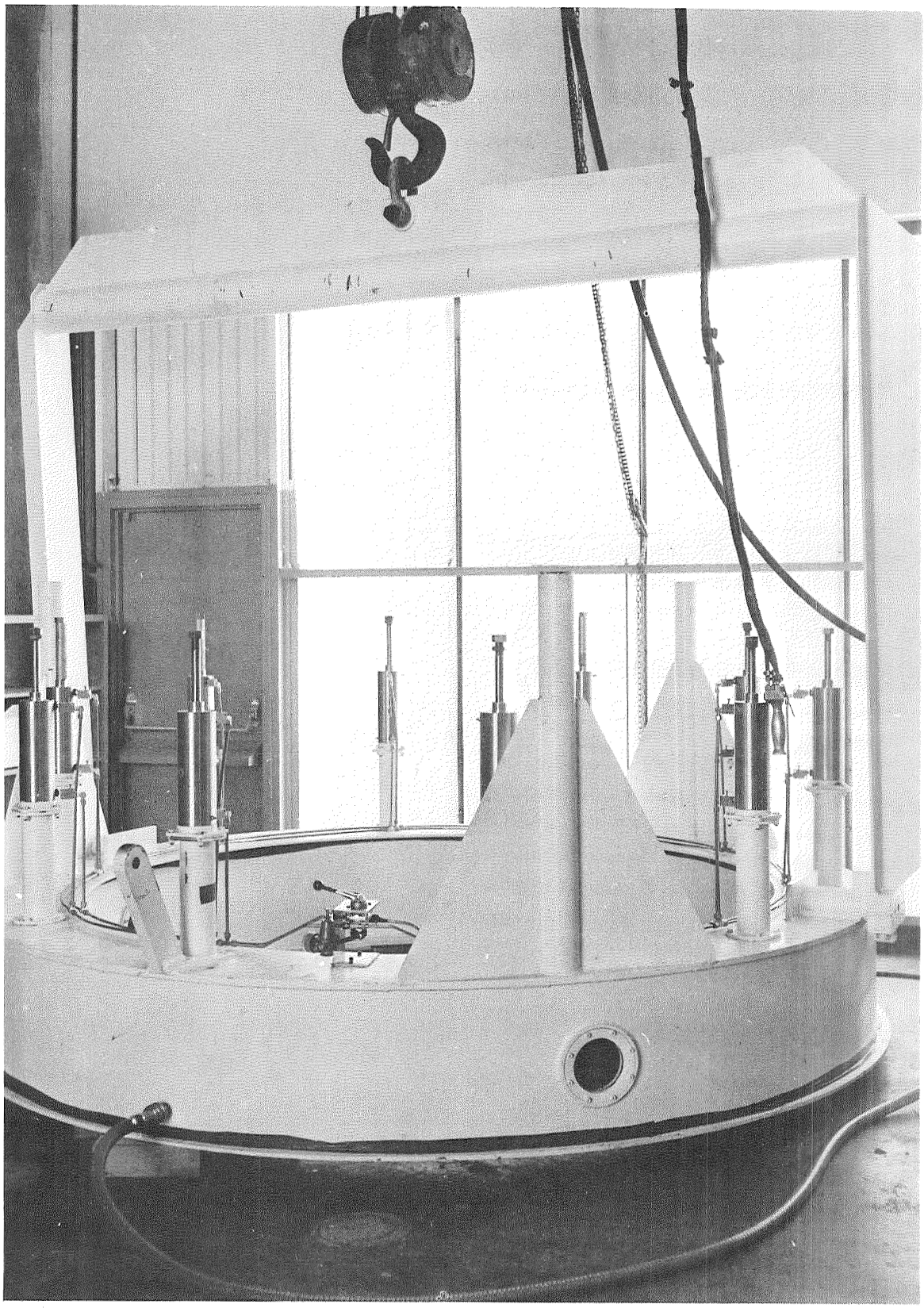

Figure 53. - Prepare the Bond Fixture for Adhesive Cure

Figure 54. - Flexible Seal, Side View

Figure 55. - Flexible Seal, Top View

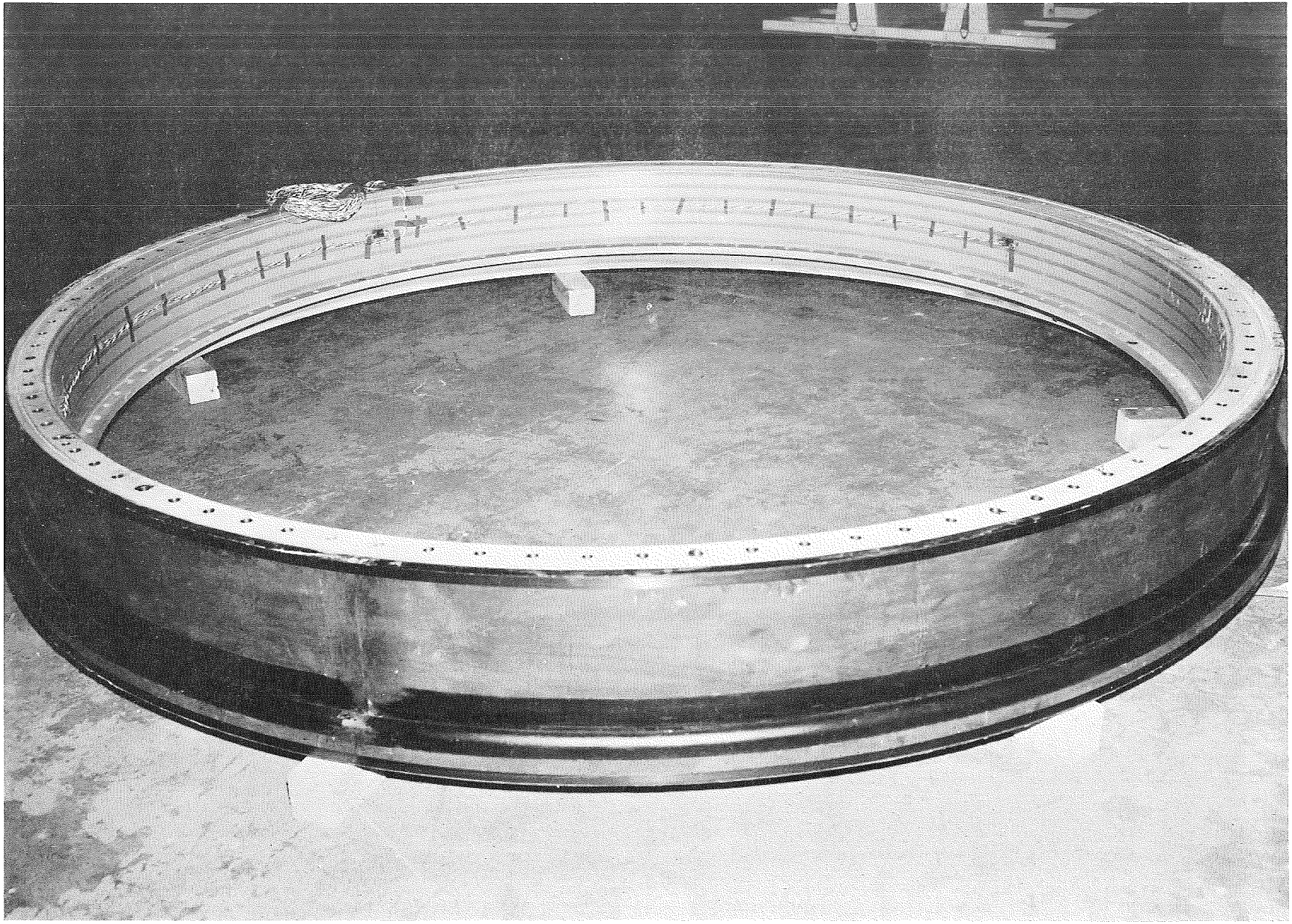

Figure 56. - Flexible Seal for 260-In.-Dia Motor

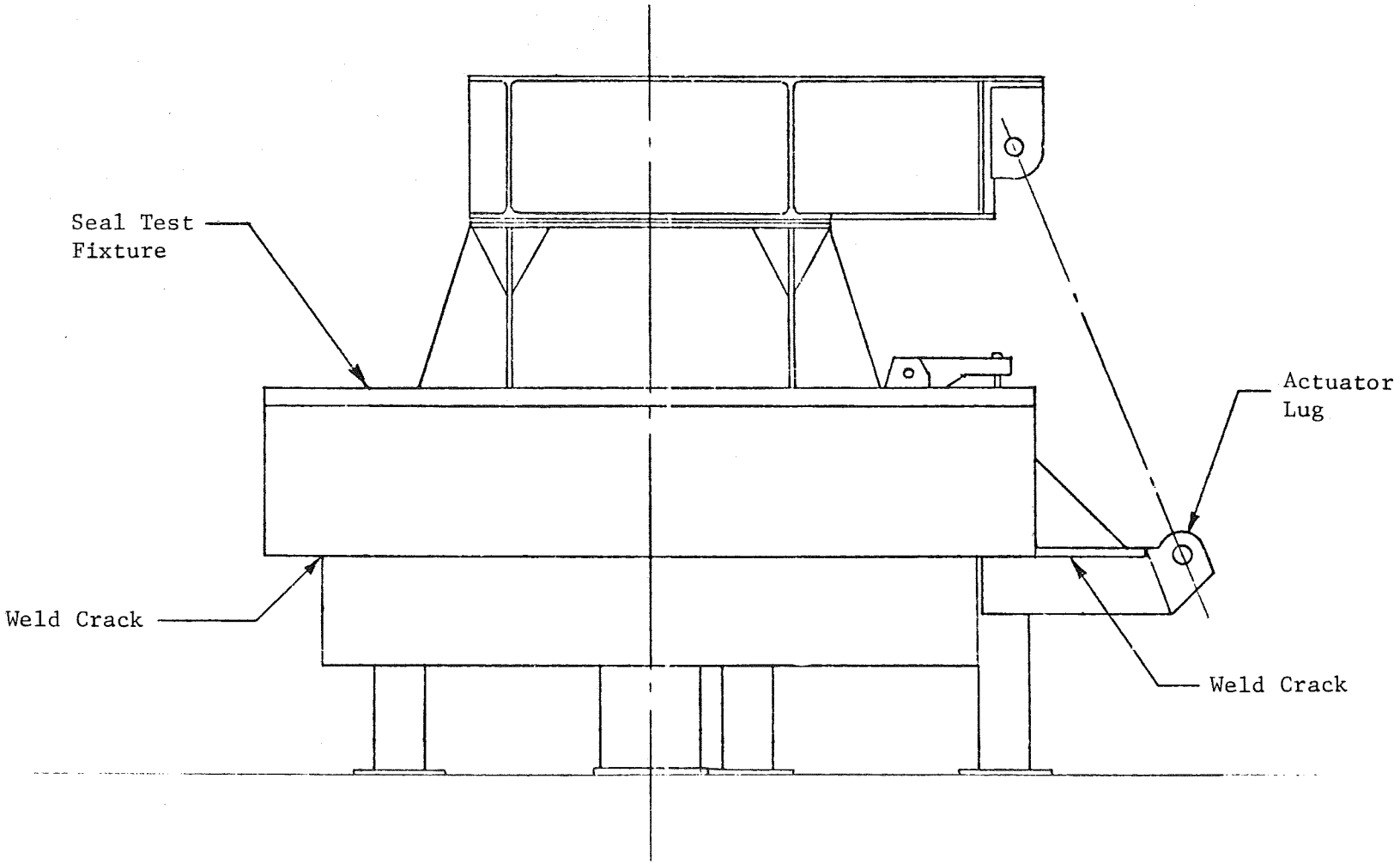

Figure 57. - Location of Weld Cracks in Test Fixture

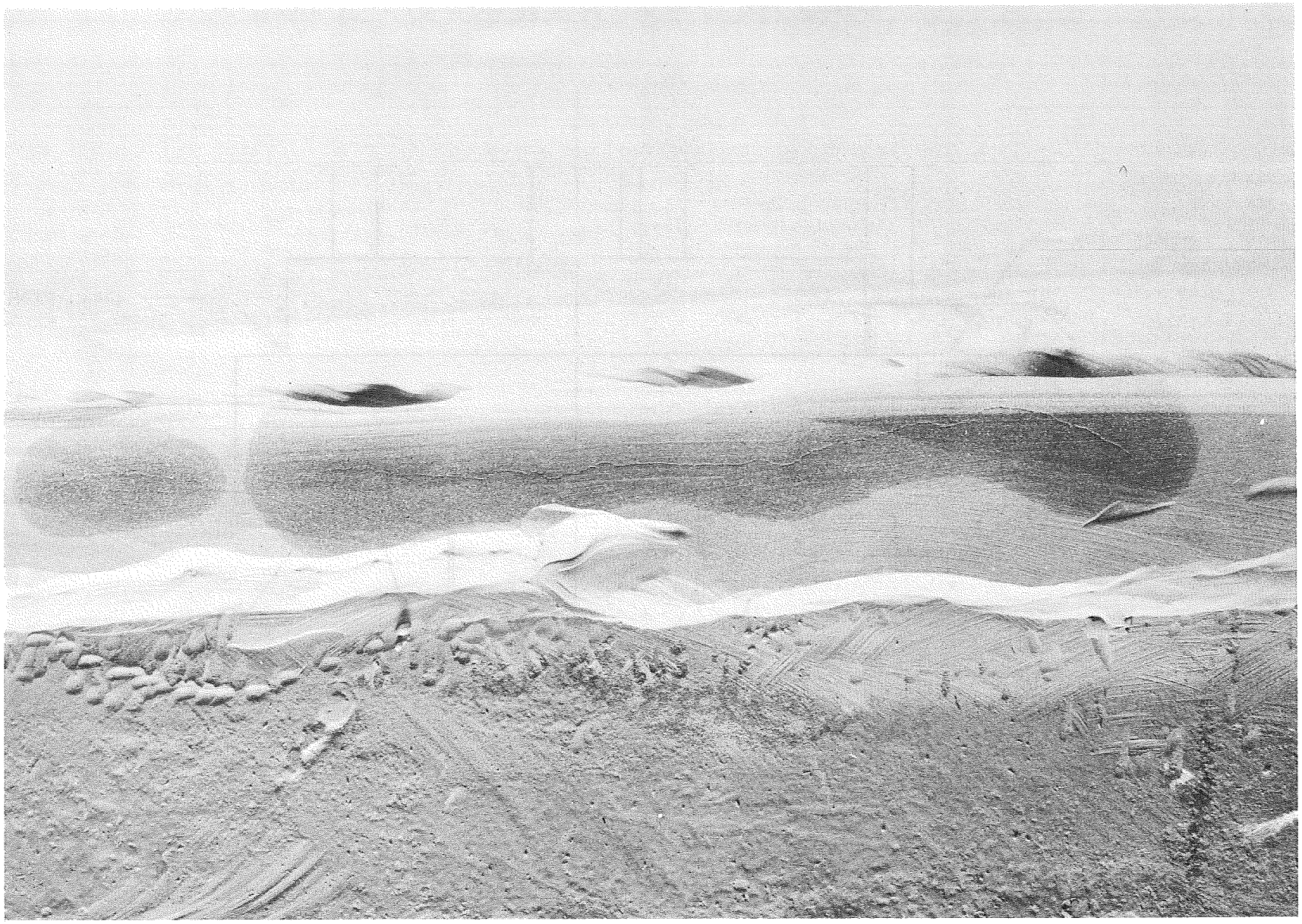

Figure 58. - Weld Crack at Tank Structure of the Test Fixture

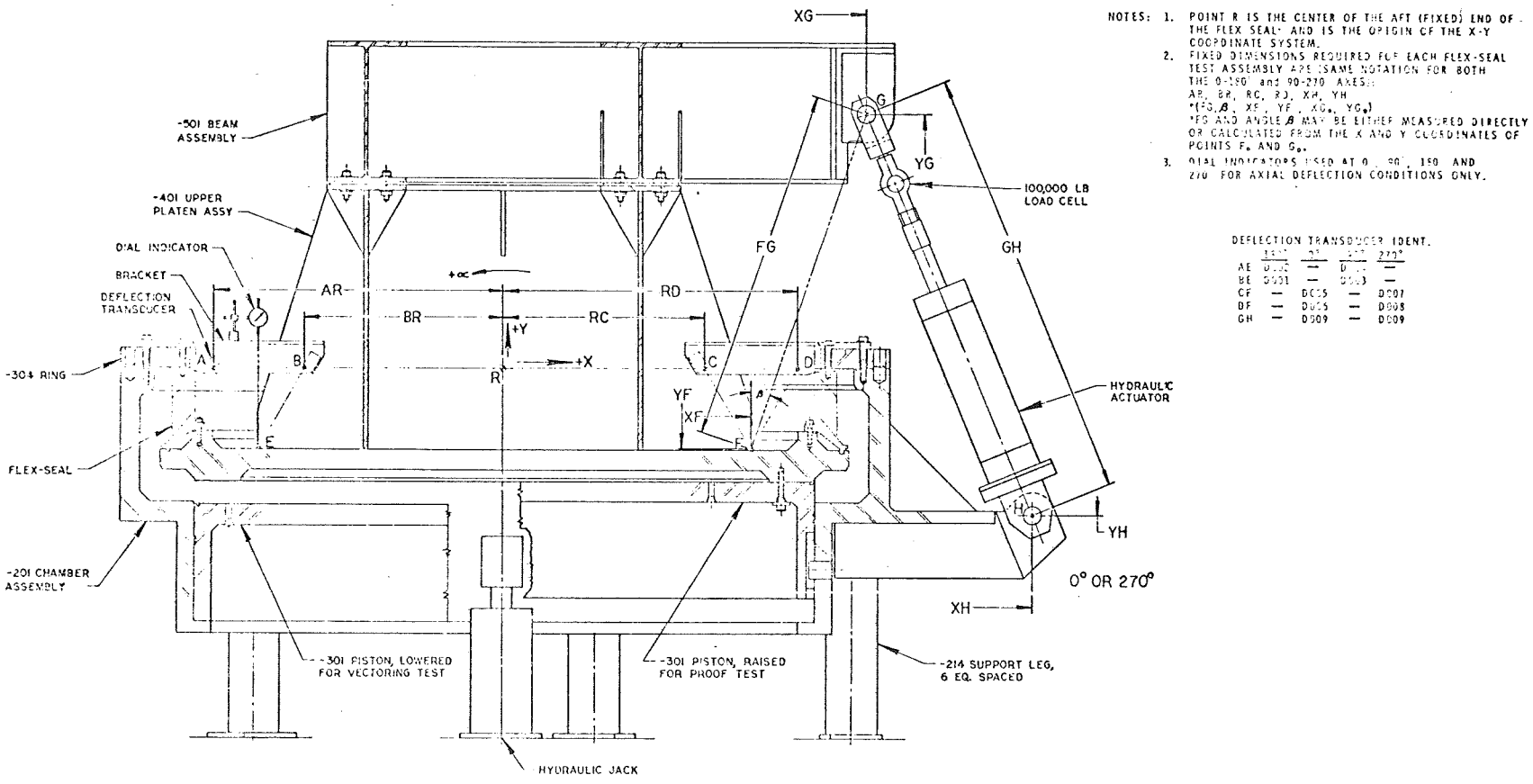

NOTES:
1. POINT R IS THE CENTER OF THE AFT (FIXED) END OF THE FLEX SEAL AND IS THE ORIGIN OF THE X-Y COORDINATE SYSTEM.
2. FIXED DIMENSIONS REQUIRED FOR EACH FLEX-SEAL TEST ASSEMBLY ARE (SAME NOTATION FOR BOTH THE 0-180 and 90-270 AXES):
   AR, BR, RC, RD, XH, YH
   *(FG, β, XF, YF, XG, YG)
   *FG AND ANGLE β MAY BE EITHER MEASURED DIRECTLY OR CALCULATED FROM THE X AND Y COORDINATES OF POINTS F and G.
3. DIAL INDICATORS USED AT 0°, 90°, 180° AND 270° FOR AXIAL DEFLECTION CONDITIONS ONLY.

DEFLECTION TRANSDUCER IDENT.

	180°	90°	270°
AE	D005	—	D[illegible]	—
BE	D001	—	D003	—
CF	—	D005	—	D007
DF	—	D005	—	D008
GH	—	D009	—	D009

Figure 59.- Assembly of the Flexible Seal on the Test Fixture

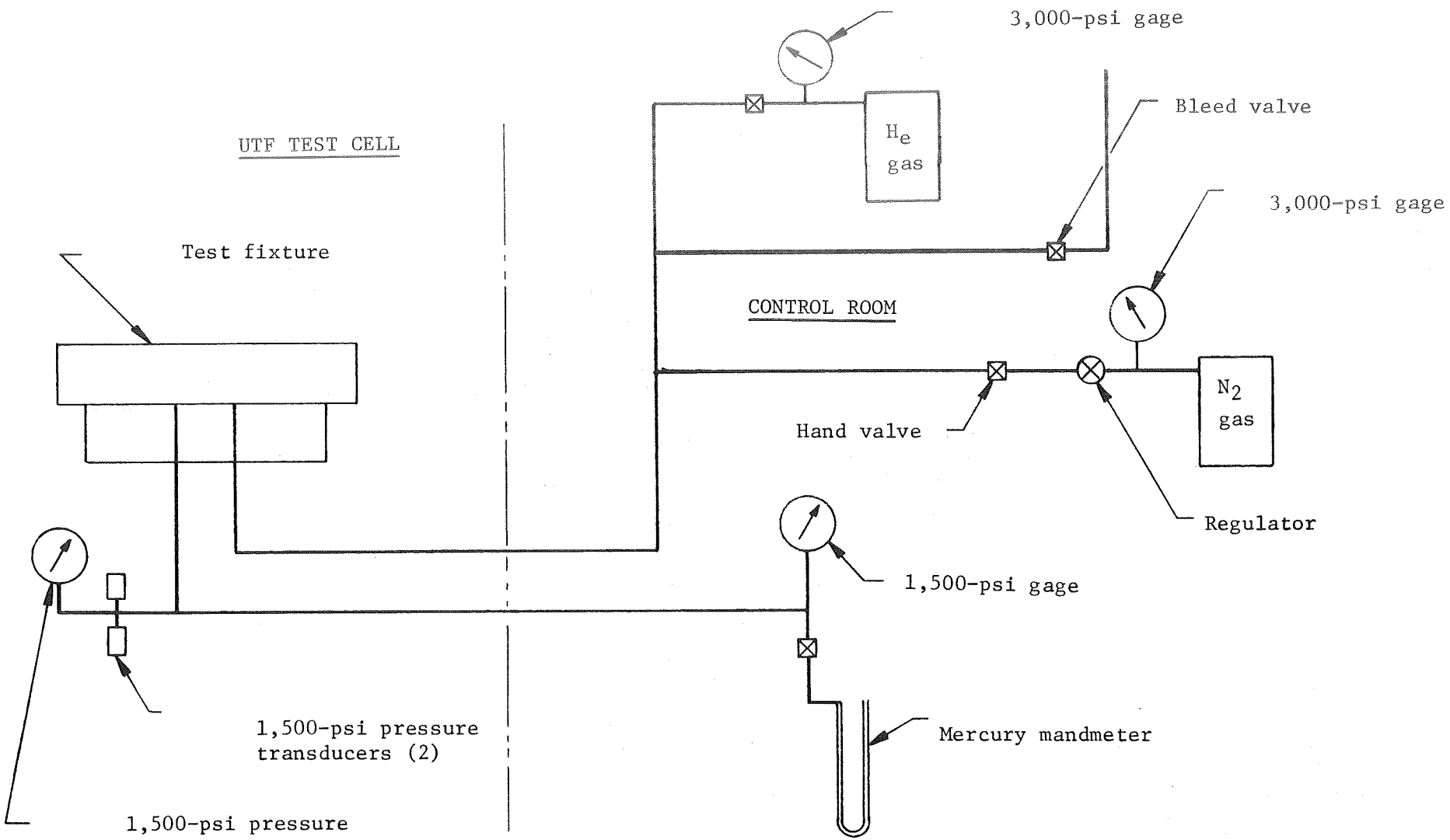

Figure 60. - Gas Pressure System Schematic

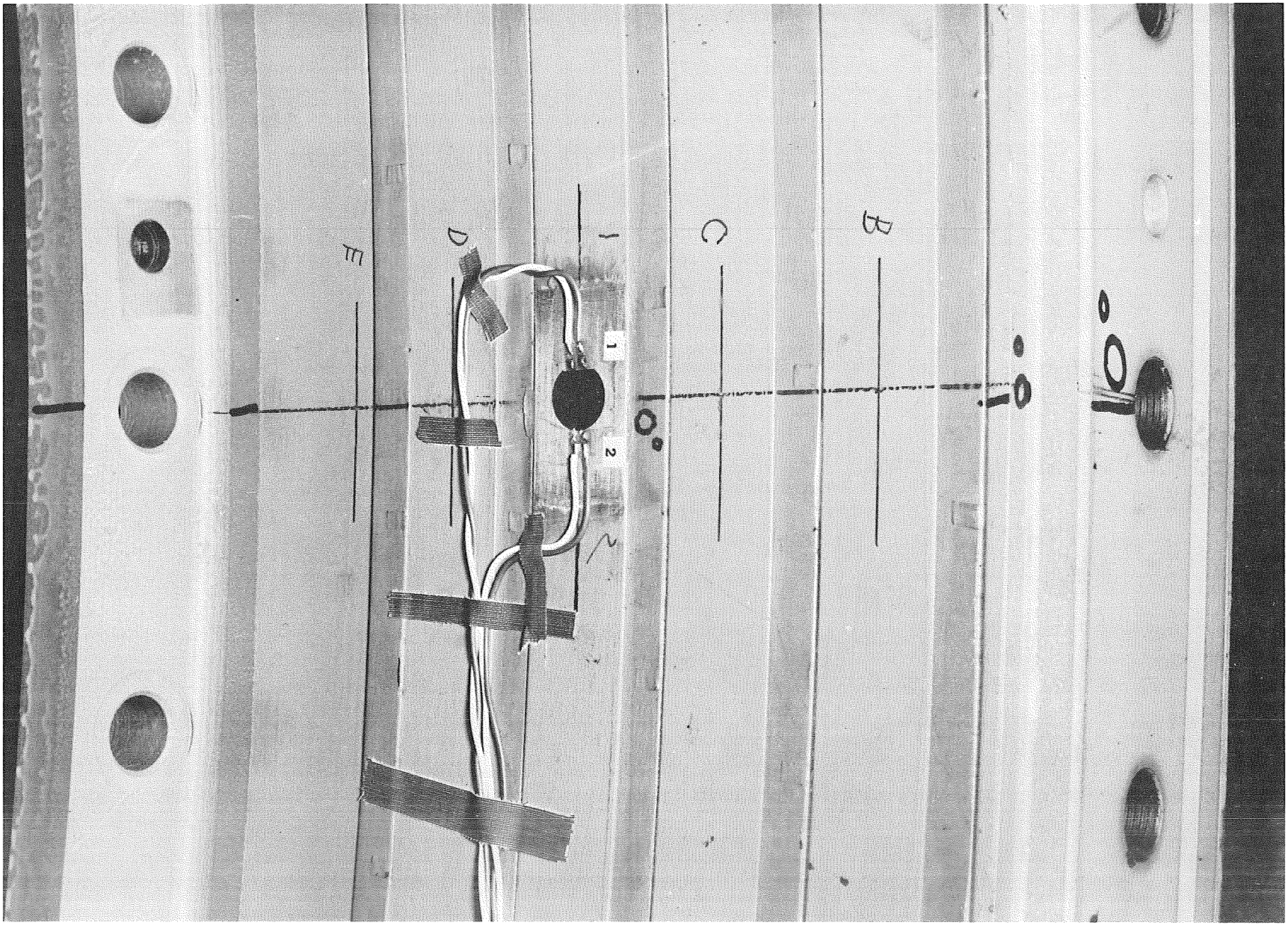

Figure 61. - Typical Strain Gage Installation on the Steel Shim

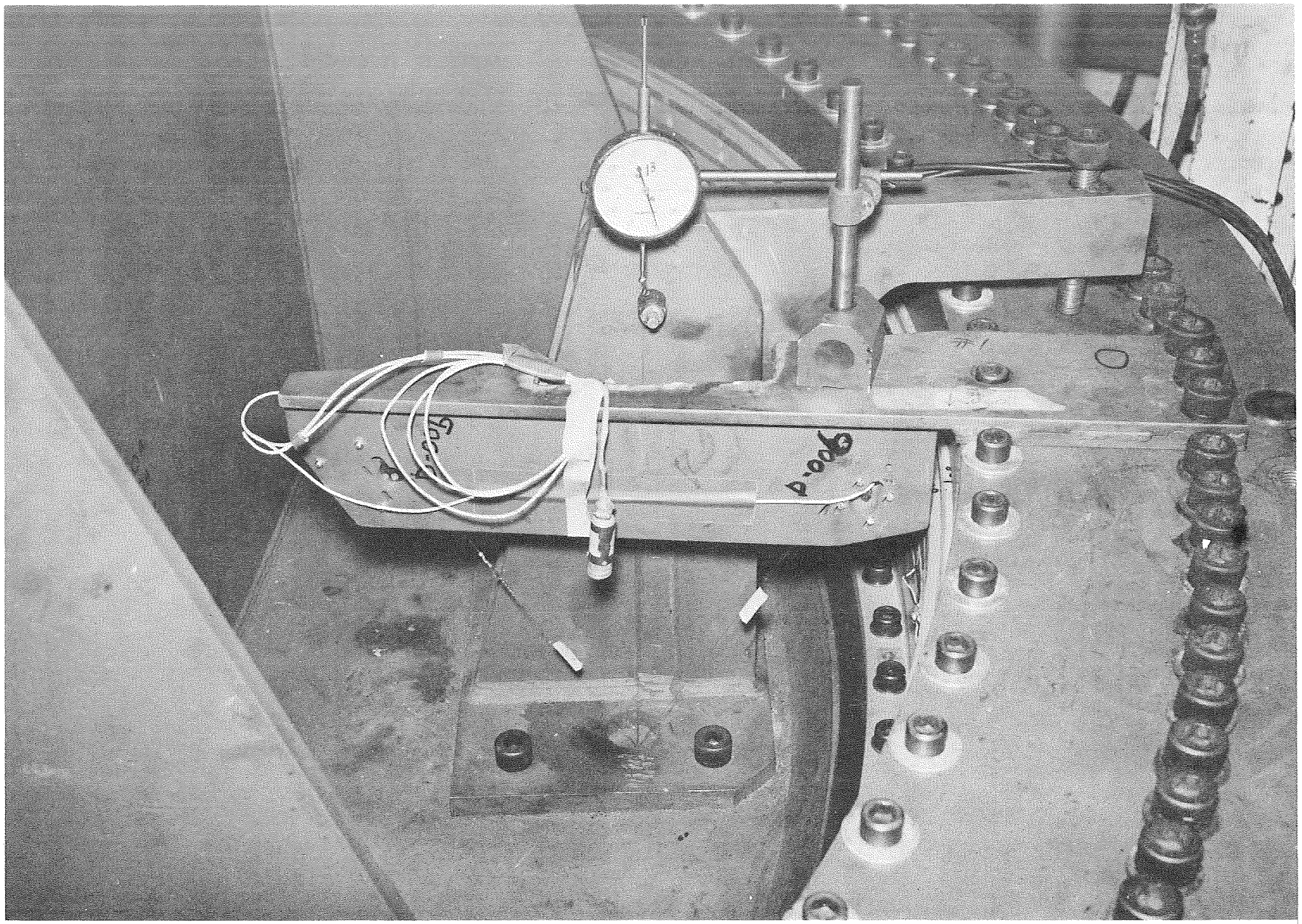

Figure 62. - Typical Dial Gage Installation

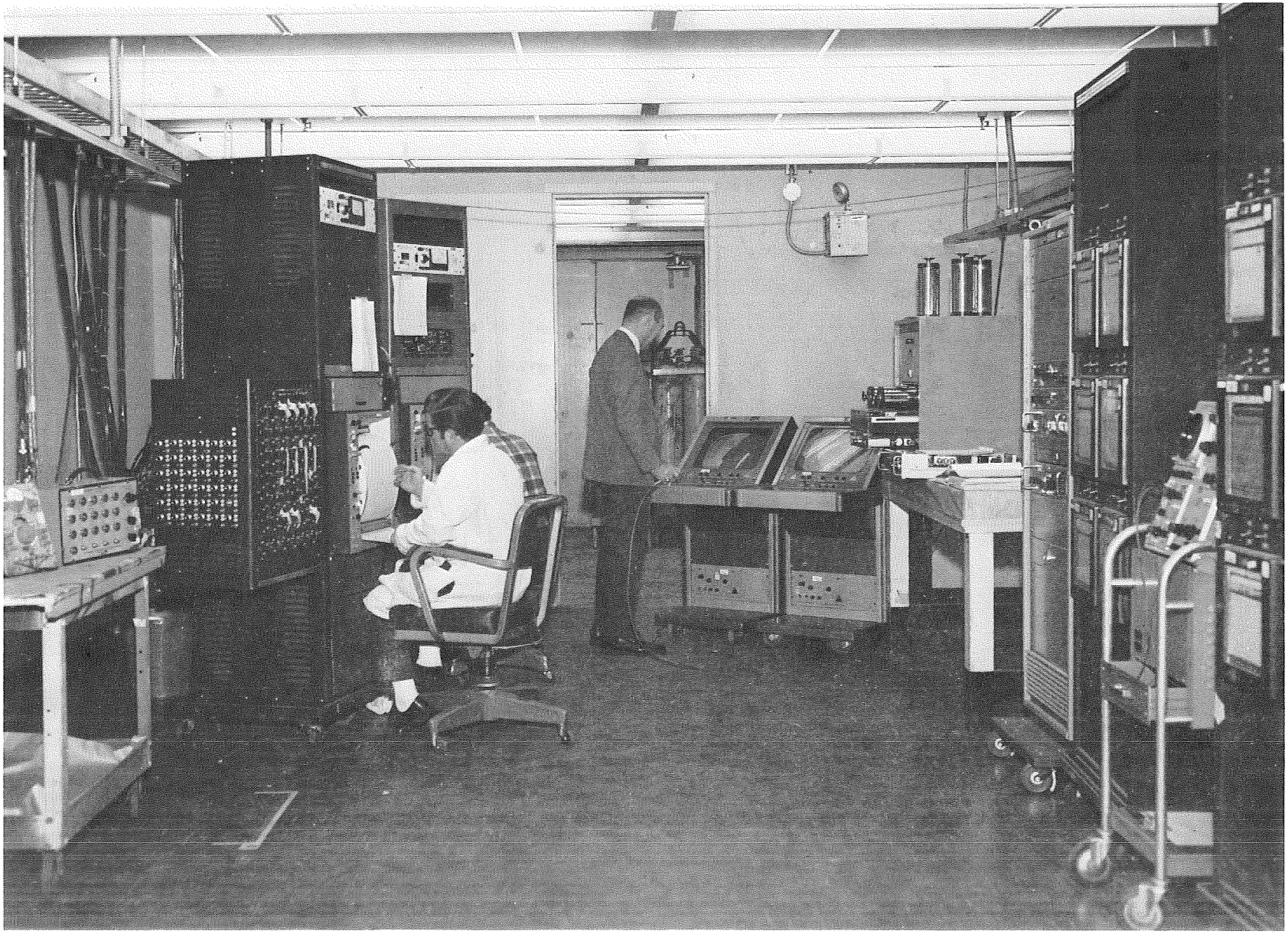

Figure 63. - Control Room Recording Equipment

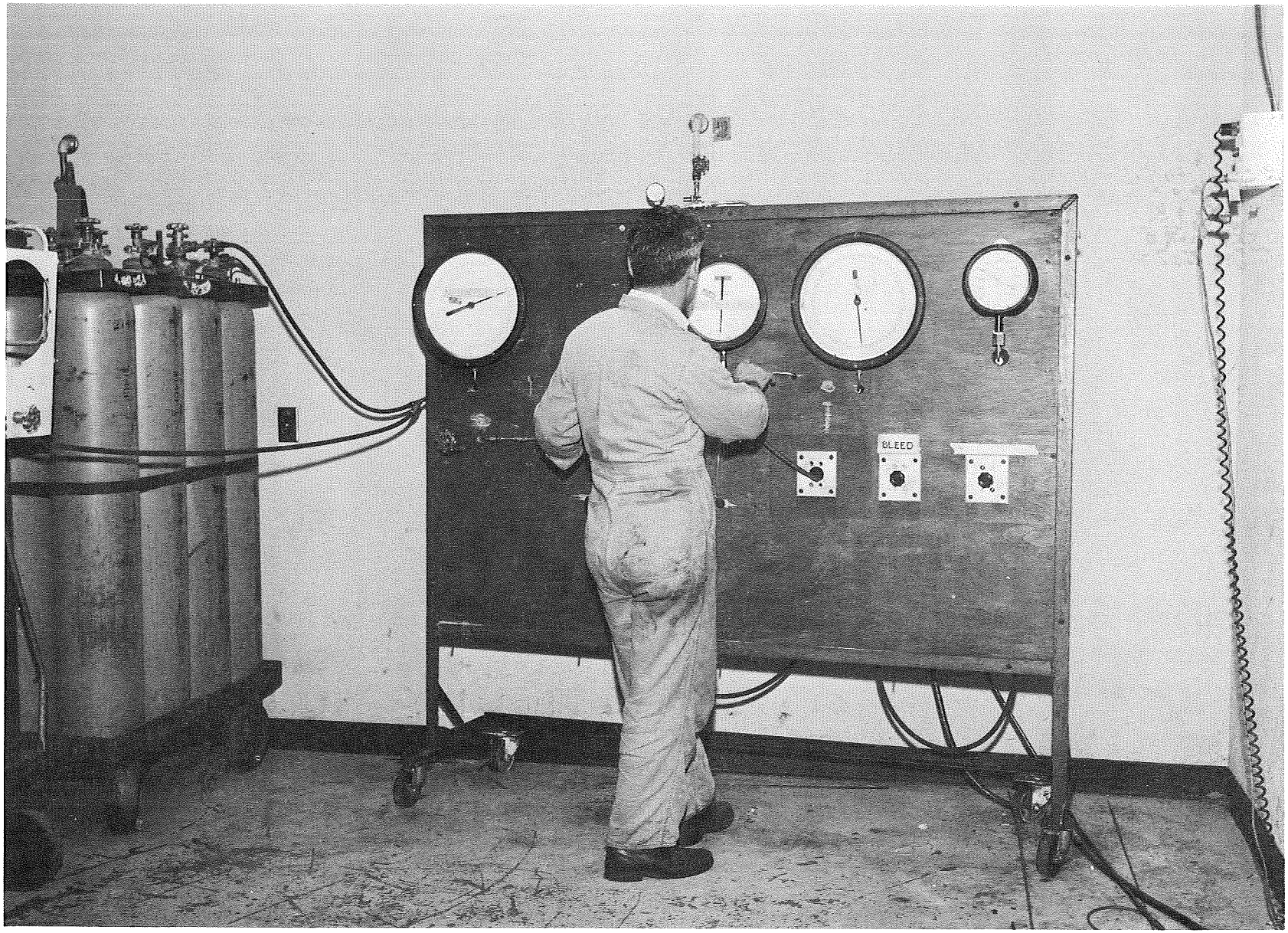

Figure 64. - Pressure Gage Panel

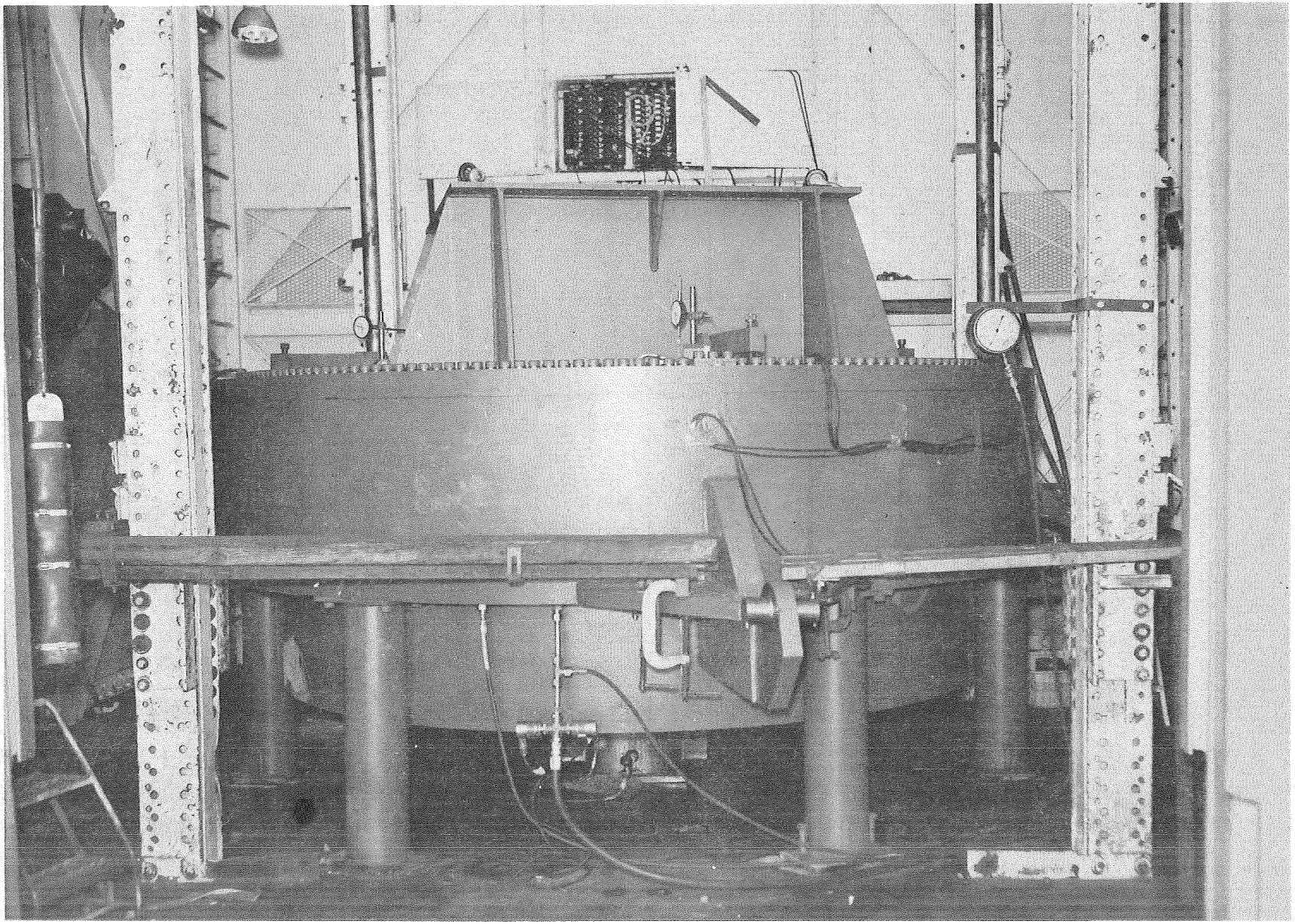

Figure 65. - Seal Proof Pressure Test Setup

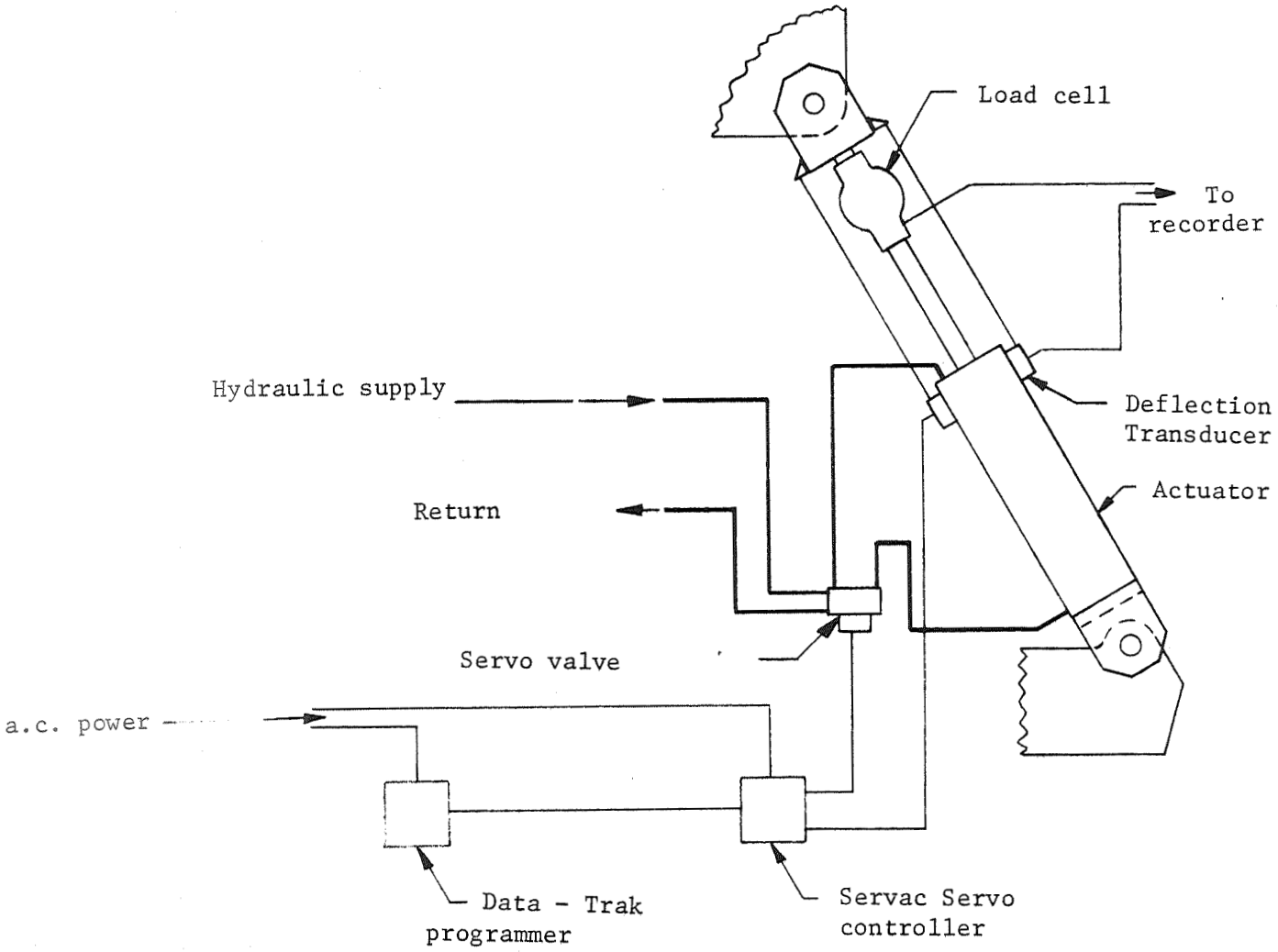

Figure 66. - Seal Actuation System Schematic

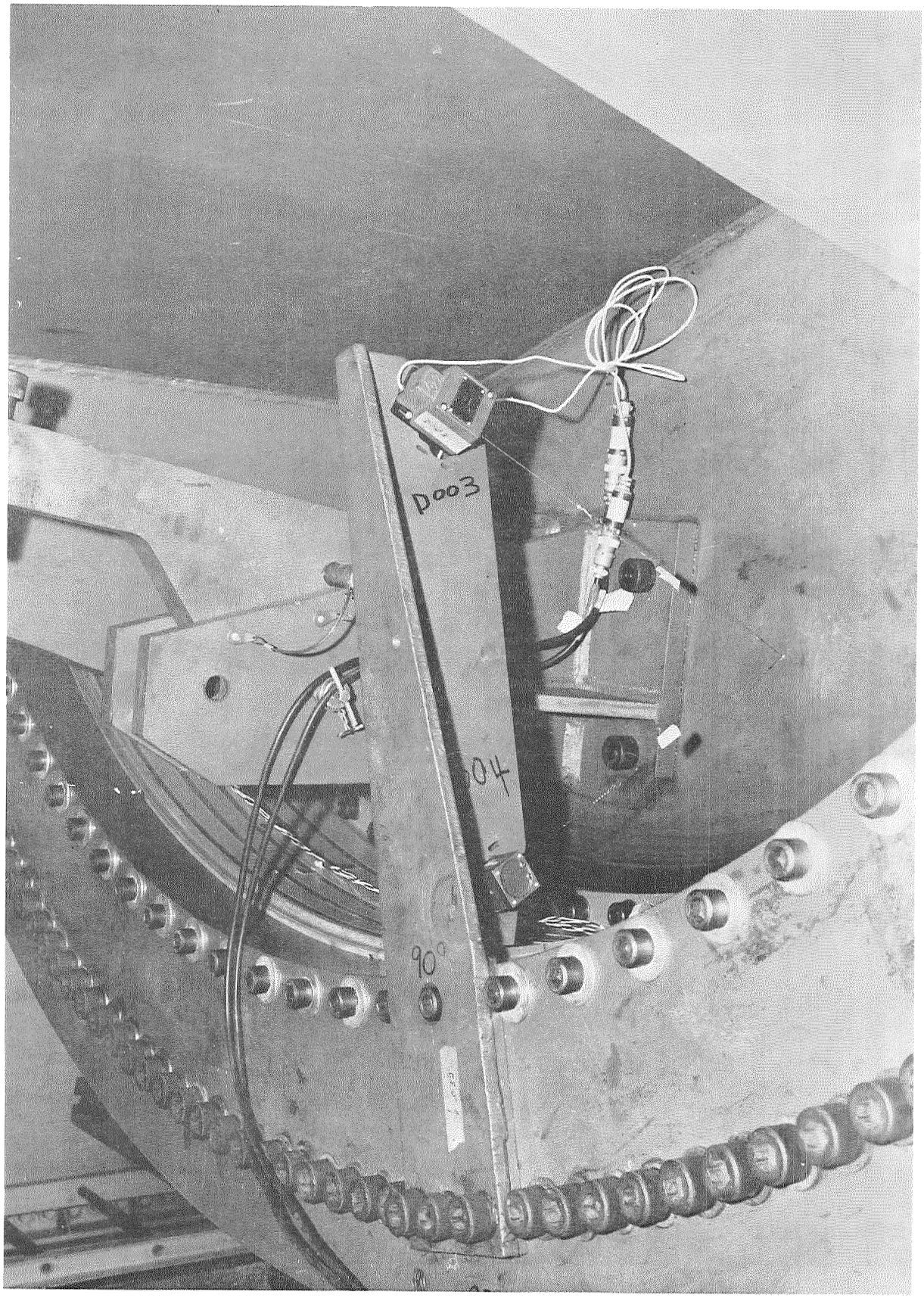

Figure 67. - Typical Deflection Potentiometer Installation

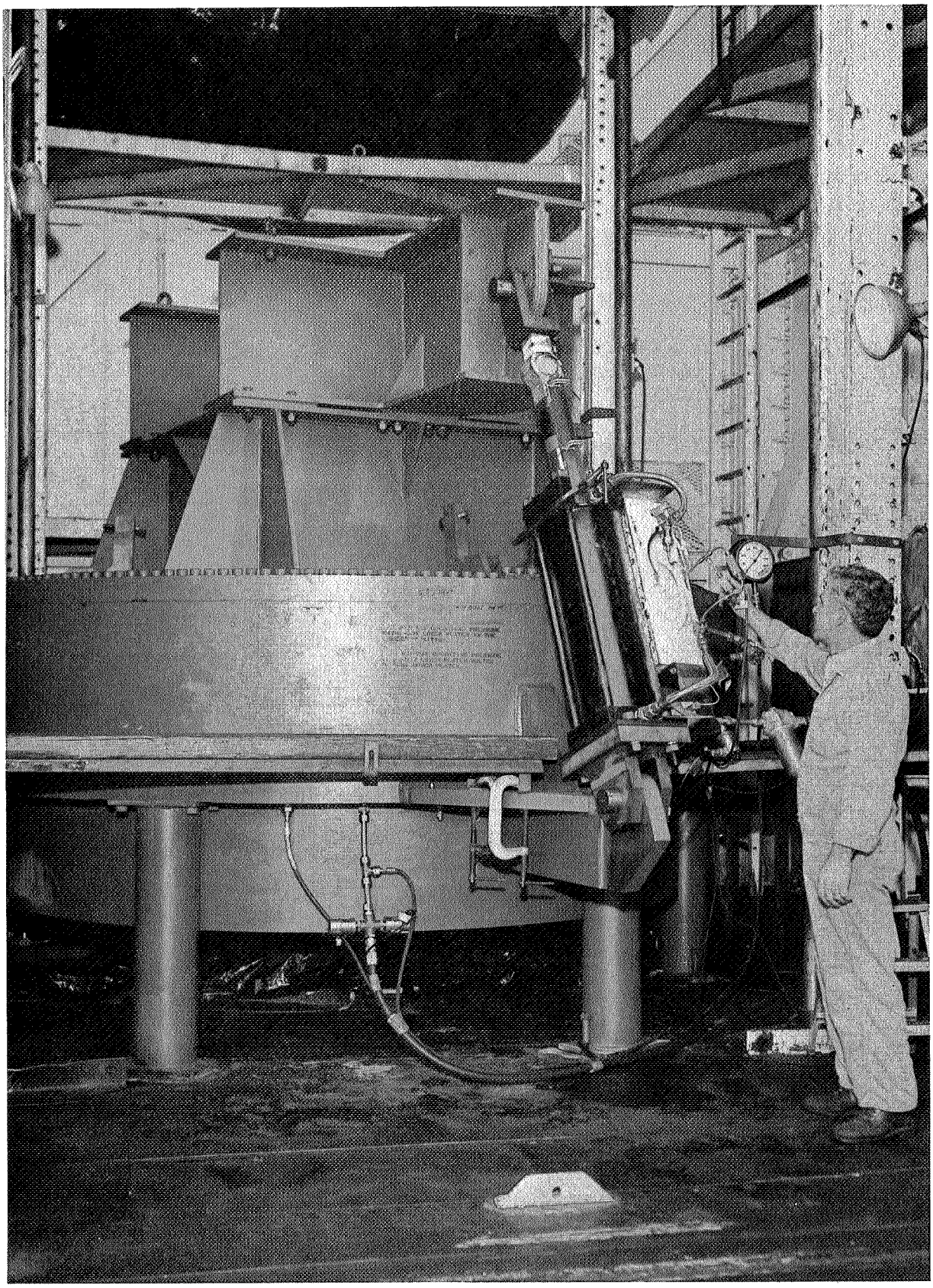

Figure 68. - Seal Vectoring Test Setup

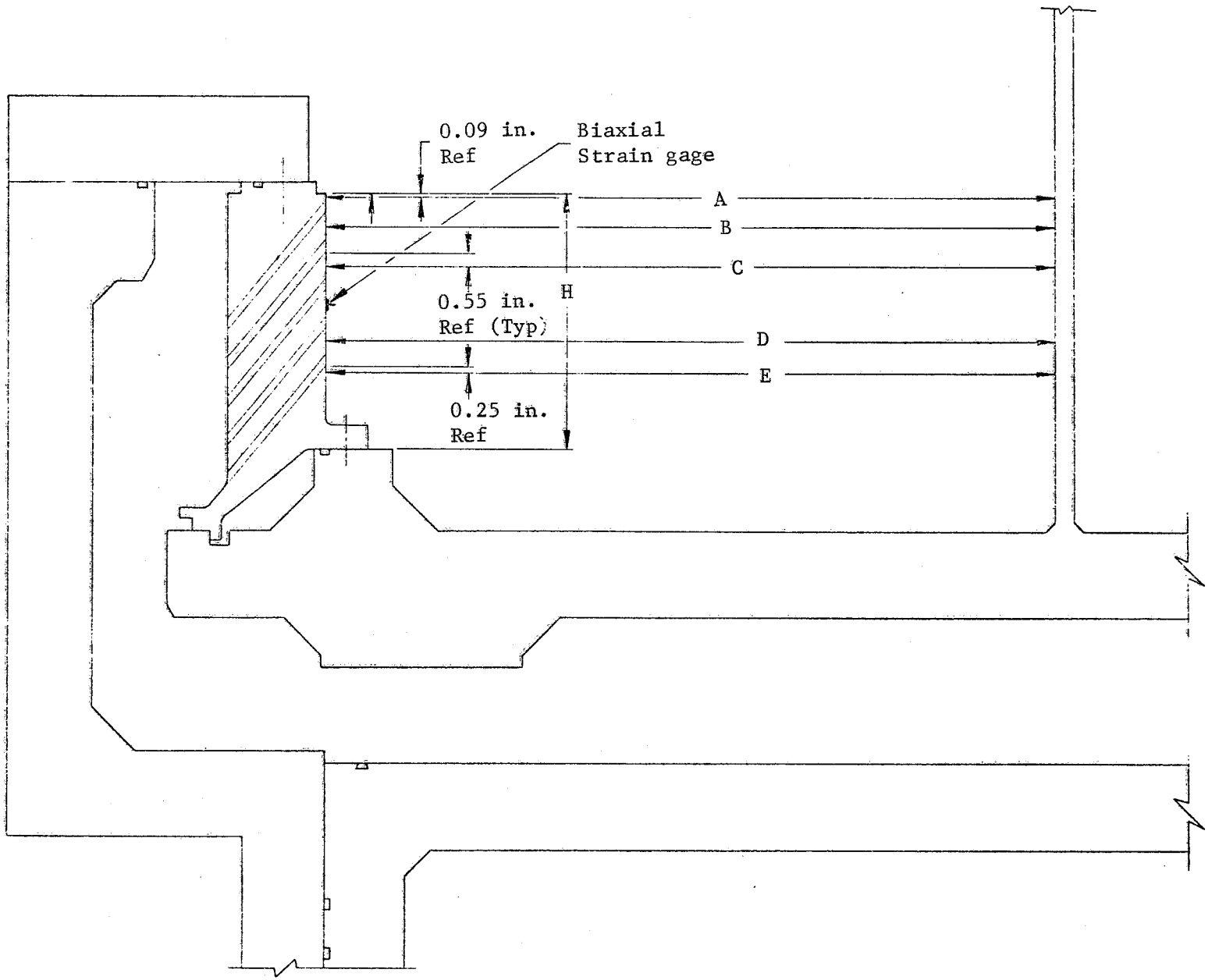

Figure 69. - Seal Height and Laterial Measurement Locations

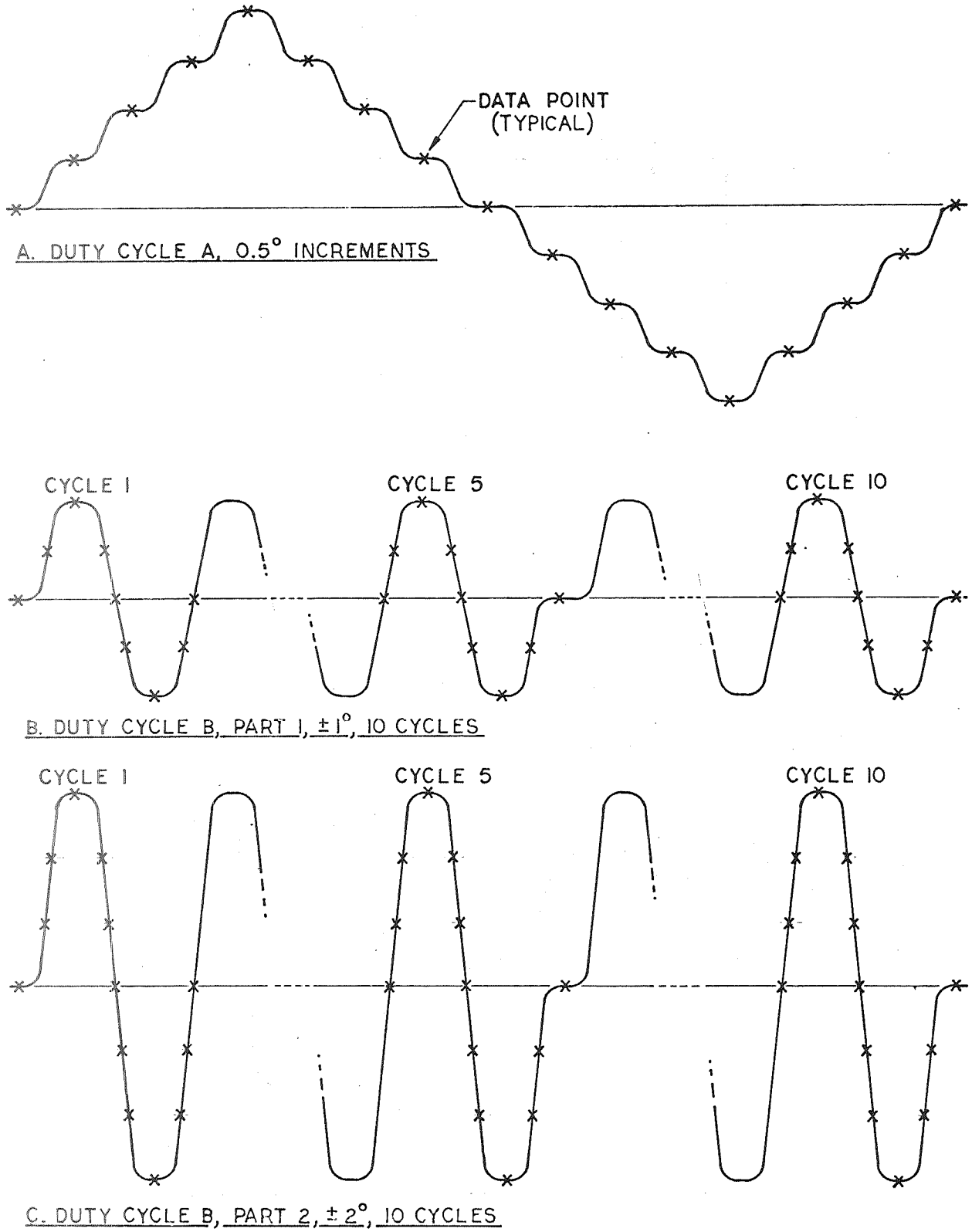

Figure 70. - Seal Vectoring Duty Cycle

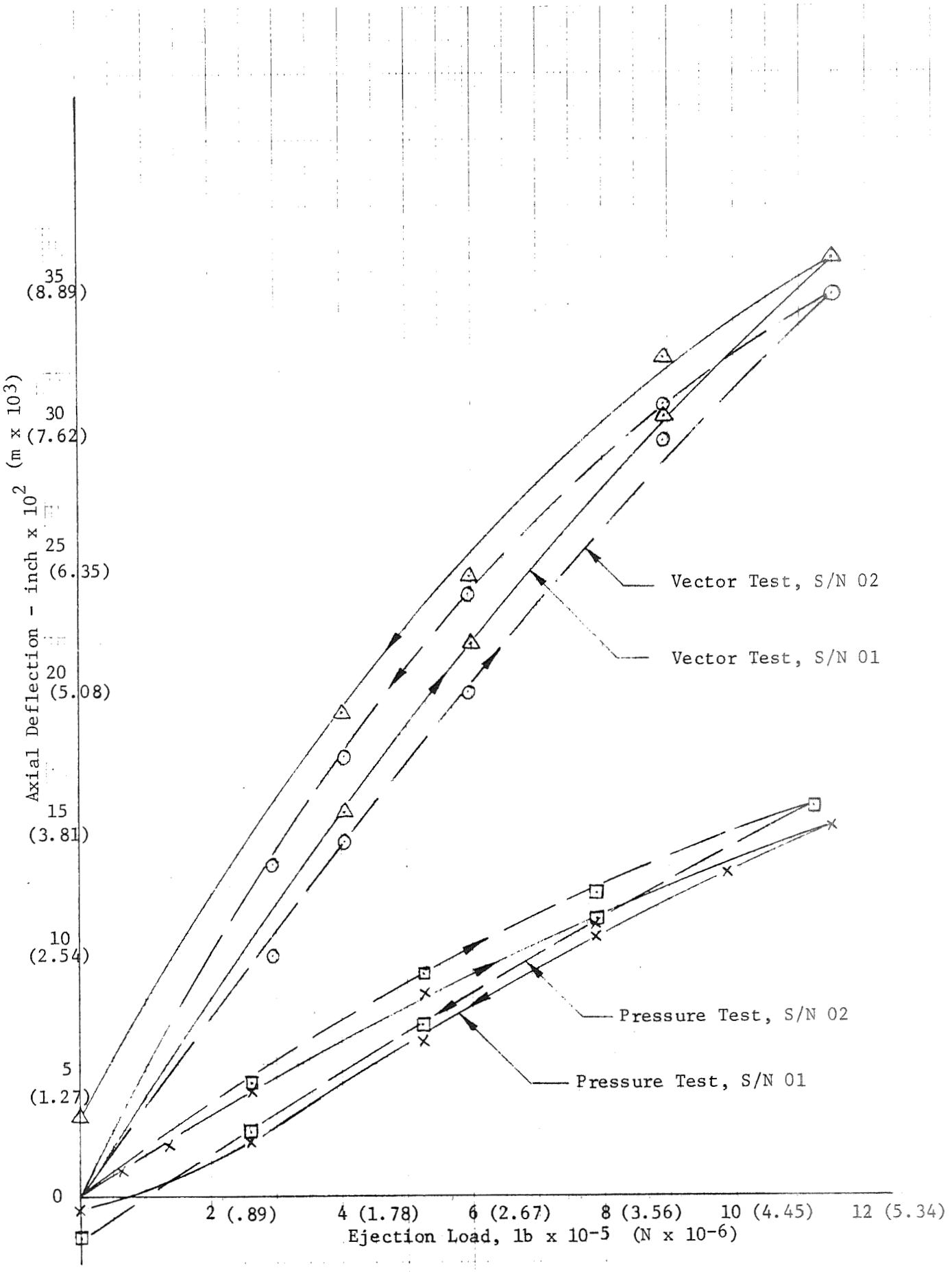

Figure 71. - Axial Deflection vs Ejection Load

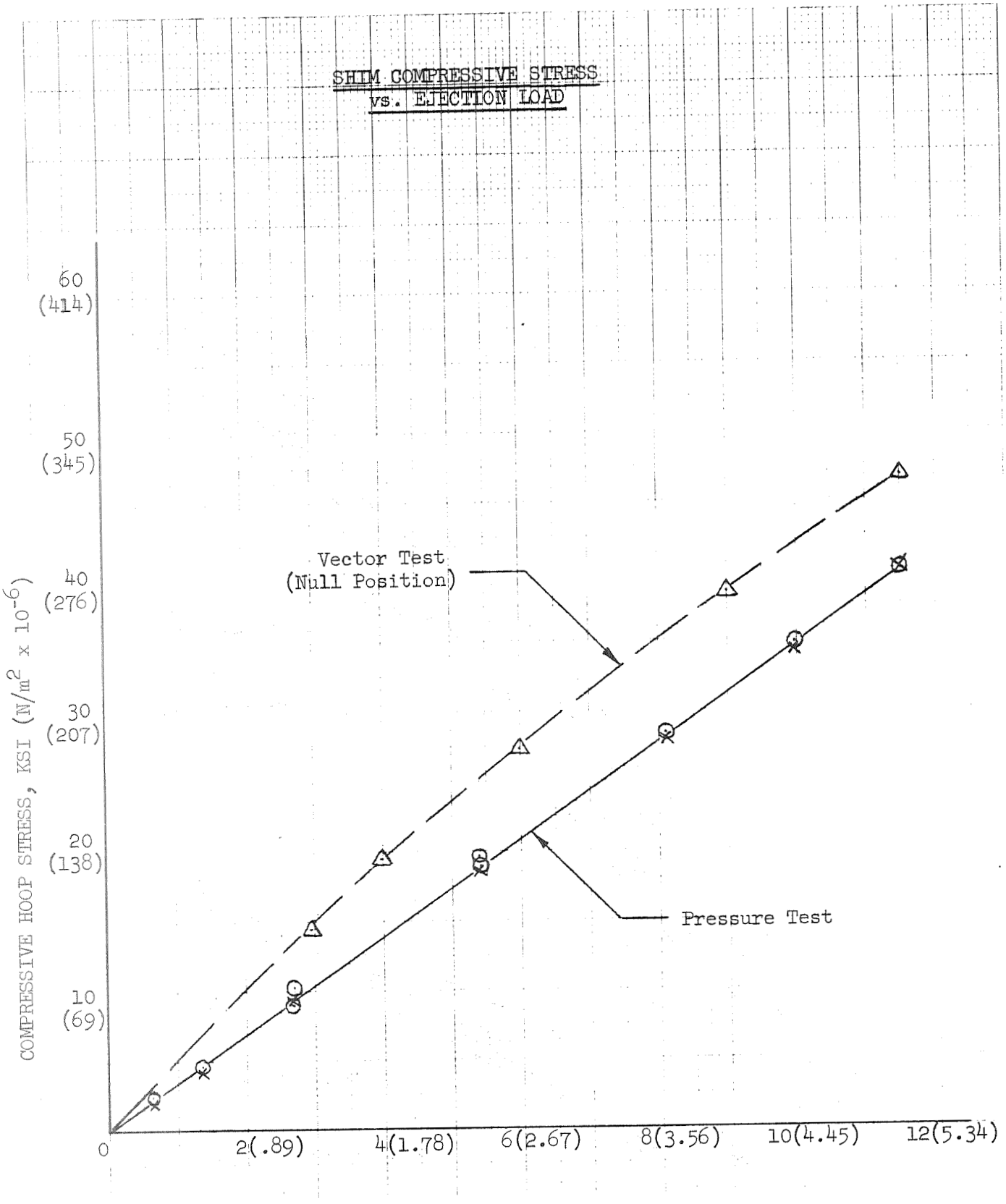

Figure 72. - Ejection Load, lb x 10^{-5} (N x 10^{-6})

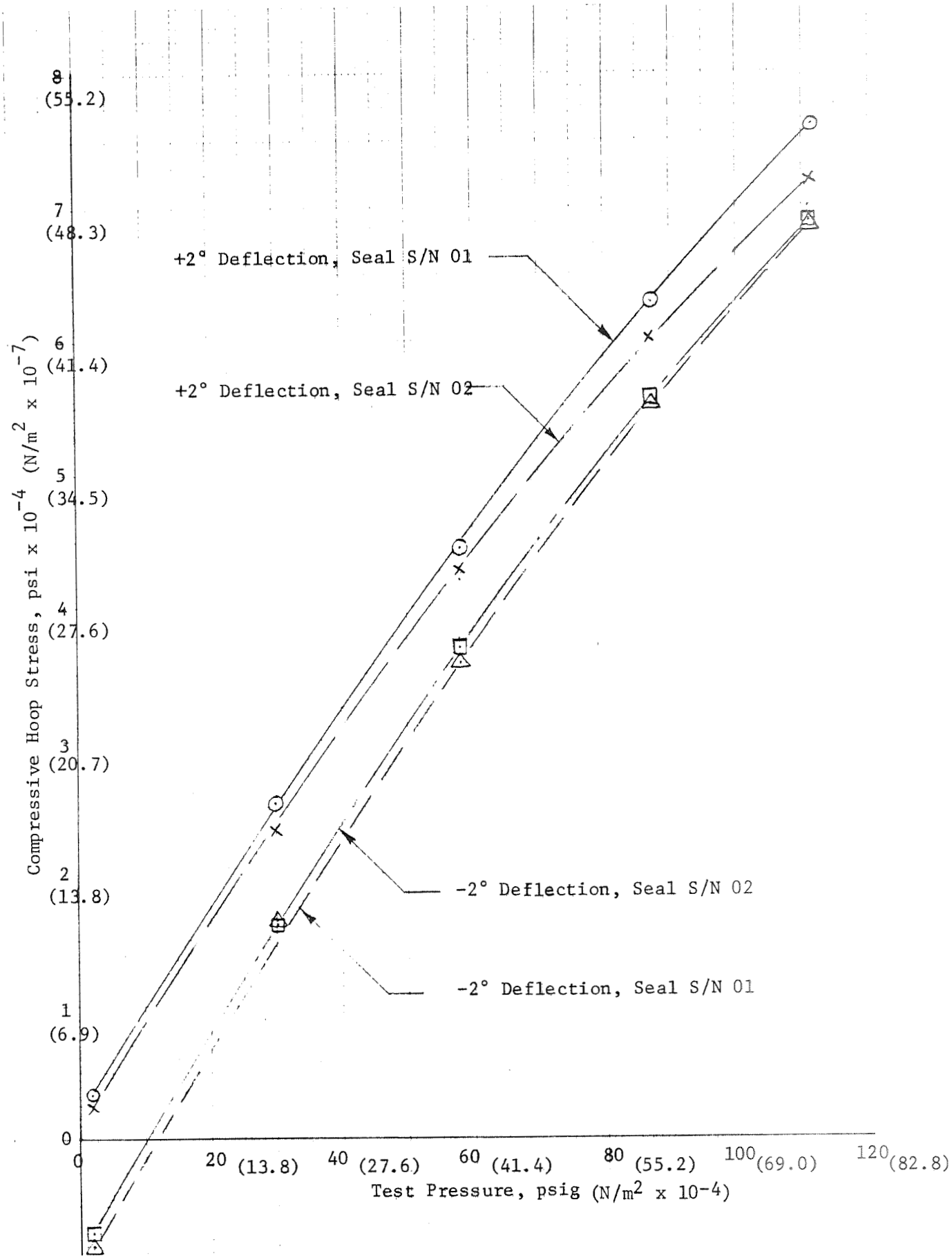

Figure 73. - Variation of Shim Hoop Stress vs Test Pressure

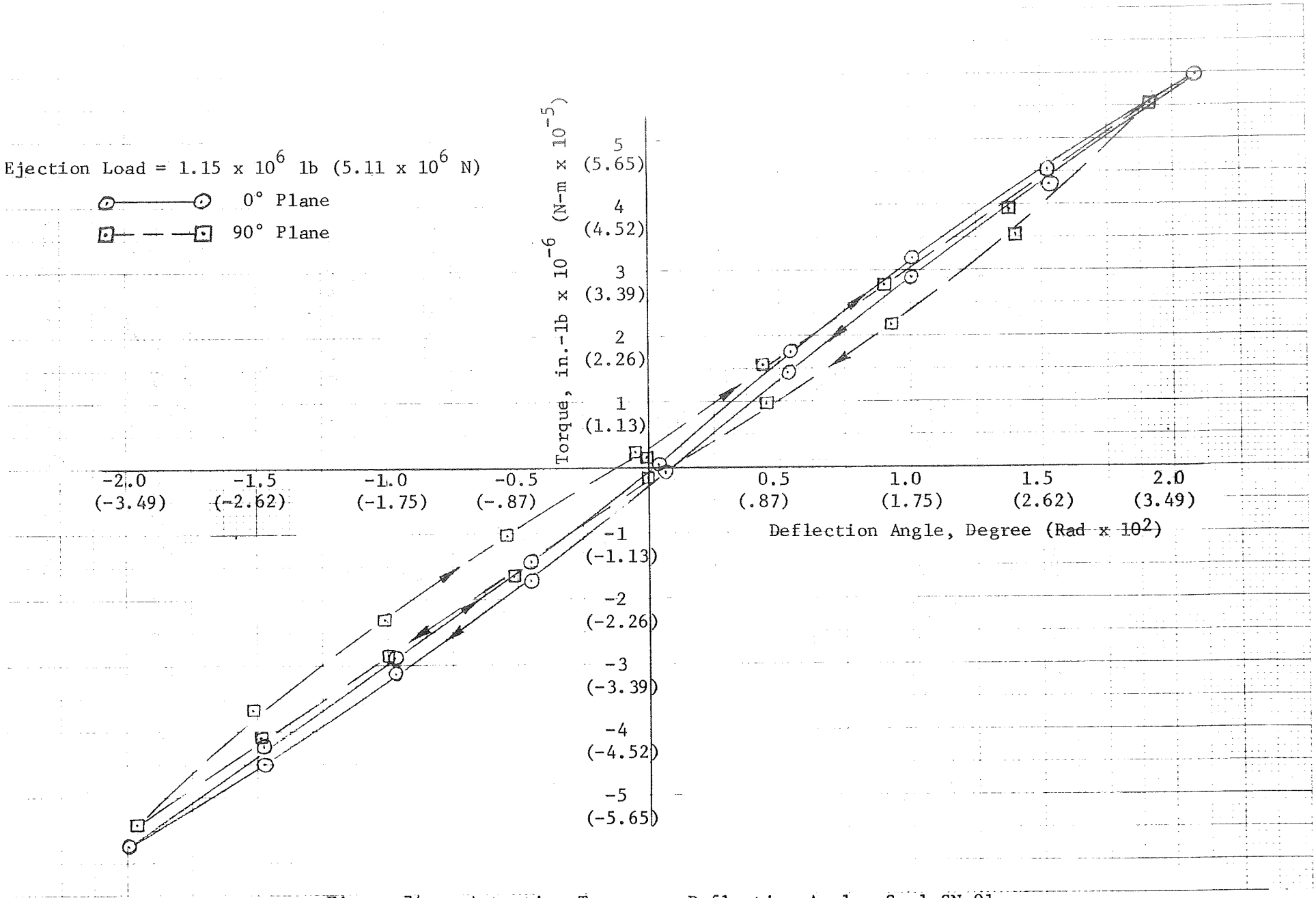

Figure 74. - Actuation Torque vs Deflection Angle, Seal SN 01

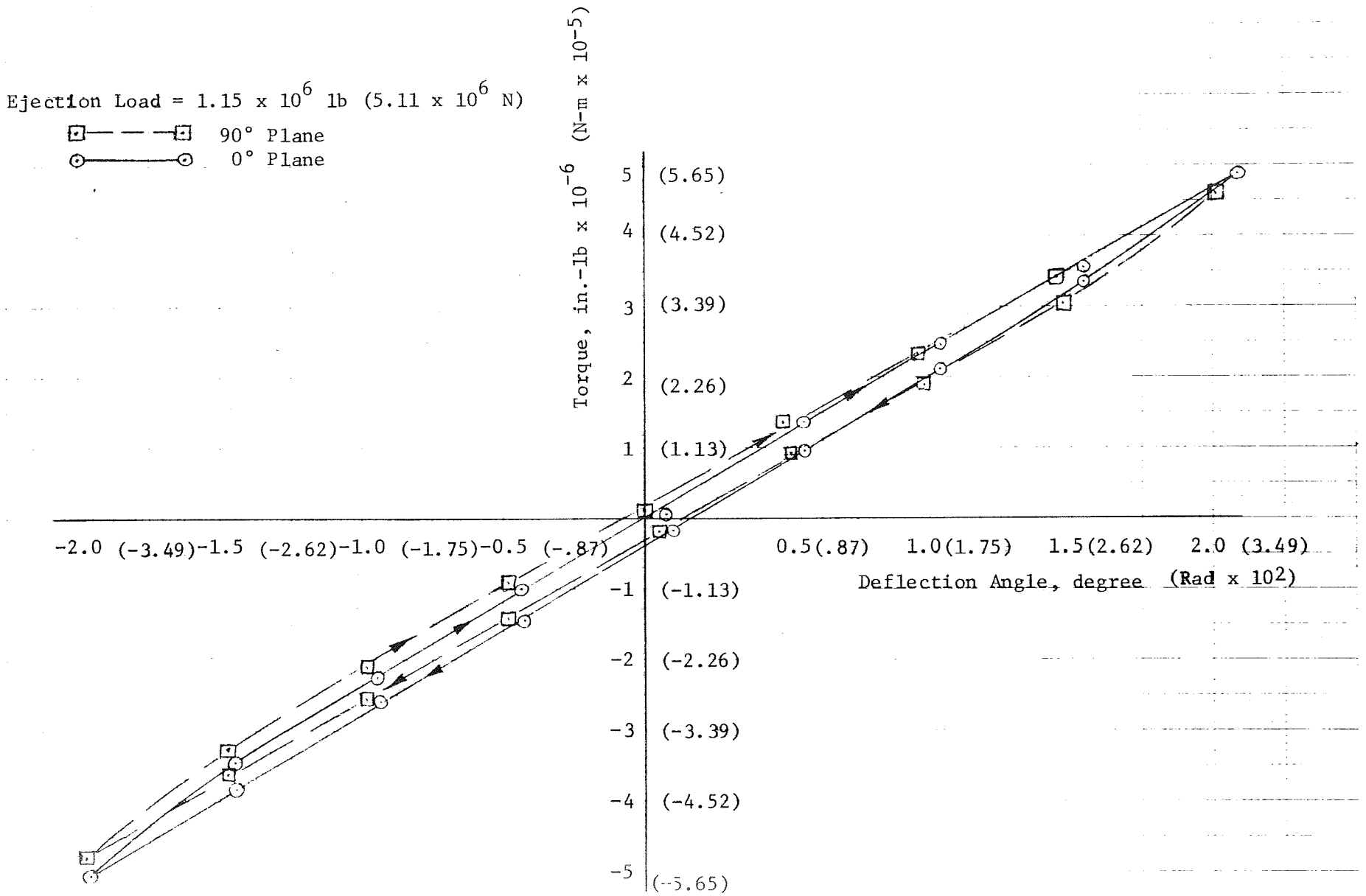

Figure 75. - Actuation Torque vs Deflection Angle, Seal SN 02

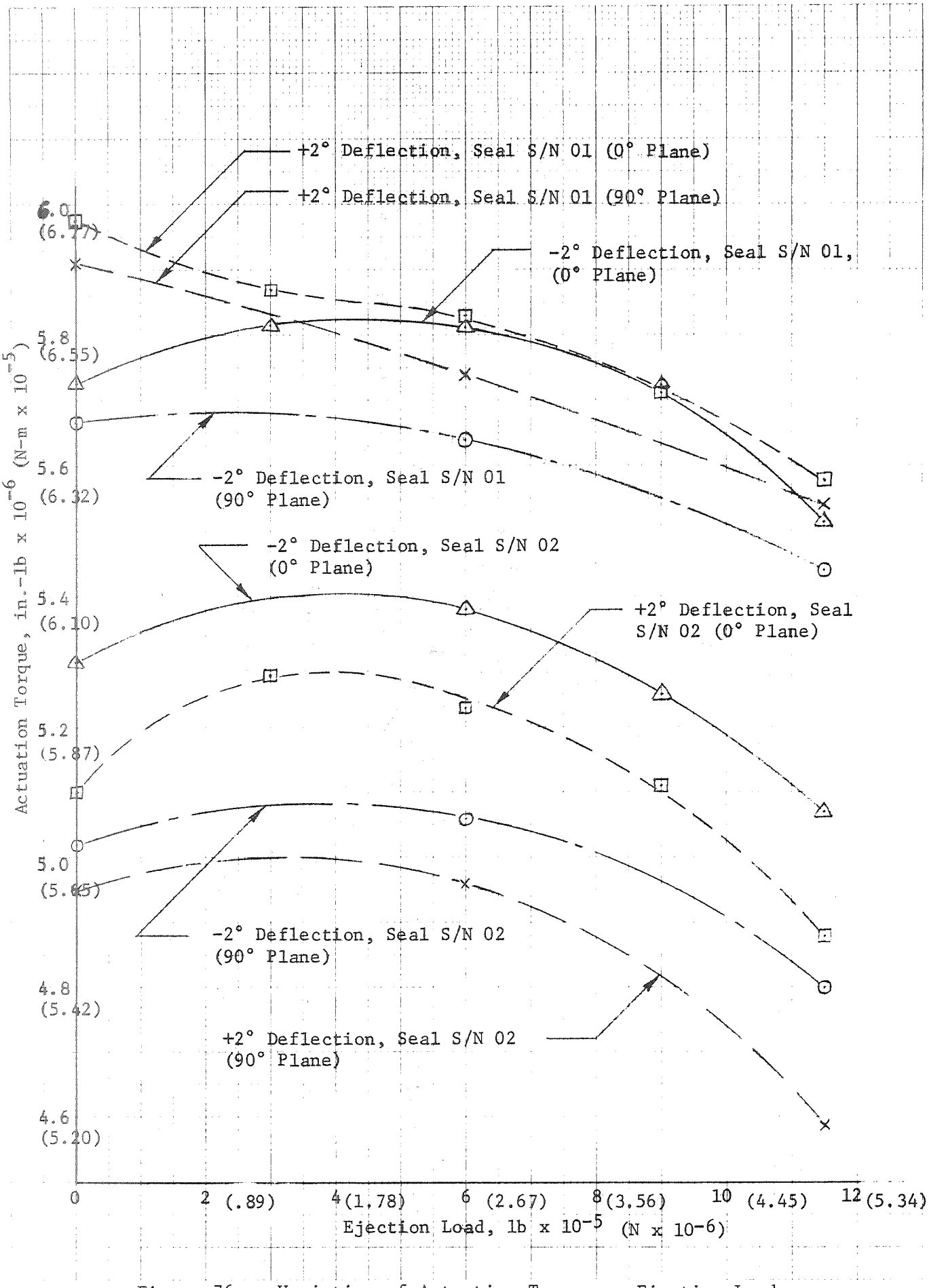

Figure 76. - Variation of Actuation Torque vs Ejection Load

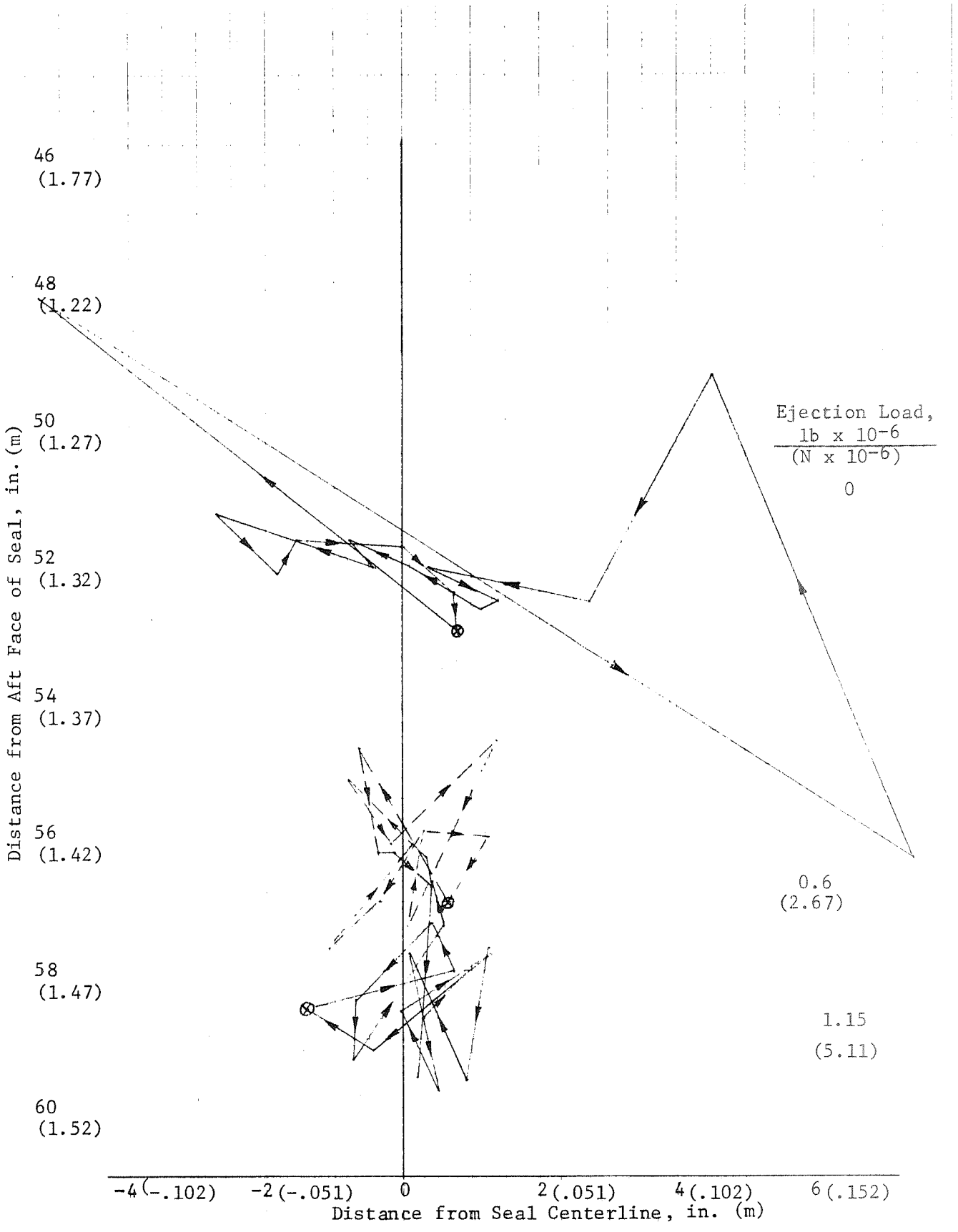

Figure 77. - Pivot Point Excursion for ± 2° Deflection Angle

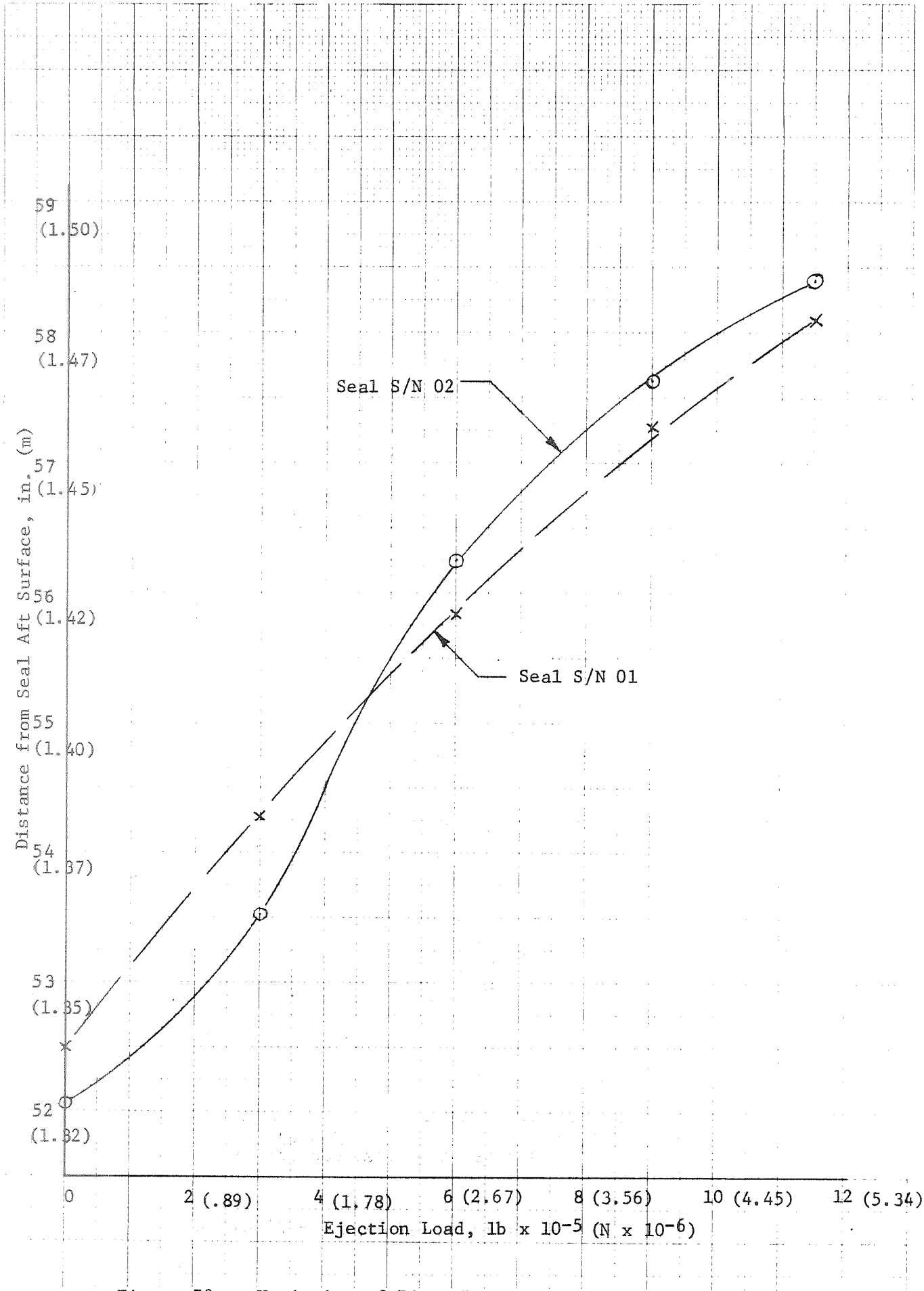

Figure 78. - Variation of Pivot Point Location vs Ejection Load

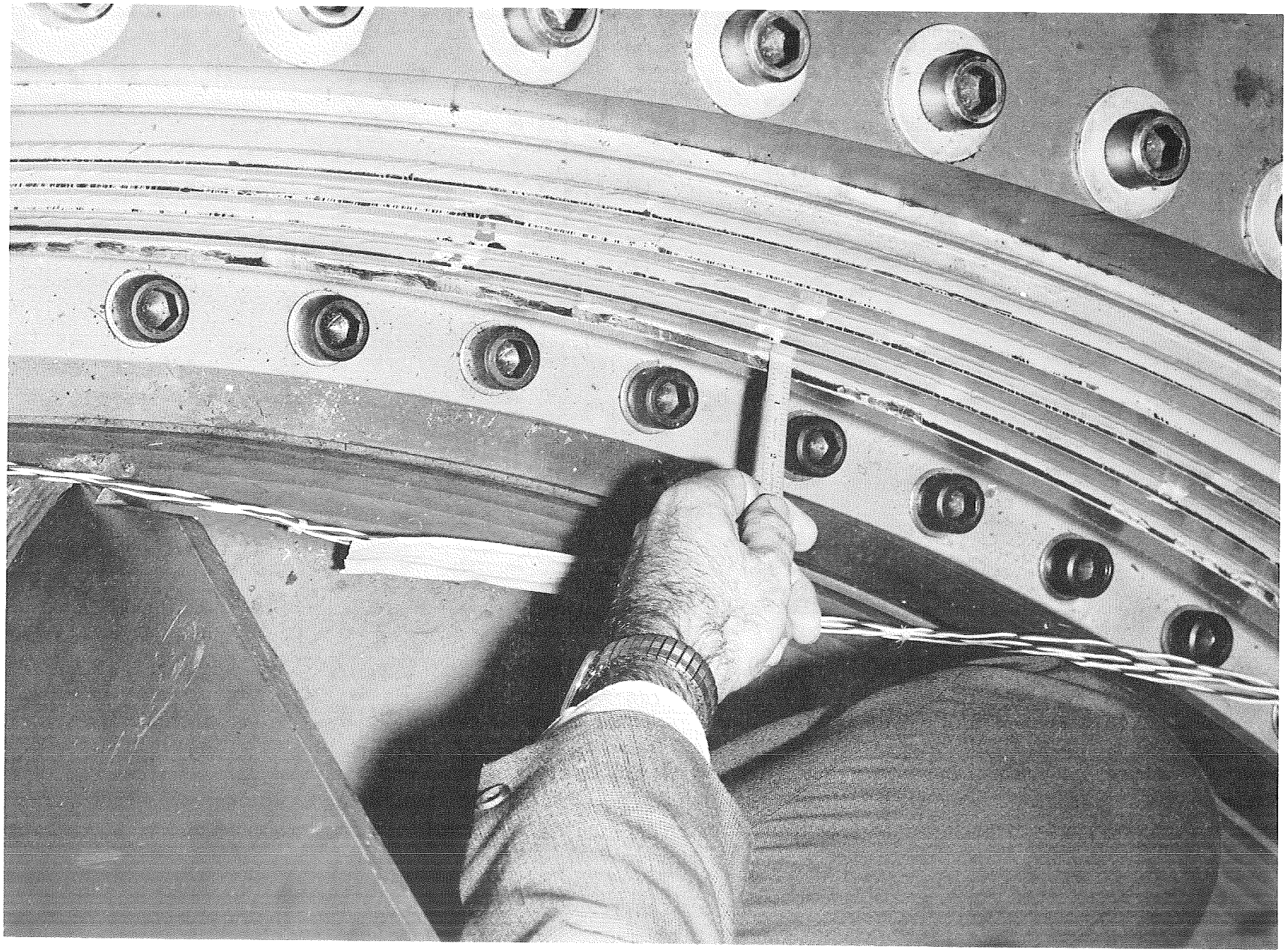

Figure 79. - Seal Unbonded Areas Between Rubber Pads and Shims

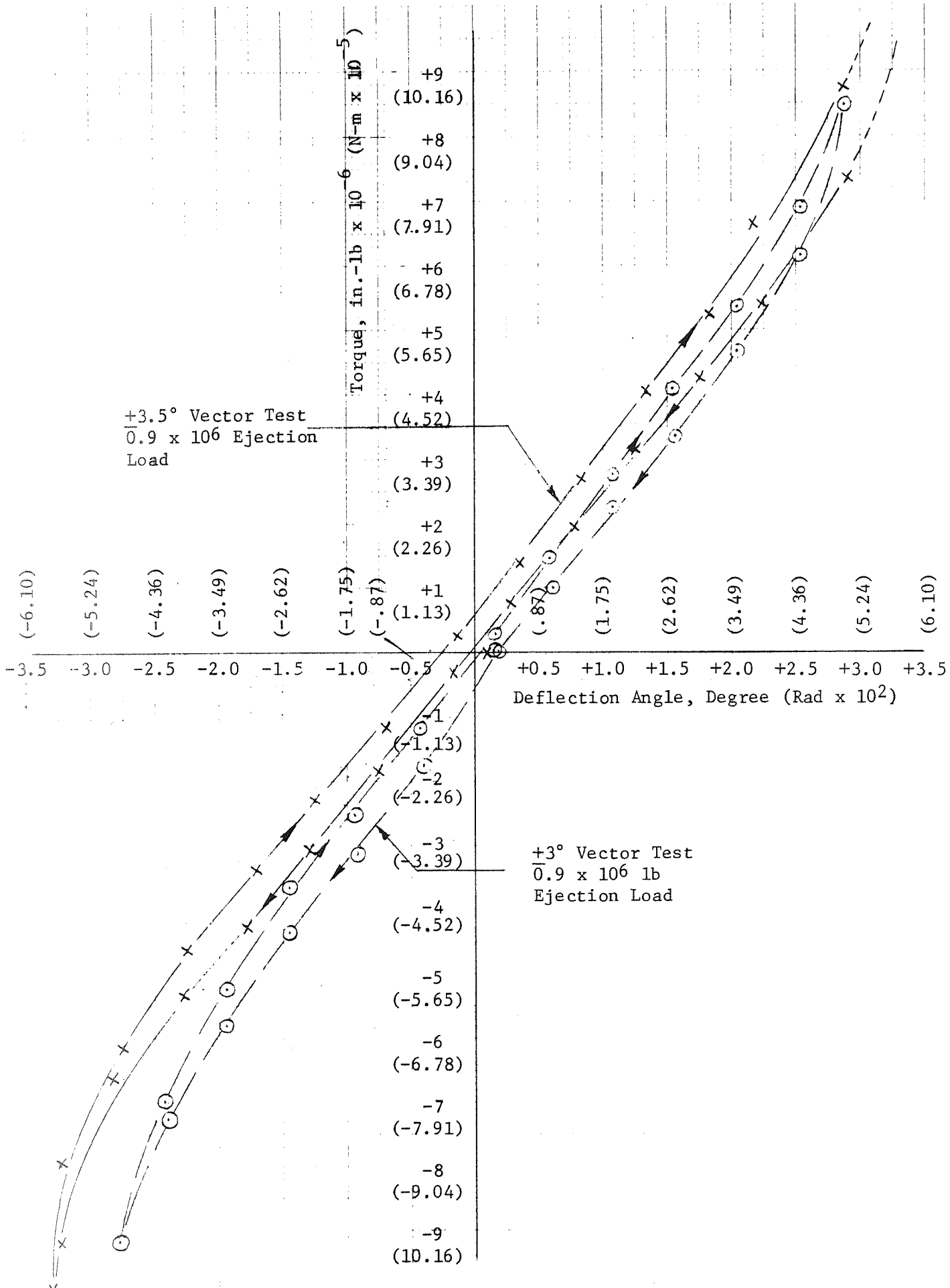

Figure 80. - Actuation Torque vs Deflection Angle, Over-Rotation Test

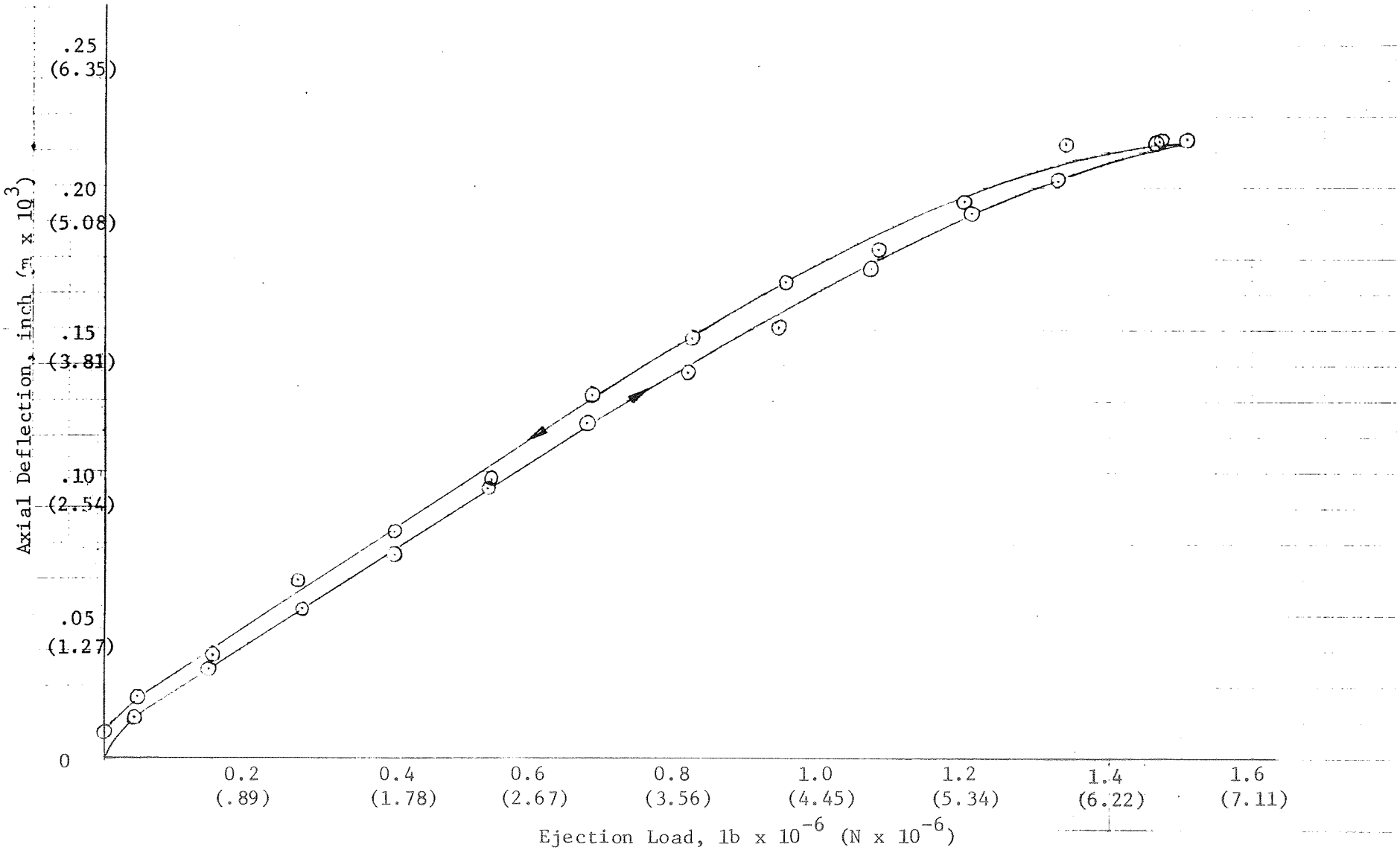

Figure 81. - Axial Deflection vs Ejection Load, Destruct Test

APPENDIX A

FLEXIBLE SEAL FAILURE MODE EVALUATION

Appendix A

FLEXIBLE SEAL FAILURE MODE EVALUATION

I. INTRODUCTION

This analysis was prepared as part of a program to design, fabricate and test flexible seals for a 260-in. (6.6 m) dia solid rocket motor movable nozzle. The scope of this analysis includes the identification of principle failure modes of the seal assembly and the estimation of their probability of occurrence during program testing and under anticipated flight conditions.

II. FAILURE MODE CHARACTERIZATION

The analysis was limited to only those failure modes related directly to the seal, since the nozzle shell, the conical shell and their protective inserts and insulation are not the primary subsystem being evaluated on this contract. As shown in Figure 1, there are three basic failure modes involved with the flexible seal: (a) the structural failure of the seal, (b) the requirement for torque in excess of that available, and (c) the premature burn through of the insulation boot protecting the flexible seal surface. Although all three are possible under flight conditions, only the first two will be evaluated in the test program.

III. PROBABILITY CALCULATION FOR EXCESS TORQUE AND BOOT BURN THROUGH FAILURE MODES

The calculation of the probability of occurrence of torque requirement in excess of the design capability and boot burn through prior to the end of action time was made using the basic requirement vs capability formula:

Appendix A

$$\Phi = \frac{\bar{X}_C - \bar{X}_R}{\sqrt{\sigma_C^2 + \sigma_R^2}}$$

where $\bar{X}_C$ and σ_C are the estimated average and standard deviation of the capability parameter

$\bar{X}_R$ and σ_R are the estimated average and standard deviation of the requirement parameter

Φ is the number of pooled standard deviations between the two parameters which can be equated to failure probability by reference to standard statistical tables of the normal distribution.

In calculation of the probability of excess torque, the requirement average was estimated from the approximate design formula:

$$T = \frac{.615\ G\ W^{1.5}\ R^{1.5}}{N\ t} \qquad \left(\frac{1.95}{1.45}\right)$$

where T = torque per degree deflection, in.-lb/degree

G = rubber seal modulus, $lb/in.^2$

W = seal radial width, in.

R = inner seal radius, in.

t = pad thickness, in.

N = number of pads

The ratio of 1.95/1.45 was determined in the preliminary stress analysis to be the amount required to adjust the results from the approximate design formula

to those obtained in the computer analysis. The variability of the required torque was estimated from this formula by the propagation of variance technique:

$$\frac{\sigma_T}{\bar{T}} = \sqrt{\left(\frac{\sigma_G}{\bar{G}}\right)^2 + \left(\frac{1.5\ \sigma_W}{\bar{W}}\right)^2 + \left(\frac{2.5\ \sigma_R}{\bar{R}}\right)^2 + \left(\frac{\sigma_t}{\bar{t}}\right)^2}$$

Using the values tabulated in Figure 2, a value of 4.60×10^6 in. lb (5.20×10^5 N-m) was obtained for $\bar{T}$ and $.266 \times 10^6$ in. lb ($.30 \times 10^5$ N-m) for T. Assuming that the capability ($\bar{X}_C$) is fixed at 5.00×10^6 in. lb (5.65×10^5 N-m) with no variance, the probability of the requirement exceeding the capability is calculated to be 0.67. Figure 3 illustrates the relationship between torque capability and the probability of exceedence and indicates that a capability of 5.87×10^6 (in. lb (6.63×10^5 N-m) would be required to reduce the probability of exceedence to 10^{-6}, the design goal needed to assure a motor reliability of .999.

In calculating the probability of premature insulation boot burn through, the capability ($\bar{X}_C$) was expressed in seconds of available protection as follows:

$$\bar{X}_C = \frac{t_i}{e_r}$$

where t_i = insulation thickness, inches

e_r = insulation erosion rate, inches/sec

The requirement ($\bar{X}_R$) was expressed in seconds of protection required prior to the end of action time as follows:

$$\bar{X}_R = \frac{t_w}{r_w} + \frac{t_{to}}{r_{to}}$$

where t_w = maximum thickness of propellant consumed during web time, inches

Appendix A

r_w = propellant burning rate prior to web time, inches/sec

t_{to} = maximum propellant thickness consumed during tail-off, inches

r_{to} = propellant burning rate during tail-off, inches/sec

The standard deviations for the capability and requirement distributions were determined from the following formula:

$$\frac{\sigma_C}{\bar{X}_C} = \sqrt{\left(\frac{\sigma_{t_i}}{\bar{t}_i}\right)^2 \left(\frac{\sigma_{e_r}}{e_r}\right)^2}$$

$$\sigma_r = \sqrt{\left[\frac{1}{r_w} \sigma_{t_w}\right]^2 + \left[\frac{t_w}{(r_w)^2} \sigma_{r_w}\right]^2 + \left[\frac{1}{r_{to}} \sigma_{t_{to}}\right]^2 + \left[\frac{t_{to}}{(r_{to})^2} \sigma_{r_{to}}\right]^2}$$

Using the values tabulated in Figure 4, a value of 250 seconds was obtained for $\bar{X}_C$ with a standard deviation of 17.4 seconds (6.95%). The nominal requirement value ($\bar{X}_R$) of 147.5 seconds was found to have a standard deviation of 1.92 seconds. Figure 5, which illustrates the relationship between boot thickness and the probability of premature boot burn through, indicates that the current nominal design thickness of .500 is adequate.

IV. DETERMINATION OF PROBABILITY OF SEAL MECHANICAL FAILURE

The preliminary stress analysis identified failure of the rubber pads in shear as the most likely mode of mechanical failure. Because of the complexity of the relationships, shear forces cannot be related to the design parameters

governing them by simple formulas. Instead they are calculated by a computer program employing the finite element technique. The only feasible method for estimating the probable distribution of the shear requirement, therefore, is to employ Monte Carlo simulation techniques in conjunction with the computer program used in the basic stress analysis. In performing such a Monte Carlo simulation, the parameters that are normally input into the computer as a single value are allowed to vary in a number of simulation runs to the degree that they could be expected to in a series of motors. Thus, instead of producing a single value result such as maximum shear stress, a distribution of probable shear stresses is obtained. It used to be considered necessary to make hundreds of simulation runs to characterize such a distribution, however, for preliminary estimating purposes, it is sufficient to make a limited number of runs and calculate a standard deviation of the output parameter from these.

The values for averages and standard deviations used in this analysis as input parameters to the computer simulation runs are shown in Figure 6.

Figure 7 presents a tabulation of the input parameter values actually used in each simulation run. These actual values were calculated for each input parameter by selecting eight values from a table of random standard deviations and adding or subtracting that number of standard deviations from the nominal values for the eight runs.

It should be noted that two input parameters, ejection force and Poisson's ratio, were not varied independently since they were considered to be functions of other input parameters that were being varied. Ejection force (F_{ej}) for example was calculated for each run from the formula:

Appendix A

$$F_{ej} = 13{,}400\ P_c - 9.02 \times 10^6$$

where P_c = maximum chamber pressure

Poisson's ratio (ν) was calculated in similar fashion by:

$$\nu = \frac{3K - 2G}{6K + 2G}$$

where K = rubber bulk modulus

G = rubber shear modulus

The results obtained for eight simulation runs are shown in Figure 8.

When plotted, the correlation between chamber pressure and maximum shear appeared to be extremely high. A regression analysis yielded a correlation coefficient of +.9994 indicating that 99.73% of the variability of maximum shear was associated with chamber pressure (or ejection force) and only .27% was a function of the variability of all of the other input parameters. Since similar plots for other elements yielded similar results, it was concluded that the variability of shear stress could be estimated directly from the variability of chamber pressure (or ejection force) from the following relationship:

$$\left(\frac{\sigma_{F_y}}{\overline{F}_y}\right)^2 = \left(\frac{m\,\sigma_{P_c}}{\overline{P}_c}\right)^2 = \left(\frac{S_{ey}}{\overline{F}_y}\right)^2$$

where: σ_{F_y} and $\overline{F}_y$ = the standard deviation and average maximum shear

σ_{P_c} and $\bar{P}_c$ = the standard deviation and average maximum chamber pressure

m = the slope of the linear relation between maximum pressure and maximum shear

S_{ey} = standard error of estimate from maximum pressure vs maximum shear regression analysis

Using values of 103.7 for $\bar{F}_y$, 117.266 for m, and .4008 for S_{ey}, a value of 216% was obtained for $\frac{\sigma_Y}{\bar{F}_y}$.

Because of the difficulty of running a combined simulation of axisymmetric and torque loading, the simulation was performed only for the axisymmetric case, with the reasoning that the percentage variability obtained for the axisymmetric case would be a good estimate of that of the combined loads. Accordingly, the standard deviation of maximum shear was estimated at 21.6% of the total of 104.3 psi (7.2×10^5 N/m^2) (axisymmetric) plus 17.9 psi (1.23×10^5 N/m^2) (torque), yielding a value of 26.4 psi (1.82×10^5 N/m^2) for 1σ. Although this percentage (21.6% may seem to be high compared to the 1.6% for chamber pressure, it must be remembered that the ejection force standard deviation is actually 17.1% of its mean.

As a final step, the probability of maximum shear (combined axisymmetric and torque loading) exceeding the material capability was calculated. For the capability nominal, the value of 292 psi (20.2×10^5 N/m^2) derived in the interim stress analysis was employed. A standard deviation of 10%, based on propellant variability experienced, was assumed. This resulted in a probability of failure

of 3×10^{-6} only slightly greater than the target value of 1×10^{-6}. Figure 9 presents the relation between probability of failure and shear strength nominal, assuming a standard deviation of 10% for shear strength capability.

V. CONCLUSIONS AND RECOMMENDATIONS

Based on the preliminary design information available, the probability of occurrence of the seal structural failure in shear and the insulation burn through failure mode, is less than or close to the desired allocation of 10^{-6}. The probability that the torque required will exceed the actuator capability is excessive, indicating that a significant increase in torque capability is required.

Because the probabilities are dependent to a large degree on variability of rubber shear stress and modulus, it is recommended that the estimated values used here, which were based on experience with similar materials be verified by a laboratory test program of the candidate material. Such a program should measure lot-to-lot variability as well as within-lot variability in order to realistically reflect probable manufacturing conditions. The effects of aging upon these parameters should also be investigated.

Failure Mode Name	Failure Mode Orgin	Failure Mode Definition	Method of Evaluating Prob. of Occurrence Using R/C Analysis
Seal Structural Failure in Shear	Excess variability of factors affecting stress in pads (chamber pressure, pad and shim thickness, pad Young's and bulk modulus, etc.)	Required shear stress exceeds material capability.	Requirements from Monte Carlo simulation of finite element stress analysis. Capability nominal of 292 psi with $\sigma/X = 20\%$ (20.2×10^5 N/m^2).
Excess Toruqe Required	Excess variability of parameters affecting torque (shear modulus, pad thickness, etc.)	Required torque for 1.95° (.034 rad) exceeds available actuation torque of 5×10^6 in.-lb (5.65×10^5 N-m).	Requirement distribution calculated from approximate relationship $T/\theta = \frac{.615\ G\ (WR)^{1.5}}{N\ t/r}$ adjusted by factor determined by computer analyses. Capability is fixed value 5×10^6 in. lb (5.65×10^5 N-m).
Insulation Boot Burnthrough	Excessive variability in boot erosion rate.	Boot burnthrough prior to end of action time.	Capability distribution calculated from time required to erode through boot. Requirement distribution calculated from time required for propellant to burn through maximum web thickness. σ/X for erosion assumed = 6.8%.

Flexible Seal Failure Mode Analysis

Figure 1

Appendix A

Name	Design Nominal $\bar{X}$	Estimated Standard Deviation σ	Basis for Estimate of
Rubber Shear Modulus, lb/in.^{2} (N/m^2)	25 (1.72×10^5)	1.25	Batch to batch variability of modulus of 10 batches of V-45 rubber at 300% strain.
Seal Radial Width, in. (m)	4.00 (.102)	.0141	The RSS combination of 1/6 of the total drawing tolerance for both pads and shims.
Inner Seal Radius, in. (m)	54.0 (1.37)	.00833	1/6 of the total drawing tolerance.
Pad Thickness, in. (m)	.3 (.0076)	.0087	Total within sheet and between sheet $\sigma/\bar{X}$ % estimated from nine sheets of rubber.
Number of Pads	5	None	----

Parameters Used in Calculating Excess Torque Probability

Figure 2

Appendix A

Probability Of Excessive Torque	Φ or Equivalent No. of Pooled Standard Deviations Between $\bar{X}_R$ and $\bar{X}_C$	Torque Capability ($\bar{X}C$) in. lb (N-m)
.067	1.50	5.00×10^6 (design nominal) (5.65×10^5)
.01	2.32	5.22×10^6 (5.90×10^5)
.001	3.09	5.42×10^6 (6.13×10^5)
.0001	3.72	5.60×10^6 (6.32×10^5)
.00001	4.25	5.73×10^6 (6.48×10^5)
.000001	4.75	5.87×10^6 (6.64×10^5)

Relation of Probability of
Excessive Torque to Torque Capability

Figure 3

Appendix A

Name	Design Nominal $\bar{X}$	Estimated Standard Deviation σ	Basis for Estimate of
Insulation Thickness, in. (m)	.50 (0.127)	.0083	1/6 of total drawing tolerance.
Insulation Erosion Rate, in./sec. (m/sec)	.002 (5.1×10^{-5})	.000136	Motor to motor variability of maximum erosion in fwd and aft heads of 12 Minuteman Wing VI motors.
Propellant Thickness Consumed Prior to Web Time, in. (m)	85.0 (2.16)	.1870	The RSS combination of 1/6 of case and insulation drawing tolerances, observed bore diameter variability, and estimated maximum core shift of .25 inch. (.00635 m)
Propellant Thickness Consumed During Tail-off, in. (m)	2.5 (.0635)	.005	"
Propellant Burning Rate Prior to Web Time, in./sec. (m/sec)	.606 (.0154)	.00818	Variability between 12 pot increments of liquid strand burning rate for 260-SL-1 and 260-SL-2.
Propellant Burning Rate During Tail-Off, in/sec. (m/sec)	.333 (.00845)	.0045	Variability between 12 pot increments of liquid strand burning rate for 260-SL-1 and 260-SL-2.

Parameters Used in Calculating
Premature Burnthrough Probability

Figure 4

Appendix A

Probability of Premature Boot Burnthrough	Φ or Number of Pooled Standard Deviations Between $\bar{X}_R$ and $\bar{X}_C$	$\bar{X}_C$, Boot Thickness, in. (m)
.001	3.09	.378 (.0096)
.0001	3.72	.398 (.0101)
.00001	4.25	.422 (.0107)
.000001	4.75	.440 (.0112)
$10^{-8.2}$	5.86	.450 (.0114) (Design Nominal)

Relation of Probability of Premature Boot Burnthrough to Boot Thickness

Figure 5

Appendix A

Parameter	$\bar{X}$	σ	Source of σ
Ejection Force (F_{ej}), lb(N)	1,000,000 (4.45×10^6)	171,000	*
Max. Chamber Pressure (P_c), lb/in.^{2} (N/m^2)	750 (5.17×10^6)	12.7	RSS combination of variability of burning rate, propellant weight, web thickness, throat area, etc.
Young's Modulus of Rubber (E_R), lb/in.^{2} (N/m^2)	81** (5.59×10^5)	4.1	Batch-to-batch variability of modulus of 10 batches of V-45 rubber at 300% strain.
Young's Modulus of Steel (E_S), lb/in.^{2} (N/m^2)	29,000,000 (2.0×10^{11})	58,000	Based on variability of % of basic chemical ingredients from heat to heat.
Pad Thickness (t_p), in. (m)	.30 (.0076)	.0087	Total within sheet and between sheet σ/X estimated from nine sheets of rubber.
Shim Thickness (t_s), in. (m)	.70 (.0178)	.0033	1/6 of total drawing tolerance.
Seal Radial Width, ($W_p + W_s$), in. (m)	4.00 (.102)	.0141	RSS combination of 1/6 of total drawing tolerance for both pads and shims.
Poisson's Ratio of Rubber (ν)	.4999	*	*

* Values used in simulation runs were derived as functions of other input parameters, i.e., parameter does not vary independently.

**The maximum value of 81 was used instead of the nominal 75 to make the simulation results compatible with previous analysis. The results were not significantly affected.

Shear Stress Simulation Input
Parameter Averages and Standard Deviation

Figure 6

Run	Chamber Pressure, psia	Ejection Force, lbs x 10^{-6}	Young's Modulus, Steel x 10^{6}	Young's Modulus, Rubber	Poisson's Ratio, Rubber	Pad Thickness, in.	Shim Thickness, P in.	Radial Width, in.
1	768.8	1.250	28.97	77.8	.4,999,543	.288	.704	3.968
2	760.0	1.134	28.97	81.8	.4,999,526	.286	.703	4.002
3	756.1	1.082	29.06	76.0	.4,999,550	.284	.694	3.998
4	735.9	.811	29.07	88.3	.4,999,501	.296	.701	3.993
5	773.7	1.312	29.00	79.4	.4,999,536	.282	.697	3.982
6	738.0	.838	29.04	82.3	.4,999,524	.304	.706	4.015
7	746.3	.950	29.02	77.1	.4,999,546	.31	.697	4.034
8	731.5	.751	29.00	84.0	.4,999,517	.283	.700	3.994
Design Nominal	750	1.000	29.0	81.0	.4,999,520	.300	.700	4.000
Range of σ's:								
High	+1.863	*	+1.244	+1.779	**	+1.125	+1.728	+2.432
Low	-1.454	*	- .575	-1.218	**	-2.005	-1.796	-1.262

*Same as Chamber Pressure.
**Same as Young's Modulus Rubber
SI units omitted for clarity.

Monte Carlo Simulation Input Values, Flex Seal Nozzle

Figure 7

Appendix A

Run No.	Ejection Force, lb x 10^{-6} ($N \times 10^{-6}$)	Maximum Chamber Pressure, psi ($N/m^2 \times 10^{-4}$)	Maximum Shear, psi (Element 1-36) ($N/m^2 \times 10^{-4}$)	Next Highest Shear, psi (Element 2-36) ($N/m^2 \times 10^{-4}$)
1	1.250 (5.55)	768.8 (530)	134.4 (92.7)	95.0 (65.5)
2	1.134 (5.05)	760.0 (524)	118.8 (81.9)	84.2 (58.0)
3	1.082 (4.81)	756.5 (521)	111.1 (76.6)	79.7 (55.0)
4	.811 (3.61)	735.9 (508)	827 (57.0)	59.9 (41.4)
5	1.212 (5.40)	773.7 (534)	127.7 (88.0)	91.0 (62.8)
6	.838 (3.73)	738.0 (509)	84.5 (58.2)	61.5 (42.5)
7	.950 (4.22)	746.3 (515)	96.8 (66.7)	70.6 (48.6)
8	.751 (3.34)	731.5 (505)	73.6 (50.7)	53.3 (36.8)

Monte Carlo Simulation Results

Figure 8

Appendix A

Probability of Shear Requirement Exceeding Capability	Φ or Number of Pooled Standard Deviations Between $\bar{X}_R$ and $\bar{X}_C$	Pad Shear Strength, psi $\bar{X}_C$ ($N/m^2 \times 10^{-4}$)
.01	2.32	200 (138)
.001	3.09	230 (159)
.0001	3.72	260 (179)
.00001	4.25	287 (198)
.000003	4.32	292 (202) (Design Nominal)
.000001	4.75	325 (224)

Relation of Probability of Maximum Shear Requirement Exceeding Capability to Pad Shear Strength

Figure 9

APPENDIX B

ENGINEERING DRAWINGS AND SPECIFICATIONS

Appendix B

I. ENGINEERING DRAWINGS

Drawing No.	Title
1148903	Flexible Seal - 260-in.-dia Motor
1148904	End Ring, Fwd - Conical, Flexible Seal
1148905	End Ring, Aft - Conical, Flexible Seal
1148906	Shim - Conical, Flexible Seal
1148907	Pad - Conical, Flexible Seal
1148993	Boot, Elastomeric - Conical, Flexible Seal

II. SPECIFICATION

Specification No.	Title
AGC-34463	Compound, Natural Rubber
AGC-34230	Insulation, Butadiene Acrylonitrile, Unvulcanized
AGC-36592	Seal Assembly, Flexible, Fabrication of
AGC-36420	Insulation, Rubber, Butadiene Acrylonitrile, Autoclave Cure Fabrication of

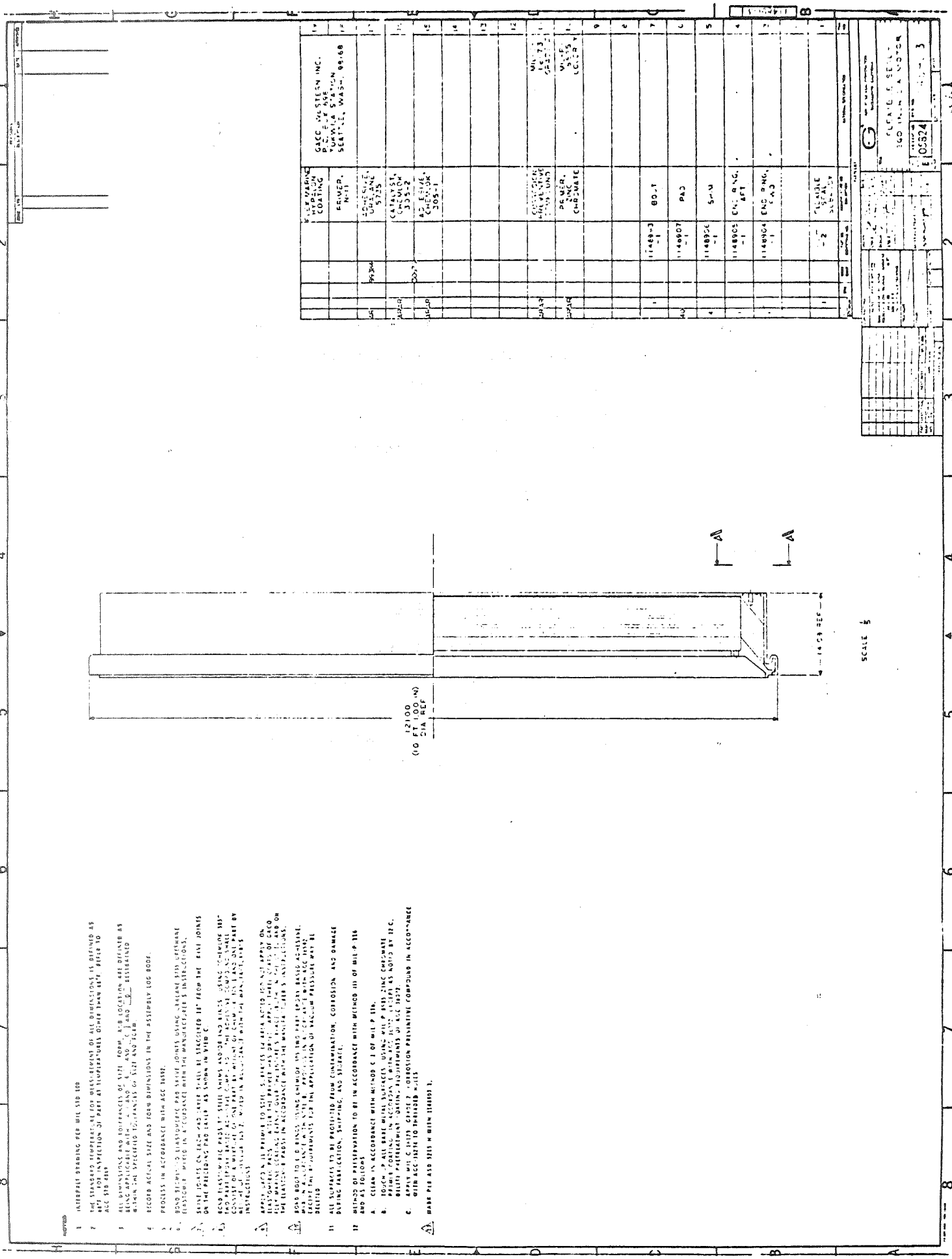

Drawing 1148903, Flexible Seal - 260-in.-dia Motor (Sheet 1 of 2)

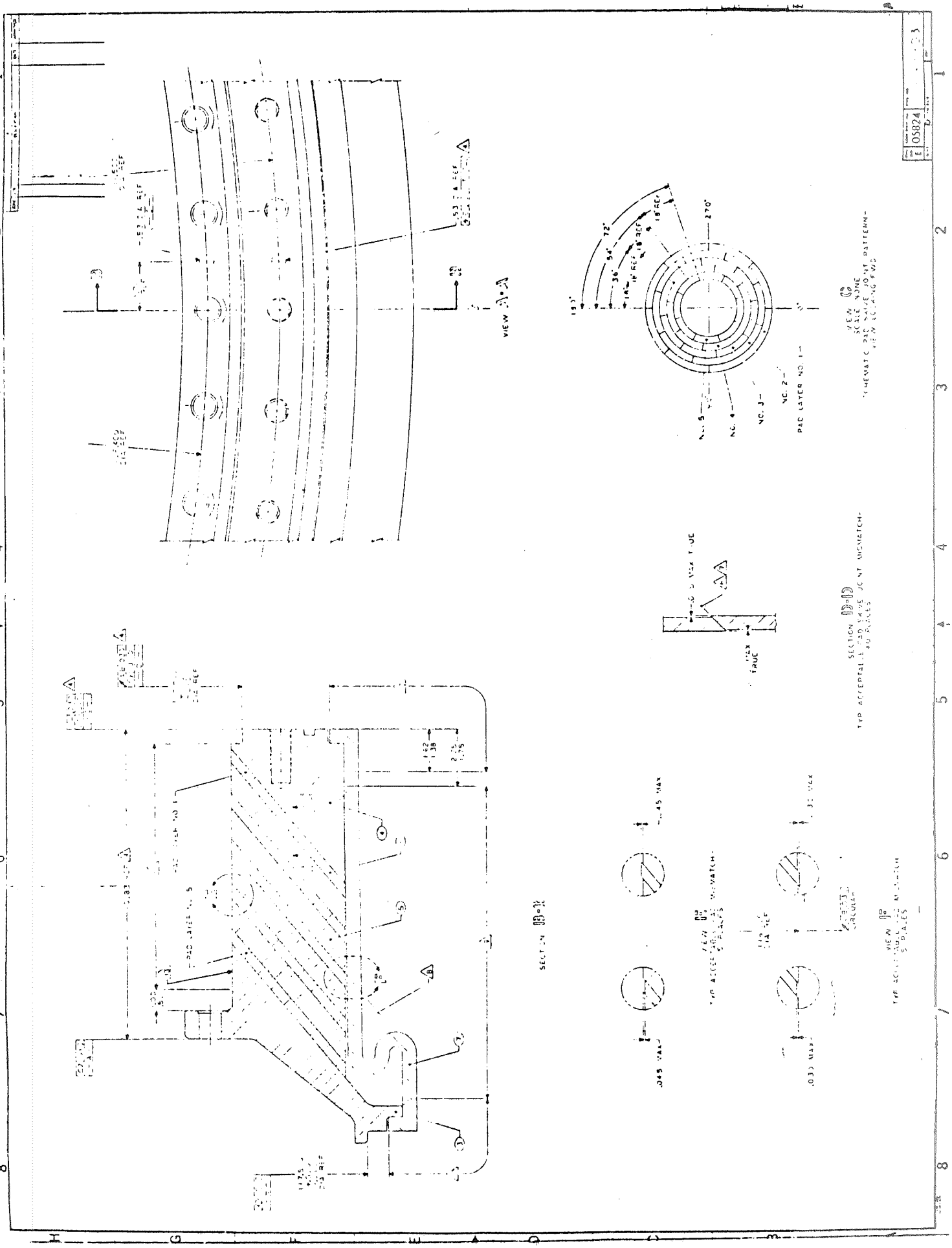

Drawing 1148903, Flexible Seal - 260-in.-dia Motor (Sheet 2 of 2

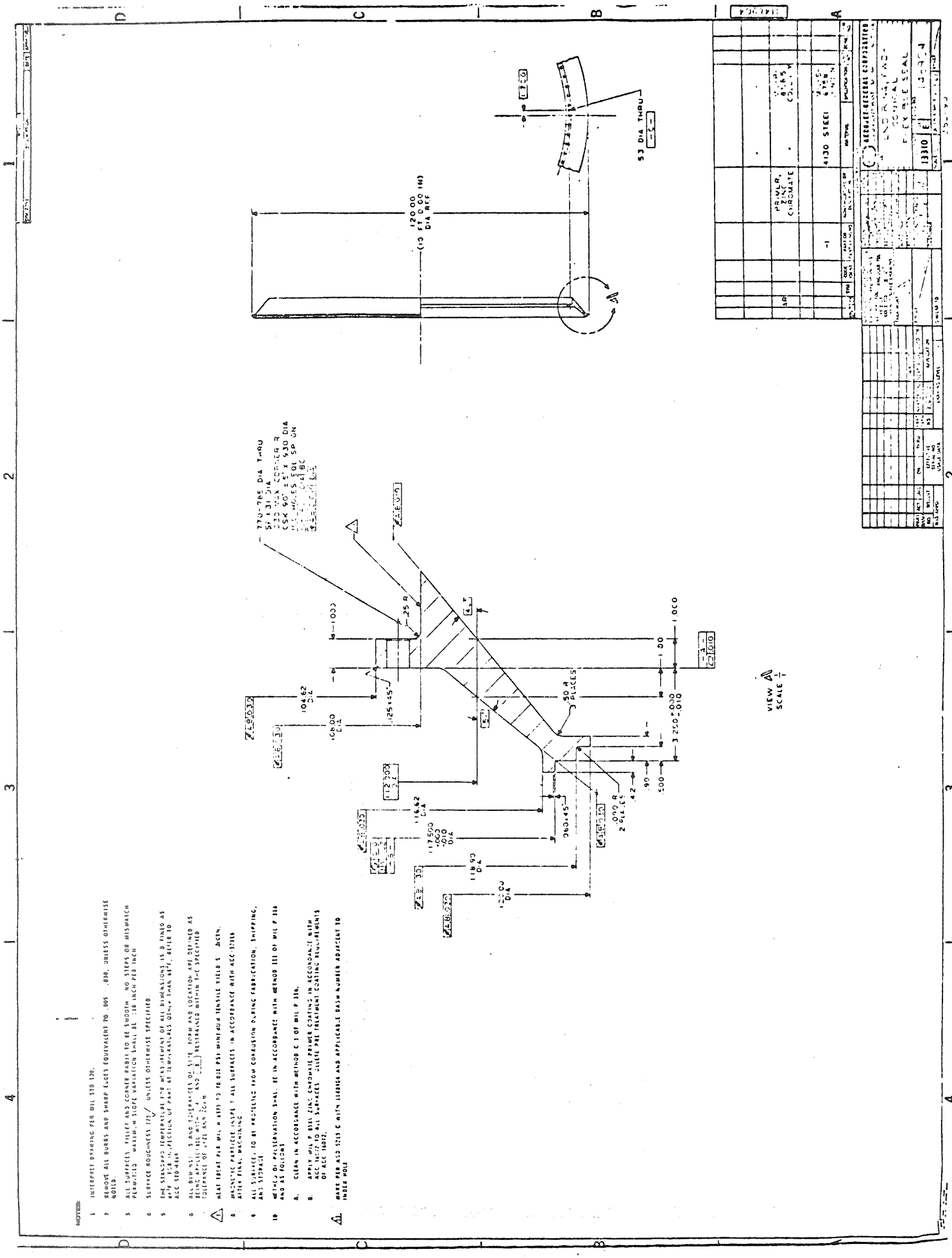

Drawing 1148904, End Ring, Fwd - Conical, Flexible Seal

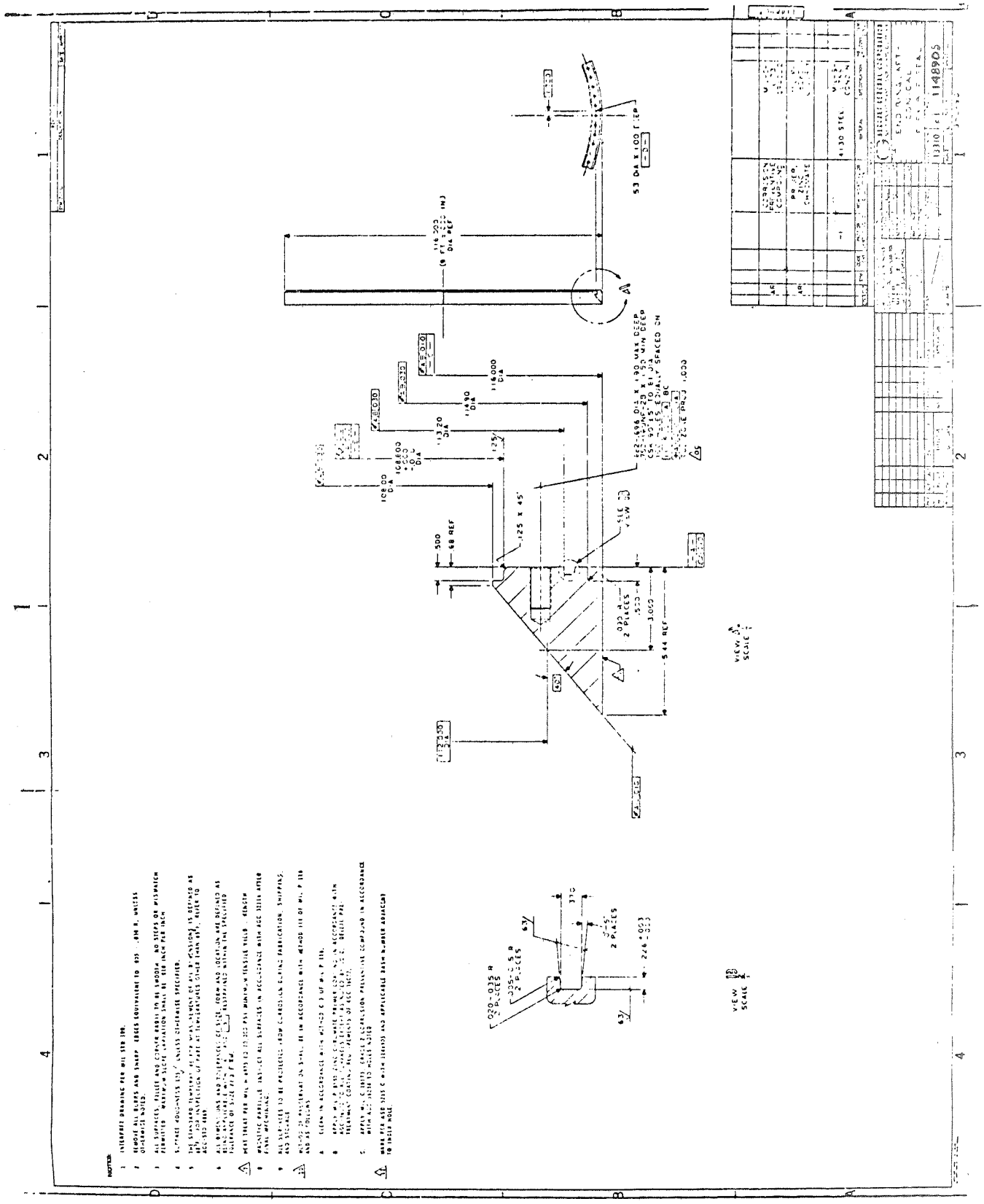

Drawing 1148905, End Ring, Aft - Conical, Flexible Seal

NOTES:

1. INTERPRET DRAWING PER MIL-STD-100.
2. REMOVE ALL BURRS AND SHARP EDGES EQUIVALENT TO .005 .030 R. UNLESS OTHERWISE NOTED.
3. SURFACE ROUGHNESS 125/ UNLESS OTHERWISE SPECIFIED.
4. THE STANDARD TEMPERATURE FOR MEASUREMENT OF ALL DIMENSIONS IS DEFINED AS 68°F. FOR INSPECTION OF PARTS AT TEMPERATURES OTHER THAN 68°F REFER TO ACC STD 4847.
5. ALL DIMENSIONS AND TOLERANCES OF SIZE AND FORM ARE DEFINED AS BEING APPLICABLE WITH [LA] RESTRAINED WITHIN THE SPECIFIED TOLERANCE OF SIZE AND FORM.
6. A WELDED FOR WELDED OR BRAZED ASSEMBLY IS ACCEPTABLE WHEN WELDING IS PERFORMED IN COMPLIANCE WITH ACC SPEC 3 USING WELD WIRE PER ACC 4001 OR EQUIVALENT. AFTER WELDING, STRESS RELIEVE IN ACCORDANCE WITH ACC 10271.
   A. RADIOGRAPHICALLY INSPECT WELDS IN ACCORDANCE WITH ACC-STD 5131. INTERPRET PER ACC 1148, CLASS 4.
   B. MAGNETIC PARTICLE INSPECT ALL WELD SURFACES PER ACC 32116.
7. HEAT TREAT PER MIL H 6875 TO 70,000 PSI MINIMUM TENSILE YIELD STRENGTH.
8. MAGNETIC PARTICLE INSPECT ALL SURFACES IN ACCORDANCE WITH ACC 32116 AFTER FINAL MACHINING.
9. ALL SURFACES TO BE PROTECTED FROM CORROSION DURING FABRICATION, SHIPPING, AND STORAGE.
10. METHOD OF PRESERVATION SHALL BE IN ACCORDANCE WITH METHOD IIE OF MIL-P 116 AND AS FOLLOWS.
    A. CLEAN IN ACCORDANCE WITH METHOD C 3 OF MIL P 116.
    B. APPLY MIL P 8585 ZINC CHROMATE PRIMER COATING IN ACCORDANCE WITH ACC 34017 TO ALL SURFACES. DELETE PRE-TREATMENT COATING REQUIREMENTS OF ACC 34017.
11. MADE PER ASD 5215 C WITH 1148906 AND APPLICABLE DASH NUMBER.

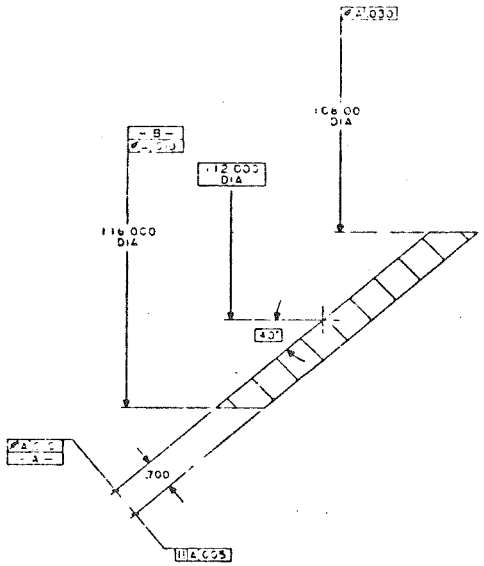

VIEW A
SCALE 1/1

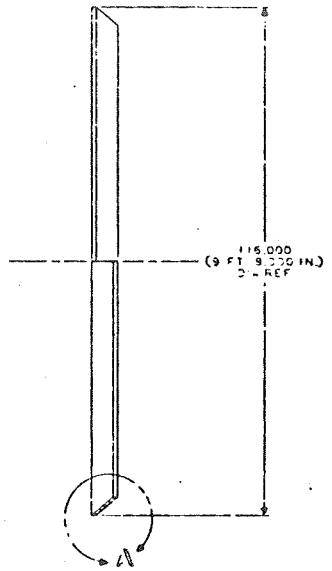

AR		POWR. ZINC CHROMATE	MIL-P-8585 COLOR Y	
	-1	4130 STEEL	MIL-S-6758A CONDN	

REVISIONS

AEROJET-GENERAL CORPORATION

SHIM - CONICAL FLEXIBLE SEAL

13310 E 1148906

SCALE 2/1 SHEET 1 OF 1

Drawing 1148906, Shim - Conical, Flexible Seal

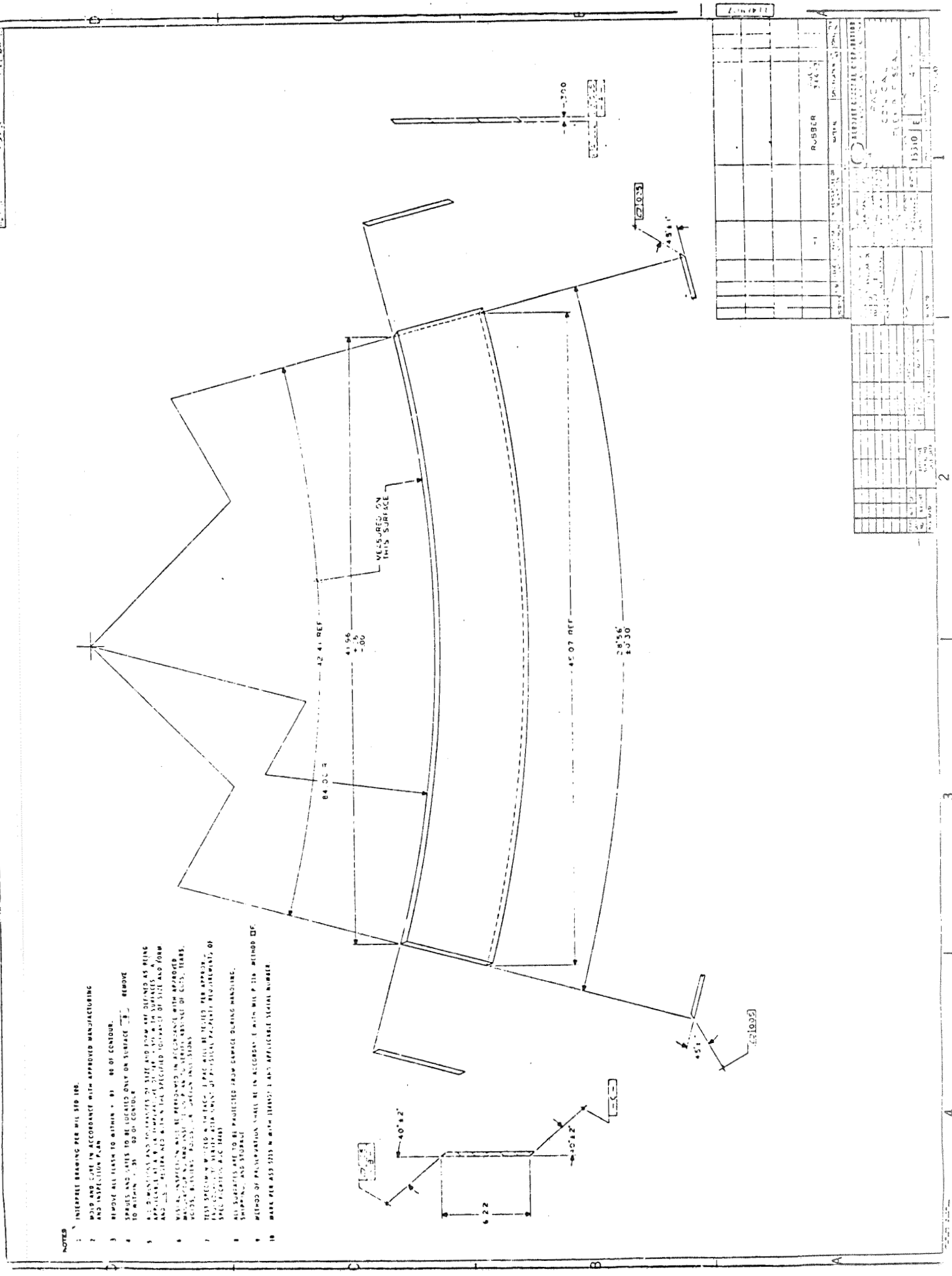

Drawing 1148907, Pad - Conical, Flexible Seal

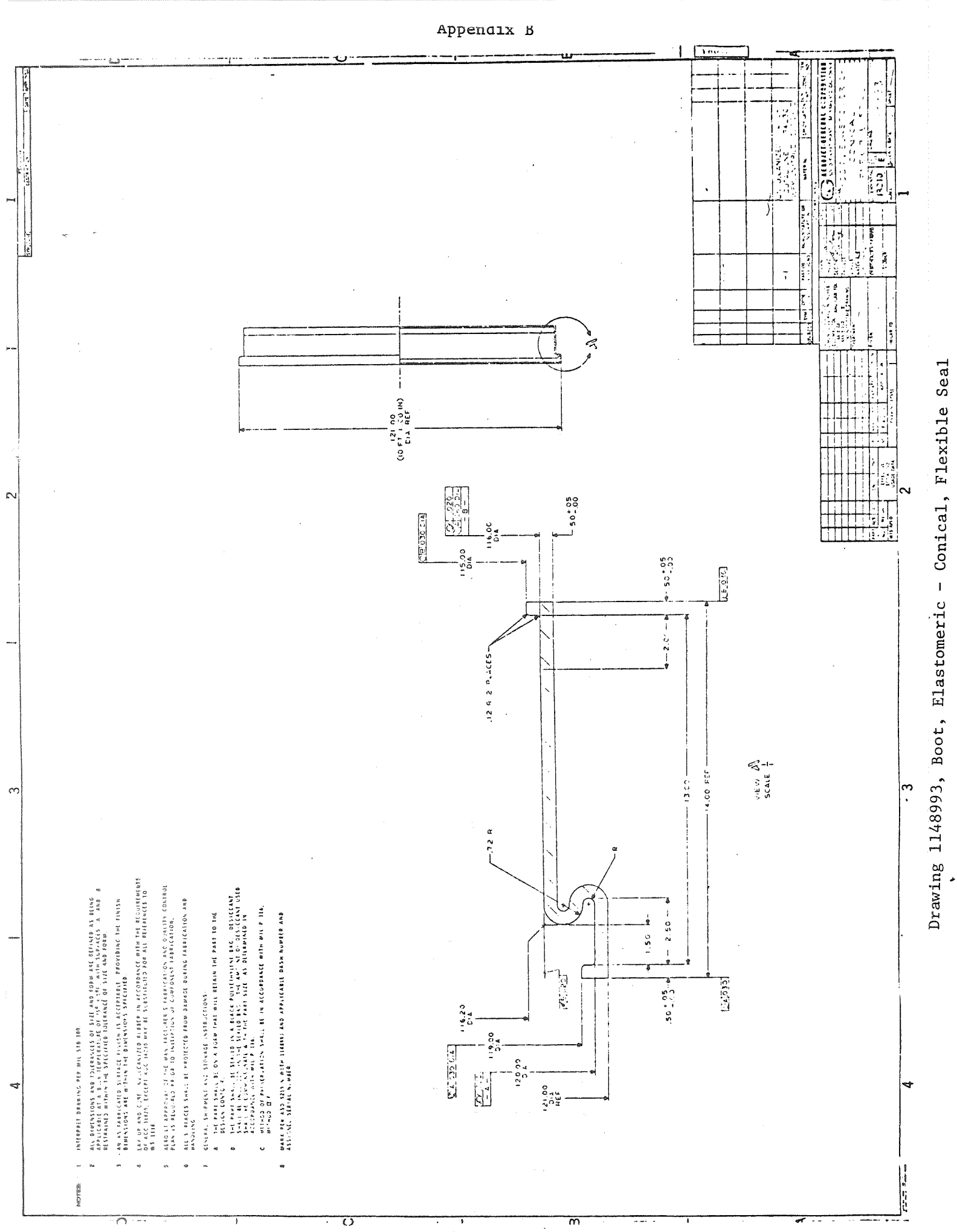

Drawing 1148993, Boot, Elastomeric - Conical, Flexible Seal

AEROJET-GENERAL CORPORATION

CODE IDENT. NO. 05824

SPECIFICATION AGC- 34463

COMPOUND, NATURAL RUBBER

SUPERSEDING:			
AGC- DATE	AGC- DATE	AGC- DATE	
RELEASES (REPLACE PAGES IN SPECIFICATION WITH LATEST CHANGE BELOW)			
REV LTR	RELEASE DATE	PAGE NUMBERS 1 2 3 4 5 6 7	PAGE ADDITIONS
	30 Oct 69		

Authorized for Release:

A. S. Hedin

A S Hedin
Specifications and Standards
Solid Rocket Operations
Sacramento

1. SCOPE

1.1 This specification covers the requirements for uncured, natural rubber compound.

2. APPLICABLE DOCUMENTS

2.1 Department of Defense documents. - Unless otherwise specified, the following documents, listed in the issue of the Department of Defense Index of Specifications and Standards in effect on the date of invitation for bids, shall form a part of this specification to the extent specified herein.

STANDARD

Federal

Fed. Test Method Std. No. 601	Rubber: Sampling and Testing

(Copies of documents required by contractors in connection with specific procurement functions should be obtained as indicated in the Department of Defense Index of Specifications and Standards.)

2.2 Other documents. - Unless otherwise specified, the following documents, of the issue in effect on the date of invitation for bids, shall form a part of this specification to the extent specified herein.

American Society for Testing and Materials

ASTM D 15	Methods of Sample Preparation for Physical Testing of Rubber Products
ASTM D 2240	Indentation Hardness of Rubber and Plastics by Means of a Durometer

(Copies of ASTM standards may be obtained from the American Society for Testing and Materials, 1916 Race Street, Philadelphia, Pa. 19103)

3. REQUIREMENTS

3.1 Qualification. - The rubber compound furnished under this specification shall be a product which has been tested and has passed the qualification tests specified herein.

3.2 Material. - The material shall be an elastomeric compound formulated and processed to the requirements specified herein.

3.3 Physical properties. - The physical properties of the cured rubber compound shall conform to the following:

		Min	Max
(a)	Specific gravity, 25°C	0.97	1.05
(b)	Hardness, Shore A	20	30
(c)	Shear strength, psi	500	---
(d)	Shear modulus at 50 psi shear stress	20	26

3.4 Shelf life. - The uncured material shall have a shelf life of at least six months from the date of manufacture when stored at 75°F, maximum.

3.5 Workmanship. - The material shall be uniform in quality and free from impurities and other defects that would prevent its use for the purpose intended.

4. QUALITY ASSURANCE PROVISIONS

4.1 Supplier responsibility. -

4.1.1 Inspection. - Unless otherwise specified, the supplier is responsible for the performance of all inspection requirements as specified herein and may use any facilities acceptable to the Aerojet-General Corporation (AGC).

4.1.2 Processing changes. - The supplier shall make no changes in processing techniques or other factors affecting the quality of the product without prior approval of AGC.

4.2 Sampling. - The qualification and quality conformance inspection samples shall consist of sufficient quantities of randomly selected material to perform the tests specified in 4.5 and 4.6.

4.3 Lot size. - A lot shall consist of material produced in one continuous production run, not exceeding 24 hours, without change in materials or process, and offered for delivery at one time. A lot shall not exceed 1000 pounds.

4.4 Classification of tests. - The inspection and testing of the material shall be classified as follows:

(a) Qualification tests
(b) Quality conformance inspection

4.5 Qualification tests. - The qualification tests shall be conducted at an activity designated by AGC. Qualification testing shall consist of the following inspections:

(a) Quality conformance inspections
(b) Shelf life

4.6 Quality conformance inspections. - Inspection of individual lots shall consist of tests to determine compliance with the following requirements of Section 3.

(a) Examination
(b) Specific gravity
(c) Hardness
(d) Shear strength
(e) Shear modulus

4.7 Test specimen preparation. - Unless otherwise specified in the contract or purchase order, the supplier shall prepare three slabs in accordance with ASTM D 15, Sections 7 through 10; and four, quadruple lap shear specimens, as shown in Figure 1, for testing. Quadruple lap shear specimens shall be prepared as follows:

(a) The size and assembly of the test specimen shall be as shown in Figure 1.
(b) Apply primer and adhesive to degreased, grit-blasted metal strips. (Primer and adhesive shall be capable of providing bond strength in excess of the shear strength of the rubber compound.)
(c) Mold rubber compound specified herein.
(d) Cure the assembled test specimens in accordance with the manufacturer's cure procedure

4.8 Test methods. - Tests shall be in accordance with the following:

	Requirement	Method
(a)	Examination	4.8.1
(b)	Specific gravity	FTMS 601, Method 14011
(c)	Hardness	ASTM D 2240 1/
(d)	Shear strength	4.8.2
(e)	Shear modulus	4.8.2
(f)	Shelf life	4.8.3

1/ Using a Type A durometer.

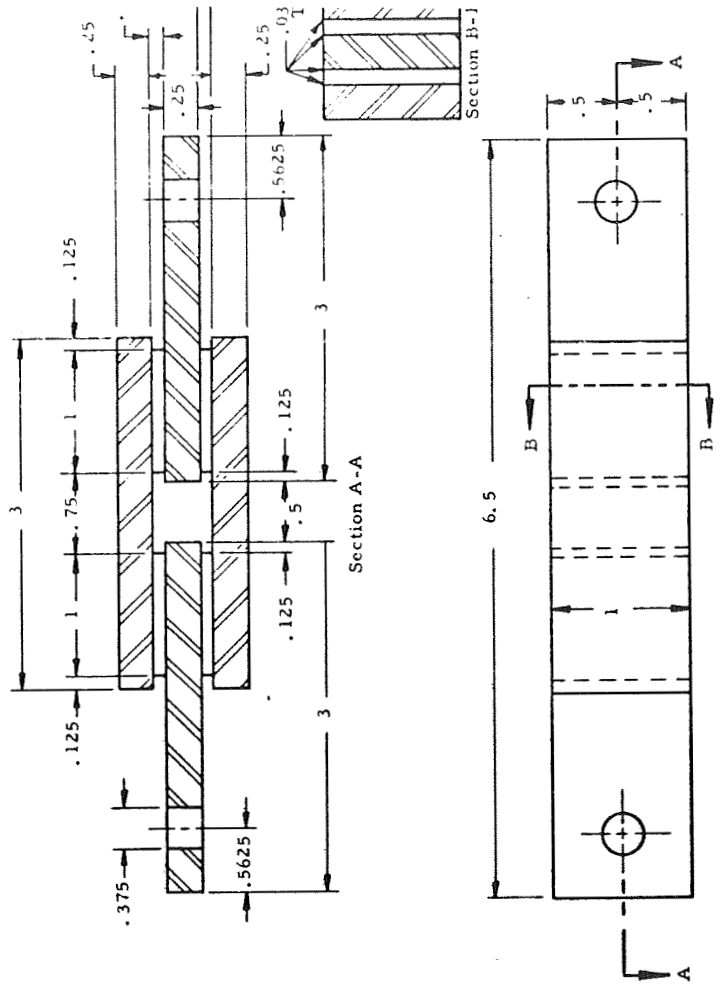

NOTE: All dimensions are in inches

Quadruple Lap Shear Test Specimen

Figure 1

5

4.8.1 Examination. - The material shall be examined for conformance to the requirement of 3.5.

4.8.2 Shear strength and modulus. - The shear strength and shear modulus of the material shall be verified as follows:

4.8.2.1 Equipment. -

(a) Testing machine with an automatic recorder
(b) Grips for holding the specimens during testing
(c) An environmental test chamber or controlled room
(d) A calibrated, indicator pyrometer or thermometer

4.8.2.2 Procedure. -

(a) Set the crosshead speed of the tester at one-half inch per minute (in./min); the recorder chart speed at 5.0 in./min, with the test temperature at 74° ± 5°F.
(b) Zero and calibrate the tester in accordance with the operating instructions of the tester.
(c) Condition and test the specimen at 74° ± 5°F.
(d) Insert the test specimen in the grips of the tester and carefully center.
(e) Start the tester and observe the chart recorder.

4.8.2.3 Calculations. - Calculate the shear strength and shear modulus as follows:

(a) Shear strength, psi = $\frac{\text{Load at failure}}{2 \times \text{length of pad} \times \text{width of pad}}$

(b) Shear stress, psi = $\frac{\text{Load}}{2 \times \text{length} \times \text{width}}$

(c) Shear strain, in./in. = $\frac{\text{Increase in crosshead separation}}{2 \times \text{thickness of pad}}$

(d) Shear modulus = $\frac{\text{Shear stress}}{\text{Shear strain}}$

4.8.2.4 Test reports. - Shear stress shall be calculated for increments of shear strain as follows: 0.1, 0.2, 0.3, 0.4, 0.5, 0.75, 1.0, 2.0, 3.0, 4.0, 5.0, 6.0, 7.0, 8.0, and to failure. Tabulate results on graphs of shear stress versus shear strain. Report shear strength at failure and shear modulus at 50 pounds per square inch (psi) shear stress.

4.8.3 Shelf life. - After exposure to 75°F, maximum, for six months $^{+1}_{-0}$ week, the material shall be tested for conformance to the quality conformance inspection requirements of this specification.

5. PREPARATION FOR DELIVERY

5.1 This section is not applicable to this specification.

6. NOTES

6.1 Intended use. - The material is intended for use in a movable joint of a rocket propulsion system.

6.2 Ordering data. - Procurement documents should specify, but not be limited to, the following information:

(a) Number and revision letter of this specification, if applicable
(b) Minimum lot size, if applicable
(c) Request for three copies of test results
(d) Place of inspection
(e) The uncured material to be used in the fabrication of components within six months of the date of manufacture

6.3 Storage. - Controlled storage of the material shall be maintained in an enclosed facility at a maximum temperature of 75°F.

6.4 Qualification. - Procurement contracts will be awarded only for such products that, prior to the closing date for receipt of quotations, have been tested and approved for inclusion on the applicable Qualified Products List. The attention of suppliers is called to this requirement, and they are urged to have the products that they propose to offer to the Aerojet-General Corporation tested for qualification in order that they may be eligible to be awarded contracts for the products covered by this specification. The activity responsible for the Qualified Products List is the Aerojet-General Corporation, Sacramento, California. 95813

aerojet solid propulsion company

CODE IDENT. NO. 13310

SPECIFICATION ASPC-34230
5 April 1971

INSULATION, BUTADIENE ACRYLONITRILE, UNVULCANIZED

This cover sheet to AGC-34230, Revision D, dated 4 May 1970, is effective as of the date of release and is for the purpose of the following:

1. Revising document identification from "AGC-34230" to "ASPC-34230."

2. Revising Code Ident number from "05824" to "13310," as applicable.

3. Revising Section 2 paragraph heading from "Aerojet-General Corporation documents" to "Aerojet Solid Propulsion Company documents," as applicable.

4. Revising any "AGC" prefixed specification and/or standard referenced herein to "ASPC," "ASPC-S," or "ASPC-STD," as applicable.

5. Revising any text reference to "Aerojet-General Corporation" or "AGC" to specify "procuring activity," as applicable.

6. Revising Section 6 "Qualification" paragraph reference from "Aerojet-General Corporation" to "Aerojet Solid Propulsion Company," as applicable.

Authorized for Release:

J. L. Simms

J. L. Simms
Specifications and Standards
Engineering Services Section
Engineering Operations

aerojet solid propulsion co.

CODE IDENT. NO. 05824

SPECIFICATION AGC- 34230D

INSULATION, BUTADIENE ACRYLONITRILE, UNVULCANIZED

SUPERSEDING:		
AGC - 34230C DATE 11 September 1964	AGC - DATE	AGC - DATE

RELEASES (REPLACE PAGES IN SPECIFICATION WITH LATEST CHANGE BELOW.)

REV LTR	RELEASE DATE	PAGE NUMBERS 1 2 3 4 5 6 7 8 9 10 11 12 13 14 15 16	PAGE ADDITIONS
	30 Apr 62		
A	5 Jun 63		
B	6 Nov 63		
C	11 Sep 64		
N.F. D	4 May 65	D D D D D D D D D D D D D D D D	

Authorized for Release:

J L Smith
Specifications and Standards
Engineering Services Section
Engineering Design Department

AGC-34230

1. SCOPE

1.1 Scope. - This specification covers two classes of synthetic-rubber insulation formulated from nitrile butadiene-acrylonitrile copolymer.

(D) 1.2 Classification. - The material shall be classified according to the method of packaging, as follows. If no class is specified, AGC-34230-1 applies.

Suffix	Class	Designation
-1	I	Rolls or sheets of unvulcanized stock separated by embossed polyethylene film.
-2	II	Rolls or sheets of unvulcanized stock separated by unembossed polyethylene film.

Each classification shall be called out by referencing the specification number plus the suffix number designating the classification desired. Example: "Use material in accordance with AGC-34230-1."

2. APPLICABLE DOCUMENTS

2.1 Department of Defense documents. - Unless otherwise specified, the following documents, of the issue listed in the Department of Defense Index of Specifications and Standards in effect on the date of invitation for bids, shall form a part of this specification to the extent specified herein.

SPECIFICATION

Federal

TT-T-548 Toluol (for Use in Organic Coatings)

STANDARDS

Federal

Fed. Test Method Std. No. 601 Rubber: Sampling and Testing of

Military

MIL-STD-105	Sampling Procedures and Tables for Inspection by Attributes
MIL-STD-129	Marking for Shipment and Storage

(Copies of documents required by contractors in connection with specific procurement functions should be obtained as indicated in the Department of Defense Index of Specifications and Standards.)

2.2 Other documents. - Unless otherwise specified, the following documents, of the issue in effect on the date of invitation for bids, shall form a part of this specification to the extent specified herein.

PUBLICATIONS

American Society for Testing and Materials

ASTM C 177	Method of Test for Thermal Conductivity of Materials by Means of the Guarded Hot Plate
ASTM D 865	Method of Heat Aging of Vulcanized Natural or Synthetic Rubber by Test Tube Method
ASTM D 1646	Method of Test for Viscosity and Curing Characteristics of Rubber by the Shearing Disk Viscometer

(Copies may be obtained from the American Society for Testing and Materials, 1916 Race Street, Philadelphia 3, Pa.)

2.3 Aerojet-General Corporation documents. - Unless otherwise specified, the following document, of the latest issue in effect, shall form a part of this specification to the extent specified herein.

SPECIFICATION

AGC-34278	Adhesive, Rubber, Vulcanizing

3. REQUIREMENTS

3.1 Qualification.- The material furnished under this specification shall be a product which has been tested and passed the qualification tests specified herein.

3.2 Preproduction.- The material shall be subjected to preproduction tests as specified herein.

3.3 Unvulcanized material.- The unvulcanized material shall be in accordance with the following.

3.3.1 Mooney viscosity.- The Mooney viscosity of the material shall not be more than 80 for the first seven days after the date of manufacture.

3.3.2 Scorch characteristic.- The time required for the Mooney viscosity of the unaged material to increase five points above the minimum value shall not be less than 10 minutes for the first seven days after the date of manufacture.

3.4 Vulcanized material.- The vulcanized material shall be in accordance with the following:

(D) 3.4.1 Unaged material.- The unaged material shall be in accordance with the following:

		Min	Max
(a)	Specific gravity at 25° C	1.195	1.225
(b)	Shore "A" hardness	64	80
(c)	Water absorption, wt%		
	(1) After immersion	----	0.75
	(2) After immersion and drying	----	0.10
(d)	Tensile strength, psi, parallel with the grain	2000	----
(e)	Elongation, %, parallel with the grain	450	----
(f)	Laminar peel, lb/in.	125	----

3.4.2 Aged material. - The aged material shall be in accordance with the following:

		Min	Max
(a)	Shore "A" hardness	71	85
(b)	Tensile strength, psi. parallel with the grain	2000	----
(c)	Elongation, %, parallel with the grain	200	----

3.4.3 Thermal properties. - The vulcanized, unaged material shall have the following thermal properties:

		Min	Max
(a)	Thickness loss rate, in./sec	----	0.0055
(b)	Weight loss, g	----	3.0
(c)	Thermal conductivity, Btu-ft/hr $^{\circ}$F ft^2 at 150°F mean temp	----	0.15
(d)	Specific heat, Btu/lb $^{\circ}$F at 150°F mean temp	0.32	----

3.4.3.1 Temperature rise. - The time allowed for the unexposed surface of the material to reach the indicated temperature shall be in accordance with the following:

	Thickness, In.	Temperature, °F	Minimum Time, Sec
(a)	0.060	200	5.5
(b)	0.060	300	7.0
(c)	0.060	400	8.5

3.5 Shipping date. - The shipping date shall be at least six months prior to the expiration date (5.3 h and i).

3.6 Storage life. - Storage life of the material shall be eight months from date of manufacture.

3.6.1 Use life. - Use life of the material shall be at least six months prior to the expiration date.

4. QUALITY ASSURANCE PROVISIONS

4.1 Supplier responsibility. -

4.1.1 Inspection. - Unless otherwise specified, the supplier is responsible for the performance of all preproduction and acceptance tests specified herein and may use any facilities acceptable to the procuring activity.

4.1.2 Processing changes. - The supplier shall make no changes in processing techniques or other factors affecting the quality of the product without prior approval of the procuring activity.

4.1.3 Preproduction sample. - A preproduction sample shall be taken in accordance with 4.3. The test shall be in accordance with 4.7.

4.2 Lot size. - A lot shall consist of material produced in one continuous production run without change in materials or process, and offered for delivery at one time. A lot shall not exceed 5000 pounds of material. Minimum lot size shall be 200 pounds. Each lot is to be divided into rolls of material. A standard roll shall be 230 pounds, maximum, 36-inch nominal width.

4.3 Sampling. - Sampling for examination, preproduction tests, and acceptance tests shall be in accordance with MIL-STD-105, Inspection Level I. The acceptable quality level (AQL) shall be 1.0 percent defective. The unit of product shall be one roll of rubber. The procedure for obtaining test samples from each roll shall be as follows:

(a) Discard the first two yards from the roll.
(b) Cut a sample the full width of the roll, from the material which immediately follows, sufficient to prepare test coupons as required. Do not remove the protective film.
(c) Wrap the sample in a noncontaminating wrapper.
(d) Complete an identification label with the following information and attach it to the sample wrapper:
    (1) Number and revision letter of this specification
    (2) Material name or code number
    (3) Lot number or batch number
    (4) Sampling date and time taken
    (5) Identification of person taking the sample

4.3.1 Test coupons. - The coupon shall be vulcanized at a pressure of 500 pounds per square inch, gage (psig), minimum, using the following time and temperature:

(a) Raise the temperature to 300 ± 5°F
(b) Maintain this temperature for 120 ± 5 minutes

4.3.1.1 Grain orientation. - When the test coupon is made from more than one layer of unvulcanized material, the grain directions of all layers shall be parallel.

4.3.1.2 Coupon thickness. - When the unvulcanized material is greater in thickness than the required test coupon, the vulcanized coupon shall be reduced in thickness in accordance with Standard Fed. Test Method Std. No. 601, method 1111.

4.4 Examination. - Packaging, packing, and marking of the material shall be inspected for conformance with the requirements of 3.5 and section 5.

4.5 Classification of tests. - The inspection and testing of the material shall be classified as follows:

(a) Qualification tests
(b) Preproduction tests
(c) Acceptance tests

4.6 Qualification tests. - Qualification tests shall be conducted at an activity designated by the procuring activity. These tests shall consist of all the preproduction and acceptance tests specified herein, additional end-product tests as specified by the procuring activity, and the following tests:

(a) Water absorption
(b) Tensile strength (aged)
(c) Elongation (aged)
(d) Thermal conductivity
(e) Laminar peel
(f) Temperature rise
(g) Storage life and use life
(h) Shore "A" hardness (aged)

4.7 Preproduction tests. - Preproduction tests shall be conducted at an activity designated by the procuring activity, and shall consist of the following tests:

(a) Mooney viscosity
(b) Scorch characteristic

4.8 Acceptance tests. - Acceptance tests of individual lots shall consist of tests to determine compliance with the following requirements of section 3:

(a) Specific gravity
(b) Shore "A" hardness (unaged)
(c) Tensile strength (unaged)
(d) Elongation (unaged)
(e) Specific heat
(f) Thickness loss rate
(g) Weight loss
(h) Shipping date

4.9 Test methods. - Testing for qualification, preproduction, and acceptance shall be in accordance with the methods specified below. Samples to be tested for conformance with the requirements of aged material shall be aged at 212 ± 2° F for 168 ± 2 hours in accordance with Publication ASTM D 865.

	Characteristic	Test Procedure	Remarks
(a)	Water absorption	4.9.1	
(b)	Tensile strength	Fed. Test Method Std. No. 601, method 4111, die III	Test temperature 73.4 ± 2° F after a min of three hours conditioning at 73.4±2° F
(c)	Elongation	Fed. Test Method Std. No. 601, method 4121, die III	Same conditions as for method 4111
(d)	Temperature rise	4.9.2	
(e)	Mooney viscosity	ASTM D 1646	Test temperature 212 ± 1° F, one-minute delay, four-minute test period, large rotor
(f)	Scorch characteristic	ASTM D 1646	Small rotor; test temperature 300 ± 1° F
(g)	Specific gravity	Fed. Test Method Std. No. 601, method 14011	Specimen size 5 to 10 g, test temperature 25° C
(h)	Shore "A" hardness	Fed. Test Method Std. No. 601, method 3021	Test temperature 76 ± 6° F after a min of three hours conditioning at 76 ± 6° F

	Characteristic	Test Procedure	Remarks
(i)	Weight loss	4.9.3	
(j)	Thickness loss rate	4.9.4	
(k)	Thermal conductivity	ASTM C 177	Mean test temperature 150° F
(l)	Specific heat	4.9.5	Mean test temperature 150° F
(m)	Shipping date	4.4	
(n)	Laminar peel	4.9.6	
(o)	Storage life and use life	4.9.7	

4.9.1 Water absorption.- Water absorption shall be determined as follows:

(a) Cut four samples 4 ± 0.030 inch (in.) by 1 ± 0.030 in. by 0.25 ± 0.030 in. from a test coupon so that the 0.25-in. wide surfaces are all newly exposed.

(b) Condition the specimens for a minimum of 24 hours at 75 ± 5° F and 50 ± 5 percent relative humidity.

(c) Weigh each specimen to the nearest 0.0001 gram (g).

(d) Place the specimens in a suitable pressure test fixture. Separate the samples from each other and from the test fixture by stainless steel screens.

(e) Fill the test fixture with distilled water at 75 ± 5° F. Close the test fixture, and connect to it the hose from a cylinder containing nitrogen at a minimum of 1500 psig.

(f) Increase the pressure in the test fixture to 900 ± 10 psig, and hold for 30 ± 1 minutes.

(g) Release the pressure, disassemble the test fixture, and remove the specimens.

(h) Blot the excess water from the specimens with absorbent paper and weigh each specimen to the nearest 0.0001 g.

(i) Place the specimens in an oven at 158 ± 5°F for 240 ± 10 minutes. Remove from the oven and allow to remain at 75 ± 5° F and 50 ± 5 percent relative humidity for a minimum of 24 hours and again weigh each specimen to the nearest 0.0001 g.

(j) Record the results as weight percent increase, from the original weight, of the weights obtained in (h) and (i).

$$W_{(h)} = \frac{h - C}{C} \times 100$$

$$W_{(j)} = \frac{j - C}{C} \times 100$$

Where: C = Original weight
h = Weight after immersion
j = Weight after immersion and drying

4.9.2 Temperature rise.- The following procedure shall be used to determine temperature rise:

4.9.2.1 Test fixture.- Use a test fixture adjusted to produce the following:

(a) Fix torch perpendicular to specimen.
(b) Adjustable distance between torch-tip and sample face to 1 ± 0.030 in.
(c) Manifold pressure regulation of oxygen and acetylene to 12.5 ± 0.5 psig.
(d) Acetylene flow of 0.58 ± 0.01 cubic feet per minute (cfm) and oxygen flow of 0.57 ± 0.01 cfm.
(e) Time control up to two minutes.
(f) Torch-tip No. 2194548, General Tire and Rubber Company, Akron, Ohio.

4.9.2.2 Test.- The test shall be as follows:

(a) The specimens to be tested shall be bonded to the metal backing, conforming to SAE 4130, with the adhesives types I, II, and III described in Specification AGC-34278, and shall be in accordance with the following:

Specimen Dimensions

Size of Specimen, In.	Size of Metal Backing, In.
4 by 4 by 0.060 thick ± 0.003	Dia - 2 by 0.020 ± 0.001 thick steel disk

(b) Immerse a fiberboard specimen holder, of an appropriate size to contain the steel backing plate, in water at room temperature for 5 to 10 minutes. Remove from the water, blot off the excess, and use within one hour.

(c) Assemble the specimen in the fiberboard holder and position on the test fixture.

(d) Secure a recording thermocouple in contact with the metal backing plate and place a damp 2 in. diameter specimen holder as a cap on top of the sample.

(e) Ignite and lower the torch-tip to 1 ± 0.030 in. from the upper surface of the upper plate, with the torch-tip at 90 ± 5° to the plane of the plate.

(f) Determine the time, to the nearest 0.2 second required for the backside surface to reach temperatures of 200, 300, and 400° F, and record.

4.9.3 Weight loss. - The following procedure shall be used to determine weight loss:

(a) Cut or mold a specimen of insulating material to a diameter of approximately 2 by 0.25 ± 0.01 in. thick. Record this thickness as t_o.

(b) Weigh the specimen to the nearest 0.05 g and record this initial weight (W_i).

(c) Place the specimen in the specimen holder and position it in a test fixture (4.9.2.1).

(d) With the test fixture adjusted in accordance with 4.9.2.1, except that the torch shall be directed away from the specimen, ignite the flame and verify the adjustment of the manifold pressure and flow meters.

(e) Lower the torch-tip to the test position and allow to oscillate at 10 ± 0.25 cycles per minute through a 60° arc.

(f) At the end of 30 seconds, remove the flame from the specimen, remove the specimen holder with sample from the test fixture, and cool them by immersing in a container of dry ice.

(g) Weigh and record the final weight of the sample (W_f) to the nearest 0.05 g and determine the weight loss as follows:

$$W = W_i - W_f$$

Where: W = Weight loss, g
W_i = Initial weight, g
W_f = Final weight, g

4.9.4 Thickness loss rate.- The following procedure shall be used to determine thickness loss rate.

(a) After weighing the specimen in 4.9.3 (g), saw the specimen in two on a line that cuts through the approximate center of the eroded area.

(b) Measure to the nearest 0.01 in., on the face of the cut, the minimum thickness of virgin material (t_v) (see figure 1). Record the average of three determinations.

(c) Calculate the thickness loss rate as follows:

$$\text{TLR, in./sec} = \frac{t_o - t_v}{E}$$

Where: t_o = Original thickness of sample, in.
t_v = Minimum thickness of virgin material left after exposure, in.
E = Exposure time, seconds

4.9.5 Specific heat.- Specific heat shall be determined in a change-of-phase calorimeter. The specimen, prepared by laminating one sheet from each sample roll and cured in accordance with 4.9.6 to form a composite (weight W) shall be heated to a temperature (T_1) and then placed in a vaporizing medium of Freon 114 maintained at a constant temperature (T_2).

Calculate the specific heat in accordance with the following equation:

$$\text{Specific heat at } \frac{T_1 + T_2}{2} = \frac{h_v\,(m)}{W(T_1 - T_2)}$$

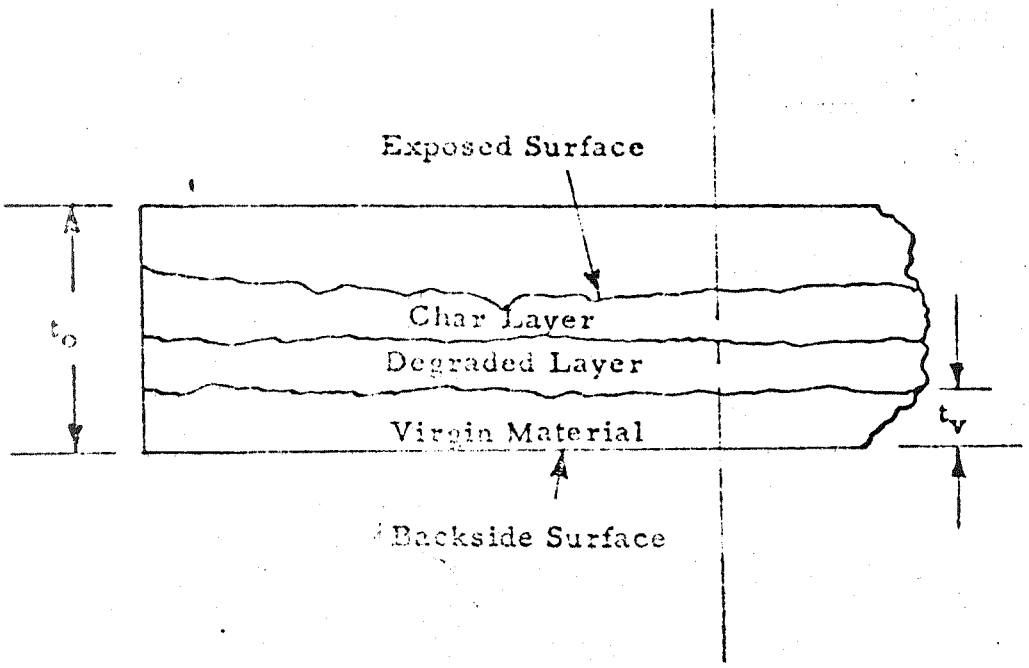

TEST SPECIMEN AFTER EXPOSURE
TO OXY-ACETYLENE FLAME

Where. h_v = The heat of vaporization limitation of Freon 114, BTU/lb

m = The amount of Freon 114 passed off as gas (corrected for normal environmental losses), lb

W = Weight of the specimen, lb

T_1 = Temperature of the specimen, °F

T_2 = Temperature of the Freon 114, °F

4.9.6 Laminar peel.- An even number of 12-inch-long pieces of unvulcanized rubber shall be freshened on both sides with toluol, in accordance with Specification TT-T-548. The freshened pieces shall be laminated to nominal 0.5 in. thickness, rolling the air from between the layers. Release the plies with polytetrafluoroethylene for a distance of 6 in. from one end and with the same number of sheets of rubber on both sides. Cure for 2 ± 0.1 hours at 300 ± 10° F and 500 pounds per square inch pressure, minimum. Cut approximately one-inch-wide strips from the cured laminate. Determine laminar peel at 180° peel and 20 in. per minute cross-head speed.

4.9.7 Storage life and use life.- The unvulcanized, calendered material shall be stored in a clean, dry container, in a dark, dry area at a temperature not exceeding 80° F for the specified time; and upon vulcanizing shall be tested for, and meet the requirements of.3.4.

5. PREPARATION FOR DELIVERY

5.1 Packaging.- The material shall be packaged in rolls or flat sheets. The material used in packaging shall not stick to the material when stored for extended periods or leave residue on the material that would affect the usability of the material.

5.1.1 Separation of material.- Rolls or sheets of unvulcanized stock shall be separated by polyethylene film, as specified for AGC-41250-1 requirements set for AGC-41250-1.

5.2 Packing.- Outside packages shall be heavy corrugated paper cartons or wooden containers. Unless otherwise specified, the material shall be packed in a manner to insure carrier acceptance and safe delivery. The lowest rate to the point of delivery specified by the purchase order or contract

5.3 Marking.- Each container shall be marked in accordance with Standard MIL-STD-129. Marking shall include, but not be limited to, the following information:

(a) Manufacturer's name
(b) Material trade name
(c) Lot number
(d) The number and revision letter of this specification
(e) Net weight
(f) Date of manufacture
(g) Use life and expiration date
(h) Date of shipment
(i) Class of material
(j) The following statement

This material shall be stored in a clean, dry container in a dark, dry area.	
Storage Temperature, °F, max	Storage Time, Months
80 1/	6

1/ 20% of the time may be above 80° F but below 100° F

6. NOTES

6.1 Intended use.- The material described herein is intended for use as an insulation material in rocket motors.

6.2 Ordering data.- Procurement documents should specify, but not be limited to, the following information:

(a) Number and revision letter of this specification
(b) Type and size of container desired
(c) Place of inspection
(d) Minimum lot size, if applicable
(e) Place of delivery
(f) Request for three copies of laboratory analysis of preproduction and acceptance test requirements
(g) Class of material

6.3 Storage conditions. - The unvulcanized, calendered material should be stored in a clean, dry container, in a dark, dry area at a temperature not exceeding 80°F, except 20 percent of the storage life may be below 100°F. The material should be discarded after the expiration date.

6.3.1 Storage life. - Storage life of the unvulcanized material is defined as the time after manufacture during which the material, stored in accordance with 6.3, upon vulcanizing will meet the requirements outlined in 3.4.

6.3.2 Use life. - Use life of the unvulcanized material shall be defined as the time after shipment, during which the material stored in accordance with 6.3, upon vulcanizing, will meet the properties outlined in 3.4.

(D) 6.4 Deleted.

(D) 6.5 Qualification. - Procurement contracts will be awarded only for such products that, prior to the closing date for receipt of quotations, have been tested and approved for inclusion on the applicable Qualified Products List. The attention of suppliers is called to this requirement, and they are urged to have the products that they propose to offer to Aerojet Solid Propulsion Company tested for qualification, in order that they may be eligible to be awarded contracts for the products covered by this specification. The activity responsible for the Qualified Products List is the Aerojet Solid Propulsion Company, Sacramento, California, 95813; and information pertaining to qualification of products may be obtained from that activity.

(D)

SHT 1/1

aerojet solid propulsion co.

CODE IDENT. NO. 05824

SPECIFICATION AGC- 36592

SEAL ASSEMBLY, FLEXIBLE, FABRICATION OF

SUPERSEDING:			
AGC- DATE	AGC- DATE	AGC- DATE	
RELEASES (REPLACE PAGES IN SPECIFICATION WITH LATEST CHANGE BELOW)			
REV LTR	RELEASE DATE	PAGE NUMBERS 1 2 3 4 5 6 7	PAGE ADDITIONS
	8 Apr 70		

Authorized for Release:

J. L. Smuts

J L Smuts
Specifications and Standards
Engineering Services Section
Engineering Design Department

1. SCOPE

1.1 This specification covers the assembly of a component designated as a flexible seal.

2. APPLICABLE DOCUMENTS

2.1 Department of Defense documents. - Unless otherwise specified, the following documents, listed in the issue of the Department of Defense Index of Specifications and Standards in effect on the date of invitation for bids, shall form a part of this specification to the extent specified herein.

SPECIFICATIONS

Federal

TT-M-261 Methyl-Ethyl-Ketone (for Use in Organic Coatings)

Military

MIL-A-9067 Adhesive Bonding, Process and Inspection Requirements for

STANDARDS

Military

MIL-STD-129 Marking for Shipment and Storage

(Copies of documents required by contractors in connection with specific procurement functions should be obtained as indicated in the Department of Defense Index of Specifications and Standards.)

2.2 Other documents. - Unless otherwise specified, the following documents, of the issue in effect on date of invitation for bids, shall form a part of this specification to the extent specified herein.

PUBLICATIONS

American Society for Testing and Materials

ASTM D 1002 Strength Properties of Adhesive in Shear by Tension Loading (Metal-to-Metal)

(Copies of ASTM documents may be obtained from American Society for Testing and Materials, 1916 Race Street, Philadelphia, Pa. 19103)

2.3 Aerojet-General Corporation documents. - Unless otherwise specified, the following documents, of the latest issue in effect, shall form a part of this specification to the extent specified herein.

SPECIFICATIONS

AGC-13855	Primer, Vinyl-Phenolic Resin-Base, FM-47, Preparation of
AGC-36237	Sandblasting to Clean Metal Surfaces, Requirements for

STANDARDS

AGC-STD-3003	Chemicals and Materials: Sampling and Testing
Method	
2109	Sodium Thiosulfate Standard Solutions
2116	Starch Indicator Solution, Preparation of

QUALITY ENGINEERING DIRECTIVES

QED No. LRU-101	Ultrasonic Inspection of Elastomers
QED No. UL-101	Laser Inspection for Unbond using the "Speckle-Shift" Technique
QED No. UU-101	Ultrasonic Inspection Metal-Insulation or Liner Bond

3. REQUIREMENTS

3.1 Rubber component integrity. - Upon receipt of the rubber components and prior to the start of fabrication of the seal, the rubber components shall show no evidence of any type of defect when inspected in accordance with 4.4.1.1.

3.2 Surface preparation. -

3.2.1 Steel surfaces. - The faying steel surfaces shall be cleaned and primed as follows.

3.2.1.1 Solvent clean. - Clean, unsized cheesecloth, wet with methyl-ethyl-ketone (MEK) conforming to TT-M-261; or Chloroethene NU solvent, shall be used to remove all surface contaminations. Dry for 10 minutes, minimum, at 60°F, minimum.

3.2.1.2 Abrade. - In order to remove any existing primer coating, rust, and scale, abrade the surfaces in accordance with AGC-36237, except that 100-grit garnet or zirconite (zirconium silicate) abrasive shall be used.

3.2.1.3 Postabrade solvent clean. - Repeat the operation of 3.2.1.1; except MEK, only, shall be used prior to primer application.

3.2.1.4 Primer application. - Primer, in accordance with AGC-13855, Type 1, shall be sprayed on the surface within four hours after cleaning. A spray pattern and technique shall be used to ensure a uniform and complete coverage of the surface. The primer shall be air dried for 30 ± 10 minutes and subsequently cured at 325° ± 25°F for a minimum of two hours.

3.2.1.5 Storage prior to bonding. - After priming and prior to bonding, primed surfaces shall be protected from damage and contamination.

3.2.2 Rubber surfaces. - The rubber surfaces shall be cleaned and chlorinated as follows.

3.2.2.1 Solvent clean. - Thoroughly scrub the rubber surfaces with clean, unsized cheesecloth wet with hexane solvent. Allow the solvent to evaporate.

3.2.2.2 Chlorination treatment. -Submerge the rubber in a chlorinating solution for 5.0 ± 0.5 minutes. The chlorinating solution shall have the following composition by volume:

(a) 100 parts distilled water
(b) 3 parts bleach containing 5.25 percent sodium hypochlorite
(c) 0.5 part concentrated hydrochloric acid

The chlorinating solution shall have an available chlorine content of 1.0 to 1.6 grams/liter prior to use, when tested in accordance with 4.3.1.4. Fresh chlorinating solution shall be prepared within 12 hours of use. Immediately after the chlorination treatment, the rubber shall be thoroughly rinsed in distilled or deionized water and dried at 70° to 100°F for 24 hours, minimum.

3.2.2.3 Storage prior to bonding. - After cleaning and prior to bonding, each rubber component shall be individually wrapped with Kraft paper for protection against contamination.

3.3 Assembly. - Assemble the flexible seal with the center line in the vertical attitude. The bonding operation shall be performed in a fixture approved by the procuring activity. The assembly of the seal shall be accomplished by a successive buildup of alternate layers of rubber pads and steel shims, starting with one of the seal end rings. The bonding area shall have a temperature ambient between 65° and 90°F and a relative humidity at 40 to 65 percent. The bonding operation shall be performed in accordance with the requirements of MIL-A-9067 and the additional detail requirements specified as follows.

3.3.1 Rubber-to-rubber bonding. - Each layer of rubber shall be positioned in the bonding fixture in the orientation in which bonding will take place. Proper mating between sections of the layer shall be established. Adhesive, as specified on the engineering drawing, shall be applied on both surfaces of the skive joints between rubber sections of the layer. The adhesive shall be cured at ambient temperature for a minimum of four hours with the mating surfaces held firmly in contact.

3.3.2 Rubber-to-steel bonding. - The primed steel surfaces shall be wiped with clean, unsized cheesecloth wet with MEK solvent. Adhesive shall not be applied until all traces of the solvent have evaporated. The steel and rubber surfaces that are to be mated shall both be completely wetted to an even thickness with the adhesive specified on the engineering drawing. The bond interfaces between rubber and steel shall be mated under a minimum vacuum pressure differential of 27.5 inches of mercury (Hg). After the surfaces are in complete contact, a load of three to six pounds per square inch (psi) shall be uniformly applied at the bond interface. The adhesive shall be cured under a maximum of 10 inches Hg vacuum pressure differential and the interface load for a minimum of

eight hours at ambient temperature. For each bond cycle, record the vacuum pressure differential, interface load, temperature, and time. After the final cure of each bond, remove any excess adhesive which extrudes at the edges of the components prior to commencing with the succeeding bond.

3.4 Bond integrity. -

3.4.1 Rubber-to-rubber bond. - Following cure, there shall be no edge separation at the rubber-to-rubber bond joint in excess of 0.05 inch when inspected as specified in 4.3.1.2.1.

3.4.2 Rubber-to-steel bond. - Following the completion of each rubber-to-steel bond cycle, there shall be no defects allowed when inspected as specified in 4.3.1.2.2.

3.5 Bond shear strength. - The adhesive bond shear strength shall be as follows:

	Shear strength, psi	Min	Max
(a)	Rubber-to-rubber	500	---
(b)	Rubber-to-steel	1500	---

3.6 Assembly log book. - An assembly log book shall be kept to record process control data. This data shall include, but not necessarily limited to, the following:

(a) Acceptance data on rubber and steel components
(b) Acceptance data and certification on adhesive materials
(c) Vacuum pressure differential, interface load, temperature, and time for each cure cycle
(d) Humidity and temperature ambients of the processing area
(e) Manufacturing documents, including all required data, with evidence of conformance to the documents
(f) Data showing compliance with 3.5
(g) Inspection records for dimensional checks, nondestructive testing, and other requirements of this document or applicable drawings
(h) Discrepancy action reports

4. QUALITY ASSURANCE PROVISIONS

4.1 Inspection. - Unless otherwise specified, the supplier is responsible for the performance of all inspection requirements as specified herein and may use any facilities acceptable to the procuring activity.

4.2 Classification of inspections. - The inspection requirements specified herein are classified as follows:

(a) In-process inspection
(b) Quality conformance inspection

4.3 In-process inspection. - In-process inspection shall consist of the following:

(a) Examination
(b) Bond integrity
(c) Bond shear strength
(d) Chlorinating solution analysis

4.3.1 Test methods. - The test methods, inspections, and examinations shall be as follows:

4.3.1.1 Examination. - Examine process control records to determine evidence of compliance with the requirements of 3.2 and 3.3.

4.3.1.2 Bond integrity. -

4.3.1.2.1 Rubber-to-rubber. - Visually inspect rubber-to-rubber bond to determine conformance to 3.4.1.

4.3.1.2.2 Rubber-to-steel. - Visually and nondestructively inspect rubber-to-steel bond to determine conformance to 3.4.2. Ultrasonically inspect through steel in accordance with QED No. UU-101; and through rubber in accordance with QED No. UL-101.

4.3.1.3 Bond shear strength. - For each rubber-to-metal and rubber-to-rubber bond cycle, prepare bond shear test specimens in accordance with ASTM D 1002 and the following, to determine conformance to 3.5. The test specimens shall be cut from test panels, prepared using steel plates primed in accordance with 3.2.1.4. These test panels are to be processed simultaneously with the processing of each rubber-to-steel and rubber-to-rubber bond cycle, using adhesive representative of that used in the assembly of the seal. After cure of the test panels, section the panels into specimens and test in accordance with ASTM D 1002. Test the specimens in triplicate for each bond cycle.

4.3.1.4 Chlorinating solution analysis. - Test the chlorinating solution for conformance to 3.2.2.2 using the following procedure:

(a) Pipette a 75-milliliter (ml) sample of chlorinating solution into a suitable-size, tared, weighing bottle and weigh to 0.1 milligram (mg). Transfer the sample to a 250-ml volumetric flask, dilute to 250 ml with distilled water, and mix thoroughly.
(b) Pipette a 30-ml aliquot portion of the above solution into a 250-ml flask or beaker containing 50 ml of distilled water, approximately two grams (g) of potassium iodide crystals, and 2 ml of concentrated hydrochloric acid. Mix the solution thoroughly.
(c) Titrate the liberated iodine with standard 0.1 normal (N) sodium thiosulfate solution, prepared and standardized in accordance with AGC-STD-3003, Method 2109, until the mixture is straw-yellow in color.

(d) Add 5 ml of starch indicator solution, prepared in accordance with AGC-STD-3003, Method 2116, and continue titrating until the dark blue color of the iodine-starch complex disappears.
(e) Observe the temperature of the standard sodium thiosulfate solution and correct the volume consumed for the titration to 20°C.
(f) Calculate the available chlorine content of the chlorinating solution:

Available chlorine (g/liter) = A x N x 3.94

Where: A = Ml of standard sodium thiosulfate consumed
N = Normality of standard sodium thiosulfate

4.4 Quality conformance inspection. - Quality conformance inspection shall consist of the following:

(a) Rubber component integrity
(b) Examination of assembly log book

4.4.1 Test methods. - The test method and examination shall be as follows.

4.4.1.1 Rubber component integrity. - Inspect rubber components in accordance with QED No. LRU-101 to determine conformance to 3.1.

4.4.1.2 Examination. - Examine the seal assembly log book to determine evidence of compliance with 3.6.

5. PREPARATION FOR DELIVERY

5.1 Packaging. - The seal assembly shall be packaged and packed in a palletized container that provides adequate protection against physical damage, moisture, and corrosion during shipment and handling, to the extent required by the applicable drawing.

5.2 Marking. - Container shall be marked in accordance with MIL-STD-129. Marking shall include, but not be limited to, the following information:

(a) Manufacturer's name
(b) Part number
(c) Date of manufacture
(d) Unusual shipping and storage requirements
(e) Net weight

6. NOTES

6.1 Intended use. - The processing operations are intended for use in the fabrication of flexible seal assemblies for application in the 260-inch-diameter motor program.

AEROJET GENERAL

AEROJET-GENERAL CORPORATION

CODE IDENT. NO. 13310

AGC-36420A
Amendment 1
7 July 1964

DEVELOPMENT SPECIFICATION

INSULATION, RUBBER, BUTADIENE ACRYLONITRILE, AUTOCLAVE CURE FABRICATION OF

This amendment forms a part of Aerojet-General Corporation Development Specification AGC-36420A.

Paragraph 3.3.4.1, Table I Delete and substitute:

"

Table I

Autoclave Cure Cycle

Vulcanization Temperature °F	Hold Period Min (Minutes)	Autoclave Pressure, Min (psig)	Vacuum in Blanket, Min (In. of Hg Vac)
180 ± 5	180	100	20
220 ± 5	125	100	20
310 ± 5	125	100	20
150	---	50	20 "

Authorized for Release:

J. H. Yetto, Manager
Specifications and Standards
Solid Rocket Operations
Sacramento Plant

AEROJET-GENERAL CORPORATION
CODE IDENT. NO. 13310

AGC-36420A
19 February 1964
Superseding
AGC-36420
3 February 1964

DEVELOPMENT SPECIFICATION

INSULATION, RUBBER, BUTADIENE ACRYLONITRILE, AUTOCLAVE CURE FABRICATION OF

1. SCOPE

1.1 This specification establishes the requirements for fabrication of autoclave-cured butadiene acrylonitrile rubber insulation.

2. APPLICABLE DOCUMENTS

2.1 Department of Defense documents.- Unless otherwise specified, the following document, listed in the issue of the Department of Defense Index of Specifications and Standards in effect on the date of invitation for bids, shall form a part of this specification to the extent specified herein.

SPECIFICATION

Federal

TT-M-261	Methyl-Ethyl-Ketone (for Use in Organic Coatings)

(Copies of documents required by contractors in connection with specific procurement functions should be obtained as indicated in the Department of Defense Index of Specifications and Standards.)

2.2 Other documents.- Unless otherwise specified, the following document, of the issue in effect on date of invitation for bids, shall form a part of this specification to the extent specified herein.

SPECIFICATION

Department of the Navy
Bureau of Naval Weapons

WS 1138	Insulating Material, Butadiene Acrylonitrile, Unvulcanized

(Copies may be obtained from the procuring activity or as indicated by the contracting officer.)

2.3 Aerojet-General Corporation documents.- Unless otherwise specified, the following documents, of the latest issue in effect, shall form a part of this specification to the extent specified herein.

SPECIFICATION

AGC-34151	Adhesive, Epoxy Paste with Amine Curing Agents

STANDARD

AGC-STD-3003	Chemicals and Materials: Sampling and Testing

Method

9073	Spark Test, Chamber Insulation
9074	X-Ray Inspection, Chamber Insulation

3. REQUIREMENTS

3.1 Materials.- The following materials, or equivalent, approved by the Aerojet-General Corporation (AGC), shall be used:

(a) Methyl-ethyl-ketone, technical grade (MEK) conforming to Specification TT-M-261.
(b) Chlorothene NU (DOW Chemical Co., Midland, Michigan)
(c) Insulating material conforming to Specification WS 1138, class 1, except that the bondability requirement is waived.

(d) Insulating material conforming to Specification WS 1138, class 2.
(e) Adhesive prepared by dissolving 22 parts by weight of insulating material, conforming to Specification WS 1138, class 2, in 78 parts by weight of MEK.
(f) Germax cure-accelerating agent (The Goodyear Tire and Rubber Company, Akron, Ohio)
(g) Insulating material conforming to Specification WS 1138, class 1, modified with Germax cure-accelerating agent (The Goodyear Tire and Rubber Company, Akron, Ohio)
(h) Insulating material conforming to Specification WS 1138, class 2, modified with Germax cure-accelerating agent (The Goodyear Tire and Rubber Company, Akron, Ohio)
(i) Adhesive, in accordance with Specification AGC-34151, type I.
(j) MR-22 release agent (Penninsular Chemical Products, Grand Rapids, Mich.)

3.2 Tools.- The following tools, or equivalent, approved by AGC, shall be used:

(a) Gloves, cotton, lint free
(b) Cloths, cotton, clean
(c) Rollers, steel, 2.0 inches (in.) wide, maximum
(d) Stitchers, serrated or knurled steel faced, 0.5 in. wide, maximum
(e) Hypodermic needle
(f) Awl
(g) Emery cloth, 40 to 80 grit

3.3 Fabrication.-

3.3.1 Mold preparation.-

3.3.1.1 Cleaning.- The building mold shall be cleaned so that it is free of all foreign matter by wiping with a cloth wet with chlorothene NU. Allow the mold to dry until all traces of chlorothene NU have evaporated.

3.3.1.2 Mold release application.- If a mold release agent is deemed necessary, the surfaces of the mold to which the unvulcanized insulation material is to be applied shall be coated with MR-22 release agent.

3.3.2 Insulation layup procedure.- The following procedure shall be used to layup the insulation material:

(a) The layup shall be made with multiple plies of patterned pieces cut from insulation material conforming to Specification WS 1138, class 1 or class 2. The patterned pieces shall be cut from material that is free of all defects such as wrinkles, voids, delaminations, or foreign matter.

(b) The edges of the patterned pieces shall be skived or scarfed at an angle of 25 $\pm$ 5° to the surface of the pieces.

(c) All surfaces and edges of the unvulcanized patterned pieces that are to be mated shall be scrubbed with clean cloths that are dampened with MEK. Care shall be exercised in all subsequent operations to prevent contamination of the scrubbed edges and surfaces. The surfaces of the unvulcanized material shall be buffed with a wire brush within 72 hours before, or immediately after, scrubbing with MEK.

(d) The scrubbed, patterned pieces shall be used in the layup within four hours, but not until all traces of MEK have evaporated.

(e) Assemble the first layer of the insulation pieces in the mold, using steel rollers having a width of no more than 2 in., to expel all air from between the patterned pieces and the mold.

(f) Stitch the joints between pieces with steel-faced rollers having a width of no more than 0.5 in.

(g) If an air bubble exists that is too far from the edge of an insulation piece to remove with a roller or stitcher, use a hypodermic needle or awl to puncture the insulation material at as small an angle to the insulation surface as possible. Remove the trapped air and stitch the area of the puncture thoroughly.

(h) Repeat steps (c) through (g) until the required layup thickness is obtained.

(i) The distance between joints or splices of the patterned pieces in adjacent plies shall be 2 in., minimum.

(j) The patterned pieces are to be placed in the mold in such a manner that the largest pieces are used in the last ply placed on the layup.

3.3.3 Vacuum blanket procedure.-

3.3.3.1 Bleeder cloth.- The outermost ply of the layup shall be completely covered with a bleeder cloth ply. The bleeder cloth material is to be cut into patterned pieces and placed over the layup in such a manner that there are no wrinkles in the cloth. Square woven cotton, nylon, or fiberglass fabric is to be used for the bleeder ply. The cloth shall be coated with a release agent which will facilitate removal of the cloth after vulcanization of the insulation material, without contaminating the material surface.

3.3.3.2 Vacuum blanket.- The layup and the bleeder ply shall be completely encapsulated in a vacuum blanket of natural or butyl rubber, 1/8 to 3/16 in. thick. At least one vacuum port is to be installed in the vacuum blanket. It shall be so located and constructed that the bleeder cloth and unvulcanized insulation material will not be drawn into the port opening.

3.3.3.3 Evacuation.- A vacuum of 20 in. of mercury, minimum, shall be applied at room temperature to the unvulcanized layup for four hours, minimum. Any detectable leaks in the assembly shall be repaired prior to vulcanization.

3.3.4 Vulcanization.-

3.3.4.1 Autoclave cure cycle.- The insulation material shall be vulcanized under the conditions specified in table I. The vulcanization temperatures must be maintained at the center of the thickest portion of the insulation material for not less than the specified hold period. The maximum temperature of the heating media shall not be more than 25°F above the required vulcanization temperature.

Table I

Autoclave Cure Cycle

Vulcanization Temperature (° F)	Hold Period Min (Minutes)	Autoclave Pressure, Min (psig)	Vacuum in Blanket, Min (in. of Hg Vac)
180 ± 5	180	100	20
310 ± 5	125	100	20
150	---	50	20

3.3.4.2 Cure cycle verification.- Each autoclave cure cycle shall be verified by including a test block of insulation material conforming to Specification WS 1138, class 1, with each insulation component during vulcanization. The test block shall have a thickness equal to, and a width greater than, the maximum thickness of the component being cured. The test block shall be prepared so that it is exposed to the same conditions as the insulation component during vulcanization. Thermocouples located at the center and at other positions inside the test block shall be monitored and the temperatures recorded throughout the cure cycle. The test block shall be sectioned after completion of the cure cycle. The Shore "A" hardness at any point in the test block shall be 74, minimum.

3.3.4.3 Moisture test coupon.- Included with each insulation component during autoclave curing shall be a 2 in. by 1 in. by 0.5 in. coupon of insulation material. Following completion of the cure cycle, the coupon shall be tested to determine the weight loss which occurs during a 12-hour exposure to dry air in an oven at 212 ± 10° F. If a coupon weight loss of greater than 0.7 percent is obtained, the corresponding insulation component must be dried by a 12-hour exposure to dry air at 212 ± 10° F.

3.4 Finishing.-

3.4.1 Trimming.- After vulcanization, the insulation component shall be trimmed to the final dimensions in accordance with the applicable drawing.

3.4.2 Cleaning and abrading.- After removal from the mold, the insulation component shall be cleaned by wiping with a clean cloth dampened with MEK. Bonding surfaces shall then be abraded with 40 to 80 grit emery cloth and cleaned by wiping with a clean, dry cloth.

3.4.3 Finished part acceptance.- A finished part is acceptable with surface imperfections measuring up to 10 percent of the part thickness if this 10 percent dimension does not exceed 0.10 in. The final thickness, as measured from the bottom of the imperfection to the other surface, cannot be less than the minimum applicable drawing requirement. A finished part is one which has been cured, or cured and trimmed, to final dimension.

3.4.4 Repair.- Other imperfections shall be repaired as follows:

3.4.4.1 Preparation of repair area.- The area of the imperfection shall be prepared as follows:

(a) Scrub defective area with a clean cloth dampened with MEK. The cleaned area shall include the area up to at least 1 in. from the edges of the defect.
(b) Allow the area to dry until all traces of MEK have evaporated.
(c) If the condition is a cut, gouge, or depression, all defective portions of the part in the area of the condition shall be removed by abrading with 40 to 80 grit emery cloth.
(d) If the condition is a blister, cut away the blistered surface. Remove all defective portions of the part in the area of the void by abrading with 40 to 80 grit emery cloth.
(e) If the defect is an inclusion, cut away only the material necessary to remove the inclusion from the nearest surface.
(f) Remove enough material to facilitate layup of the repair material. The cavity shall be faired to an angle of at least 45° to the face of the part and abraded with 40 to 80 grit emery cloth.
(g) Scrub the area of the part which was abraded in (c), (d), or (f) with a clean cloth dampened with MEK.
(h) Allow the area to dry until all traces of MEK have evaporated.

3.4.4.2 Repair methods.- Layup and cure of material in the prepared area shall be accomplished by one of the methods outlined below. AGC approval of the repair method to be used must be received by the supplier prior to initiation of any repair procedure.

3.4.4.2.1 Air-curing method.- The procedure for completing the repair by the air-curing method shall be as follows:

(a) Mix 100 parts by weight of the adhesive specified in 3.1 (e) with 2.5 parts by weight of Germax cure-accelerating agent.
(b) Apply a minimum of two coats of the adhesive to the abraded area of the part.
(c) Dry the adhesive coat until all traces of MEK have evaporated.
(d) The adhesive-coated area of the part shall be filled with plies of insulation material to which Germax cure-accelerating agent has been added. Parts fabricated from material conforming to Specification WS 1138, class 1, shall be repaired using the material specified in 3.1 (g). Parts fabricated from material conforming to Specification WS 1138, class 2, shall be repaired using the material specified in 3.1 (h). The repair material shall be prepared and laid in place according to the layup procedures in 3.3.2.
(e) Cure the repair area under a vacuum of 24 in. of mercury, minimum, for two hours, minimum, at 190° F, minimum, or cure under a pressure of 10 pounds per square inch (psi), minimum, for two hours, minimum, at 190° F, minimum.

3.4.4.2.2 Heating iron cure method.- The procedure for completing the repair by the heating iron method shall be as follows:

(a) Apply a minimum of two coats of the adhesive specified in 3.1 (e) to the abraded area of the part.
(b) Dry the adhesive coat until all traces of MEK have evaporated.

(c) The adhesive-coated area shall be filled with plies of material of the same specification as the part. The repair material shall be prepared and laid in place according to the layup procedures in 3.3.2.

(d) The repair shall be cured by use of a heating iron at a temperature of 300 ± 10° F. under a pressure of 10 psi, minimum. The required cure time is given in table II.

Table II

Heating Iron Cure Times

Depth of Cavity (In.)	Min Cure Time (Hours)
Up to 1/8 in.	2.5
1/8 to 1/4	6
1/4 to 1/2	8
1/2 to 3/4	12

3.4.4.2.3 Precured repair method. - The procedure for completing the repair by the precured method shall be as follows:

(a) Obtain 0.030 and 0.080 in. thick patches of cured insulation material of the same specification as the part to be repaired.

(b) Prepare the patches for layup according to the procedures of 3.3.2.

(c) Prepare the adhesive specified in 3.1 (i) by mixing four parts by weight of the Part A paste with one part by weight of the Part B curing agent.

(d) If the depth of the abraded area of the part is less than 0.080 in., the surface of the abraded area shall be coated with the adhesive. An 0.080 in. thick patch prepared as in (b) shall be placed over the defect, without trapping air beneath it.

(e) If the depth of the abraded area of the part exceeds 0.080 in., the defect shall be filled with 0.030 and 0.080 in. thick patches prepared as in (b). Each piece of cured material is to be bonded to the part and to the adjacent pieces with the adhesive of (c). Care shall be taken to avoid trapping air between plies.

(f) The repair shall be cured for six hours, minimum, at 90° F, minimum, and 10 pounds per square inch, gage, minimum. A check sample of the mixed adhesive shall be exposed to the same temperature environment as the repair area during curing. The cure cycle is not to be terminated until the adhesive sample has cured.

3.4.4.3 Finishing the repair area.- The material in the repair area shall, if necessary, be ground after cure so that the surface of the repair material is flush with the adjacent material surface.

3.5 Dimensions.- The insulation part shall conform with the dimensional requirements of the applicable drawing.

3.6 Insulation defects.-

(a) There shall be no holes in the cured boots and cylindrical section insulation when spark tested in accordance with 4.1.1.4.
(b) The cured cylindrical section insulation shall have no holes, blisters, or cuts deeper than 10 percent of the part thickness, no thin areas less than 0.10 in. thick, and no foreign material, except asbestos agglomerates.
(c) The forward, aft, and nozzle insulation components shall show no voids or delaminations when X-rayed in accordance with 4.1.1.4.

4. QUALITY ASSURANCE PROVISIONS

4.1 Fabricators responsibility.- The fabricator shall be responsible for the performance of all the processing and inspection requirements as specified herein. The fabricator may utilize his own or any other inspection facilities and services acceptable to the procuring activity. Processing records and inspection records shall be kept complete and available to the procuring activity.

4.1.1 Inspection during process.- The fabricator shall establish and maintain inspection at appropriately located points in the process to verify compliance with the requirements of section 3.

4.1.1.1 Cure cycle verification.- Test blocks required in 3.3.4.2 shall be so identified as to permit positive traceability to the component being cured.

4.1.1.2 Moisture test.- Test coupons required in 3.3.4.3 shall be weighed to the nearest 0.001 gram before and after 12-hour oven exposure, and weights recorded. Test coupons shall be so identified as to permit positive traceability to the component being cured.

4.1.1.3 Precured repair.- The check sample of mixed adhesive employed to determine cure time in 3.4.4.2.3 (f) shall be considered to be cured when the sample is solidified.

4.1.1.4 Tests for insulation defects.- The following tests shall be employed to determine the location and acceptability of insulation defects:

(a) Spark tests in accordance with Standard AGC-STD-3003, method 9073.
(b) X-ray in accordance with Standard AGC-STD-3003, method 9074.

4.1.2 Processing changes.- The supplier shall make no changes in processing techniques or other factors affecting the quality of the product without prior approval of Aerojet-General Corporation.

5. PREPARATION FOR DELIVERY

5.1 This section is not applicable to this specification.

6. NOTES

6.1 This section is not applicable to this specification.

Authorized for Release:

J. H. Yetto, Manager
Specifications and Standards
Solid Rocket Plant
Sacramento

APPENDIX C

QUALITY ENGINEERING DIRECTIVES

aerojet solid propulsion company

QUALITY ENGINEERING DIRECTIVE

QED NO. LRU-101

DATE 2 June 1970

SUPERSEDES

TITLE:

ULTRASONIC INSPECTION, RUBBER TO STEEL BOND, 260 INCH FLEXSEAL PROGRAM

MANAGER, PRODUCT ASSURANCE DEPARTMENT

1. SCOPE

This directive establishes the procedure to be followed in the inspection of rubber to steel bonds in the 260" Flexseal using contact pulse/echo ultrasonics at the exposed rubber surface.

2. EQUIPMENT

Branson Sonoray, Sperry Reflectoscope, or equivalent ultrasonic instrument
3.5 Mc Lithium sulfate transducer, 0.5 x 0.75"
Bond/unbond sample
Distilled water
Sponge and/or clean cloths

3. PROCEDURE - SETUP (Branson Sonoray)

3.1 Plug the instrument into a 110V outlet

3.2 Attach the transducer to the "pulser" jack on the instrument with the appropriate search cable.

3.3 Turn the power switch to "ON" and allow the instrument to warm up 10 to 15 minutes.

3.4 Position the instrument controls as follows:

Delay	1	Coarse Gain	D
Range	2	Fine Gain	04
Damping	7	Rate Gen.	12 o'clock
Reject	9 o'clock	Range Mult.	Slow

3.5 With the instrument warmed up:

3.5.1 Adjust DELAY control to place the initial pulse at the first left vertical grid line on the scope. (Figure 1)

3.5.2 Using distilled water as a couplant, place the transducer on the rubber surface of the bond/unbond sample over an area known to be bonded. If necessary, adjust the FINE GAIN control until the scope presentation extends to the right vertical grid line. (Figure 2)

3.5.3 Place the transducer over an area of the sample known to be unbonded. Note that the scope presentation is reduced to three major pips as in Figure 3. Adjust RANGE and FINE GAIN controls to obtain maximum differentiation between bond and unbond signals.

4. PROCEDURE - INSPECTION

Place the ultrasonic instrument and an ample supply of distilled water inside the circle formed by the steel/rubber ring of the Flexseal. The instrument should be mounted on a wheeled cart or table at a height that affords easy viewing of the CRT screen. The couplant (distilled water) should be used directly from the bottle.

Saturate a sponge or pad of clean cloth with distilled water and wipe a small area of the rubber surface, leaving as much water on the surface as possible. Sweep the transducer over the moistened area in both the vertical and horizontal directions, adding distilled water as necessary to maintain acoustic coupling between the face of the transducer and the surface of the rubber. As each area is completed, wipe the rubber dry with a clean cloth or sponge.

Inspect the entire ring in this manner, and record the location and size of all unbonded areas on a map of the ring. DO NOT MARK ON THE SURFACE OF THE RUBBER. Document all unbonded areas on an Inspection Report.

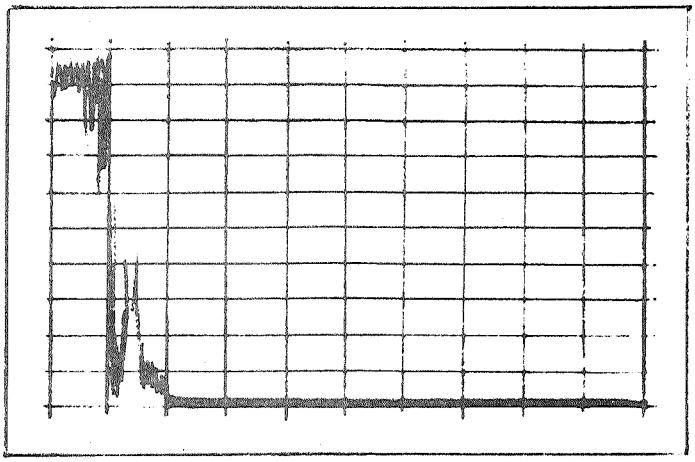

Figure 1 Initial Pulse (Unbonded Rubber)

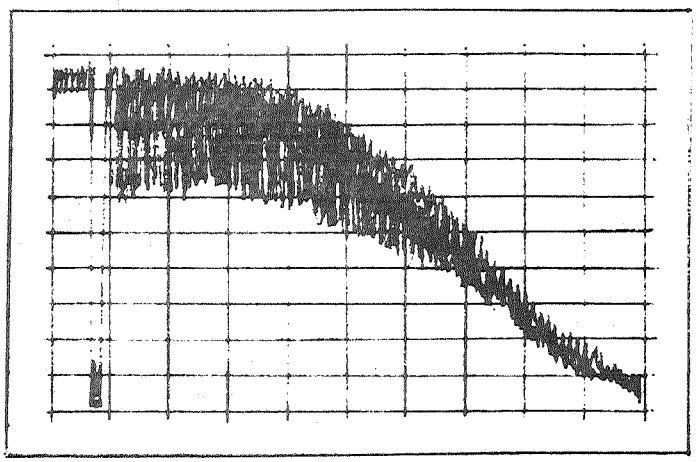

Figure 2 Rubber Bonded to Steel

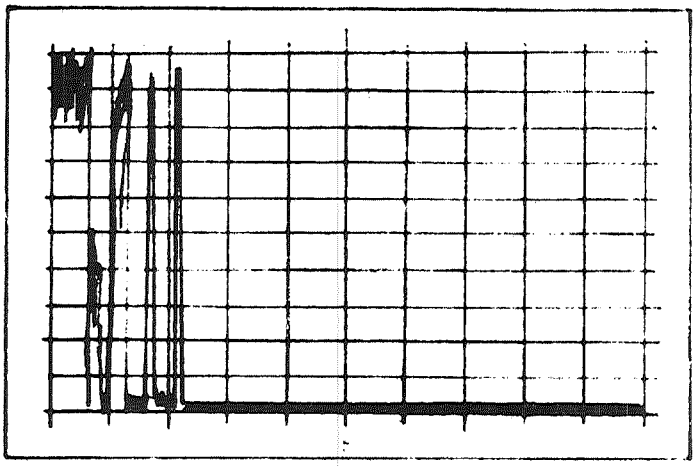

Figure 3 Rubber not Bonded to Steel

aerojet solid propulsion company

QUALITY ENGINEERING DIRECTIVE

QED NO. LRU-102

DATE 13 April 1970

SUPERSEDES

TITLE:

AUTOMATED ULTRASONIC INSPECTION (C SCAN) OF ELASTOMERS FOR EVALUATION OF INTERNAL DEFECTS

MANAGER, PRODUCT ASSURANCE DEPARTMENT

1. SCOPE

This procedure defines the use of one type of pulse-echo ultrasonic equipment to detect internal voids and delaminations in the sheet rubber components for use in the 260" Flex-Seal.

2. EQUIPMENT

Curtiss-Wright Immerscope, Model 424D
Alden Helix Recorder, Model 319CA
Automation Industries Ultragraph, Model 1047
Immersion Tank with Bridge and Carriage - Automation Industries
Plexiglass trays (54" x 18" x 3") with supports for mounting in Immersion Tank
15 Mc, medium focus Lithium Sulfate Transducer, 0.75" diameter
Distilled Water
Fotoflow Solution
Standard Samples - 6" x 6" (2)

3. PROCEDURE - SETUP AND OPERATION

a. Turn on power supply to Immerscope and Ultragraph. Allow 15 minutes for warm-up.

b. Set controls as follows:

Immerscope

Frequency	2.25
Pulse/sec	400
Gain	100
Zero suppress	Off
ST C	Off
Coarse sweep	F
Fine Sweep	Minimum
Marker	Off
Alarm	Off
Auto sweep	Off
Range marker	Off

Ultragraph

Level	8 o'clock
Contrast	4
Gate delay	12 - 12.5
Gate width	17
Intensity	Adjust as required
Set for positive recording	

Bridge and Carriage

Lines/inch	44
Bridge speed	42
Helix	On
Carriage	On
Carriage speed	45
Vert. & Rotary Drive	Off

FIGURE 1

Test Sample No. 1

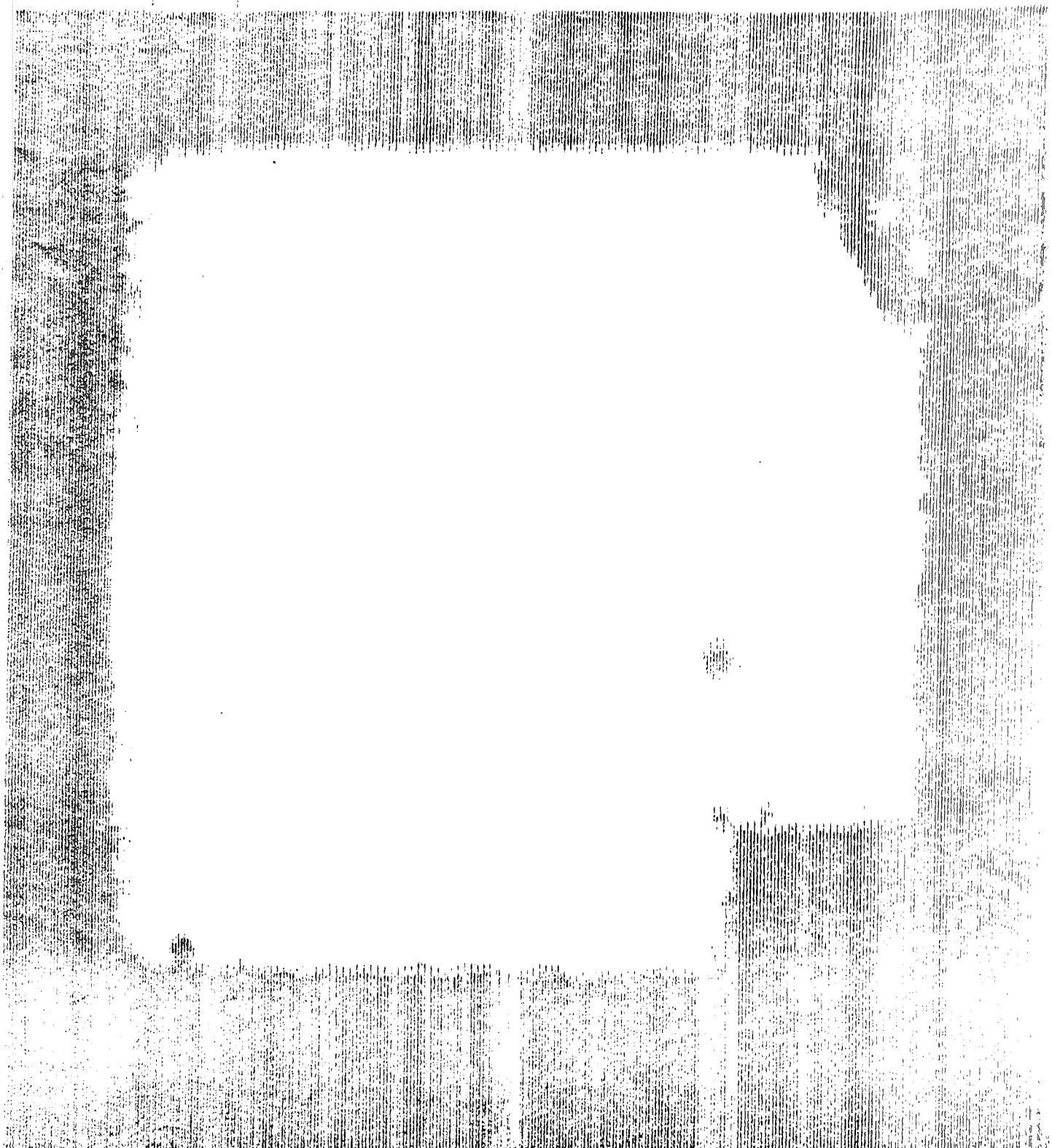

FIGURE 2

Test Sample No. 1

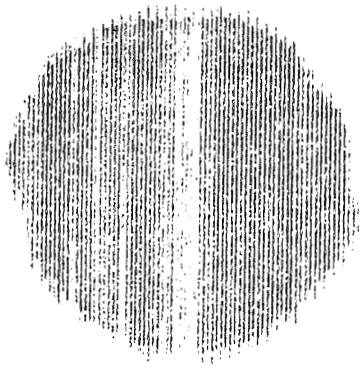

APPENDIX D

FLEXIBLE SEAL DATA ANALYSIS PROCEDURE

AEROJET-GENERAL CORPORATION
SACRAMENTO • CALIFORNIA

AGCS-0800-11 •

REPORT NO

PAGE 1 OF

SUBJECT LSR FLEX SEAL DATA ANALYSIS & PIVOT POINT CALCULATIONS

DATE

WORK ORDER

BY S. J. BROWN

CHK BY

DATE

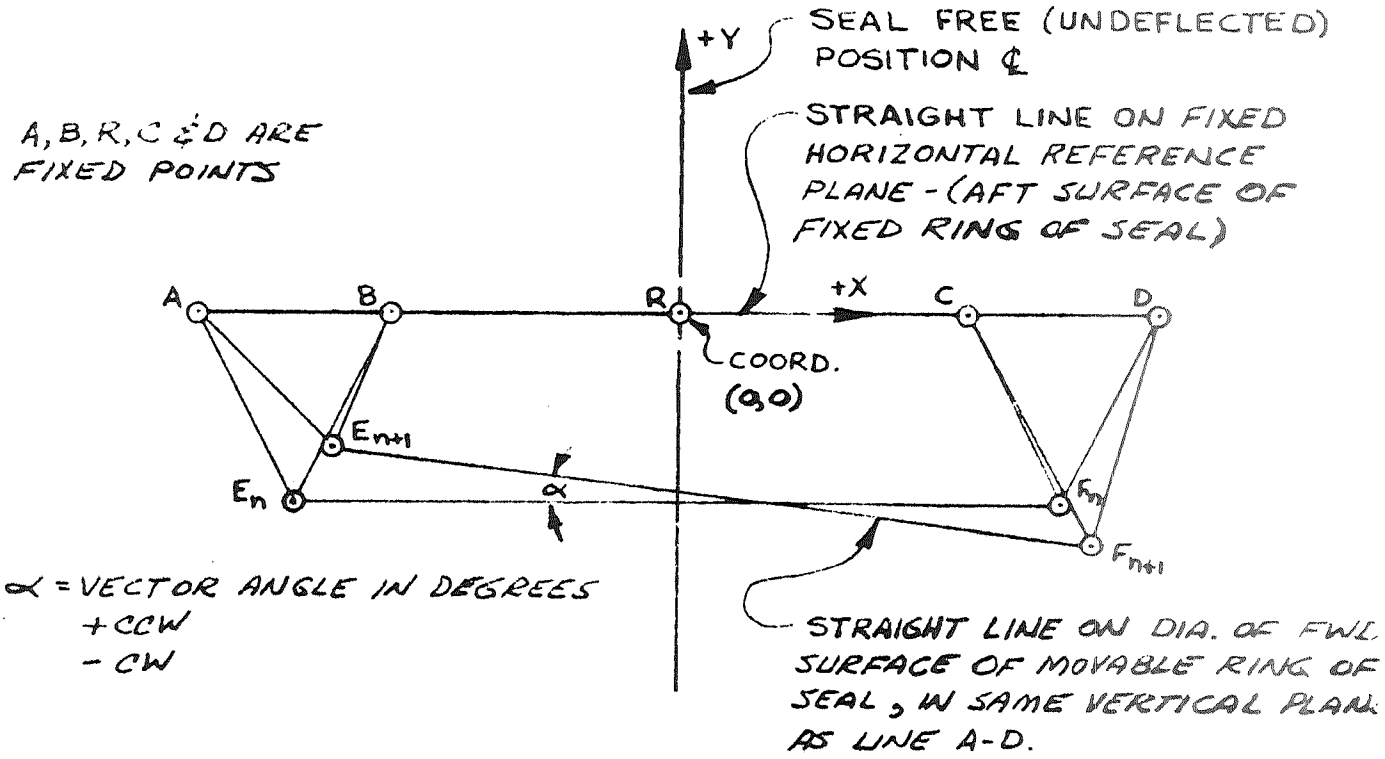

CONDITIONS:

1. POINT R IS THE ORIGIN OF THE XY COORDINATE SYSTEM.
2. AR, BR, RC & RD ARE MEASURED PRIOR TO TESTING AND ARE FIXED DIMENSIONS, NOT NECESSARILY SYMMETRIC ABOUT R.
3. EF IS MEASURED PRIOR TO TESTING AND IS A CONSTANT DIMENSION PREFERABLY, BUT NOT NECESSARILY, CENTERED ON THE SEAL ℄.
4. AE_o, BE_o, CF_o & DF_o ARE MEASURED PRIOR TO TESTING, AND ΔAE, ΔBE, ΔCF & ΔDF ARE REMOTELY MEASURED FOR EACH SEAL DEFLECTED POSITION DURING TESTING.

AEROJET-GENERAL CORPORATION
SACRAMENTO • CALIFORNIA

AGCS-0800-11 | REPORT NO. | PAGE 2 OF

SUBJECT: LSR FLEX SEAL DATA ANALYSIS & PIVOT POINT CALCULATIONS | DATE | WORK ORDER

BY: S. J. BROWN | CHK. BY | DATE

CALCULATION OF DEFLECTED POSITION AND VECTOR ANGLE

FOR SEAL POSITION n

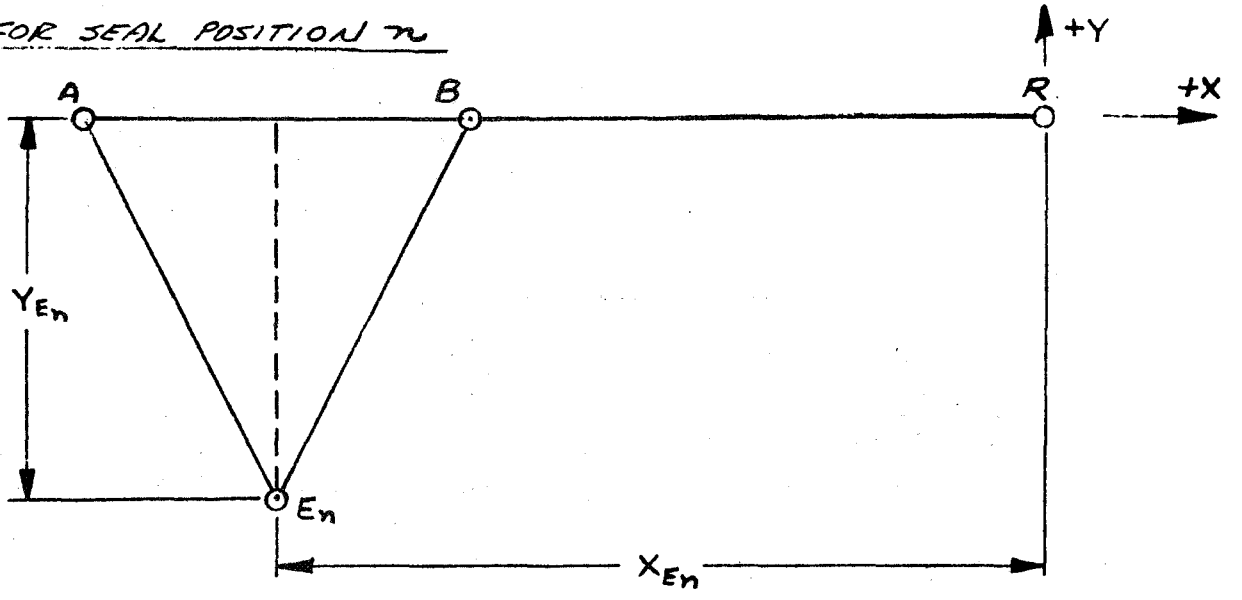

$AE_n = AE_o + (\Delta AE)_n$ FOR $n=0$, $(\Delta AE)_{n=0} = 0$ & $(\Delta BE)_{n=0} = 0$

$BE_n = BE_o + (\Delta AE)_n$

$(YE_n)^2 = (BE_n)^2 - (BR + XE_n)^2$ (PROPERTY OF RT. TRIANGLE: $a^2+b^2=c^2$)

ALSO, $(YE_n)^2 = (AE_n)^2 - (AR + XE_n)^2$ — AR & BR ARE POS.; XE_n IS NEGATIVE.

SO, $(BE_n)^2 - (BR + XE_n)^2 = (AE_n)^2 - (AR + XE_n)^2$

$(BE_n)^2 - (BR)^2 - 2(BR)(XE_n) - XE_n^2 = (AE_n)^2 - (AR)^2 - 2(AR)(XE_n) - (XE_n)^2$

$2(AR)(XE_n) - 2(BR)(XE_n) = (AE_n)^2 - (AR)^2 - (BE_n)^2 + (BR)^2$

$2(AR-BR)(XE_n) = (AE_n)^2 - (BE_n)^2 - (AR)^2 + (BR)^2$

$$\therefore \quad XE_n = \frac{(AE_n)^2 - (BE_n)^2 - (AR)^2 + (BR)^2}{2(AR-BR)}$$

$$YE_n = -\sqrt{(BE_n)^2 - (BR + XE_n)^2}$$

↑ PROVIDES FOR YE_n TO ALWAYS BE NEGATIVE

BASED ON THE PROPERTIES OF A PLANE TRIANGLE (HUDSON'S THE ENGINEERS' MANUAL) AN ALTERNATE METHOD OF COMPUTING YE_n IS AS FOLLOWS:

$S = \frac{1}{2}(AB + AE_n + BE_n)$ & $AB = AR - BR$

$$YE_n = -\frac{2}{AB}\sqrt{S(S-AB)(S-AE_n)(S-BE_n)}$$

AEROJET-GENERAL CORPORATION
SACRAMENTO • CALIFORNIA

AGCS-0800-11

REPORT NO

PAGE 3 OF

SUBJECT LSR FLEX SEAL DATA ANALYSIS & PIVOT POINT CALCULATIONS

DATE

WORK ORDER

BY S.J. BROWN

CHK. BY

DATE

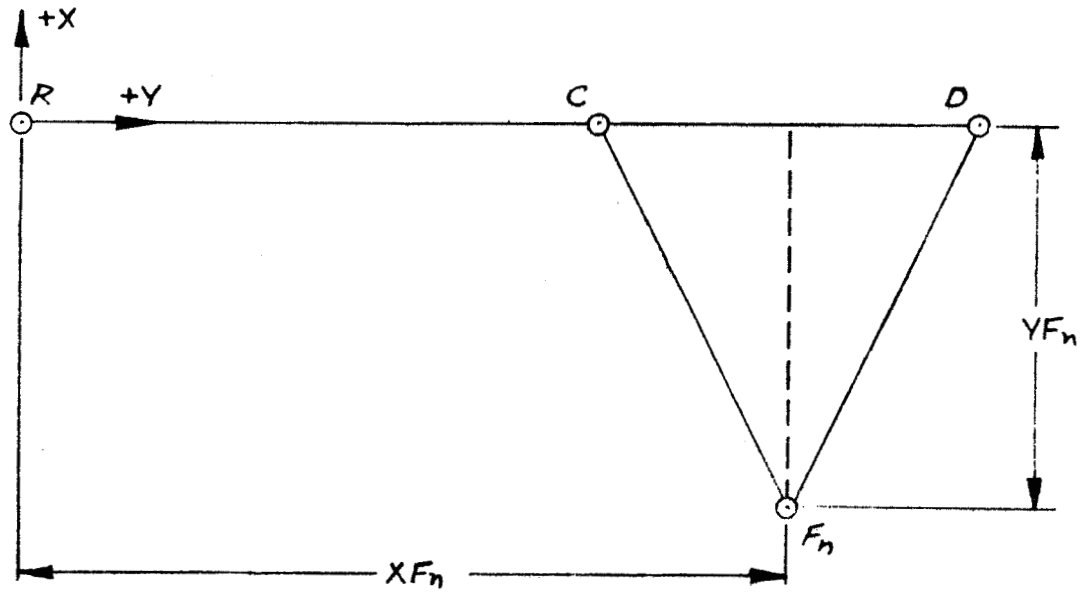

$CF_n = CF_o + (\Delta CF)_n$ } FOR $n = 0$, $(\Delta CF)_o = 0 = (\Delta DF)_o$
$DF_n = DF_o + (\Delta DF)_n$ }

$(YF_n)^2 = (CF_n)^2 - (XF_n - RC)^2$; RC, RD & XF_n ARE ALWAYS POSITIVE, YF_n NEGATIVE

& $(YF_n)^2 = (DF_n)^2 - (RD - XF_n)^2$

SO, $(CF_n)^2 - (XF_n - RC)^2 = (DF_n)^2 - (RD - XF_n)^2$

$(CF_n)^2 - (XF_n)^2 + 2(XF_n)(RC) - (RC)^2 = (DF_n)^2 - (RD)^2 + 2(XF_n)(RD) - (XF_n)^2$

$2(RC)(XF_n) - 2(RD)(XF_n) = (DF_n)^2 - (CF_n)^2 - (RD)^2 + (RC)^2$

$2(RC - RD)(XF_n) = (DF_n)^2 - (CF_n)^2 - (RD)^2 + (RC)^2$

$$XF_n = \frac{(DF_n)^2 - (CF_n)^2 - (RD)^2 + (RC)^2}{2(RC - RD)}$$

$$YF_n = -\sqrt{(CF_n)^2 - (XF_n - RC)^2}$$

ALTERNATELY,

$S = \frac{1}{2}(CD + CF_n + DF_n)$, $CD = RD - RC$

$$YF_n = -\frac{2}{CD}\sqrt{S(S - CD)(S - CF_n)(S - DF_n)}$$

AEROJET-GENERAL CORPORATION
SACRAMENTO • CALIFORNIA

AGCS-0800-11

REPORT NO.

PAGE 4 OF

SUBJECT LSR FLEX SEAL DATA ANALYSIS & PIVOT POINT CALCULATIONS

DATE.

WORK ORDER

BY S.J. BROWN

CHK. BY

DATE.

$$\alpha_n = \text{ARCTAN}\left(\frac{YF_n - YE_n}{XF_n - XE_n}\right) - \text{ARCTAN}\left(\frac{YF_o - YE_o}{XF_o - XE_o}\right)$$

INSTANTANEOUS PIVOT POINT CALCULATIONS

DEFINITION: THE INSTANTANEOUS PIVOT POINT WILL BE DEFINED, FOR ANY TWO DEFLECTED SEAL POSITIONS n AND $n-1$, AS THE POINT FROM WHICH A CONSTANT RADIUS ARC MAY BE DRAWN THROUGH BOTH POSITIONS OF ANY GIVEN POINT ON THE MOVEABLE PLANE (I.E. E_n & E_{n-1}). FOR CORRELATION AND PLOTTING PURPOSES EACH PIVOT POINT, P_n, WILL BE ASSOCIATED WITH THE AVERAGE SEAL VECTOR ANGLE OF POSITIONS n AND $n-1$, $\alpha_{P_n} = \frac{1}{2}[(\alpha_n) + (\alpha_{n-1})]$.

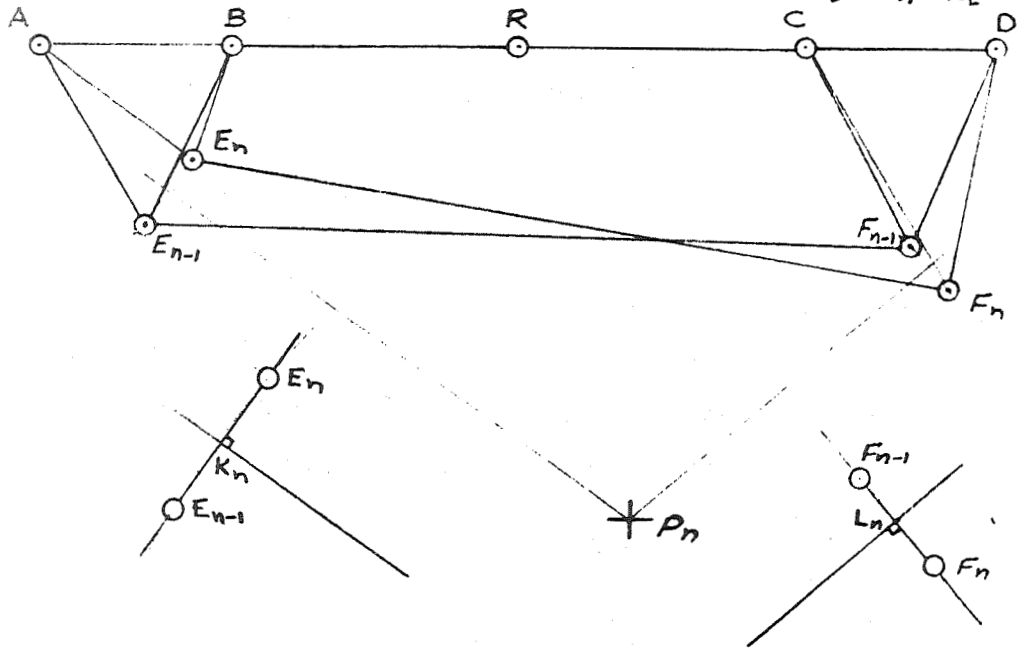

K_n IS THE MIDPOINT OF CHORD LINE E_nE_{n-1}, HAVING THE COORDINATES $\left(\frac{XE_n + XE_{n-1}}{2}, \frac{YE_n + YE_{n-1}}{2}\right)$. LINE K_nP_n BISECTS AND IS NORMAL TO LINE E_nE_{n-1}.

L_n IS THE MIDPOINT OF CHORD LINE F_nF_{n-1}, HAVING THE COORDINATES $\left(\frac{XF_n + XF_{n-1}}{2}, \frac{YF_n + YF_{n-1}}{2}\right)$. LINE L_nP_n BISECTS AND IS NORMAL TO LINE F_nF_{n-1}.

AEROJET-GENERAL CORPORATION
SACRAMENTO • CALIFORNIA

AGCS-0800-11 | REPORT NO | PAGE 5 OF

SUBJECT: LSR FLEX SEAL DATA ANALYSIS & PIVOT POINT CALCULATIONS | DATE | WORK ORDER

BY: S. J. BROWN | CHK. BY | DATE

THE SLOPE OF LINE $E_n E_{n-1} = M_E = \dfrac{YE_n - YE_{n-1}}{XE_n - XE_{n-1}}$

SO THE SLOPE OF LINE $K_n P_n = M_K = \dfrac{-1}{M_E} = \dfrac{XE_{n-1} - XE_n}{YE_n - YE_{n-1}}$

THEREFORE THE EQUATION OF LINE $K_n P_n$ IS:

$$Y_K = M_K X_K + B_K \quad \text{AND} \quad B_K = Y_K - M_K X_K = \left(\frac{YE_n + YE_{n-1}}{2}\right) - \left(\frac{XE_{n-1} - XE_n}{YE_n - YE_{n-1}}\right)\left(\frac{XE_n + XE_{n-1}}{2}\right)$$

$$B_K = \frac{YE_n + YE_{n-1}}{2} - \left[\frac{(XE_{n-1}XE_n) + (XE_{n-1})^2 - (XE_n)^2 - (XE_n XE_{n-1})}{2(YE_n - YE_{n-1})}\right] = \frac{YE_n + YE_{n-1}}{2} - \frac{(XE_{n-1})^2 - (XE_n)^2}{2(YE_n - YE_{n-1})}$$

$$B_K = \frac{(YE_n + YE_{n-1})(YE_n - YE_{n-1}) - (XE_{n-1})^2 + (XE_n)^2}{2(YE_n - YE_{n-1})} = \frac{(YE_n)^2 - (YE_{n-1})^2 - (XE_{n-1})^2 + (XE_n)^2}{2(YE_n - YE_{n-1})}$$

THEREFORE

$$\boxed{Y_K = \left(\frac{XE_{n-1} - XE_n}{YE_n - YE_{n-1}}\right) X_K + \frac{(YE_n)^2 - (YE_{n-1})^2 - (XE_{n-1})^2 + (XE_n)^2}{2(YE_n - YE_{n-1})}}$$

THE SLOPE OF LINE $F_{n-1} F_n = M_F = \dfrac{YF_n - YF_{n-1}}{XF_n - XF_{n-1}}$

SO THE SLOPE OF LINE $L_n P_n = M_L = \dfrac{-1}{M_F} = \dfrac{XF_{n-1} - XF_n}{YF_n - YF_{n-1}}$

THEREFORE THE EQUATION OF LINE $P_n L_n$ IS:

$$Y_L = M_L X_L + B_L \quad \text{AND} \quad B_L = Y_L - M_L X_L = \left(\frac{YF_n + YF_{n-1}}{2}\right) - \left(\frac{XF_{n-1} - XF_n}{YF_n - YF_{n-1}}\right)\left(\frac{XF_n + XF_{n-1}}{2}\right)$$

$$B_L = \frac{YF_n + YF_{n-1}}{2} - \frac{(XF_{n-1}XF_n) + (XF_{n-1})^2 - (XF_n)^2 - (XF_{n-1}XF_n)}{2(YF_n - YF_{n-1})}$$

$$B_L = \frac{(YF_n + YF_{n-1})(YF_n - YF_{n-1}) - (XF_{n-1})^2 + (XF_n)^2}{2(YF_n - YF_{n-1})} = \frac{(YF_n)^2 - (YF_{n-1})^2 - (XF_{n-1})^2 + (XF_n)^2}{2(YF_n - YF_{n-1})}$$

THEREFORE

$$\boxed{Y_L = \left(\frac{XF_{n-1} - XF_n}{YF_n - YF_{n-1}}\right) X_L + \frac{(YF_n)^2 - (YF_{n-1})^2 - (XF_{n-1})^2 + (XF_n)^2}{2(YF_n - YF_{n-1})}}$$

THE INSTANTANEOUS PIVOT POINT P_n IS AT THE INTERSECTION OF LINES $K_n P_n$ AND $P_n L_n$. AT THAT POINT $Y_L = Y_K = Y_P$ AND $X_L = X_K = X_P$. IN OTHER WORDS,

$$\left(\frac{XE_{n-1} - XE_n}{YE_n - YE_{n-1}}\right) \overset{X_P}{\overset{\|}{X_K}} + \frac{(YE_n)^2 - (YE_{n-1})^2 - (XE_{n-1})^2 + (XE_n)^2}{2(YE_n - YE_{n-1})} = \left(\frac{XF_{n-1} - XF_n}{YF_n - YF_{n-1}}\right) \overset{X_P}{\overset{\|}{X_L}} + \frac{(YF_n)^2 - (YF_{n-1})^2 - (XF_{n-1})^2 + (XF_n)^2}{2(YF_n - YF_{n-1})}$$

SO,

$$\boxed{X_P = \frac{\left(\dfrac{(YF_n)^2 - (YF_{n-1})^2 - (XF_{n-1})^2 + (XF_n)^2}{2(YF_n - YF_{n-1})}\right) - \left(\dfrac{(YE_n)^2 - (YE_{n-1})^2 - (XE_{n-1})^2 + (XE_n)^2}{2(YE_n - YE_{n-1})}\right)}{\left(\dfrac{XE_{n-1} - XE_n}{YE_n - YE_{n-1}}\right) - \left(\dfrac{XF_{n-1} - XF_n}{YF_n - YF_{n-1}}\right)}}$$

AGCS-0800-11

AEROJET-GENERAL CORPORATION
SACRAMENTO • CALIFORNIA

REPORT NO.

PAGE 6 OF

SUBJECT LSR FLEX SEAL DATA ANALYSIS & PIVOT POINT CALCULATIONS

DATE

WORK ORDER

BY S. J. BROWN

CHK. BY

DATE

AFTER SOLVING THE PRECEDING EQUATION FOR X_P, SUBSTITUTE THAT VALUE INTO THE PRECEDING EQUATION TO FIND $Y_L = Y_P$, DEFINING THE INSTANTANEOUS PIVOT POINT IN THE X-Y PLANE.

AEROJET-GENERAL CORPORATION
SACRAMENTO • CALIFORNIA

AGCS-0800-11

REPORT NO

PAGE 7 OF

SUBJECT
LSR FLEX SEAL ROTATIONAL TORQUE CALCULATIONS

DATE

WORK ORDER

BY
S.J. BROWN

CHK. BY

DATE

R IS A FIXED POINT AT THE ORIGIN OF THE X-Y COORDINATE SYSTEM.

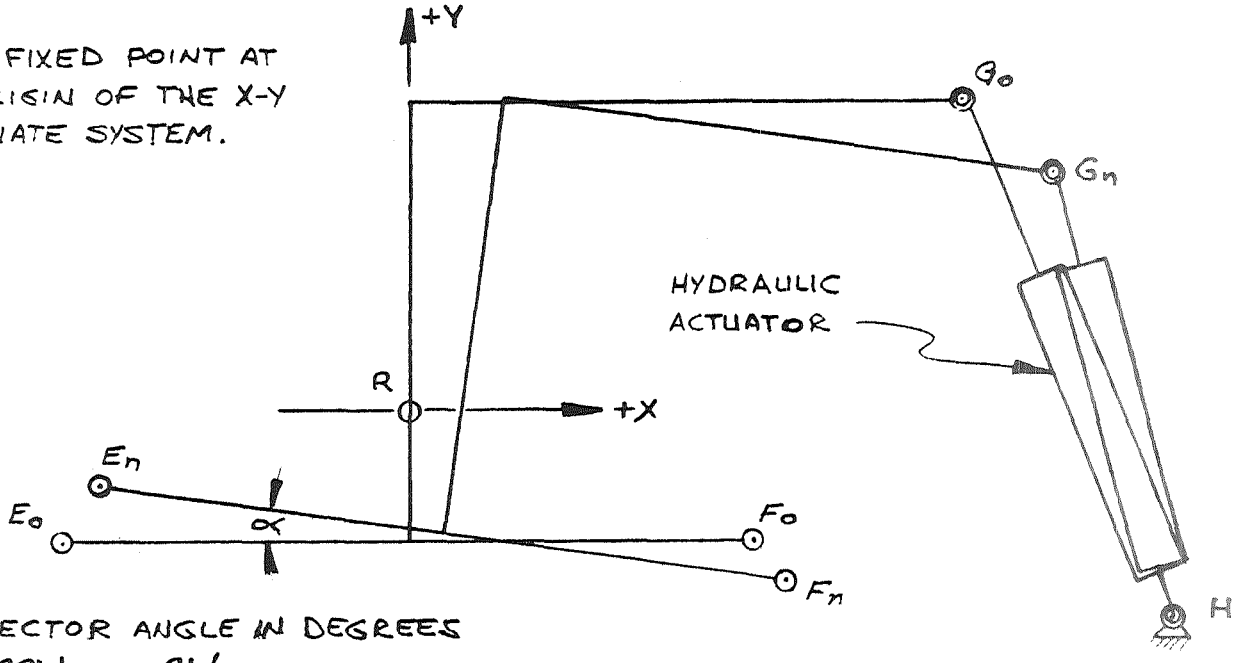

α = VECTOR ANGLE IN DEGREES
+ CCW , − CW

H IS A FIXED REACTION POINT FOR THE HYDRAULIC ACTUATOR.

GoH IS MEASURED PRIOR TO THE TEST AND ΔGH IS MEASURED REMOTELY DURING THE TEST.

Pn

Pn IS THE INSTANTANEOUS PIVOT POINT FOR POSITION n.

THE X AND Y COORDINATES FOR POINTS Eo, Fo, Go & H ARE DETERMINED PRIOR TO THE TEST AND THE NEW COORDINATES OF En, Fn & Pn ARE CALCULATED FROM TEST DATA AS SHOWN PREVIOUSLY. DIMENSION FG IS ALSO MEASURED PRIOR TO THE TEST AND IS CONSIDERED FIXED.

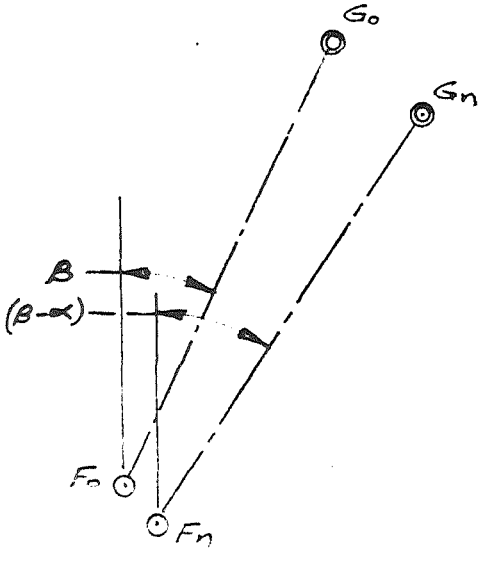

ANGLE β WILL BE DETERMINED PRIOR TO TEST BASED ON MEASUREMENTS OF POSITIONS OF Fo AND Go.

$$XG_n = XF_n + FG \sin(\beta - \alpha)$$
$$YG_n = YF_n + FG \cos(\beta - \alpha)$$

AEROJET-GENERAL CORPORATION
SACRAMENTO • CALIFORNIA

AGCS-0800-11

REPORT NO.	PAGE 8 OF
SUBJECT: LSR FLEX SEAL ROTATIONAL TORQUE CALCULATIONS	DATE
	WORK ORDER
BY S.J. BROWN	CHK. BY / DATE

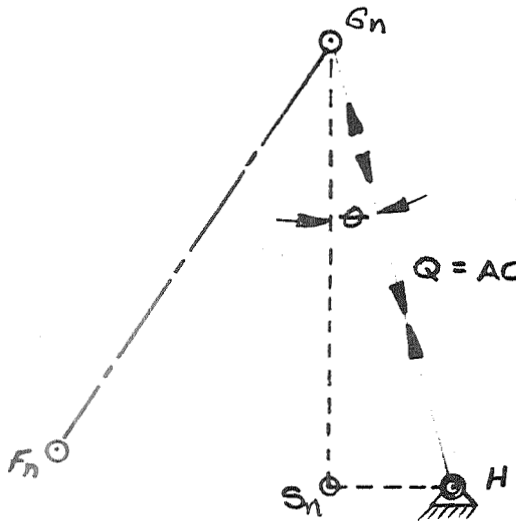

$S_nH = XH - XG_n$

$S_nG_n = YG_n - YH$

$\theta = \text{ARCTAN} \dfrac{S_nH}{S_nG_n}$

Q = ACTUATOR FORCE IN POUNDS

TORQUE ARMS

$TA1 = YG_n - YP_n$

$TA2 = XG_n - XP_n$

SEE DIAGRAM BELOW

TORQUE FORCES

$TF1 = Q \sin\theta$

$TF2 = Q \cos\theta$

OR $TF1 = Q \dfrac{S_nH}{G_nH}$, WHERE $G_nH = G_oH + \Delta GH$,

SIMILARLY FOR $TF2 = Q \dfrac{S_nG_n}{G_nH}$

THE ACTUATOR FORCE, Q, WILL BE MEASURED REMOTELY DURING THE TEST. THEREFORE, THE ACTUATION TORQUE AT POSITION n WILL BE:

$T = (TA1)(TF1) + (TA2)(TF2)$

$T = (YG_n - YP_n)(Q \sin\theta) + (XG_n - XP_n)(Q \cos\theta)$

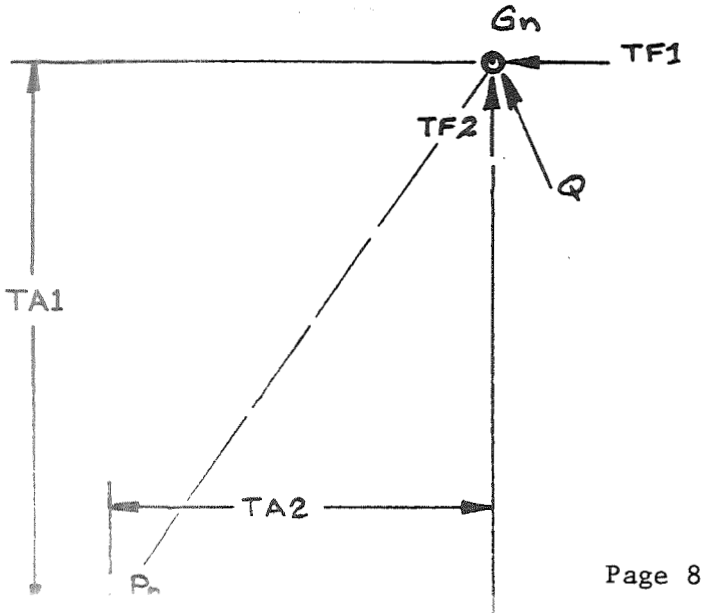

DISTRIBUTION LIST FOR FINAL REPORT NASA CR-72889

NASA Lewis Research Center
21000 Brookpark Rd.
Cleveland, Ohio 44135
Attn: Contracting Officer (1)
Mail Stop: 500-313
Solid Rocket Technology Branch (8)
Mail Stop: 500-205
Technical Library (2)
Mail Stop: 60-3
Tech. Report Control Office (1)
Mail Stop: 5-5
J. Kennard (1)
Mail Stop: 3-17
Tech. Utilization Office (1)
Mail Stop: 3-19
Patent Counsel (1)
Mail Stop: 500-311

National Aeronautics & Space Admin.
Washington, D.C. 20546
Attn: RPM/R. Wasel (3)
RPS/Robert W. Ziem (1)
ATSS-AL/Technical Library (2)

NASA Ames Research Center
Moffett Field, Calif. 94035
Attn: Technical Library (1)

NASA Langley Research Center
Langley Station
Hampton, Virginia 23365
Attn: Robert L. Swain (1)
Technical Library (1)

NASA Goddard Space Flight Center
Greenbelt, Maryland 20771
Attn: Technical Library (1)

NASA Manned Spacecraft Center
2101 Webster Seabrook Road
Houston, Texas 77058
Attn: Technical Library (1)

NASA George C. Marshall Space
Flight Center
Redstone Arsenal
Huntsville, Alabama 35812
Attn: Technical Library (1)
S&E-ASTN-PJ/D. Burrows (1)

Jet Propulsion Laboratory
Calif. Institute of Technology
4800 Oak Grove Drive
Pasadena, California 91103
Attn: Richard Bailey
Technical Library (1)

Scientific & Technical Information
Facility
NASA Representative
P.O. Box 33
College Park, Maryland 20740
Attn: CRT (6)

GOVERNMENT INSTALLATIONS

AF Space Systems Division
Air Force Unit Post Office
Los Angeles, California 90045
Attn: Col. E. Fink (1)

AF Research & Technology Division
Bolling AFB, D.C. 20332
Attn: Dr. Leon Green, Jr. (1)

AF Rocket Propulsion Laboratory
Edwards AFB, California 93523
Attn: RPM/Mr. C. Cook (2)

AF Materials Laboratory
Wright Patterson AFB, Ohio 45433
Attn: MANC/D. Schmidt (1)
MAAE (1)

AF Ballistic Missile Division
P.O. Box 262
San Bernardino, California
Attn: WDSOT (1)

Structures Division
Wright Patterson AFB, Ohio 45433
Attn: FDT/R. F. Hoener (1)

Army Missile Command
Redstone Scientific Information Center
Redstone Arsenal, Alabama 35809
Attn: Chief, Document Section (1)

DISTRIBUTION LIST (cont)

Ballistic Research Laboratory
Aberdeen Proving Ground,
Maryland 21005
Attn: Technical Library (1)

Picatinny Arsenal
Dover, New Jersey 07801
Attn: Technical Library (1)

Navy Special Projects Office
Washington, D.C. 20360
Attn: H. Bernstein (1)

Naval Air Systems Command
Washington, D.C. 20360
Attn: AIR-330/Dr. O. H. Johnson (1)

Naval Propellant Plant
Indian Head, Maryland 20640
Attn: Technical Library (1)

Naval Ordnance Laboratory
White Oak
Silver Spring, Maryland 20910
Attn: Technical Library (1)

Naval Ordnance Test Station
China Lake, California 93557
Attn: Technical Library (1)
C. J. Thelen (1)

Naval Research Laboratory
Washington, D.C. 20390
Attn: Technical Library (1)

Chemical Propulsion Information Agency
Applied Physics Laboratory
8621 Georgia Avenue
Silver Spring, Maryland 20910 (1)

Defense Documentation Center
Cameron Station
5010 Duke Street
Alexandria, Virginia 22314 (1)

Defense Materials Information Center
Battelle Memorial Institute
505 King Avenue
Columbus, Ohio 43201 (1)

Materials Advisory Board
National Academy of Science
2101 Constitution Ave., N.W.
Washington, D.C. 20418
Attn: Capt. A. M. Blamphin (1)

Institute for Defense Analysis
1666 Connecticut Ave., N.W.
Washington, D.C.
Attn: Technical Library (1)

Advanced Research Projects Agency
Pentagon, Room 3D154
Washington, D.C. 20301
Attn: Tech. Information Office (1)

INDUSTRY CONTRACTORS

Aerojet Solid Propulsion Company
P.O. Box 13400
Sacramento, California 95813
Attn: Dr. B. A. Simmons (1)
L. Westphal (2)
Tech. Information Center (1)

Aerojet-General Corporation
P.O. Box 296
Azusa, California 91702
Attn: Technical Library (1)

Aerospace Corporation
2400 East El Segundo Boulevard
El Segundo, California 90245
Attn: Technical Library (1)
Solid Motor Dev. Office (1)

Aerospace Corporation
P.O. Box 95085
Los Angeles, California 90045
Attn: Technical Library (1)

Atlantic Research Corporation
Shirley Highway at Edsall Road
Alexandria, Virginia 22314
Attn: Technical Library (1)

Battelle Memorial Library
505 King Avenue
Columbus, Ohio 43201
Attn: Edward Unger (1)

Boeing Company
P.O. Box 3999
Seattle, Washington 98124
Attn: Technical Library (1)

Chrysler Corporation
Space Division
Michoud Operations
New Orleans, Louisiana
Attn: Technical Library (1)

Douglas Missiles & Space Systems
Huntington Beach, California
Attn: T. J. Gordon (1)

Hercules Company
Allegany Ballistics Laboratory
P.O. Box 210
Cumberland, Maryland 21502
Attn: Technical Library (1)

Hercules Company
Bacchus Works
P.O. Box 98
Magna, Utah 84044
Attn: Technical Library (1)

Lockheed Missiles & Space Company
P.O. Box 504
Sunnyvale, California
Attn: Technical Library (1)

Lockheed Propulsion Company
P.O. Box 111
Redlands, California 93273
Attn: Bud White (1)

Martin Marietta Corporation
Baltimore Division
Baltimore, Maryland 21203
Attn: Technical Library (1)

Mathematical Sciences Corporation
278 Renook Way
Arcadia, California 91107
Attn: M. Fourney (1)

Philco Corporation
Aeronutronics Division
Ford Road
Newport Beach, California 92660
Attn: Technical Library (1)

Rocketdyne
Solid Propulsion Operations
P.O. Box 548
McGregor, Texas
Attn: Technical Library (1)

Rocketdyne
6633 Canoga Avenue
Canoga Park, California 91304
Attn: Technical Library (1)

Rohm and Haas
Redstone Arsenal Research Division
Huntsville, Alabama 35807
Attn: Technical Library (1)

Rohr Corporation
Space Products Division
8200 Arlington Boulevard
Riverside, California (1)

Thiokol Chemical Corporation
Wasatch Division
Brigham City, Utah 84302 (1)

Thiokol Chemical Corporation
Elkton Division
Elkton, Maryland 21921
Attn: Technical Library (1)

Thiokol Chemical Corporation
Huntsville Division
Huntsville, Alabama 35807
Attn: Technical Library (1)

TRW, Inc.
Structures Division
23444 Euclid Avenue
Cleveland, Ohio 44117
Attn: L. Russell (1)

TRW Systems
One Space Park
Redondo Beach, California 90278
Attn: M. Lipow (1)

United Technology Center
P.O. Box 358
Sunnyvale, California 94088
Attn: Technical Library (1)